Time Curve of Heat Release for Compartment Fires with Fuel of Wooden Cribs

Nilsson, Leif

1974

LUND INSTITUTE OF TECHNOLOGY · LUND · SWEDEN · 1974

DIVISION OF STRUCTURAL MECHANICS AND CONCRETE CONSTRUCTION · BULLETIN 36

LEIF NILSSON

TIME CURVE OF HEAT RELEASE FOR COMPARTMENT FIRES WITH FUEL OF WOODEN CRIBS

Sigma-Tryck

TIME CURVE OF HEAT RELEASE FOR COMPARTMENT FIRES WITH FUEL OF WOODEN CRIBS

Leif Nilsson

Lund Institute of Technology, Sweden, 1974

PREFACE

In the present report, the experimentally obtained results from a large test series for a systematical determination of the time curve corresponding to the energy released per unit time in a fully developed fire process, by the heat- and mass balance equation of the fire cell, are analyzed. The experimental test series analyzed embraces a study dealing with the influence of variations in the size of the fire load, piling density, stick thickness, ventilation properties of the fire cell and thermal properties of the enclosing structures of the fire cell, on the combustion rate, gas temperature and radiation. The experimental test results have been partly published before and will be further described in some other connection. Based on the concept of energy released per unit time, primarily its maximum value, a differentiated classification of compartment fires is further performed in the present report with division into ventilation- and fuel bed controlled fire processes in the rigorous sense and crib controlled fire process. In addition, a method based on equivalent porosity factor and equivalent stick thickness is outlined relating the fire load in the form of a regular wood crib to a realistic fire load in the form of furniture, textile goods and other equipments.

Since the research activity on structural fire research in Sweden is largely concentrated to the Division of Structural Mechanics and Concrete Construction at Lund Institute of Technology where the report has been prepared, an open and broad cooperation among the persons involved becomes natural and herewith I would like to convey my best thanks to all who have, somehow or other, been engaged in the project.

In the first place, I would like to give my special thanks to professor Ove Pettersson, Head of the Division of Structural Mechanics and Concrete Construction, who has given rise to a great part of the ideas presented here and who has given me valuable stimulus and personal encouragement in the course of the work.

I would further like to thank research engineer Sven-Erik Magnusson and university lecturer Sven Thelandersson who have placed a func-

tioning computer program at my disposal and who, in addition, on many occasions, have discussed different problems with great interest.

Mrs. Birgit Ohlsson and Mrs. Mary Lindqvist have typed the manuscript, Mrs. Ann Schollin has drawn the figures and Mahmood Mazlumolhosseini has been responsible for the translation. Their contribution is marked by precision and skillfulness and I would like to express my best thanks to each of them for their cooperation.

The investigation has been mostly financed by the Swedish Council for Building Research. Thanks to the kind disposition of the Council, further knowledge has been provided for, through the present report, facilitating an improved and differentiated design of the structural fire protection according to the principles held by present fire technological research at the Division of Structural Mechanics and Concrete Construction

Finally, I would like to express my best thanks to my dear wife Gun-Britt, who has followed the successive progress of the work with active interest and who has been a great support for me the whole time.

April, 1974

Leif Nilsson

CONTENTS

PRINCIPAL NOTATIONS

A	Area of vertical openings in the enclosing structure	m^2
A_s	Area of the surface of the fire load initially exposed to fire	m^2
A_t	The total internal surface area of the fire cell	m^2
$(A\sqrt{H})$	Air flow factor (ventilation factor)	$m^{5/2}$
$(A\sqrt{H}/A_t)$	Opening factor	$m^{1/2}$
C	A coefficient ≤ 1	
H	Height of vertical opening in the enclosed space	m
I	Enthalpy	MJ/m^3
I_B	Heat energy stored per unit time in the gas volume of the fire cell	MJ/h
I_C	Heat energy released per unit time during combustion	MJ/h
I_L	Energy removed per unit time through exchange of hot gases with cold air	MJ/h
I_R	Energy radiated per unit time through the openings of the fire cell	MJ/h
I_W	Energy supplied to the enclosing wall, floor and ceiling structures per unit time	MJ/h

I_{Cav}	Mean value of the heat energy released per unit time during the time period the weight of the fuel decreases from 80% to 30% of the initial weight	MJ/h
I_{Cd}	Mean value of the heat energy released per unit time during the time interval which is determined by values of 0.75 I_{Cmax} on the ascending and descending parts of the energy-time curve respectively	MJ/h
I_{Cg}	Mean value of the heat energy released per unit time during the time interval which is determined by values of 0.75 I_{Cmax} and 0 respectively on the descending part of the energy-time curve during the glowing phase	MJ/h
I_{Cm}	Mean value of the heat energy released per unit time during the time interval between ignition and the time corresponding to the maximum energy development, I_{Cmax} respectively	MJ/h
I_{Cmax}	The maximum value of the energy-time curve	MJ/h
I_{Cr}	Mean value of the heat energy released per unit time during the time interval between ignition and the time corresponding to 0.75 I_{Cmax}, on the descending part of the energy-time curve, respectively	MJ/h
L	Length of the individual stick in the crib	cm
M	The total fuel quantity in the fire cell	MJ

N	The number of layers of sticks in a crib	number
Q	The quantity of gases leaving the fire cell per unit time through the vertical openings	kg/h
Q_a	The gas flow, Q, modified by a factor $C < 1$, that is $Q_a = C \cdot Q$	kg/h
R	Combustion rate	kg wood per unit time
R_{80-30}	Mean value of the combustion rate during the flaming phase, referred to the weight decrease of the fire load from 80% to 30% of the initial weight	kg wood per unit time
R_d	Mean value of the combustion rate during the time interval which is determined by the values 0.75 I_{Cmax} on the ascending and descending part of the energy-time curve respectively	kg wood per unit time
R_g	Mean value of the combustion rate during the time interval which is determined by the values 0.75 I_{Cmax} and 0 respectively on the descending part of the energy-time curve during the glowing phase	kg wood per unit time
R_r	Mean value of the combustion rate during the time interval between ignition and the time corresponding to 0.75 I_{Cmax} on the descending part of the energy-time curve	kg wood per unit time
T	Fire duration, defined as the duration of the flame phase	h

X		
W	Heat value of the fuel	MJ/kg
W_{av}	Mean value of the heat value during the time period the weight of the fuel decreases from 80% to 30% of the initial weight	MJ/kg
W_d	Mean value of the heat value during the time interval which is determined by the values 0.75 I_{Cmax} on the ascending and descending part of the energy-time curve respectively	MJ/kg
W_g	Mean value of the heat value during the time interval which is determined by the values 0.75 I_{Cmax} and 0, respectively, on the descending part of the energy-time curve during the glowing phase	MJ/kg
W_r	Mean value of the heat value during the time interval between ignition and the time corresponding to 0.75 I_{Cmax} on the descending part of the energy-time curve	MJ/kg
b	Thickness of each individual stick in the crib	mm
c	Specific heat of the enclosing structure	$MJ/kg \cdot {}^{o}C$
c_p	Specific heat of the gases	$MJ/kg \cdot {}^{o}C$
g	Gravitational acceleration	m/s^2
n	Number of sticks in each of the crib	number
q	Fire load	MJ per square meter of the enclosing area

r	Hydraulic radius	mm
t	Time co-ordinate	h
t_d	The time interval which is determined by the values 0.75 I_{Cmax} on the ascending and descending part of the energy-time curve respectively	h
t_g	The time interval which is determined by the values 0.75 I_{Cmax} and 0, respectively, on the descending part of the energy-time curve during the glowing phase	h
t_m	The time interval between ignition and the time corresponding to the maximum value I_{Cmax} on the energy-time curve	h
t_r	The time interval between ignition and the time corresponding to 0.75 I_{Cmax} on the descending part of the energy-time curve	h
t_1	The time interval between the times corresponding to 0.75 I_{Cmax} and 0.5 I_{Cmax}, respectively, on the descending part of the energy-time curve	h
t_2	The time interval between the times corresponding to 0.75 I_{Cmax} and 0.25 I_{Cmax}, respectively, on the descending part of the energy-time curve	h
v_i	Penetration rate of the fire perpendicular to the exposed surface of a wooden lath	mm/min

x	Position co-ordinate	m
α_i	Coefficient of heat transfer at the surface exposed to fire (internal surface)	$W/m^2.^oC$
α_u	Coefficient of heat transfer at the surface not exposed to fire (external surface)	$W/m^2.^oC$
γ	Density of the enclosing structure	kg/m^3
ε_{res}	Resultant emissivity for radiation between flames, combustion gases and the surface exposed to fire (internal surface)	
ε_{fl}	Emissivity of flames	
ε_i	Emissivity of the surface exposed to fire	
ϑ	Temperature	^oC
ϑ_o	Temperature of the outside air	^oC
ϑ_g	Temperature of the combustion gases in the fire chamber	^oC
ϑ_i	Temperature of the surface exposed to fire (internal surface)	^oC
ϑ_u	Temperature of the surface not exposed to fire (external surface)	^oC
λ	Coefficient of thermal conductivity	$W/m.^oC$

ϑ_{80-30}	Mean value of the gas temperature in the fire chamber during the time period in which the weight of the fuel decreases from 80% to 30% of the initial weight	^{o}C
ϕ	Porosity factor	$cm^{1.1}$
Φ	Ventilation parameter	kg/s
ρ	Density of the air	kg/m^3

1. INTRODUCTION.

1.1 Development trends. Main characteristics of fire technological design.

In spite of the intensive research in the field of structural fire protection in the recent years, our knowledge regarding a qualified fire technological design of bearing and partitioning constructions is still incomplete. This is of course unfortunate especially in regard to the huge direct and indirect costs which ensure from fire damages every year. Thus the direct fire damages in Sweden alone during the year 1970 can be estimated to approximately 350 MCr, while the total value of the direct and indirect expenses at the same period (expenses for preventive measures, fire extinction and administration) reaches the roughly approximative value of 1 1/2 billion crowns per year.

In tact with an increasing knowledge, new design methods, standards, and testing methods would be developed so that the risks of fire are more properly determined and a successively improved cost-benefit criterion is obtained. This concept applied to a well-defined situation - for example in a community - means minimizing the total costs of fire extinction system, preventive fire protection plus the cost of fire damage risk which is defined as the sum of the costs of all types of fire damages, each weighed according to its risk (Σ individual cost x individual risk). The path to such a complete point is, however, very long and it necessitates qualified solutions of more limited partial problems. Accordingly the present activity, for example in regard to bearing and partitioning constructions, is primarily directed towards acquiring increased knowledge about the fire process, properties of construction material within the actual temperature range during the fire exposure, temperature-time field, behaviour and bearing capacity in the course of the fire exposure. A further activity which is fundamental in this case is directed towards improvement, coordination and standardization of the testing equipments and testing methods.

A fundamental objective of a fire differentiated fire-technological design is the development of a procedure which would basically be equivalent with the essential features of a statical design of bearing structures. In brief, this implies an evaluation of the existing quantity of combustible material in a fire cell (fire loading), of the corresponding gas temperature-time curve of the fire cell and of temperature condition of the construction together with the corresponding minimum bearing capacity which, with the prescribed safety, would exceed the actual value for the loading throughout the whole fire process.

The research work which is either planned for the future, or is going on, or is already completed may roughly be sorted into one of the following main groups. These groups comprise the fundamental steps in a qualified fire technological design, Pettersson (1965):

a) Combustion-technological characterization of the fire load of a fire cell for the usually occuring types localities and buildings (flats, offices, schools, hospitals, stores, libraries etc.).

b) Study of energy development, necessary air supply and gas production during a fire process and evaluation of the gas smoke temperature obtained in the fire chamber as a function of time.

c) Evaluation of the thermal properties of the relevant construction material within the whole temperature range of a fire both for heating and cooling phase.

d) Evaluation of the non-stationary temperature field arising in a structure when the fire exposure is as in b).

e) Evaluation of the behaviour and bearing capacity of a loaded and fire-exposed structure with respect to the temperature field determined according to d), knowing the corresponding changes in strength and deformation properties of the material.

In order that a fire technological design procedure, performed with theoretical calculations according to the above outlined

pattern, shall be possible it is required that the given problems under b)-e) are made clear for a complete fire process which is normally divided into ignition phase, flaming phase, glowing and cooling phase, compare FIG. 1. Here in this paper both the last two phases are designated by cooling phase.

Published research has hitherto been largely concentrated on experimental studies, preferably on the flaming phase of the fire process while ignition and cooling phases have only been studied to a limited extent. This fact is reflected in the current Swedish Building Standards 1967 by which a fire technological design of a building or part of a building, may be carried out according to three rather different alternatives with respect to precision while for cooling phase it is briefly stated that gastemperature-time curve of the fire cell may be chosen with a linear cooling rate of 10°C per minute provided that no other solution is found to be more suitable. This implies that in a continuous fire process the two consecutive phases of heating and cooling respectively, would have different criteria as far as the precision is concerned. For structures with little heat resistance, such as non-insulated or lightly insulated steel constructions, this undifferentiated characterization would exert an unfavourable influence which is of course unsatisfactory.

1.2 Scope of the present work.

The present publication is primarily devoted to the problem of the liberated energy per unit time in a fire with wooden combustibles in a closed room with a window opening. The work is based upon experimental model studies performed by the author results of which have partly been reported in another publication - Nilsson (1971) - and will be more completely accounted for later. The problem is tackled with the purpose of developing an approximate method for engineering use which would form a basis for a differentiated and practical design in such structures as bearing and partitioning constructions during fire exposure.

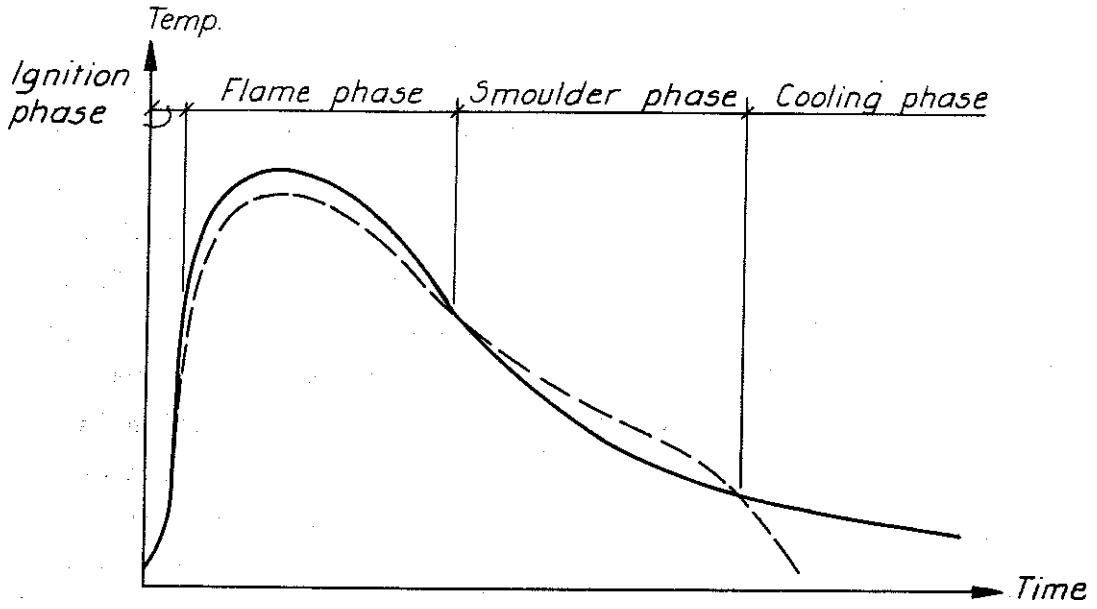

FIG. 1 The main phases of the fire process characterized by time curves for the temperature of the fire chamber (—) determined by thermocouples, and for the radiation temperature (---).

Solving the problem requires parallel theoretical studies and experimental works. The research performed up to now has almost been wholly directed towards the flaming phase of the fire process while ignition and cooling phases have only been studied to a limited extent.

Of the published theoretical studies on the fire process the works by Kawagoe-Sekine (1963), Ödeen (1963) and Magnusson - Thelandersson (1970, 1971) should specially be mentioned here. In both of the first-mentioned works which have been performed simultaneously and independent of each other, the authors have set up the heat balance equation corresponding to fire in a closed room and by solving this equation they have evaluated the temperature-time curves of the fire chamber for some fundamental cases. When applying the equation to fuels which were more complicated from combustion point of view, such as wooden combustibles, the extent of the problem was restricted to embrace only the flaming phase of the fire process while the cooling phase was left untreated due to incomplete theory.

An extension of the theory in which even the cooling phase is generally included appears in the works of Magnusson-Thelandersson. This theory extension requires, among other things, the solution of two problems which have earlier been treated incompletely, that is partly evaluation of the liberated energy per unit time as a function of time for the whole fire process and partly an extension and completion of the heat balance equation the terms of which had earlier been solely set up for the heating phase.

The first-mentioned problem was tackled through making comparative calculation by computer, with varying time curves for the liberated energy per unit time in such full scale fire tests which have already been performed and reported in the existing literature and the results of which fulfil certain requirements regarding the specifications of the problem. Accordingly, for every test the energy-time curve which rendered a satisfactory agreement between the temperature-time curve of the smoke gases as measured through tests and that calculated through a theoretical model,

was iteratively determined. After working out the obtained results they could be systematized so that the time curve for the liberated energy per unit time could generally be assumed to be approximately known, whereupon the complete gas temperature-time curve of the fire process with different values of fire loading and opening factor for different types of fire cells in regard to the thermal properties of the enclosing constructions, was determined. Compare Section 2.

In working out the experimental basis, a schematization was found to be necessary since the tests analysed by the authors were incompletely described with respect to the detailed properties of the fire loading and thermal characteristics of the enclosing constructions.

Since the author in an earlier report, Nilsson (1971), has among other things, shown that an increase in the piling density of a wooden lath pile may result in a multiple increase of the mean combustion rate during the flaming phase, it seems to be an urgent matter that the influence of variations in the detailed properties of the fire loading on the time curve for the liberated energy and for the gas temperature be taken into consideration while doing heat balance computations for a fire cell.

The most significant influences on the fire process of a fire cell are as follows:

a) The quantity and type of the combustible material in the fire cell

b) Piling density of the fire loading and particle shape

c) Distribution of the fire loading in the fire cell

d) Geometry of the fire cell

e) Thermal characteristics of the enclosing constructions of the fire cell, and

f) The quantity of air supplied to the fire cell per unit of time

Thus, properties of the fire loading and ventilation conditions of the fire cell combined together determine if the fire process is going to be governed by fuel bed or by ventilation.

In the former case the combustion rate during the flaming phase is predominantly determined by size, location, particle shape and piling density of the fire loading while the air supplied through windows and door openings is of minor importance.

In the latter case, the air quantity available for combustion will determine the combustion rate and thereby the gas temperature-time curve of the fire cell as well, while size of the fire loading and other properties exert less influence.

During the recent years, the influence of different parameters on the fire process in a closed room described primarily by gas temperature-time curve, combustion rate and radiation conditions has been experimentally studied, in a systematic way, at the Division of structural mechanics and concrete constructions, Lund Institute of Technology. The varying parameters which have been taken into account consist of opening factor and air flow factor belonging to the fire cell, thermal properties of the enclosing structures and size, piling density and particle shape of the fire loading. Opening factor is defined as $A\sqrt{H}/A_t$ and air flow factor as $A\sqrt{H}$, in which A_t (m^2) denotes the inner surface area of the walls, floor and ceiling which bound the fire cell from its surroundings, A (m^2) is the total opening area of the fire cell (windows, doors etc.) and H is a weighted mean value of the height of the openings. The experimental studies which have been performed in different model scales have taken place indoors inside a large laboratory hall which has implied that other conditions such as air temperature, relative air humidity and air velocity have almost been unchanged from test to test. Since shape of the fire cell and the more important properties of the fire loading have been carefully specified, an extensive material has been obtained which is quite suitable for theoretical analysis.

The purpose of the present paper is to analyse theoretically the influence of the different parameters on the liberated energy per unit of time in a complete fire process, in fires of the type wooden combustibles for different combination of the opening factor $A\sqrt{H}/A_t$, size of the fire loading as well as piling density, and the type of material composing the enclosing structures of the fire cell. The objective, herewith, is to find energy-time curves which are more differentiated than those described earlier in the literature and which thereby make improved heat balance computations of the fire process in a fire cell possible.

Based on the above-mentioned experimental tests to be shortly described in Section 3 and by applying the theoretical model, valid for a complete fire process, which has been given by Magnusson-Thelandersson (1970, 1971) and which would shortly be referred to in Section 2, the influence of some different parameters on the time curve for the energy development and gas temperature-time curve of the fire cell is analysed in Sections 4-7. The parameters which are treated here are composed of piling density of the fire loading described in Section 4, size of the fire loading in Section 5, particle thickness of the fire loading in Section 6 and thermal properties of the enclosing structures of the fire cell in Section 7. In parallel with the study of the influence of all the parameters, a study of the influence of the size of the window opening is included. In Section 8, the results obtained in Sections 4-7 are recapitulated in diagrams in order to give a basis which can be used in practical applications for estimating the influence of the different factors. Besides, a comparison is made between, on one side, the values summarized in Sections 4-7 which is based on the author's experimental studies on a model scale and, on the other side, the results obtained from tests performed on a full scale where the fire loading was composed of wooden lath piles or real furniture. The idea is, thereby, among other things, to find a method to make a correspondence between actual conditions during a fire process with loading consisting of actual furniture with values of the piling density corresponding to a wooden lath pile. Thereby systematical studies of the more important influences, with the aid of simply shaped fire loading on a model scale, could be made possible.

2. COMPUTATION MODEL AND COMPUTER PROGRAM.

2.1 Computation model.

A theoretical calculation of the heat and mass balance equations for the temperature-time curve of a fire process is based on the identity between the energy liberated per unit time during combustion on one side and the energy per unit time removed through openings and enclosing structures of the fire cell on the other, that is

$$I_C = I_L + I_W + I_R + I_B \qquad (1)$$

in which

I_C = the liberated energy per unit time during combustion (MJ/h)

I_L = the energy removed per unit time through exchange of hot gases with cold air (MJ/h)

I_W = the energy per unit time supplied to such enclosing structures as walls, floors, and ceilings and to possible enclosed structures (MJ/h)

I_R = the energy radiated per unit time through the openings of the fire cell (MJ/h)

I_B = the energy stored per unit time in the gas volume of the fire cell (MJ/h).

The Equation is schematically illustrated in FIG. 2.

A first development of a practical method from Equation (1), for evaluation of the gas temperature-time curve of a fire process during a fire in a closed room was simultaneously published by Kawagoe-Sekine (1963) and Ödeen (1963). The different terms in Equation (1) were thereby set up under the following simplified conditions:

a) The temperature is at any moment distributed uniformly in the whole fire chamber

b) The coefficient of heat transfer is the same at any point on the internal boundary surfaces of the fire cell

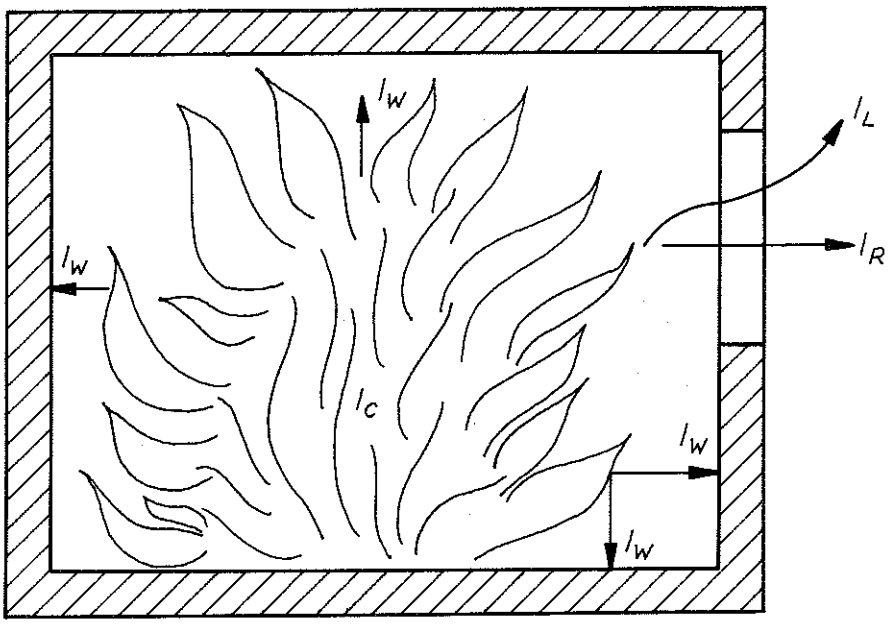

FIG. 2 Schematical illustration of the terms I_C, I_L, I_W and I_R entering into the heat balance equation.

c) There is a one-dimentional heat flow through enclosing walls, floor and ceiling which except for possible window- and door openings is uniformly distributed.

The above conditions render satisfactory precision in the ordinary practical cases.

For the terms I_C and I_L Kawagoe-Sekine and Ödeen set up expressions which make considerable restrictions in the application of the calculation procedure. For a complete fire process the method is applicable only in fires with well-defined fuels without glowing phase, e.g. liquid fuels. Roughly the method can also be used for determining the gas temperature-time curve during the flaming phase for the fire technologically more complicated fuels such as wood fuel in which case vigorously simplified assumptions concerning the combustion rate should be made.

An extension and generalisation of the method devised by Kawagoe-Sekine and Ödeen to a theoretical evaluation of the gas temperature-time characteristics of a complete fire process with fuels of the type wooden combustibles requires the solution of two complicated fundamental problems, that is, partly determination of the heat quantity liberated per unit time as a function of time and partly making a survey of the prevailing thermodynamical conditions when the rate of combustion is not any longer limited by the size of the openings of the fire cell.

Both of the problems are treated in detail by Magnusson and Thelandersson (1970, 1971) which in ordinary cases render acceptable solutions of the problems, moreover, they also set up the heat and mass balance relations required for a theoretical evaluation of the gas temperature-time curve of a complete fire process, in fires with wooden combustibles in a closed room, that is with such fuels which are frequently used in connections with buildings.

For this type of fuels, a theoretical description, for instance, of such a fundamental parameter as combustion rate gets complicated due to the fact that the combustion occurs both in the solid

constituents and in the gases formed during pyrolysis in such a manner that the influence on the combustion rate is not clear at the present. This means that for a fuel with a combustion mechanism similar to that of wooden combustibles, we lack, for example, the necessary knowledge for translating the weight decrease of the fuel per unit time registered during a fire process to energy liberated per unit time, or are equally ignorant of distribution of the total effective heat value on different phases of the fire process.

After this introductory brief outline it is shortly shown below how the different terms in Equation (1) are treated partly in the works by Kawagoe-Sekine and partly in the more general publications by Magnusson and Thelandersson.

The term I_B indicates the energy which is stored in the gas volume of the fire cell per unit time. In relation to other energy quantities actual during a fire process, this energy is insignificant and can be neglected with a satisfactory approximation.

The term I_R indicates the energy radiated through the openings of the fire cell per unit time. This energy is calculated by the Stefan-Boltzmann's law

$$I_R = A(E_g - E_o) \qquad (2)$$

where

A = area of the opening (m^2)

$$E_g = 5.77 \left(\frac{\vartheta_g + 273}{100}\right)^4$$

$$E_o = 5.77 \left(\frac{\vartheta_o + 273}{100}\right)^4$$

ϑ_g = temperature of the smoke gases (^oC)

ϑ_o = air temperature (^oC)

Equation (2) indicates the radiation, provided that the surroundings of the fire cell is considered as a black body. This approximation is acceptable in the present connection specially when considering

the fact that the radiation fraction is of the order of magnitude of 15% of the total energy.

The term I_W indicates the energy supplied to the enclosing walls, floor and ceiling per unit time. The desired non-stationary heat flow to the enclosing structures of the fire chamber is obtained by solving the general equation of heat conduction for the one-dimensional case.

$$c \cdot \gamma \frac{\partial \vartheta}{\partial t} = \frac{\partial}{\partial x} \left(\lambda_x \cdot \frac{\partial \vartheta}{\partial x} \right) \tag{3}$$

in which

ϑ = temperature of the wall material (^{o}C)
t = time (h)
x = position coordinate (m)
c = specific heat of the wall material for the actual position co-ordinate (MJ/kg ^{o}C)
γ = density of the wall material (kg/m^3)
λ_x = thermal conductivity of the wall material (W/m ^{o}C)

Equation (3) can be solved according to a numerical procedure which, in connection with fire, has been stated by many authors including Odenmark (1935) and later further developed by Ödeen (1963) and others. Summarily, this procedure implies that the enclosing walls, floor and ceiling structures are divided into n elements, each Δx_k thick, whereafter a heat balance equation is set up for each element based on the fact that the difference between the energy quantity per unit area entering an element and the energy leaving the element during the time Δt, causes a temperature change in the element which depends on the heat properties of the material. If at time t, the temperature at the mid point of the k:th layer is denoted by ϑ_k and the corresponding temperature at time $t + \Delta t$ by $\vartheta_k + \Delta\vartheta_k$, the following relations are obtained:

$$\begin{aligned}
&\phi_1 \cdot \frac{\Delta \vartheta_1}{\Delta t} = \psi_1 (\vartheta_g - \vartheta_1) - \psi_2 (\vartheta_1 - \vartheta_2) \\
&\vdots \\
&\phi_k \cdot \frac{\Delta \vartheta_k}{\Delta t} = \psi_k (\vartheta_{k-1} - \vartheta_k) - \psi_{k+1} (\vartheta_k - \vartheta_{k+1}) \\
&\vdots
\end{aligned} \tag{4}$$

$$\phi_n \cdot \frac{\Delta\vartheta_n}{\Delta t} = \psi_n(\vartheta_{n-1} - \vartheta_n) - \psi_{n+1}(\vartheta_n - \vartheta_o)$$

where

$$\phi_k = \Delta x_k \cdot c(x,\vartheta)\cdot\gamma$$

$$\psi_1 = \frac{1}{\frac{1}{\alpha_i(\vartheta)} + \frac{\Delta x_1}{2\cdot\lambda(x,\vartheta)}}$$

$$\vdots$$

$$\psi_k = \frac{1}{\frac{\Delta x_{k-1}}{2\cdot\lambda(x,\vartheta)} + \frac{\Delta x_k}{2\cdot\lambda(x,\vartheta)}}$$

$$\vdots$$

$$\psi_{n+1} = \frac{1}{\frac{\Delta x_n}{2\cdot\lambda(x,\vartheta)} + \frac{1}{\alpha_u(\vartheta)}}$$

with

$\alpha_i(\vartheta)$ = coefficient of heat transfer at the internal fire exposed surface ($W/m^2\ ^oC$)

$\alpha_u(\vartheta)$ = coefficient of heat transfer at the external surface ($W/m^2\ ^oC$)

$\lambda(x,\vartheta)$ = thermal conductivity at section x for temperature ϑ

$c(x,\vartheta)$ = the specific heat at section x for temperature ϑ

γ = the density at section x

The coefficient of heat transfer α_i can be divided into two parts, that is partly a convection fraction which with satisfactory precision can be chosen to be a constant = 25 $W/m^2\ ^oC$ and partly a radiation fraction which strongly dominates at the temperatures prevalent in connection with fire. This renders the following relation for the coefficient of heat transfer α_i:

$$\alpha_i = \frac{5.77\cdot\varepsilon_{res}}{\vartheta_g - \vartheta_i}\left[\left(\frac{\vartheta_g+273}{100}\right)^4 - \left(\frac{\vartheta_i+273}{100}\right)^4\right] + 25 \qquad (5)$$

where

ϑ_i = temperature of the internal surface

ε_{res} = the resultant emissivity for the radiation between flames - smoke gases and the internal surface.

ε_{res} is determined by the equation

$$\frac{1}{\varepsilon_{res}} = \frac{1}{\varepsilon_{fl}} + \frac{1}{\varepsilon_i} \tag{6}$$

where

ε_{fl} = emissivity of the flames and the smoke gases

ε_i = emissivity of the fire exposed surface

As an approximative expression for the coefficient of heat transfer at the outer surface not in touch with the fire, Ödeen (1963) gives the following formula:

$$\alpha_u = 8.7 + 0.033\ \vartheta_u \tag{7}$$

where ϑ_u = temperature at the external surface.

After solving the system of differential equations of the first order (4), the energy supplied to the enclosing structures I_W is obtained from

$$I_W = A_T \cdot \psi_1 \cdot (\vartheta_g - \vartheta_1) \tag{8}$$

where A_T indicates the total enclosing area of the structure excluding the openings. The relation assumes that the enclosing structure possess a uniform shape.

In cases where the enclosing structures consist of different materials or have different thicknesses I_W is obtained from the relation

$$I_W = \sum_j I_{W,j} = \sum_j A_j\ \psi_{1,j}\ (\vartheta_g - \vartheta_{1,j}) \tag{9}$$

where A_j denotes the area of the partial structure j.

The term I_L indicates the energy which is transported from the openings of the fire cell through convection due to the difference in density between the surrounding air and the hot gases of the fire

chamber. A formulation of the term I_L requires a generally valid expression based on the magnitude of the air exchange.

Assuming

that the statical pressure distribution varies linearly from the floor to the ceiling in the fire chamber

that there exists a level corresponding to a neutral plane where the pressure inside the fire cell is as large as the pressure outside

that the temperature in the fire chamber is uniformly distributed

and

that the vertical acceleration of the gases is neglected

the magnitude of smoke gases flowing out and the cold air flowing in can be determined as a function of the temperature difference, $\vartheta_g - \vartheta_o$, and position of the neutral plane, by applying Bernoulli's equation, Kawagoe (1958), Thomas-Hinkley-Theoblad-Simms (1963), Ahlqvist-Thelandersson (1968), Magnusson-Thelandersson (1970, 1971). Using the condition that the difference between quantity of gas flowing in and flowing out is the same as the difference between the quantity of gas produced and consumed during the combustion, the position of the neutral plan can be calculated as a function of temperature and combustion rate.

In doing so it is assumed on one hand, that the same quantity of air is consumed as the quantity of smoke gas produced upon liberation of a certain quantity of energy, independent of the magnitude of the combustion rate; on the other hand, since the expression for I_L should be applicable during the whole fire process, the combustion rate should be able to vary from zero to a maximal value with respect to the actual opening factor. Knowing the position of the neutral plane, following expression is obtained for I_L:

$$I_L = Q \cdot c_p (\vartheta_g - \vartheta_o) \qquad (10)$$

where

Q = gas flow from the fire cell (kg/h)

c_p = specific heat of the smoke gases (MJ/kg $^{\circ}$C)

The gas flow Q is obtained from the expression

$$Q = \varphi \cdot A\sqrt{H} \qquad (11)$$

where φ is a proportionality factor which is approximately temperature-independent within the range prevalent during fire.

Equation (11) assumes that the vertical acceleration of the gases can be neglected which, in some cases is not correct, cf. Thomas-Heselden-Law (1967). When large window openings exist in a fire cell consideration should be paid to this vertical acceleration, which results in decreased pressure difference and horisontal gas velocity and thus a lower gas flow than that indicated by Equation (11). If this fact is not taken into consideration during a theoretical analysis of the experimental tests, it could, in some cases, become impossible to obtain agreement between the calculated and the measured gas temperature-time curve since according to the computation procedure, too much energy disappears through the openings without any effect on the fire process. In the literature, Thomas-Heselden-Law (1967), it is stated that in unfavourable cases, the gas flow can be reduced to 1/4 of that obtained when vertical acceleration is neglected.

The above mentioned conditions can be taken into consideration through modifying the Equation (11) by a multiplication factor $C \leq 1$, that is

$$Q_a = C \cdot \varphi \cdot A\sqrt{H} \qquad (12)$$

As an illustration to how two different C-values influence a theoretical evaluation of the gas temperature-time curve of a fire process, curves evaluated by Magnusson-Thelandersson and obtained partly for $C = 1$ and partly for $C = 0.8$, under otherwise constant conditions, are shown in FIG. 3. Since both curves are evaluated for a genuine full-scale test, Ehm-Arnault (1969), the experimentally registered gas temperature-time curves have also been inserted which, in this case, show that the higher C-values render too low temperatures.

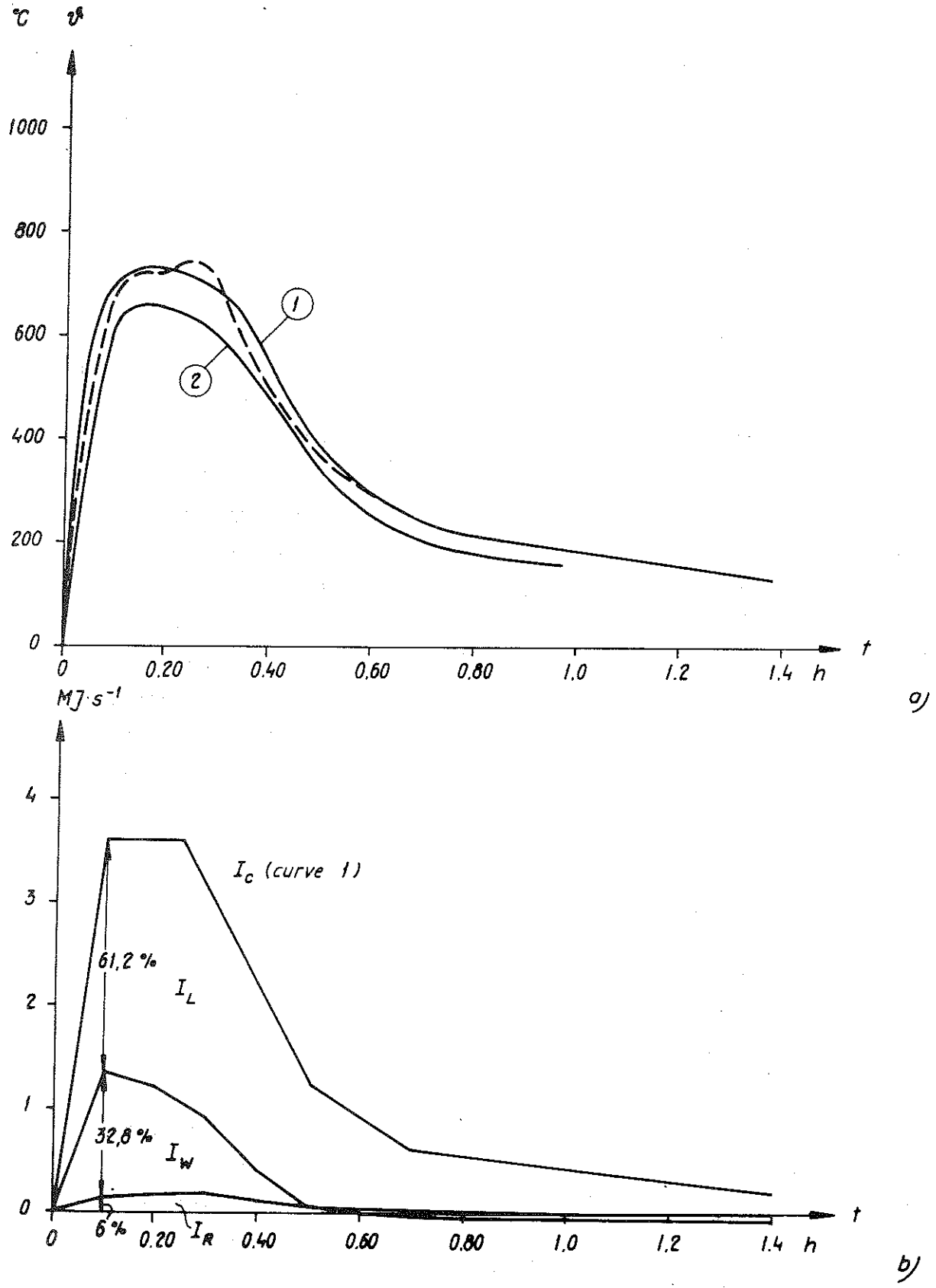

FIG. 3 The experimentally measured (------) and theoretically calculated gas temperature-time curves for a full-scale test where curve (1) has been determined for $Q = 0.8\varphi A\sqrt{H}$ kg/s and curve (2) for $Q = \varphi A\sqrt{H}$ kg/s. Opening factor $A\sqrt{H}/A_t = 0.091$ m^2. Fire load q = 90 MJ/square meter enclosing surface. Figure b) indicates the time variations of the terms I_C, I_L, I_W and I_R.

Based on theoretical analysis of some fifty full-scale tests performed independently at different places Magnusson and Thelandersson have come to the conclusion that a reduction of the gas flow ($C < 1$) can only be realized at so high values for the window openings that the opening factor $A\sqrt{H}/A_t$ becomes greater than 0.06 $m^{1/2}$, and that even with large openings the factor C only exceptionally falls below the value 0.7 to 0.8.

As mentioned above, the term I_C which indicates the liberated energy per unit time, can normally be given with satisfactory precision for liquid fuel. For wooden combustibles, on the other hand, it is somewhat difficult to indicate this variation satisfactorily, since for this type of fuel the combustion simultaneously takes place both in the solid constituents and in the gases formed during pyrolysis in such a way that it has hitherto been impossible to clarify.

For the term I_C, Kawagoe-Sekine and Ödeen use the following relation

$$I_C = R \cdot W \tag{13}$$

where

R = the combustion rate (kg/h)
W = the heat value (MJ/kg)

In the case when the combustion is limited by the access of air, which is true for the flaming phase for fires governed by ventilation, Kawagoe (1958) has given the following approximate relation for the combustion rate for fire loadings of wood fuel type:

$$R = k \cdot A\sqrt{H} \quad \text{(kg wood/min)} \tag{14}$$

where k in the normal case has the order of magnitude of 5.5 ($kg/m^{5/2} \cdot min$).

In Kawagoe-Sekine's works (1963) the liberated heat quantity per unit time for wood fuel was assumed to be 10.78 MJ per kg wood during the flaming phase implying a reduction in the nominal heat value of the wood which amounts to 17.5 - 18.9 MJ per kg wood at a complete combustion.

Since Equation (14) is only applicable in cases where the combustion rate is limited by access of air, the problem should be solved in a different manner when the fire process is governed by other factors, e.g., during the cooling phase.

In order to find a temporary approximate solution to the problem, Magnusson and Thelandersson (1970, 1971) have chosen the following analytical technique. Based on the results described in the literature obtained in such model and full scale tests which have been reported with satisfactory precision, they assume a reasonable energy-time curve I_C for each particular test, whereafter the gas temperature-time curve of the fire process is calculated. A necessary condition for such an attempt is that the total energy liberated during the fire process should be equal to the energy available in the beginning of fire, that is, the following relation should be satisfied:

$$\int_0^\infty I_C dt = M \cdot W \qquad (15)$$

where

M = the total fire load (kg)
W = the nominal heat value (MJ/kg)
t = time coordinate

The calculated gas temperature-time curve is compared with that measured in the test whereupon the energy distribution assumed for the fire process is modified if necessary, until agreement is reached between the calculated and experimentally obtained temperature curves.

In the analysis it was assumed that the maximum heat energy liberated during ventilation-controlled fires has the maximum value given by Equation (14). After analysis of some fifty tests, the results could be systematised and generalized so that polygon-shaped energy-time curves as in FIG. 3b were obtained, one for each combination of opening factor - fire load. The results are summarized in FIG. 4, which gives the possibility to determine the distribution of the heat quantity during the entire fire process with a precision which is sufficient in most practical cases. As shown in

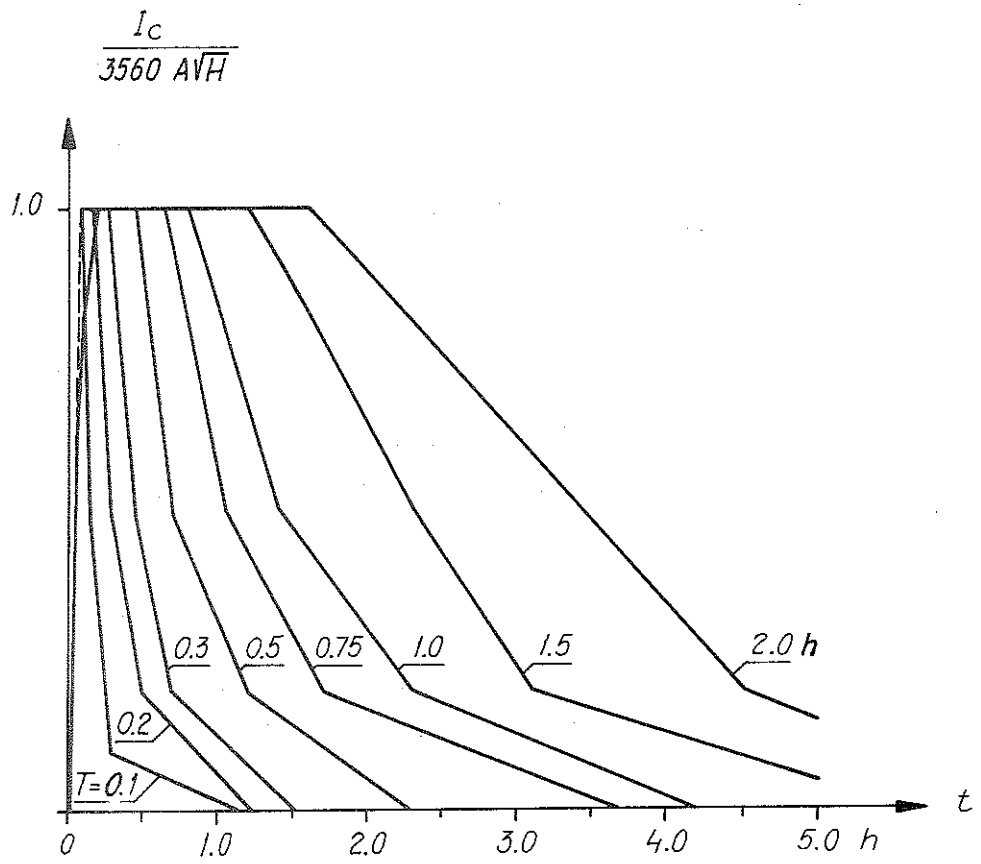

FIG. 4 Time graphs of the energy released per unit time in the process of combustion, I_C, expressed in a relative dimensionless form by putting $3560\ A\sqrt{H}$ equal to unity. The eight curves shown in this figure correspond to different values of the duration of the fire defined as the duration of the flame phase by the expression $T = q\ A_t/6300\ A\sqrt{H}$ (h). The dash-line portion of the curve for the ignition phase belongs to the curves relating to the lowest four values of the duration of fire.

the figure the liberated energy is reported in a dimensionless form through division by the factor $330 \cdot A\sqrt{H} \cdot 10.78$ MJ$\cdot$m$^{5/2}$/h which according to the authors corresponds to the maximum energy liberated in a fire process which is limited by access of air.

At the time when the works by Magnusson and Thelandersson came into being the existing literature did not allow the possibility to consider, in a detailed manner, such influences on the fire process and energy-time curves as piling density of the fire loading and particle shape plus the size of the window opening. This circumstance leads to the fact that the theoretically calculated gas temperature-time according to Magnusson and Thelandersson's procedure, can, in certain cases, become considerably higher than that obtained at a corresponding real fire. It is true that the results obtained would be on the safe side, but it may also imply uneconomical solutions. It has further been shown, Heselden-Thomas-Law (1970), that the order of magnitude of the factor k in Equation (14) may in certain cases, with very small openings, amount to double as much as the normal value. If such a high value for the combustion rate implies a corresponding high value for the energy liberated per unit time, a theoretical treatment of the problem based on the curves described in FIG. 4 can give results not on the safe side.

By applying the program presented by Magnusson and Thelandersson, the present investigation aims at finding out if significant deviations from the energy-time curves given by the two authors are obtained in case more important influences on the fire process are taken into consideration, and if this is the case, then it is the aim to illustrate how large these deviations could become and when they should specially be observed.

2.2 Computer program.

In order to solve the system of Equations (4), a modified application of Runge-Kutta's method is used, see Fox (1962). In treating the system from time t to $t + \Delta t$, at which the computer itself chooses a predetermined suitable integration interval Δt, depending on the precision, computations are performed five times.

Each time the value of the gas temperature ϑ_g evaluated immediately at the previous time is used. Recapitulating the heat balance equation with the pertaining terms entering the equation, we can write:

$$I_C = I_L + I_W + I_R \qquad \text{(Equation (1))}$$

$$I_L = \varphi(\Delta\vartheta)\cdot c_p \cdot A\sqrt{H}(\vartheta_g - \vartheta_o) \qquad \text{(Equations (10) and (11))}$$

$$I_W = \sum_j I_{W,j} = \sum A_j \psi_{1,j}(\vartheta_g - \vartheta_{1,j}) \qquad \text{(Equation (9))}$$

$$I_R = A(E_g - E_o) \qquad \text{(Equation (2))}$$

from which the following expression is obtained for the smoke gas temperature:

$$\vartheta_g = \frac{I_C + \varphi(\Delta\vartheta)\cdot A\sqrt{H}\cdot\vartheta_o + \sum_j A_j\cdot\psi_{1,j}\cdot\vartheta_{1,j} - I_R}{\varphi(\Delta\vartheta)c_p\cdot A\sqrt{H} + \sum_j A_j\cdot\psi_{1,j}} \qquad (16)$$

The program worked out by Magnusson and Thelandersson can, through its form, be applied to a fire cell with the enclosing structures of at most three types where two should be assumed to be homogeneous while the third can be composed of at most three layers. The fact that most of the construction materials either through physical or chemical transformations, possess a specific heat which is discontinously dependent on the temperature, is considered in the program. This change in property motivates the use of the enthalpy of the material, instead of the temperature, as the independent variable when calculating the temperature field. As a complementary illustration, FIG. 5 shows a flow diagram which illustrates the calculation procedure used in determining the smoke gas temperature of a fire cell and which is used in the present theoretical study performed to find out the influence of different parameters on the energy distribution for fires taking place in a closed room with one window opening.

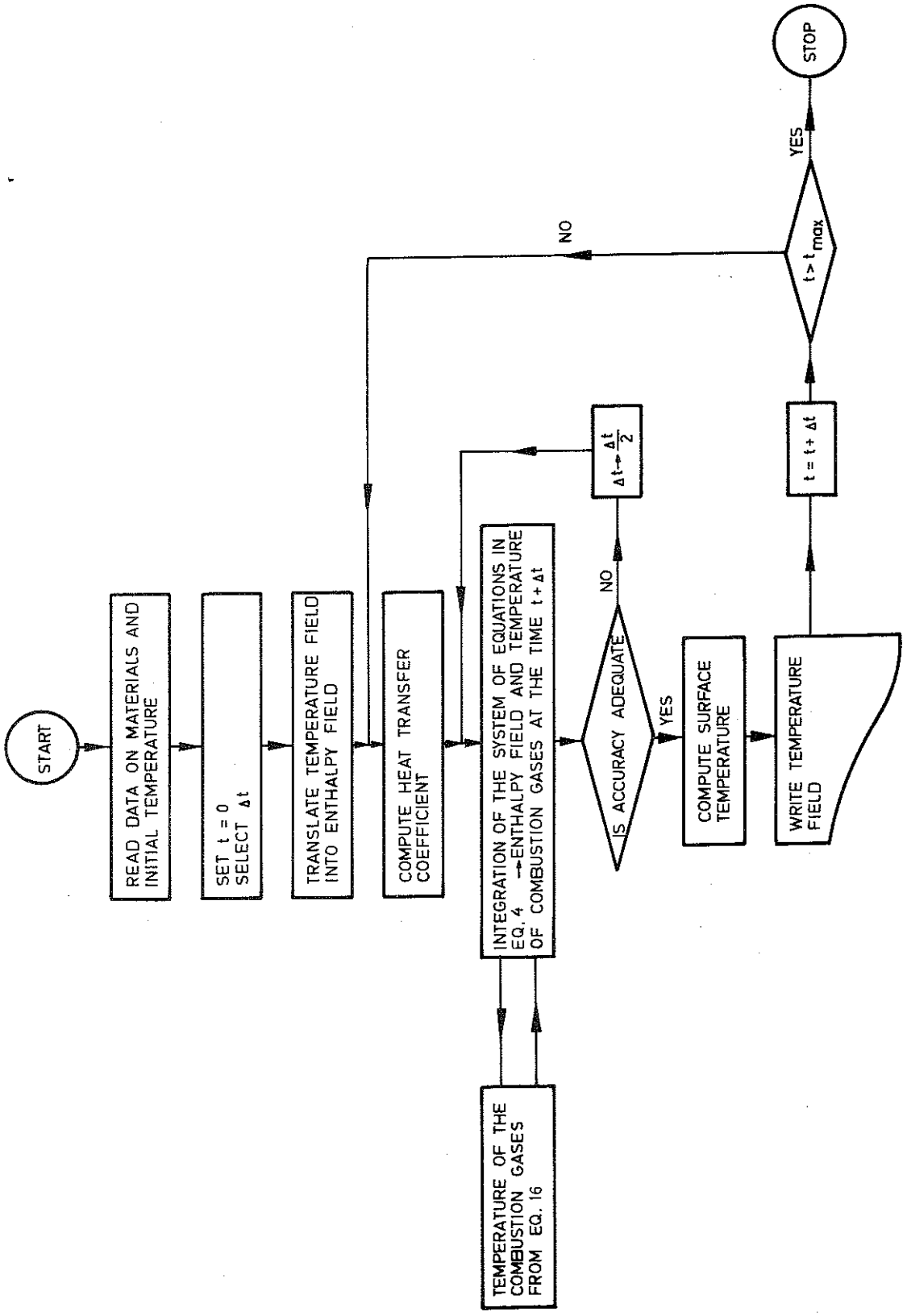

FIG. 5 Flow diagram which schematically shows the calculation procedure for determining the smoke gas temperature in a fire cell.

3. BRIEF DESCRIPTION OF THE ANALYSED TEST SERIES.

The present report deals with analysing the experimental studies of the fire process which, except for a few full-scale tests performed elsewhere and discussed in section 8, have been recovered from a test series performed by the author and co-workers in model scale with results which have been partially described in an earlier report by the author (1971) and Olsson-Sjöholm (1972) and which is partially under revision for a complete report later in some other connection. The test series was planned with the objective of finding out the influence of the essential factors on the time curve for the combustion rate, energy development and gas temperature. Choice of model scale tests is partly necessitated by the desire to perform the tests indoors for an improved precision and partly by the consideration that the quantity of fuel consumed in a large number of tests should be reasonable from an economical point of view. Three cubical, closed fire chambers at the model scale with one window opening and with the internal lateral dimensions measuring 500, 750 and 1000 mm respectively, were used in the tests. The main part of the test, on the occasion, were performed in the model fire chamber with the internal lateral dimensions of 750 mm and the fire processes analysed in this paper belong to the model scale test at this scale.

FIG. 6 shows a sketch and FIG.7 a photography of the fire chamber as viewed from the front side. The figures also show the form of the basket in which the fuel was piled, plus the system for determining the combustion rate expressed as the decrease in weight per unit time.

A side view of the fire cell is given in FIG. 8 from which the location of the radiation meter and connection cables for the thermocouples, used for temperature measurements in the fire cell, may also be observed.

Since in the investigation, a determination of the influence of the opening factor on the combustion rate and energy development, was one of the fundamental goals, the front of the fire cell was made exchangeable. The window opening of the fire cell was chosen in a square form and the dimensions given to this opening were

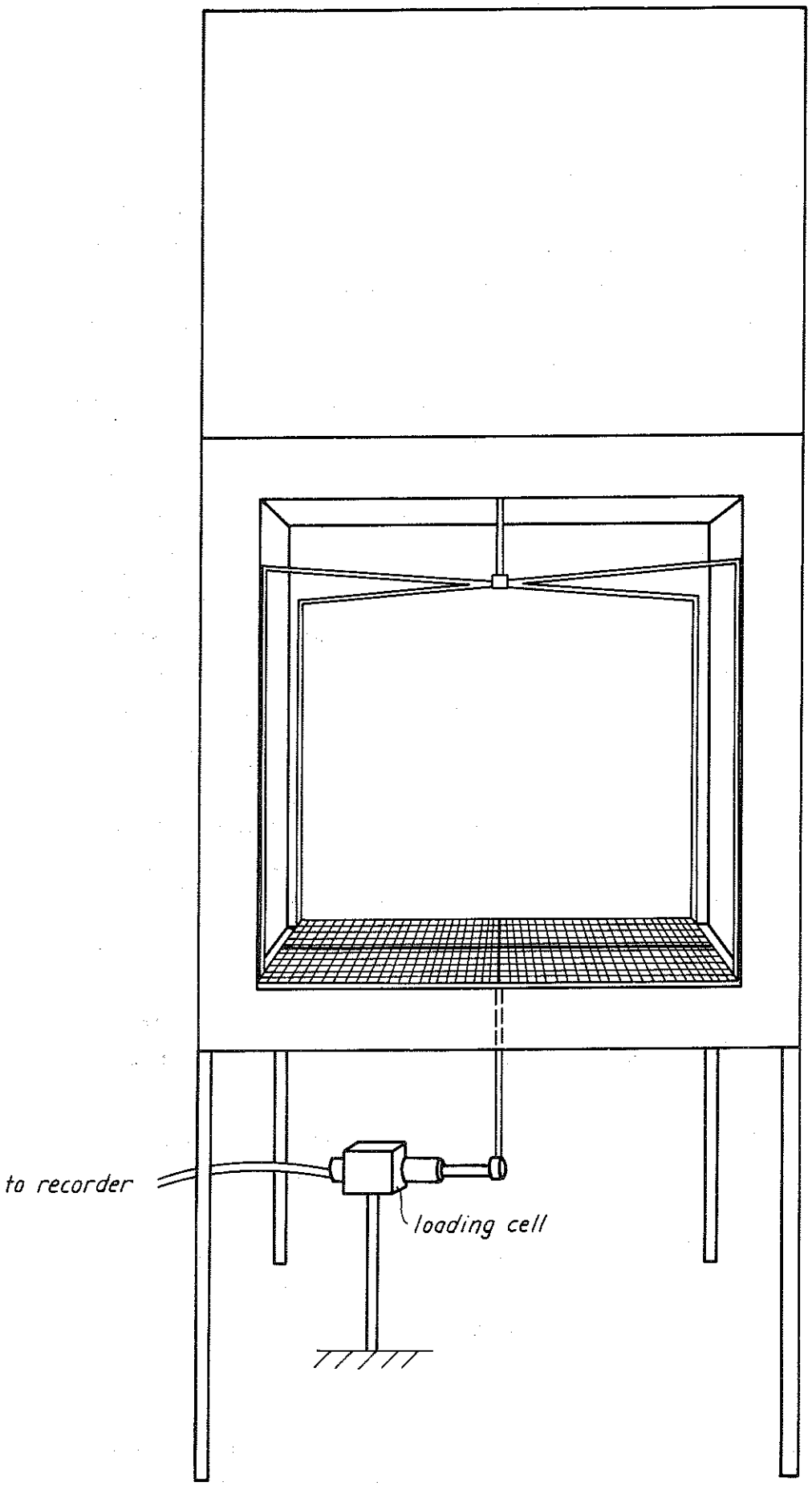

FIG. 6 The model fire chamber used during the investigation, as viewed from the front.

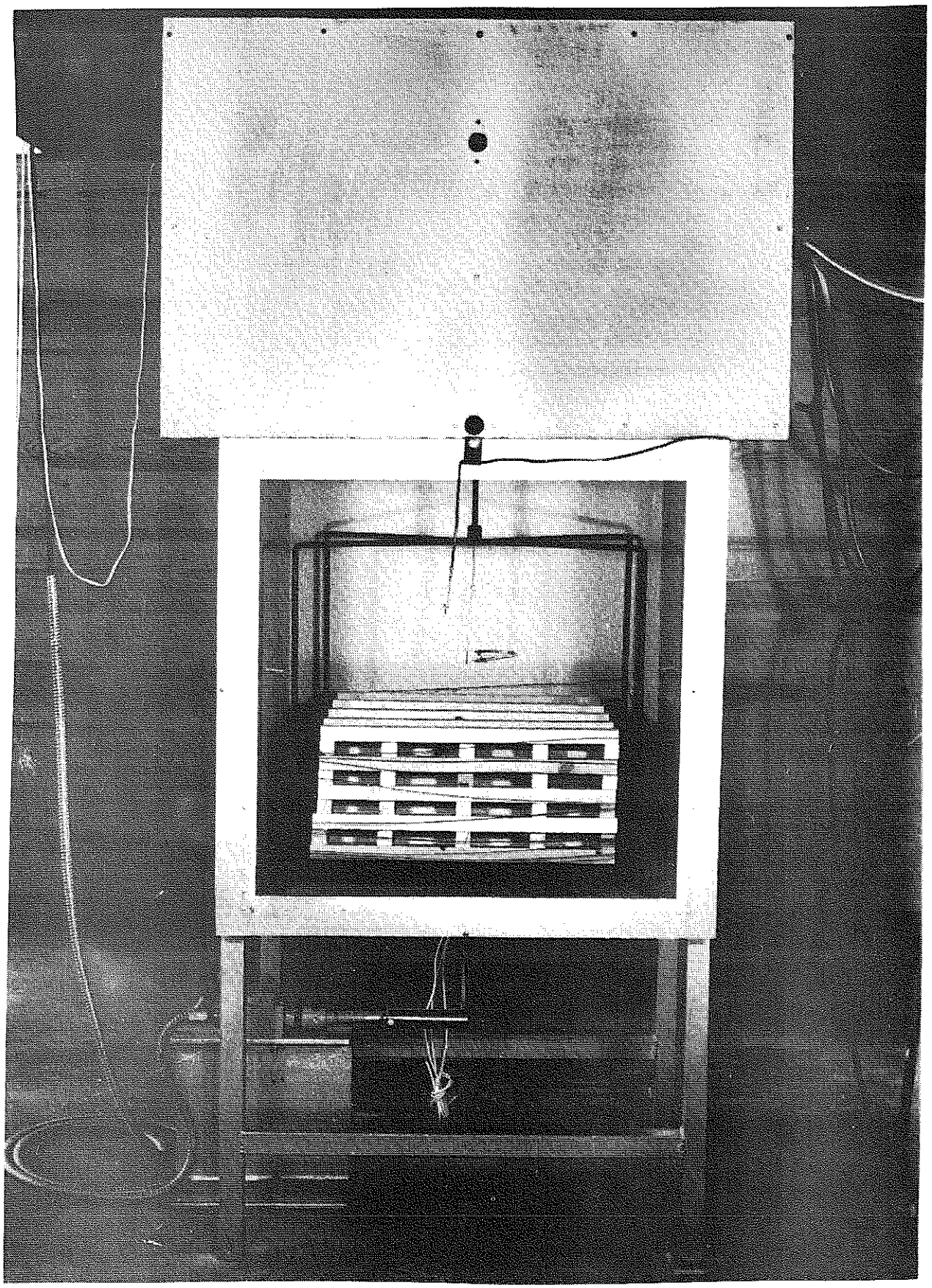

FIG 7 Photograph showing the model fire chamber.

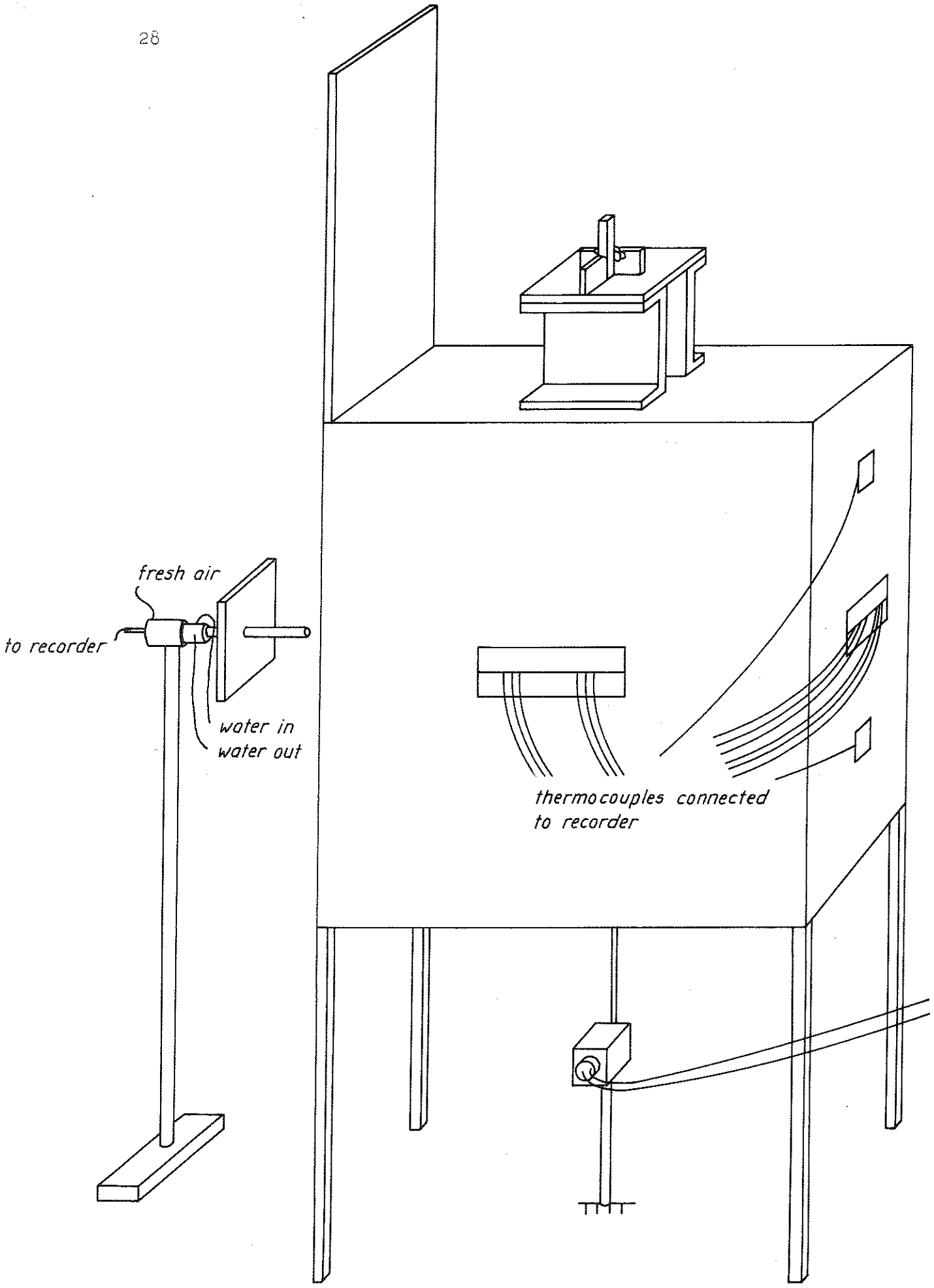

FIG. 8 Side view of the fire chamber including a part of the measuring system.

such that the five different values, namely, 0.020, 0.032, 0.040, 0.070 and 0.114 $m^{1/2}$ were obtained for the opening factor, which together cover a broad and realistic range of variation. The lateral dimensions corresponding to the different values of the opening factor were 340, 412, 449, 562 and 683 mm respectively.

Since the test series even embraces a study of the influence of different thermal properties of the enclosing structures of the fire chamber on the fire process, the following enclosing surfaces have been included in the test series, the materials counted from the external surface towards the internal surface are as follows:

a) 1.5 mm steel sheet (section 7)
b) 1.5 mm steel sheet + 10 mm asbestos disk having the density of 1020 kg/m^3 (sections 4-7)
c) 1.5 mm steel sheet + 125 mm light weight concrete with the density of 500 kg/m^3 (section 7).

A summary of the coefficients of thermal conductivity for asbestos disk, light weight concrete, and steel sheet as a function of temperature used in the analysis is given in TAB. 1.

During the tests the fuel consisting of sticks was piled in a basket, the dimension of which was somewhat less than the lateral internal dimension of the fire cell. The basket was horisontally braced without friction by a special arrangement, see FIG. 6-8. Thus, the risk for the basket or any stick to bump into a wall resulting in erroneous registration of the combustion rate was eliminated. The fuel basket rested on a loading cell connected to a line printer through which a determination of the combustion rate as the weight decrease of the fuel per unit time, in accordance with the developed practice, was made possible.

Since a detailed knowledge of gas temperature-time curve of the fire process at varying conditions is essential for a theoretical determination of the energy liberated per unit time corresponding to the weight decrease of the fire loading or of the fuel per unit time at each time during the fire process, an extensive survey of the gas temperature-time process obtained in the tests is a fundamental requirement. For temperature measurements unprotected

TAB. I The variation of coefficient of thermal conductivity with temperature for asbestos disk with a density of 1020 kg/m^3, light weight concrete with a density of 500 kg/m^3 and steel sheet.

Asbestos dish		Light weight concrete		Steel sheet	
T	λ	T	λ	T	λ
^{o}C	W/m^{o}C	^{o}C	W/m^{o}C	^{o}C	W/m^{o}C
216	0.155	0	0.100	0	81
549	0.134	385	0.150	100	73
673	0.116	525	0.189	300	54
881	0.110	700	0.206	500	44
1024	0.121	865	0.212	700	35
1500	0.116	1500	0.400	2000	29

thermocouples of Chromel-Alumel type manufactured by Honeywell were used, the types used being 9 B2 N2, 20 GA. The measuring points on which the analysis described in this paper are based, were located inside, 30 mm from the internal surface of the fire cell corresponding to the mid-section of the walls with no openings, and arranged in such a manner that the connection cable nearest the joint followed an isotherm. Besides the combustion rate and the gas temperature-time process, the changes in radiation as a function of time and the intensity of the smoke gas were also registered. These latter magnitudes have not been used in the analysis described in this paper. For a more detailed description of the measurement techniques used in the test series, the reader is referred to the author's report (1971).

Except for the tests reported in section 6 which embrace a study of the influence of varying stick thickness on the fire process, the fire loading consisted of firwood sticks with a square cross sectional area, 25 x 25 mm^2, due to the fact that the number of stick layers and number of sticks in each layer varied from test to test, the sticks had variable lengths but were adjusted in such a manner that the number of running meters of stick for each fire loading was constant (This is only partly applicable to the tests in section 6).

Prior to the tests the fuel was stored in an air conditioned room at a temperature of 20°C and the relative air humidity of 43% until equilibrium was reached with the surrounding air. The corresponding moisture ratio amounts to 9.3% calculated on the basis of the weight per unit volume.

In choosing the sticks it was attempted to make a varied selection so that the particularly resinous firwood was not used predominantly in the same test. In spite of such a selection, a relatively large variation in the density of the timber was obtained from test to test, cf. TAB. II, III, VI and VIII. In all the tests, the fire process was initiated by ignition of petrol or alcohol in a little bowl, centrally located under the basket containing the wood pile. The influence of the small variations in the characte-

ristics of the ignition liquid on the fire process is estimated to be negligible, since, in all the tests, this liquid had burnt out before any significant combustion had taken place in the wood pile.

All the tests were performed indoors in a large laboratory hall with a free ceiling height of about 10 meters, and thus the influence of disturbances and factors which were difficult to control, such as wind and climate variations, was eliminated. The smoke gases developed during the tests were ventilated away through a metal cover located over the fire cell and discharged into the open air through a specially designed metal channel.

FIG. 9 illustrates an outline of the test arrangement, showing the fire cell, measuring device for registration of the combustion rate and radiation, metal cover plus parts of the metal exhaust channel.

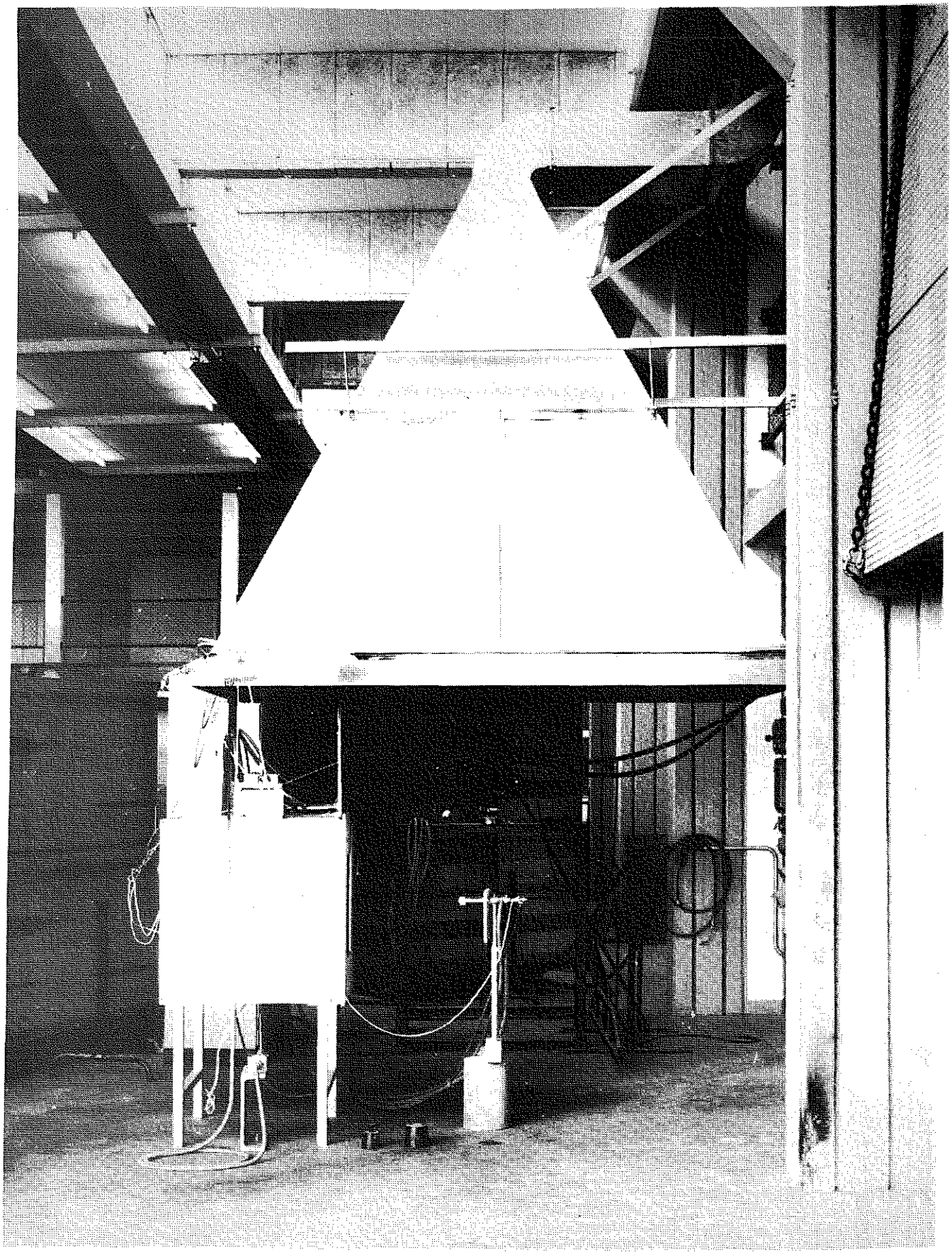

FIG 9 Survey of test arrangement and ventilation cowl.

4. POROSITY- AND OPENING FACTORS.

4.1 Definition of the porosity factor.

In order to characterize the piling density of a crib, namely porosity, Gross (1962) has introduced the porosity factor ϕ, defined through the relation

$$\phi = N^{0.5} \cdot b^{1.1} \cdot \frac{A_v}{A_s} \tag{17}$$

with

$$A_s = 2nb \left\{ 2NL + b \left[N-n(N-1) \right] \right\} \tag{18}$$

$$A_v = (L-nb)^2 \tag{19}$$

In the formula b denotes the thickness (square cross section) and L the length of each wooden stick, n the number of sticks per layer, N the number of layers of the wooden stick pile, A_s the area of all the sticks in the pile, initially exposed to the air and A_v the free horizontal area for vertical air flow through the pile, cf. FIG. 10.

The porosity factor has been originally introduced to characterize a crib for a fire taking place in the open air. As an illustration of the application of the factor in such a connection, FIG. 11 shows the flaming phase characteristics obtained by Gross (1962) through model scale tests, concerning the combustion rate of wood fuel for fire in the open air. The figure gives the relation, experimentally obtained, between the mean combustion rate R in % per sec. during the flaming phase, that is that part of the fire process in which the weight decrease of the fuel is approximately constant, and the porosity factor ϕ applied to a square crib with the lateral length of 10b. With respect to the model scale and the variations in wood sort, the combustion rate has been given under the modified form $FRb^{1.6}$, where F denotes the ratio of the coefficient of thermal conductivity of Oregon pine which has been used in the main part of the tests and that of the actual wood sort.

From the figure it is observed that three different stages can be distinguished, that is

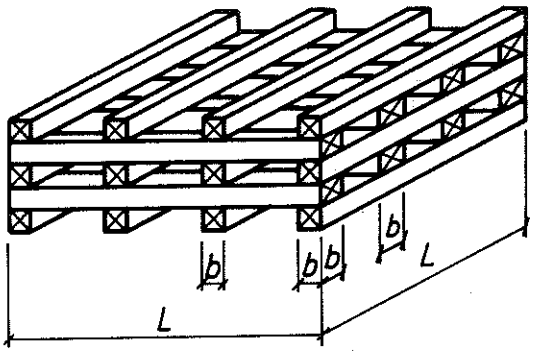

N layer
n sticks / layer
L the lenght of each wooden stick
b the thickness of each stick (square cross section)

FIG 10 Crib with some relevant descriptions.

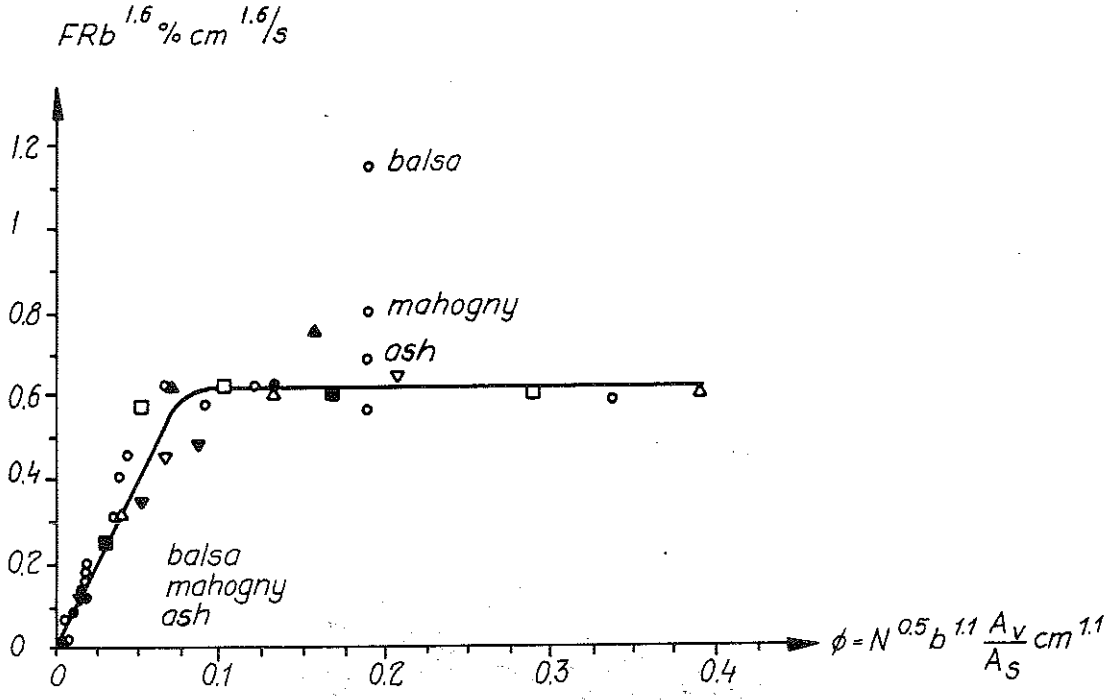

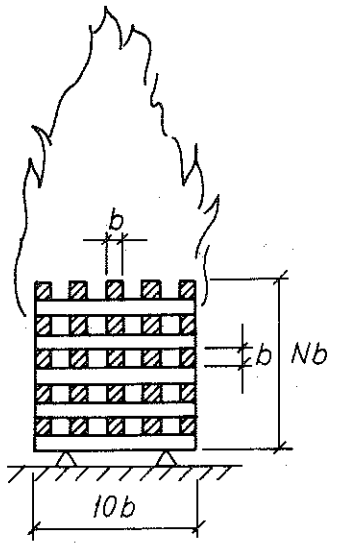

	b cm	n	N	
○	0.16	3, 5, 7	10	
○	0.32	3, 5, 7	10	
○	0.64	3, 5, 7	10	
○	1.27	3, 5, 7	10	
□	1.90	3, 5, 7	10	
○	1.90	3, 5, 7	7	
○	1.90	3*, 5, 7	5	
■	1.90	3*, 5, 7	3	
△	2.54	3, 5, 7	10	
▽	3.81	3*, 5, 7	10	
▲	9.15	7, 8	10	
▼	1.0	4, 5, 7	10	FOLK (1937)

No sustained burning

* No sustained burning

FIG. 11 Experimentally determined relationship between the scaled rate of burning $FRb^{1.6}$ and the porosity factor ϕ, characteristic of the pile of wood, for combustion in the open of a square pile of wood cribs.

a) an incomplete combustion with an approximately linear relation between the scale modified combustion rate and the porosity factor

b) a complete combustion, where the scale modified combustion rate is independent of the porosity factor, and

c) a non-continuing combustion at a porosity factor larger than about 0.4 $cm^{1.1}$, that is, with a very exposed crib.

Since the flaming stage characteristics shown in the figure have been obtained for the combustion in the open air, the properties of the crib (the exposed area of the sticks, chimney area of the pile, and the number of layers of sticks) have alone been determinative for the combustion rate during the whole fire process. This implies that the fire process can be classified as the type fuel bed controlled. For fire in a closed fire cell with window opening, the obtained characteristics would generally depend on both the properties of the crib and the size and form of the window opening which limits the air supply available for the combustion. Depending on which of these quantities are decisive for the fire process in each individual case, the process would be governed by either fuel bed or ventilation. At extremely large window openings the conditions for fire in a closed fire cell will approach those prevailing for fire in the open air with the differences which can be caused by the variations in the combustion air and smoke gas flow through the crib in both cases.

It should be emphasized that the porosity factor defined according to Equations (17) - (19) is strongly limited in its application, since the pile should have a regular shape according to FIG. 10. In cases where the regularity of the piling pattern is left out in such a manner that the chimney effect is noticeably affected, the fire process may possibly be influenced to a non-negligible extent. For regularly piled, square sticks, the porosity factor gives a uniquely defined crib which is essential both for decreasing the number of the influencing factors and making the reproducibility of the tests possible in a simple manner. That the piling density of a crib has a fundamental importance for the development of a fire process has already been established in a report described

by the author (1971). This relation will also be verified in the present report. The variations in piling density of the fire loading constitutes the main cause to the dispersion in results from similar tests described in an undifferentiated manner in the existing literature.

The magnitude ϕ is included in Equation (17) with the dimension length$^{1.1}$. Of course a modified dimensionless form is to prefer since it would give a simpler interpretation between different model scales and the full scale. A dimensionless description of the porosity of a crib would also facilitate a future coupling of a conventional, genuine fire loading to the porosity. By conventional fire loading it is here ment that which exists in the more usual types of buildings and localities. This varies to a high degree between different types of localities and even from one time to another. The last mentioned relation can be illustrated by the furniture which is normally found in the usual apartments and which consisted mainly of wood for some decades ago but which, to a large extent, has been replaced by plastics of different types. From the results described by Gross and shown in FIG. 11, attempts have been made to transform ϕ to a modified dimensionless form with maintained principal feature for the given R-ϕ curve. However, these attempts have not been successful why the definition of porosity factor given by Gross has been preserved.

4.2 Analysis of the experimental results with respect to the influence of the porosity factor and the opening factor.

In order to study the combined influence of porosity and opening factors, at otherwise constant conditions, on the energy-time curve during the combustion, the calculation procedure given by Magnusson and Thelandersson (1970, 1971) as briefly discussed in section 2 has been applied to a number of fire tests performed at model scale and described in an earlier report published by the author (1971). The selected values for the size of the opening factor has been $A\sqrt{H}/A_t$ = 0.020, 0.032, 0.040, 0.070 and 0.114 $m^{1/2}$. The

selected range of variation for the opening factor embraces most of the actual cases in practice and contains fire processes controlled both by fuel bed and ventilation. Five values for the porosity factor have been experimentally studied namely $\phi \approx 0.1$ cm$^{1.1}$ implying a densely packed crib, $\phi \approx 0.25$, 0.50 and 0.70 cm$^{1.1}$ corresponding to representative values in the middle of the range plus $\phi \approx 1.0$ cm$^{1.1}$ corresponding to a rather open crib. The last mentioned value has been deemed to be interesting from the point of view of investigating if the corresponding open distance between the sticks is so large that the optimal spacing for maximum energy development has been exceeded or if the rather significant influence on the fire process, observed earlier, embraces only the mean combustion rate and gas temperature or whether it embraces even the energy development, see Nilsson (1971).

All the tests analysed in this section have been performed in a cubical model fire cell which starting from outside is composed of 1.5 mm steel plate and 10 mm asbestos disk with the internal lateral dimension of 750 mm and the presumed constant fire loading q which has been theoretically assumed to be 35.0 MJ per square meter of the enclosing surface.

The desired energy-time curve developed during the fire process for the treated tests have been obtained according to the same method which has been applied by Magnusson and Thelandersson, that is a reasonable I_C-time curve was set up with the condition that the total energy developed during the fire should be equal to the total energy of the fire loading, whereafter, based on the assumed energy distribution, the gas temperature-time curve was calculated. This curve was compared with the corresponding one obtained by experiment and if satisfactory agreement was not obtained, the I_C-curve and thus even the theoretically calculated gas temperature-time curve was modified until the corresponding gas temperature-time curves approximately coincided. As an illustration, FIG. 12 shows partly the gas temperature-time curves experimentally registered at two measuring points in the fire chamber, placed centrally throughout every wall side, 30 mm from the wall surface,

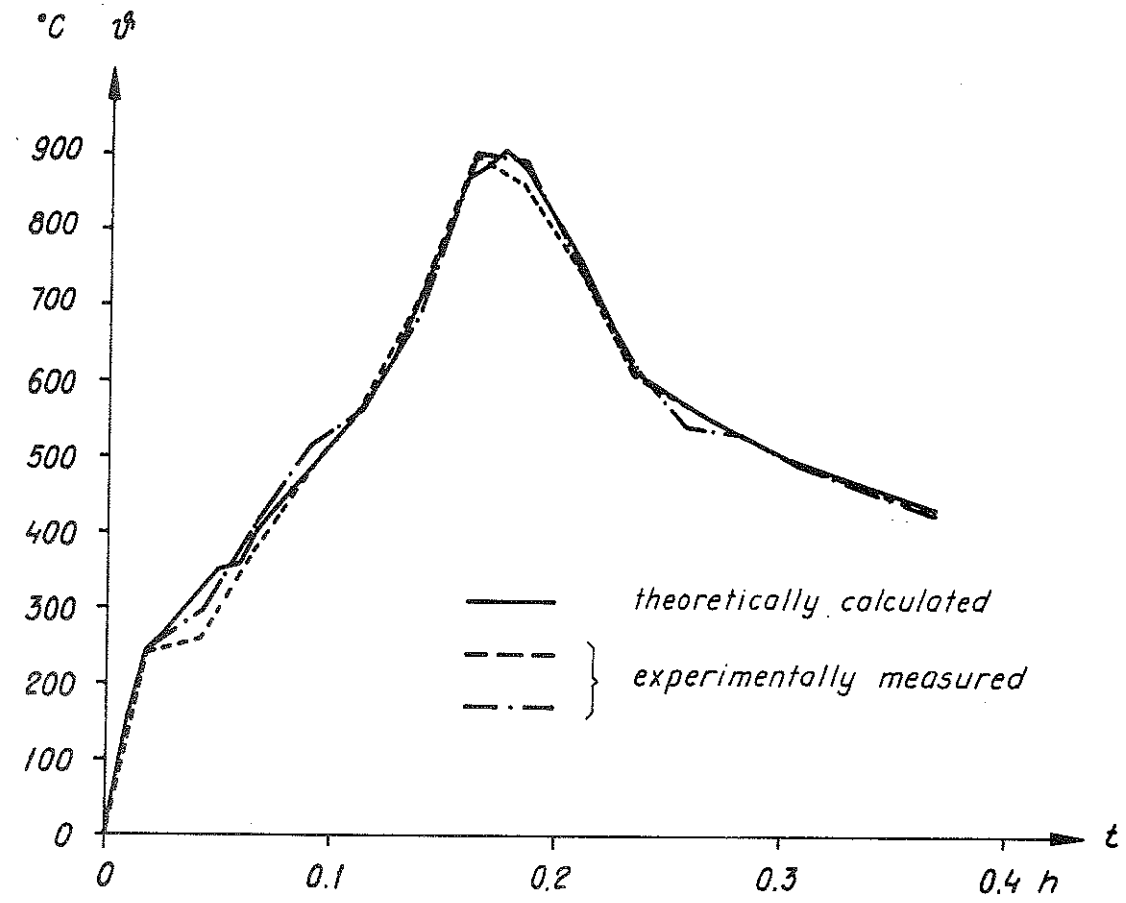

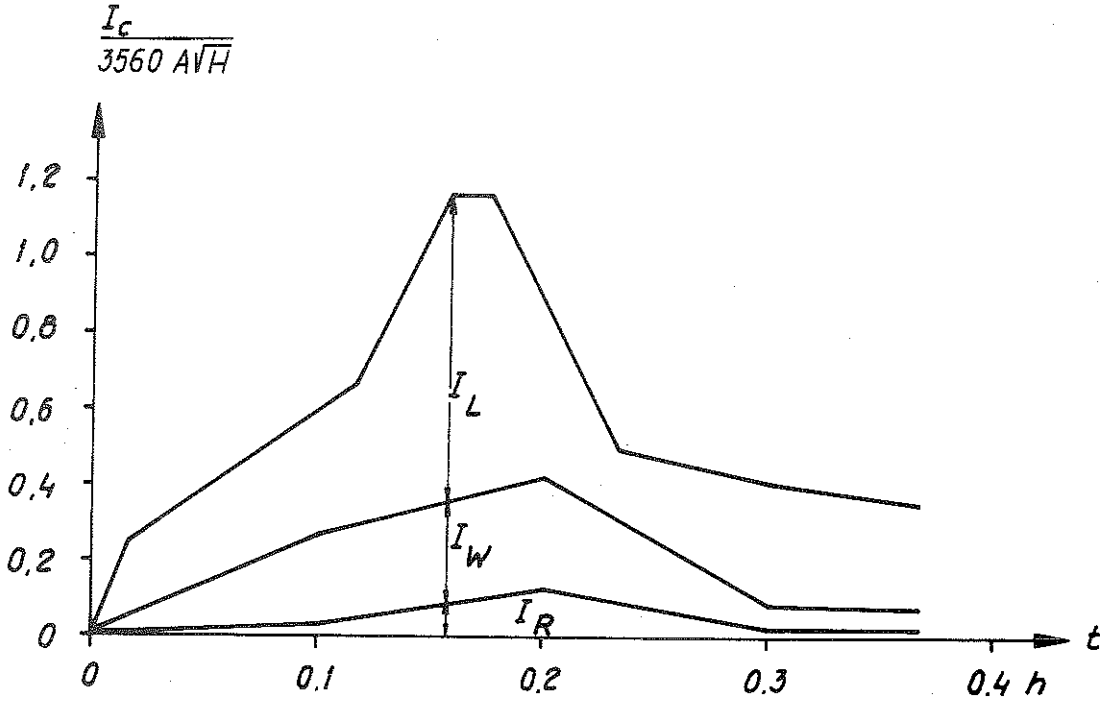

FIG. 12 Illustration of the temperature-time curves measured experimentally and those theoretically calculated and the assumed energy-time curve with the corresponding division of the energi into terms I_L, I_W and I_R.

which have been estimated to render representative values and partly, the theoretically computed gas temperature-time curve, the assumed energy-time curve and division of the energy into the terms I_W, I_L and I_R, that is the energy removed through the enclosing structures, convection and radiation respectively.

The energy-time relations theoretically calculated have been summarized in FIG. 13-17, where each figure gives difinite curves for one opening factor $A\sqrt{H}/A_t$ and five porosity factors ϕ. The energy illustrated along the vertical axis is expressed in dimensionless form by division with the factor $330 \cdot A\sqrt{H} \cdot 10.78 \approx 3560\ A\sqrt{H}$ MJ/h. Furthermore, Table II gives a summary of such brief characteristics for each individual test that a general picture is obtained. The table also gives primary values and other fundamental magnitudes used in the further discussion. The table gives

the opening factor $A\sqrt{H}/A_t$ ($m^{1/2}$);

the porosity factor ϕ ($cm^{1.1}$);

the theoretically assumed fire loading q (MJ per m^2 enclosing surface);

the real fire loading for the actual test (MJ per m^2 enclosing surface);

the ratio between gas flow Q_a, used in the calculations and the value which is given by equation (11), $Q = \varphi A\sqrt{H}$;

the mean combustion rate during the flaming phase, R, determined by Kawagoes formula (14) $R = 330\ A\sqrt{H}$ (kg wood per h);

the mean value of the combustion rate experimentally obtained during the flaming phase R_{80-30}, referred to the decrease in weight from 80% to 30% of the initial weight (kg wood per h);

the maximum value of I_{Cmax} indicating the energy liberated per unit time, determined from energy-time relations based on theoretical calculations given in FIG. 13-17;

the time interval t_m from ignition to the mean time at which the maximum value I_{Cmax} is reached (h), cf. FIG. 18;

the mean value of the energy liberated per unit time I_{Cm} during the time interval t_m defined as above, (MJ/h);

the time interval t_r from ignition to the time corresponding to the value 0.75 I_{Cmax} on the descending part of the energy-time curve (h), cf. FIG. 18;

the mean value of the energy liberated per unit time I_{Cr} during the time interval t_r defined as above, (MJ/h);

the mean value of the combustion rate R_r expressed as the decrease in weight of the fuel per unit time during the time interval t_r, (kg/h);

W_r, which gives the ratio between the mean value of the energy liberated per unit time, I_{Cr}, and the mean value of the combustion rate R_r, effectively expressing the heat value per kg of fuel during the time interval t_r, (MJ/kg);

the time interval t_d between the times corresponding to 0.75 I_{Cmax} on the asending and descending parts of the energy-time curve respectively, cf. FIG. 18;

the mean value of the energy liberated per unit time, I_{Cd}, during the time interval t_d, defined as above, (MJ/h);

the mean value of the combustion rate, R_d, expressed as the decrease in weight of the fuel per unit time during the time interval t_d, (kg/h);

W_d, which gives the ratio between the mean value of the energy liberated per unit time, I_{Cd}, and the mean value of the combustion rate R_d, effectively expressing the heat value per kg of fuel during the time interval t_d, (MJ/kg);

the time interval t_1 between the times corresponding to 0.75 I_{Cmax} and 0.5 I_{Cmax} respectively, on the descending part of the energy--time curve (h), cf. FIG. 18;

the time interval t_2 between the times corresponding to 0.75 I_{Cmax} and 0.25 I_{Cmax} respectively, on the descending part of the energy--time curve (h), cf. FIG. 18;

the time interval t_g which together with t_r defines the total fire duration, when energy is developed (h), cf. FIG. 18;

the mean value of the energy liberated per unit time I_{Cg} during the time interval t_g defined as above, (MJ/h);

the mean value of the combustion rate R_g, defined as the decrease in weight of the fuel per unit time during the time interval t_g, (kg/h);

W_g, which gives the ratio between the mean value of the energy liberated per unit time I_{Cg} and the mean value of the combustion rate R_g, effectively expressing the heat value per kg of fuel during the time interval t_g, (MJ/kg);

the mean value of the energy liberated per unit time I_{Cav} during the same period as for R_{80-30}, (MJ/h);

W_{av}, which gives the ratio between the mean value of the energy liberated per unit time, I_{Cav}, and the mean combustion rate, R_{80-30}, effectively expressing the heat value per kg of fuel during the active phase of the fire (MJ/kg);

the mean value of the gas temperature in the fire chamber ϑ_{80-30} during the flaming phase, referred to weight decrease of the fire loading from 80% to 30% of the initial weight, (°C);

the ratio between the mean combustion rate R_{80-30} and the mean temperature of the fire cell ϑ_{80-30}, (kg/°C·h);

the ratio between the mean value of the energy liberated per unit time during the flaming phase, I_{Cav}, and the mean temperature of the fire cell ϑ_{80-30}, (MJ/°C·h).

The magnitudes described in columns 8-24 of TAB. II, defined according to FIG. 18, are essentially new in the literature. They have been chosen to give a detailed description of the energy-time curve of the energy developed during the fire process. Since this curve is calculated based on the real gas temperature-time curve, the latter is reflected by the former. The characteristics shown in the table are intended to illustrate partly the more intensive phase of the fire process and partly the glowing- and cooling phases through some values which describe the energy development, some noticeably interesting periods of time and the corresponding heat values calculated. In order to facilitate the calculations, the I_C-t curve has been approximated by a polygon-shaped curve. However, the obtained differences are estimated to be practically negligible.

Even if, in most of the cases, the maximum value of the energy--time curve is reached during the flaming phase, conventionally defined as the time interval for R_{80-30}, this is not generally valid. This is illustrated in FIG. 19 in which for the tests C 40

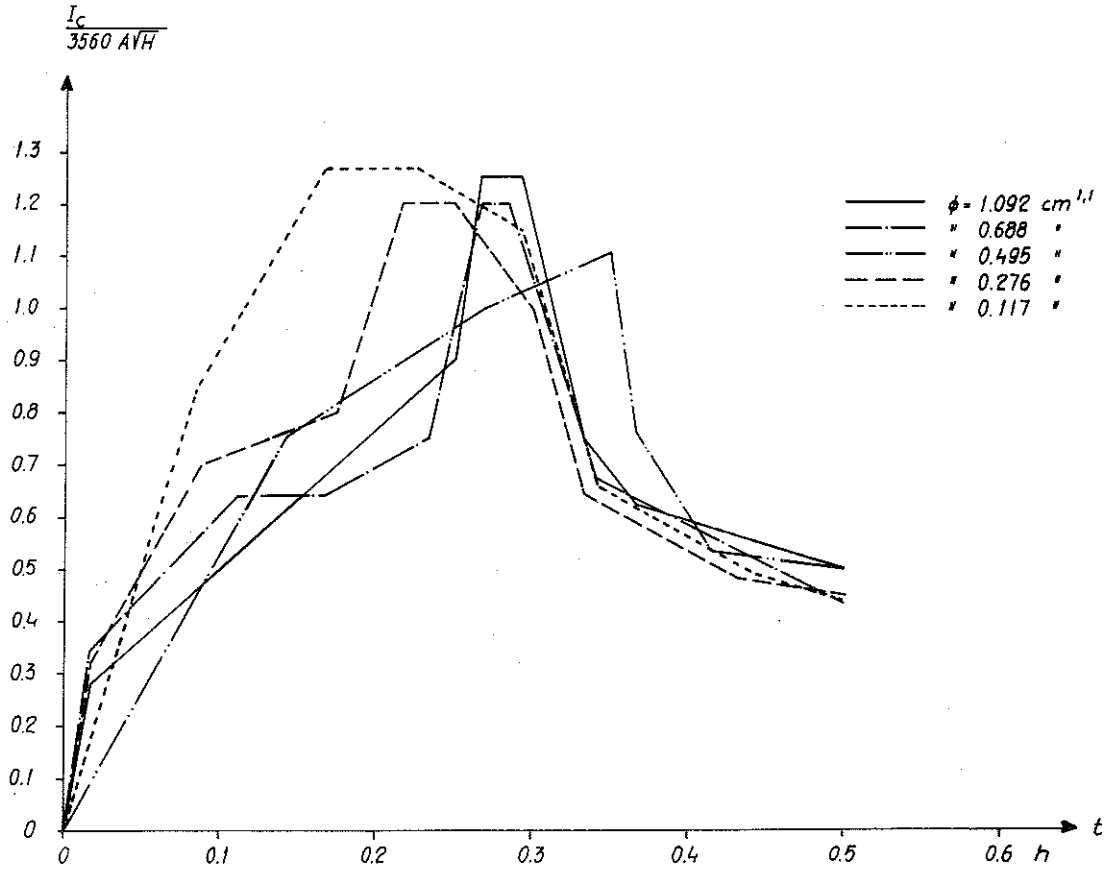

FIG 13 Theoretically calculated energy-time curve for the energy developed during the fire process for varying porosity factor, ϕ ($cm^{1.1}$). Opening factor $A\sqrt{H}/A_t$ = 0.020 $m^{1/2}$, fire load q = 35 MJ/square meter enclosing surface. The enclosing structures of the fire cell are composed of 10 mm asbestos disk having a density of 1020 kg/m^3 and 1.5 mm steel sheet.

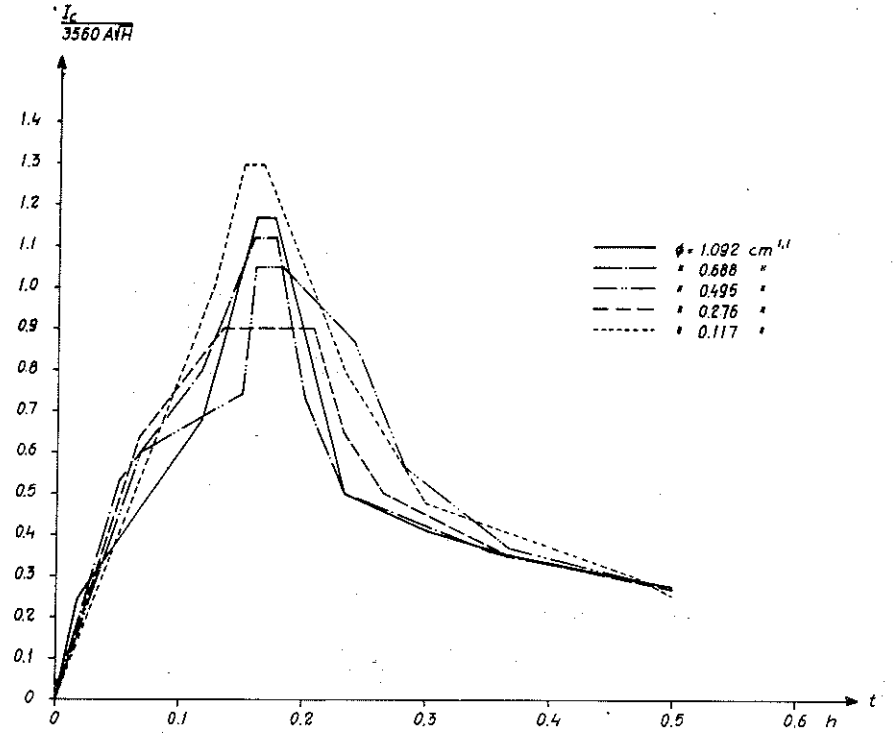

FIG 14 Theoretically calculated energy-time curve of the energy developed during the fire process for varying porosity factor ϕ ($cm^{1.1}$). Opening factor $A\sqrt{H}/A_t$ = 0.032 $m^{1/2}$, fire load q = 35 MJ/square meter enclosing surface. The enclosing structures of the fire cell are composed of 10 mm asbestos disk having a density of 1020 kg/m^3 and 1.5 mm steel sheet.

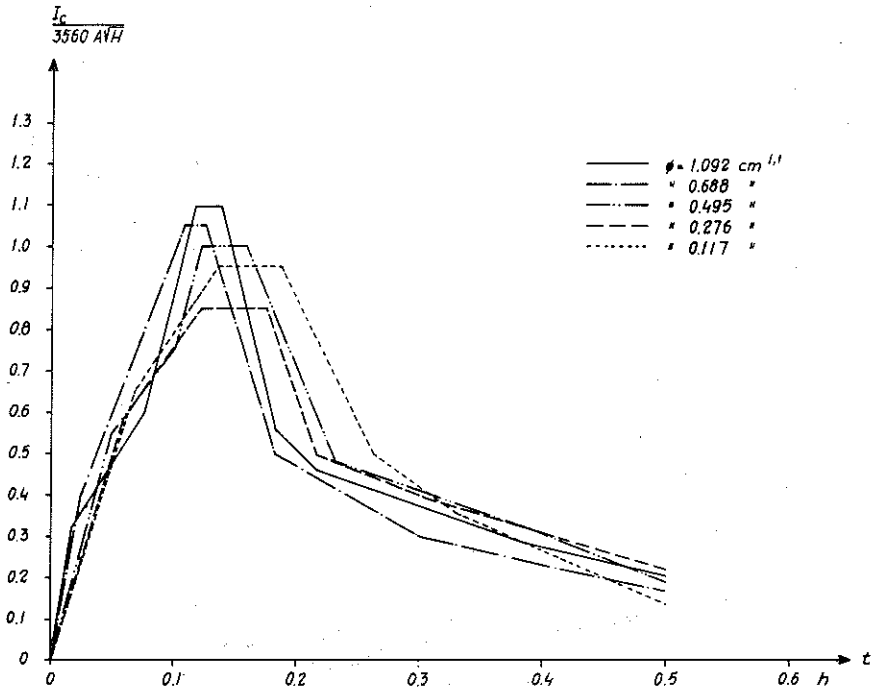

FIG 15 Theoretically calculated energy-time curve for energy developed during the fire process for varying porosity factor, ϕ ($cm^{1.1}$). Opening factor $A\sqrt{H}/A_t$ = 0.040 $m^{1/2}$, fire load q = 35 MJ/square meter enclosing surface. The enclosing structures of the fire cell are composed of 10 mm asbestos disk having a density of 1020 kg/m^3 and 1.5 mm steel sheet.

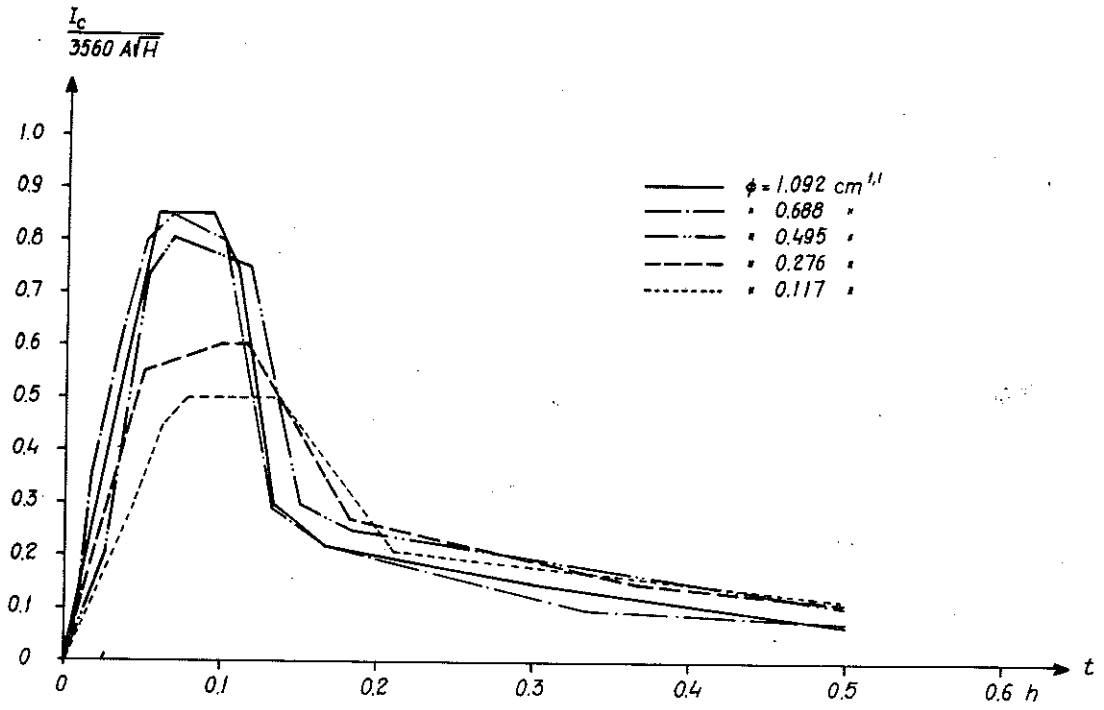

FIG 16 Theoretically calculated energy-time curve for energy developed during the fire process for varying porosity factor, ϕ (cm$^{1.1}$). Opening factor $A\sqrt{H}/A_t$ = 0.070 m$^{1/2}$, fire load q = 35 MJ/square meter enclosing surface. The enclosing structures of the fire cell are composed of 10 mm asbestos disk having a density of 1020 kg/m^3 and 1.5 mm steel sheet.

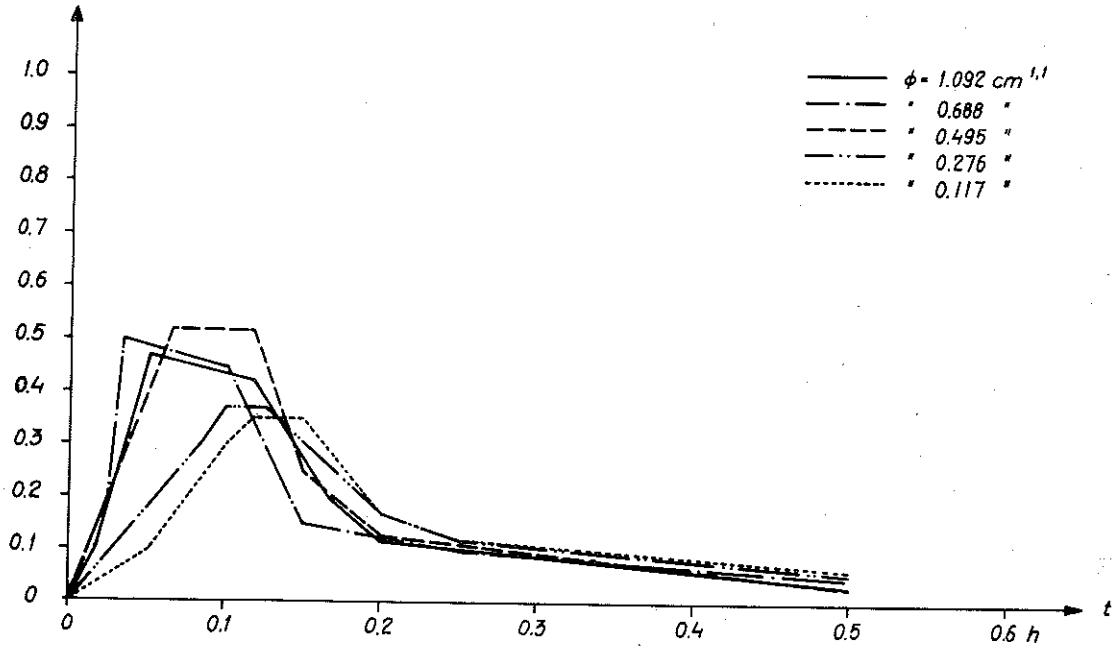

FIG 17 Theoretically calculated energy-time curve for energy developed during the fire process for varying porosity factor, ϕ (cm$^{1.1}$). Opening factor $A\sqrt{H}/A_t$ = 0.114 m$^{1/2}$, fire load q = 35 MJ/square meter enclosing surface. The enclosing structures of the fire cell are composed of 10 mm asbestos disk having a density of 1020 kg/m^3 and 1.5 mm steel sheet.

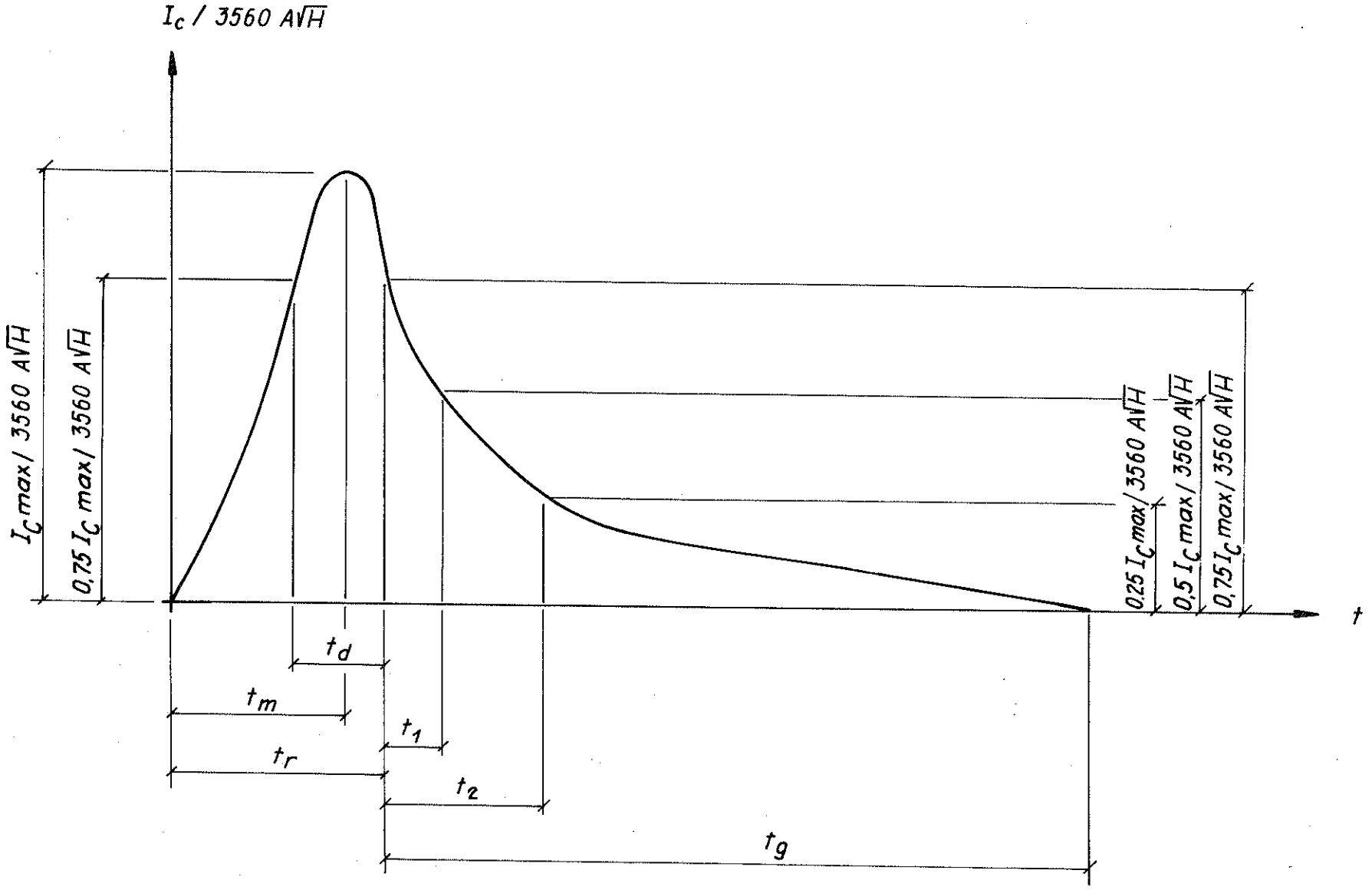

FIG 18 Definition of the parameters characterizing the energy-time curve.

TAB. II Characteristics and primary values with several magnitudes summarized for tests embracing a study of the influence of varying porosity- and opening factors on the fire process.

$\frac{A\sqrt{H}}{A_t}$	ϕ	q_{teor}	q	$\frac{Qa}{\varphi A\sqrt{H}}$	$R=330A\sqrt{H}$	R_{80-30}	I_{Cmax}	t_m	I_{Cm}	t_r	I_{Cr}	R_r	$W_r=\frac{I_{Cr}}{R_r}$	t_d	I_{Cd}
$m^{1/2}$	$cm^{1,1}$	MJ/m^2 o.y.	MJ/m^2 o.y.		kg/h	kg/h	MJ/h	h	MJ/h	h	MJ/h	kg/h	MJ/kg	h	MJ/h
(1)	(2)	(3)	(4)	(5)	(6)	(7)	(8)	(9)	(10)	(11)	(12)	(13)	(14)	(15)	(16)
0.020	0.117	35.0	37.0	1.0	22.3	26.5	305	0.196	196	0.312	230	19.00	12.1	0.207	283
0.020	0.276	35.0	36.4	1.0	22.3	25.1	288	0.233	170	0.309	193	19.42	10.0	0.120	265
0.020	0.495	35.0	35.3	1.0	22.3	27.1	252	0.309	159	0.365	178	16.02	11.1	0.203	240
0.020	0.688	35.0	35.3	1.0	22.3	26.2	288	0.276	152	0.316	166	18.39	9.0	0.072	260
0.020	1.092	35.0	37.0	1.0	22.3	26.9	300	0.279	149	0.317	165	19.00	8.7	0.065	281
0.032	0.117	35.0	37.0	1.0	35.6	28.6	499	0.159	248	0.210	297	22.39	13.2	0.087	449
0.032	0.276	35.0	36.9	1.0	35.6	38.6	346	0.171	238	0.230	261	26.48	9.9	0.151	324
0.032	0.495	35.0	37.3	1.0	35.6	37.1	403	0.171	216	0.253	265	24.85	10.7	0.101	370
0.032	0.688	35.0	37.2	1.0	35.6	47.0	430	0.166	245	0.194	267	30.99	8.6	0.072	389
0.032	1.092	35.0	36.5	1.0	35.6	45.9	449	0.167	220	0.200	251	29.15	8.6	0.065	413
0.040	0.117	35.0	37.1	1.0	44.6	27.1	456	0.163	301	0.229	336	23.94	14.0	0.154	418
0.040	0.276	35.0	37.8	1.0	44.6	41.7	408	0.148	275	0.200	303	29.88	10.2	0.128	379
0.040	0.495	35.0	37.5	1.0	44.6	43.5	480	0.140	285	0.193	327	30.57	10.7	0.093	453
0.040	0.688	35.0	34.8	1.0	44.6	51.6	504	0.117	306	0.152	340	35.99	9.5	0.077	455
0.040	1.092	35.0	38.0	1.0	44.6	51.2	528	0.127	289	0.160	330	37.38	8.8	0.066	485
0.070	0.117	35.0	37.4	0.8	77.9	42.7	420	0.104	282	0.165	323	34.30	9.4	0.114	398
0.070	0.276	35.0	39.0	0.8	77.9	54.2	504	0.108	368	0.147	391	41.10	9.5	0.106	470
0.070	0.495	35.0	40.5	0.8	77.9	66.0	673	0.067	340	0.128	481	48.75	9.9	0.084	631
0.070	0.688	35.0	37.4	0.8	77.9	67.3	715	0.067	451	0.110	538	53.13	10.1	0.074	665
0.070	1.092	35.0	35.1	0.8	77.9	61.6	715	0.075	444	0.114	524	48.00	10.9	0.071	675
0.114	0.117	35.0	35.5	0.7	127.0	40.4	479	0.134	245	0.175	292	29.98	9.7	0.085	443
0.114	0.276	35.0	35.7	0.7	127.0	47.0	506	0.112	277	0.159	331	42.16	7.9	0.082	462
0.114	0.495	35.0	37.9	0.7	127.0	59.3	712	0.092	453	0.133	523	42.97	12.2	0.083	676
0.114	0.688	35.0	36.2	0.7	127.0	60.9	657	0.060	424	0.115	515	48.76	10.6	0.086	631
0.114	1.092	35.0	35.2	0.7	127.0	56.0	616	0.077	404	0.135	476	40.02	11.9	0.097	586

R_d	$W_d = \frac{I_{Cd}}{R_d}$	t_1	t_2	t_g	I_{Cg}	R_g	$W_g = \frac{I_{Cg}}{R_g}$	I_{Cav}	W_{av}	ϑ_{80-30}	$\frac{R_{80-30}}{\vartheta_{80-30}}$	$\frac{I_{Cav}}{\vartheta_{80-30}}$	Försök nr
kg/h (17)	MJ/kg (18)	h (19)	h (20)	h (21)	MJ/h (22)	kg/h (23)	MJ/kg (24)	MJ/h (25)	MJ/kg (26)	°C (27)	kg/°C·h (28)	MJ/°C·h (29)	
23.02	12.3	0.045	0.323	0.679	76	1.73	44.0	295	11.16	836	0.032	0.35	C53
21.96	12.1	0.274	0.415	0.862	72	1.14	63.1	221	8.80	717	0.035	0.31	C51
22.17	10.8	0.066	0.422	0.740	72	1.25	57.6	218	8.05	724	0.037	0.30	C49
21.36	12.2	0.072	0.416	0.952	69	1.02	67.6	170	6.50	663	0.040	0.26	C47
14.45	19.4	0.049	0.309	0.927	77	1.16	66.4	173	6.43	660	0.041	0.26	C45
30.16	14.9	0.055	0.234	0.464	133	5.18	25.6	419	14.63	847	0.034	0.49	C42
32.90	9.9	0.070	0.243	0.713	89	1.40	63.5	326	8.46	740	0.052	0.44	C40
24.61	15.0	0.045	0.137	0.605	95	1.45	65.6	304	8.19	747	0.050	0.40	C38
34.86	11.2	0.031	0.296	0.784	93	1.44	64.5	315	6.70	689	0.068	0.46	C36
38.28	10.8	0.026	0.268	0.783	91	1.50	60.7	323	7.03	749	0.061	0.43	C34
25.92	16.1	0.047	0.196	0.378	125	4.36	28.6	418	15.40	775	0.035	0.54	C31
36.09	10.5	0.079	0.306	0.563	116	2.28	50.9	384	9.21	700	0.060	0.55	C29
39.49	11.5	0.037	0.251	0.474	131	2.73	48.0	427	9.82	732	0.059	0.58	C27
44.66	10.2	0.046	0.102	0.618	106	1.92	55.2	437	8.47	762	0.068	0.57	C25
40.71	11.9	0.026	0.244	0.631	118	2.10	56.2	398	7.78	716	0.071	0.55	C23
38.07	10.5	0.035	0.329	0.706	103	2.16	47.6	412	9.65	591	0.072	0.70	C20
48.90	9.6	0.030	0.220	0.597	122	2.42	50.4	489	9.00	659	0.082	0.74	C18
59.61	10.6	0.014	0.165	0.606	122	2.54	47.9	647	9.81	753	0.088	0.86	C16
56.91	11.7	0.014	0.067	0.860	76	1.54	49.3	673	9.99	752	0.089	0.89	C14
54.34	12.4	0.012	0.067	0.546	107	2.31	46.3	681	11.05	748	0.082	0.91	C12
37.20	11.9	0.024	0.241	0.688	99	2.28	43.4	424	10.49	448	0.090	0.94	C9
40.52	11.4	0.032	0.215	0.630	105	2.46	42.8	452	9.63	473	0.099	0.95	C5
52.31	12.9	0.016	0.067	0.464	120	3.36	35.7	698	11.77	641	0.092	1.09	C7
52.16	12.1	0.020	0.095	0.608	101	2.22	45.5	657	10.79	704	0.086	0.93	C3
48.69	12.0	0.026	0.091	0.482	111	2.80	39.6	634	11.01	590	0.095	1.07	C1

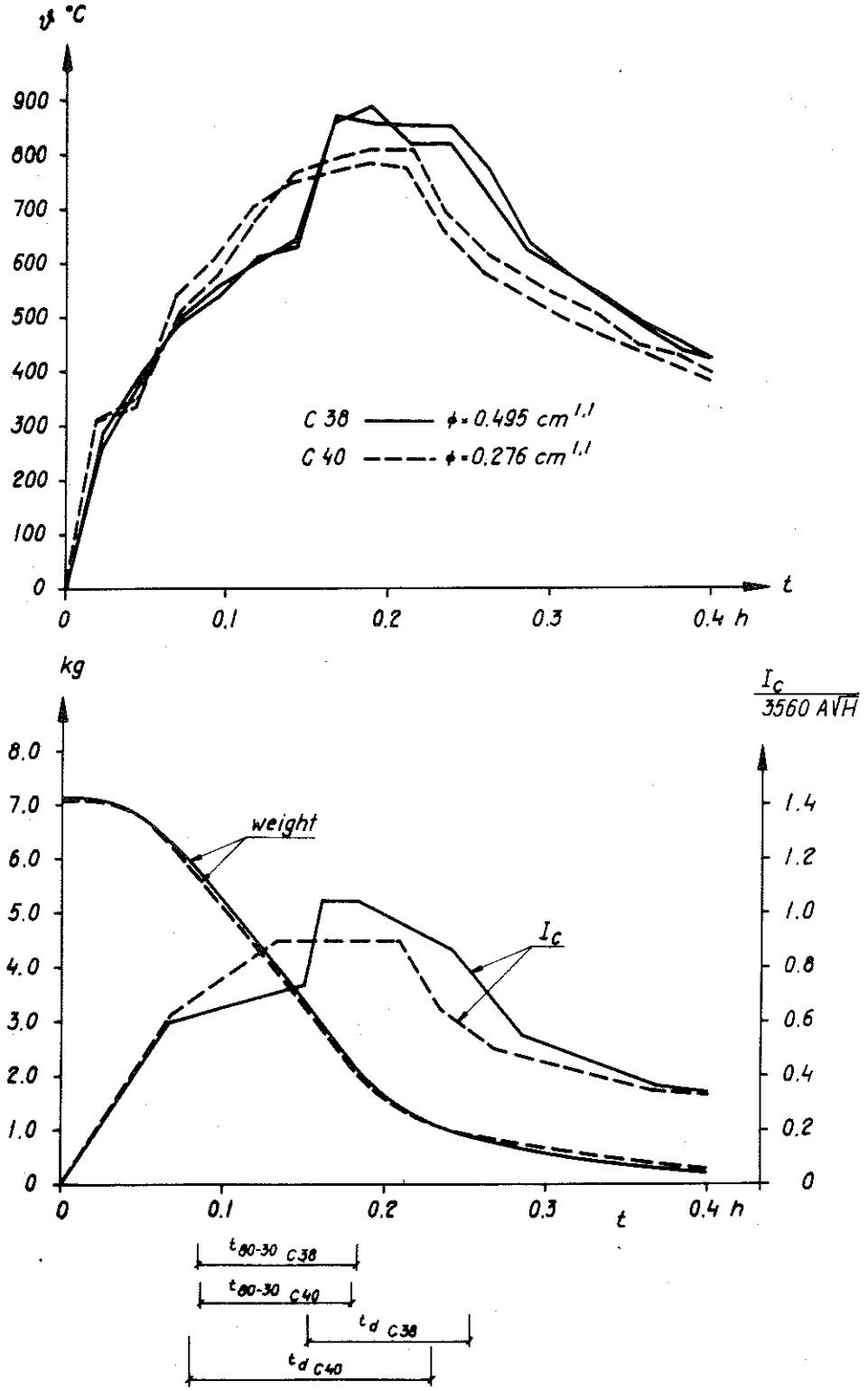

FIG. 19 Experimentally registered temperature-time curves and the curves showing the weight decrease as a function of time plus the theoretical calculated energy-time curves for the two tests C38 and C40. Opening factor $A\sqrt{H}/A_t$ = 0.032 $m^{1/2}$, fire load q = 35 MJ/square meter enclosing surface. Porosity factors ϕ = 0.276 for test nr C40 and 0.495 $cm^{1.1}$ for test nr C38.

and C 38 - opening factor $A\sqrt{H}/A_t$ = 0.032 $m^{1/2}$, porosity factor ϕ = = 0.276 and 0.495 $cm^{1.1}$ respectively - the recorded gas temperature--time curves, the experimentally registered time curves for the combustion rate expressed as the decrease in weight of the fuel per unit time, and the theoretically calculated energy-time curves are described. From the figure it is observed that the gas temperature--time curve and the curve showing the weight decrease exhibit poor agreement. The calculated energy-time curve is directly based on the real temperature-time curve, why this curve describes the fire process more adequately than the curve which shows the weight decrease. For this reason, in working out the results, emphasis has been placed on magnitudes which characterize the energy-time curve. However parallel discussions are even made concerning the more conventional magnitudes in order to partly give a general picture of the influence of different parameters on the fire process as far as possible and partly find such relations which make a theoretical, differentiated determination of the fire process and its gas temperature--time curve possible for each individual case in the future.

From TAB. II it is observed that with a constant value for the porosity factor the magnitudes I_{Cmax}, I_{Cm}, I_{Cr} and I_{Cd} increase with increasing opening factor up to $A\sqrt{H}/A_t \approx 0.07$ $m^{1/2}$ whereafter these magnitudes either remain approximately constant or somewhat decrease with further increase of the opening factor. This fact is even illustrated by FIG. 20-22 which, in a diagram form render the relations found between I_C-characteristics I_{Cm}, I_{Cr}, and I_{Cd} respectively and the porosity factor ϕ at different values for the opening factor $A\sqrt{H}/A_t$. The relation is uniquely substantiated for higher values of the porosity factor, $\phi > 0.7$ $cm^{1.1}$. For very small ϕ-values the relations found exhibit a high degree of irregularity. On the whole, the results described show that the growth of the I_C-magnitudes is asymptotical and not linear which would be the case if Kawagoes formula (14) were applicable without any restrictions. That this formula has a highly limited validity may be observed from FIG. 13-17 in which $I_{Cmax}/3560\ A\sqrt{H}$ strongly decrease with increasing opening factor. This relation can be illustrated by the values corresponding to the opening factors 0.020, 0.040 and 0.114 $m^{1/2}$ which posess the variation range of 1.25-1.1, 1.1--0.85 and 0.5-0.35 respectively. With respect to the fact that the

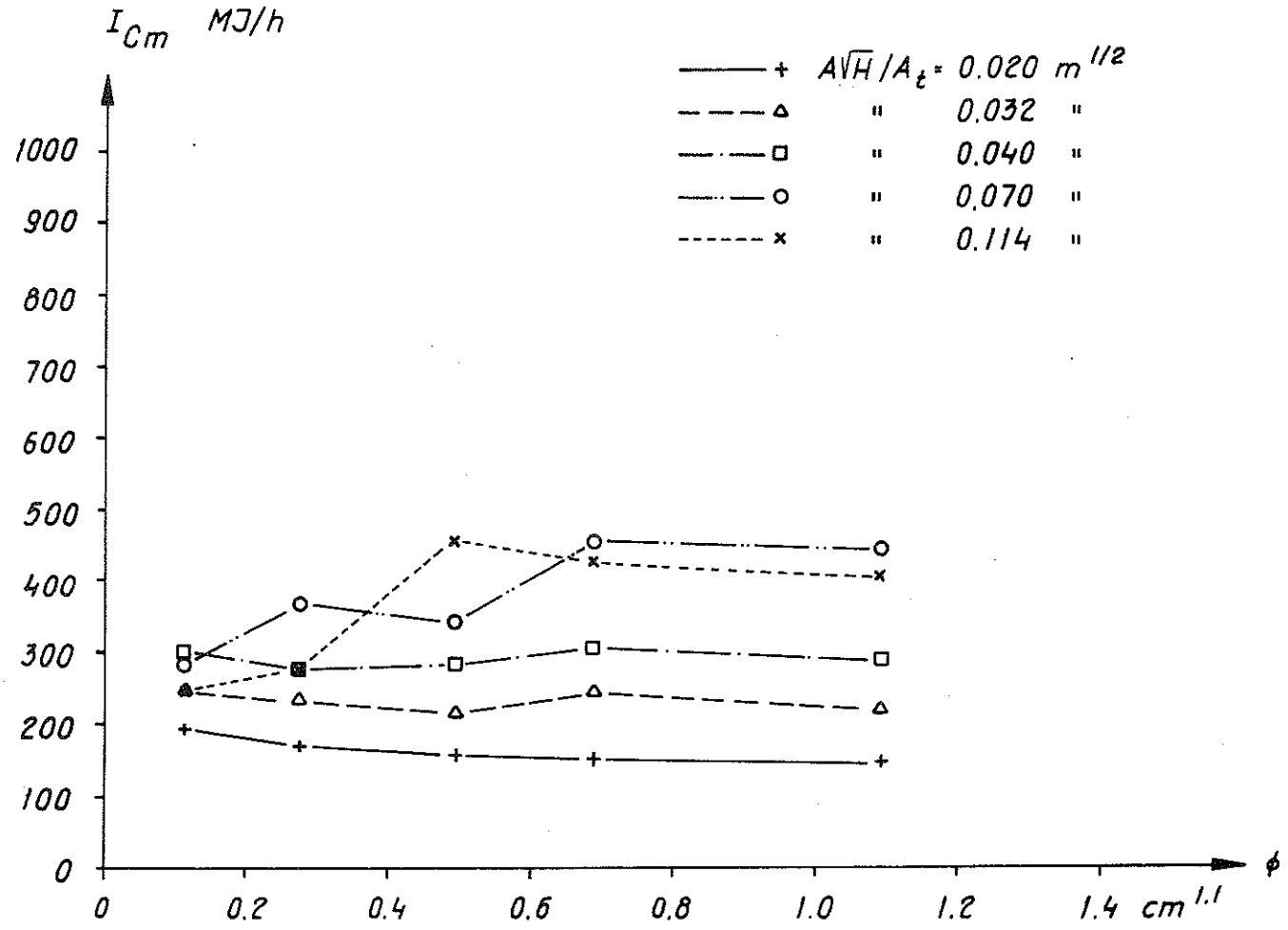

FIG. 20 By a theoretical analysis of the experimental results obtained relation between I_{Cm} (MJ/h) and the porosity factor, ϕ ($cm^{1.1}$), for varying opening factor, $A\sqrt{H}/A_t$ ($m^{1/2}$). Fire load 35 MJ/square meter enclosing surface. The enclosing structures of the fire cell are composed of 10 mm asbestos disk having a density of 1020 kg/m^3 and 1.5 mm steel sheet.

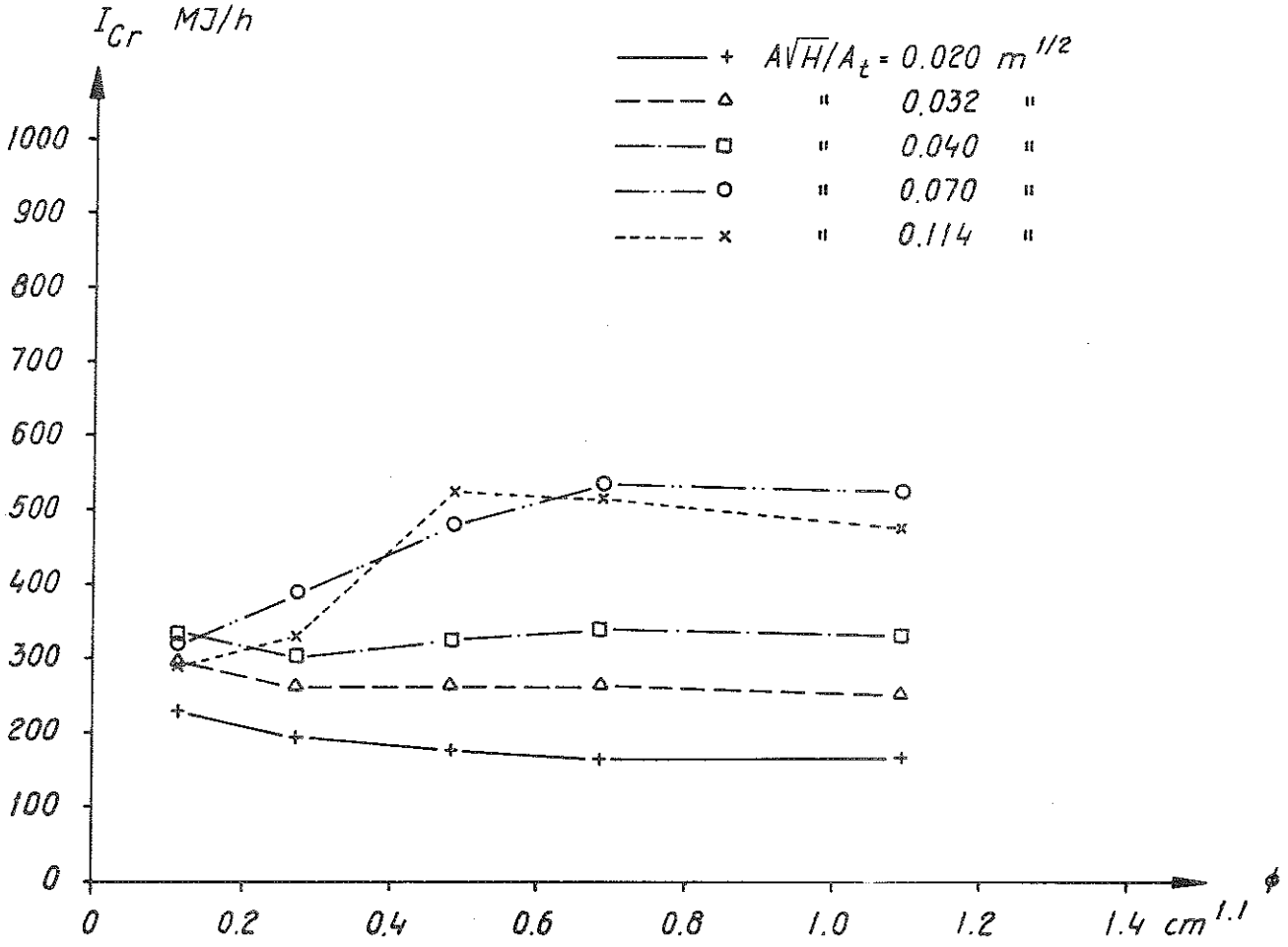

FIG. 21 By a theoretical analysis of the experimental results obtained relation between I_{Cr} (MJ/h) and the porosity factor, ϕ ($cm^{1.1}$), for varying opening factor, $A\sqrt{H}/A_t$ ($m^{1/2}$). Fire load 35 MJ/square meter enclosing surface. The enclosing structures of the fire cell are composed of 10 mm asbestos disk having a density of 1020 kg/m^3 and 1.5 mm steel sheet.

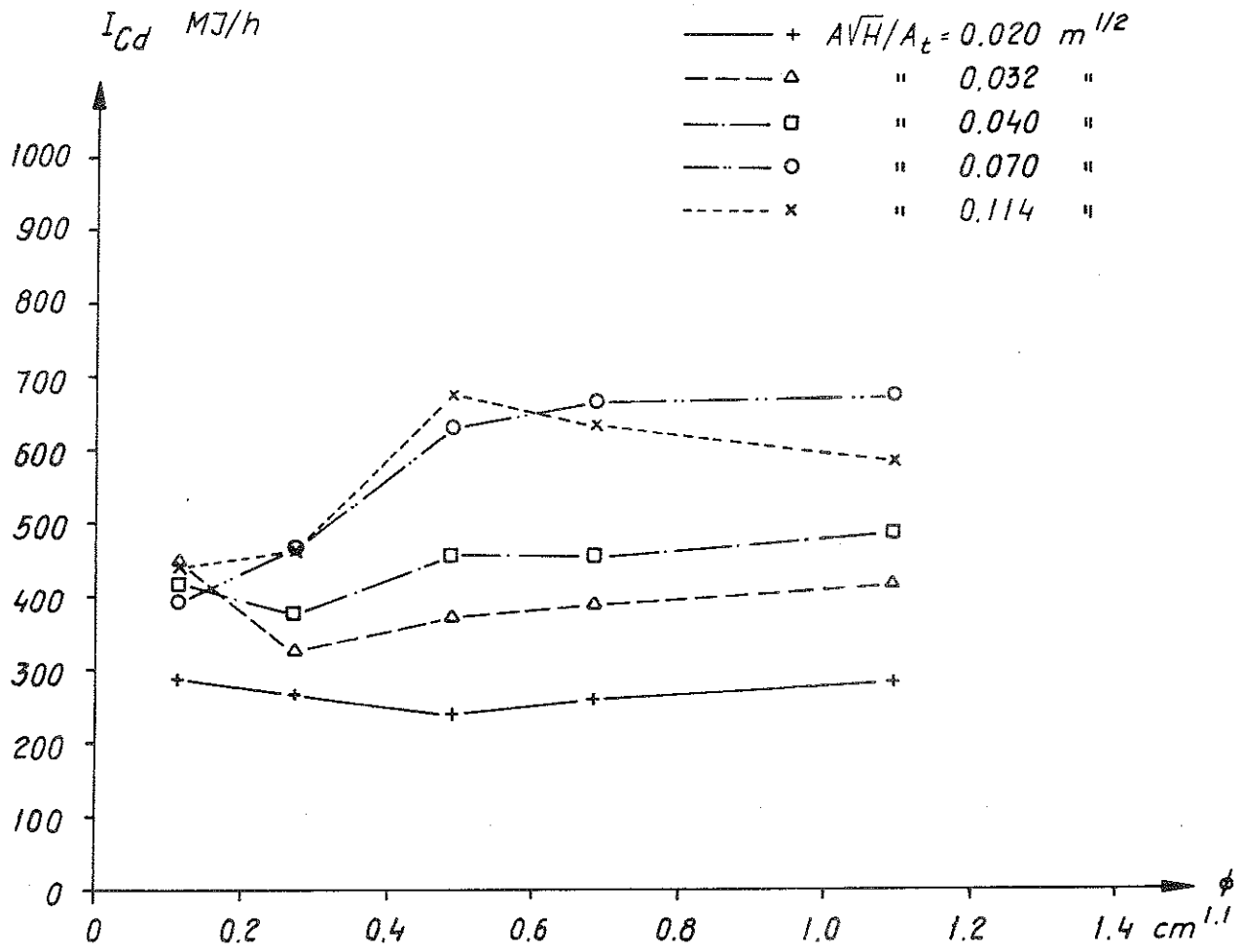

FIG. 22 By a theoretical analysis of the experimental results obtained relation between I_{Cd} (MJ/h) and the porosity factor, ϕ ($cm^{1.1}$), for varying opening factor, $A\sqrt{H}/A_t$ ($m^{1/2}$). Fire load 35 MJ/square meter enclosing surface. The enclosing structures of the fire cell are composed of 10 mm asbestos disk having a density of 1020 kg/m^3 and 1.5 mm steel sheet.

expression $R = k \cdot A\sqrt{H} \cdot 10.78$, with $k = 5.5$ kg/min·m$^{5/2}$ = 330 kg/h·m$^{5/2}$, is assumed to describe the maximum mean combustion rate during the active phase of the fire which is controlled by ventilation, the order of magnitude of the value 1.25 is remarkably high, specially considering the fact that I_{Cmax} has, in some cases, such a time protraction that the mean combustion rate is exceeded during the flaming phase implying an energy development which is higher than that maximally presumed. In determining the combustion rate R, according to the mentioned expression, it should be remembered that the value obtained is very rough since several influencing factors such as porosity of the fire loading, particle shape and location plus the thermal data for the enclosing structures of the fire cell are not considered. The fact that, at small opening factors, the combustion rate can exceed the value given by equation (14) above, that is $k > 5.5$ kg/min·m$^{5/2}$, is confirmed by experiences described in the literature. As an example see Heselden-Thomas-Law (1970), who in summarizing a large number of model and full scale tests, performed at different places, establish that for small window openings of the order of magnitude of 1/10 of the front side or less, the value of k can amount to 9 or 10 kg/min·m$^{5/2}$.

For large values of the opening factor, $A\sqrt{H}/A_t > 0.07$ m$^{1/2}$, the ratio $I_{Cmax}/3560\ A\sqrt{H}$ would be much lower than one, for all values of the porosity factor, proving the fact that, within this range, the fire process has changed from being ventilation controlled to fuel bed controlled. The energy developed per unit time does not then increase with increasing opening factor, but remains roughly constant or somewhat decreases. From the results summarized it can be observed that the transition point, or more correctly, the transition range between ventilation controlled and fuel bed controlled, fire process depends on both the opening factor of the fire cell and porosity of the fire loading. The corresponding influence for the magnitude I_{Cav} is to be found in column 25 of TAB. II. This magnitude which expresses the mean value of the energy liberated per unit time during the same time as for R_{80-30}, is determined from the curves described in FIG. 13-17. The values of I_{Cav} given in the table are represented in diagram form in FIG. 23, describing the relation $I_{Cav} - \phi$ for the values of the opening fac-

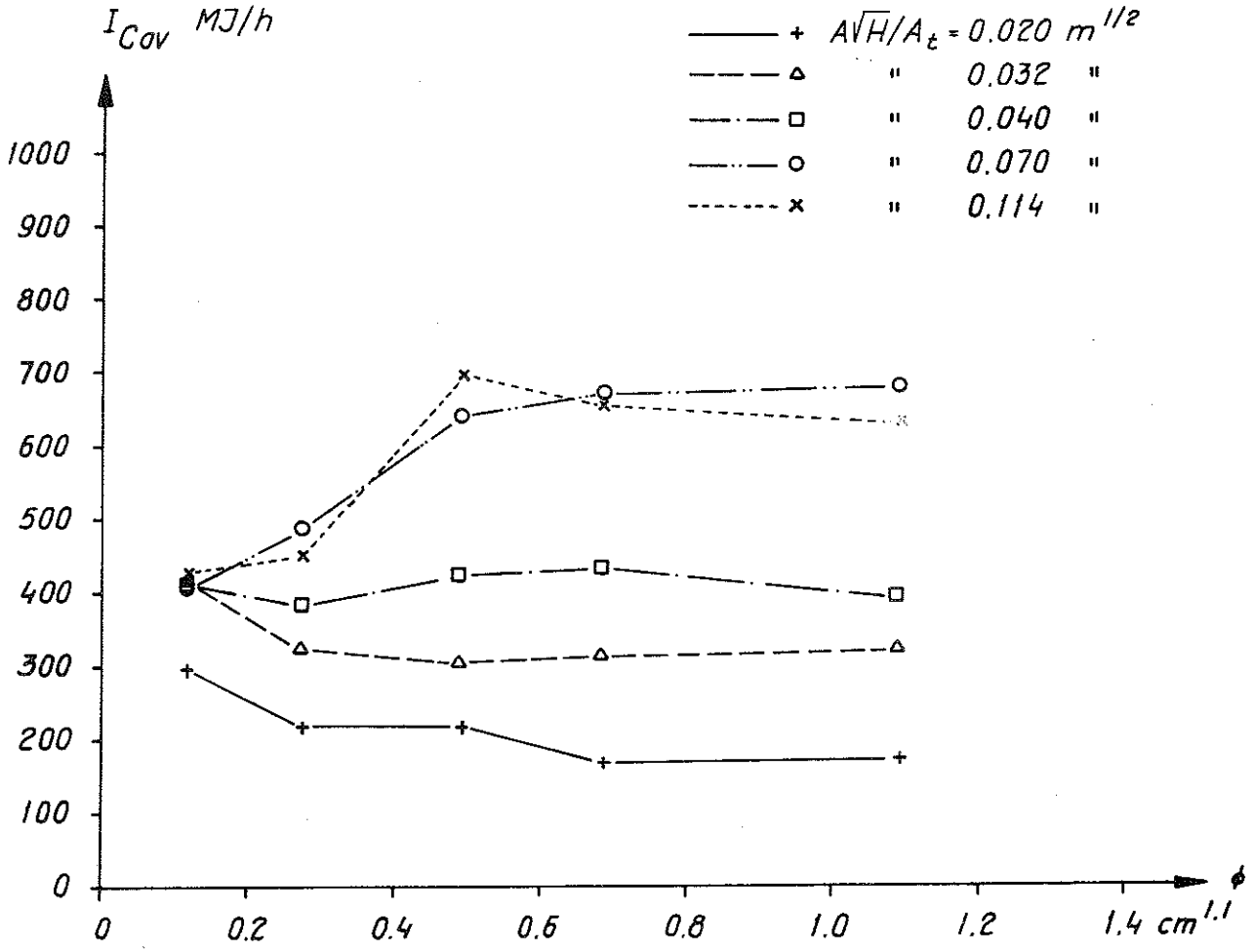

FIG. 23 By a theoretical analysis of the experimental results obtained relation between the liberated heat quantity, I_{Cav} (MJ/h), and the porosity factor, ϕ ($cm^{1.1}$), for varying opening factor, $A\sqrt{H}/A_t$ ($m^{1/2}$). Fire load 35 MJ/square meter enclosing surface. The enclosing structures of the fire cell are composed of 10 mm asbestos disk having a density of 1020 kg/m^3 and 1.5 mm steel sheet.

tors studied. The figure emphasizes the fact that an increase of the size of the window opening, beyond that corresponding to $A\sqrt{H}/A_t \approx$ $\approx 0.07\ m^{1/2}$, results in an approximately constant or somewhat reduced fire process which approaches that which is valid for fire in open air with the differences which can be caused by variations in the combustion air and smoke gas flow through the crib in both cases.

In the literature, cf. for instance Tenning (1961) and document No. 274 of CTH (1963), it is stated that the growth rate of the coal layer formed during a fire in solid or glued solid beams or wooden columns is approximately constant during the heating phase. This growth rate has the order of magnitude of 0.4 mm/min for oak or teak constructions, for a fire exposure which is in agreement with the prevailing classification test according to ISO R 834. For a more intensive fire exposure, the values, referred to, would increase, cf. Knublanch (1972). If the value 0.7 mm/min is applied to the fire loading used in the test series, it would, with an assumed effective heat value of 10.78 MJ/kg, imply that the energy developed per unit time would be of the order of magnitude of 8.4 MJ/min $\approx$ $\approx$ 500 MJ/h during the active phase of the fire. With respect to the slender dimension of the wooden sticks compared with that of solid beams or columns, it is reasonable to assume that the penetration rate of the fire for this actual case would be somewhat higher. The value of the energy liberated per unit time thus estimated is of the same order of magnitude as the value noted for I_{Cd} and I_{Cav}, which, for a fuel bed controlled process, cover the variation range of 400-700 MJ/h.

With respect to the influence of the porosity factor, ϕ, of the crib on the energy liberated per unit time, I_C, the following comments may be made:

From the FIG. 13-17 and TAB. II it is observed that, for the opening factors $A\sqrt{H}/A_t$ = 0.07 and 0.114 $m^{1/2}$ an increase of the porosity factor, ϕ, within the range $\phi < 0.5\ cm^{1.1}$ gives rise to a higher maximum energy development, I_{Cmax}, and a faster ignition process. This relation is illustrated for the opening factor 0.07 $m^{1/2}$ in FIG. 16 and TAB. II, column 8, which for ϕ = 0.117, 0.276 and 0.495 $cm^{1.1}$ give the corresponding I_{Cmax}-values amounting

to 420, 504 and 673 MJ/h respectively. For the lowest opening factor studied, $A\sqrt{H}/A_t = 0.02$, the opposite relation is true implying a maximum energy development, I_{Cmax}, which within the range $\phi < 0.5$ $cm^{1.1}$ decreases with increasing porosity factor. For the values of the opening factor situated in between, $A\sqrt{H}/A_t = 0.032$ and 0.04 $m^{1/2}$, the corresponding influence of varying porosity factor, ϕ, is substantially less. For value of the porosity factor $\phi > 0.5$ $cm^{1.1}$, variations in ϕ renders rather little influence on the maximum energy development, I_{Cmax}, for all the opening factors studied. It should however be observed that the shape of the crib, with either such high values for ϕ or such open piling that the distance between the sticks exceeds the limit value for which the spread of fire within the pile is no longer possible, has not been taken into account in the test series. With respect to the influence of the porosity factor, ϕ, the same characteristics are essentially true for the energy magnitudes, I_{Cd} and I_{Cr}, as those described for the maximum energy development, I_{Cmax}. On the whole, the same characteristics are also true for the magnitude I_{Cav} which is the mean value of the energy liberated per unit time during the conventionally defined flaming phase, determined as the time during which the weight of the fire loading decreases from 80% to 30% of the initial weight. On the other hand, the mean combustion rate, R_{80-30}, given as the weight decrease of the fire loading per unit time, exhibits a deviating pattern for $\phi < 0.5$ $cm^{1.1}$ and $A\sqrt{H}/A_t \leq 0.04$ $m^{1/2}$, within which range, R_{80-30} on the whole increases with increasing porosity factor. For the lowest opening factor described, $A\sqrt{H}/A_t = 0.02$ $m^{1/2}$, R_{80-30} is however almost independent of the porosity factor, ϕ, within the whole range studied.

From the view of combustion, it is technically interesting to analyze the relation between the parameters liberated energy per unit time, I_C, weight decrease of the fuel per unit time, R, and the effective heat value, W. For the time period t_d which defines the active phase of the fire with respect to the liberated energy, I_C, TAB. II gives the heat value, W_d, calculated as the ratio I_{Cd}/R_d within the small variation range of 9.6-12.9 MJ/kg for all the tests but four. For the time period t_r which, in addition to t_d, also embraces the ignition- and flaming processes, the corre-

sponding variation range for the heat value, $W_r = I_{Cr}/R_r$, is 7.9--12.2 MJ/kg. The dispersion in the effective heat value, W_d, or W_r as a function of the porosity factor, ϕ, decreases with increasing opening factor of the fire cell, $A\sqrt{H}/A_t$. The values obtained for the time periods t_d and t_r have a good agreement with the effective heat value of 10.78 MJ/kg which has been calculated by Kawagoe (1958) in an analysis of the composition of the smoke gases and which have been applied by some authors including Magnusson-Thelandersson for heat- and mass balance calculations for wood fuel fires in closed compartments. With respect to the heat value which is determined in a calorimetric bomb during a complete, intensive combustion and which varies between 17 and 20 MJ/kg for wood, the values of W_d and W_r described amount to approximately 45-65%.

A calculation of the corresponding magnitudes I_{Cav}, R_{80-30} and W_{av} from the test results obtained for the conventionally defined flaming phase, that is the time period during which the weight of the fire loading decreases from 80% to 30% of the initial weight, leads according to TAB. II to an effective heat value, $W_{av} = I_{Cav}/R_{80-30}$, which exhibits a larger dispersion with the porosity of the fire loading than the effective heat values, W_d, and, W_r, and which, on the whole, in addition also exhibit a tendency to increase with increasing opening factor $A\sqrt{H}/A_t$ up to $A\sqrt{H}/A_t \approx 0.07$ $m^{1/2}$, whereafter it remains approximately constant.

It is noteworthy to observe the high effective heat values, W_d, W_r, and W_{av}, computed for the lowest porosity factor, $\phi = 0.117$ $cm^{1.1}$, with the opening factors $A\sqrt{H}/A_t = 0.032$ and 0.04 $m^{1/2}$. The effective heat values thus calculated amount to 70 to 80% of those corresponding to a complete combustion in a calorimetric bomb.

For the glowing- and cooling phases of the fire process which together embrace the time period t_g, an analogous analysis renders an effective heat value $W_g = I_{Cg}/R_g$ which, on a computational basis, becomes very large. The variation range being between 25.5--67.6 MJ/kg. Phenomenologically, this incidence depends on a combination of high liberated radiation energy and a very slow weight decrease of the fire loading during these phases. Compared with

the corresponding values for the active phase of the fire t_d, the mean value of the energy liberated per unit time, I_{Cg}, during the glowing- and cooling phases amount to approximately 15-30% while the mean value of the weight decrease of the fire loading R_g, during the glowing- and cooling phases is only of the order of magnitude of 3-10% of the weight decrease, R_d. The dispersion in the magnitude W_g, is also much higher than the dispersion in the corresponding magnitudes W_d and W_r, which can be attributed to the fact that the I_C-time curve and R-time curve for several tests are mutually displaced in time to a varying and non-negligible extent. For the total energy, $I_{Cg} \cdot t_g$, liberated during the time period t_g, TAB. II gives 63.8 MJ with the variation range of 47.3-74.5 MJ, corresponding to the variation range of 34.8-40.5 MJ per square meter of the enclosing surface for the fire loading q.

Furthermore the duration of the different phases of the fire process are of decisive importance. For the time period t_d which accordingly embraces the active phase of a fire with respect to the energy liberated per unit time, I_C, TAB. II gives a strong influence of the variations in the porosity factor, ϕ, belonging to the fire loading within the ventilation controlled range, that is up to the opening factor $A\sqrt{H}/A_t \approx 0.07$ cm$^{1.1}$. Within this range, t_d decrease with increasing ϕ. On the other hand, within the fuel bed controlled range, the influence of the porosity factor, ϕ, on the time period t_d is rather insignifficant. On the whole, for low porosity factors, ϕ, the active time period of the fire phase, t_d, decreases with increasing opening factor, $A\sqrt{H}/A_t$, within the ventilation controlled range and, then remains approximately constant within the fuel bed controlled range. For high values of the porosity factor, ϕ, the influence of the variations in the opening factor, $A\sqrt{H}/A_t$, is much less.

For the magnitude t_r which indicates the time period from ignition to the time corresponding to the value 0.75 I_{Cmax} on the descending part of the energy-time curve, the influence of the variations in the porosity factor, ϕ, is rather of minor importance. With respect to the opening factor, $A\sqrt{H}/A_t$, the time period t_r decreases

with increasing opening factor from approximately 0.32 h for $A\sqrt{H}/A_t$ = = 0.02 $m^{1/2}$ to approximately 0.13 h for $A\sqrt{H}/A_t$ = 0.07 $m^{1/2}$. For high values of the opening factor, that is within the fuel bed controlled range, t_r, then remains approximately constant.

For the time period t_2 which embraces the time between the times corresponding to 0.75 I_{Cmax} and 0.25 I_{Cmax} on the descending part of the energy-time curve, different characteristics are true in certain respects. During this time period the influence of the porosity factor, ϕ, is stronger for high values of the opening factor, that is within the range controlled by the fuel, than for the lower opening factors corresponding to fire controlled by ventilation. For low values of the porosity factor, ϕ, a change of opening factor does not tend to influence the time t_2 in any certain direction. For high values of the porosity factor, the influence of the variations in the opening factor is analogous with that for the time periods t_d and t_r. For duration of the cooling phase, that is to say the time period t_g, the values calculated on the basis of the test results do not show any clear and unique tendency to depend on either the porosity factor ϕ or the opening factor $A\sqrt{H}/A_t$. For several tests the duration t_g lies within the range 0.5-0.8 h.

Another magnitude essential for the heat- and mass balance of the fire process is the quantity of fire gases carried away from the fire cell. In section 2, it is stated that the gas flow can be determined by either the first or the second of the following two formulas, depending on whether the vertical acceleration in the window openings is neglected or whether it is taken into account respectively:

$$Q = \varphi A\sqrt{H} \tag{11}$$

$$Q_a = C \cdot \varphi A\sqrt{H} \tag{12}$$

where φ is a proportionality constant and C a factor smaller than one which depends on the shape and size of the window opening as well as the geometry of the fire cell. In agreement with the experiences described by Magnusson-Thelandersson, it can be observed from TAB. II, column 5, that for the opening factor $A\sqrt{H}/A_t$ = 0.070

and 0.114 $m^{1/2}$ the value of C amounts to 0.8 and 0.7 respectively, while for the lower values of the opening factor C equals 1.

That a rough estimation of the gas flow can even be made on the basis of the registered gas temperature and combustion rate is shown by the following analysis presented by Magnusson-Thelandersson. If the terms entered into the heat balance equation are approximated according to the following relations:

$$I_C = C_1 \cdot R \tag{20}$$

$$I_L = C_2 \cdot Q \cdot \vartheta_g \tag{21}$$

$$I_W = C_3 \cdot \vartheta_g \tag{22}$$

$$I_R = C_4 \cdot \vartheta_g \tag{23}$$

with C_1-C_4 as constants, then the following equation is obtained by inserting the appropriate terms in the heat balance equation

$$Q = \frac{C_1 \cdot R}{C_2 \cdot \vartheta_g} - \frac{C_3 + C_4}{C_2} = C_5 \frac{R}{\vartheta_g} - C_6 \tag{24}$$

where C_5 and C_6 are two new constants. Accordingly, Equation (24) expresses that the gas flow, Q, is proportional with the magnitude R/ϑ_g.

If I_C in Equation (20) is instead assumed to be proportional with the mean value of the energy developed per unit time during the flaming phase, I_{Cav}, that is

$$I_C = C_7 \cdot I_{Cav} \tag{20a}$$

Equation (24) would then be transferred to

$$Q = C_8 \frac{I_{Cav}}{\vartheta_g} - C_6 \tag{24a}$$

where C_7 and C_8 are two new constants, meaning that the gas flow, Q, becomes proportional with the ratio I_{Cav}/ϑ_g.

With respect to the flaming phase of the fire process defined as the time period for a weight decrease of the fire loading from 80% to 30% of the initial value, the magnitudes $R/\vartheta_g^{\beta} = R_{80-30}/\vartheta_{80-30}^{\beta}$ and $I_{Cav}/\vartheta_g^{\beta} = I_{Cav}/\vartheta_{80-30}^{\beta}$, are described in TAB. II, columns 28 and 29 respectively. The magnitude $I_{Cav}/\vartheta_{80-30}^{\beta}$ has in addition been summarized in FIG. 24, as a function of the opening factor $A\sqrt{H}/A_t$ for varying porosity factor, ϕ. From the figure it is observed that the influence of the variations in the porosity factor, ϕ, is rather small within the range $\phi \gtrsim 0.5$ cm$^{1.1}$. Within this range, the curves indicate an approximate validity for Equation (11) up to the opening factor $A\sqrt{H}/A_t = 0.07$ m$^{1/2}$, while for larger values of the opening factor, a heat- and mass balance computation should instead be based on Equation (12), that is the influence of the vertical acceleration of the gas flow in the window opening should be taken into account. For both the lowest porosity factors, $\phi = 0.117$ and $\phi = 0.276$, FIG. 24 gives the transition from applying Equation (11) to Equation (12) at a much lower opening factor - $A\sqrt{H}/A_t \simeq 0.04$ m$^{1/2}$ - than what is true for the range $\phi \gtrsim 0.5$ cm$^{1.1}$. Compared with the magnitude $I_{Cav}/\vartheta_{80-30}^{\beta}$, the magnitude $R_{80-30}/\vartheta_{80-30}^{\beta}$ gives a more non-uniform picture of the functional relationship between the gas flow $Q(Q_a)$ and the opening factor $A\sqrt{H}/A_t$ or the air flow factor, $A\sqrt{H}$, and is thus poor as a parameter in the analysis.

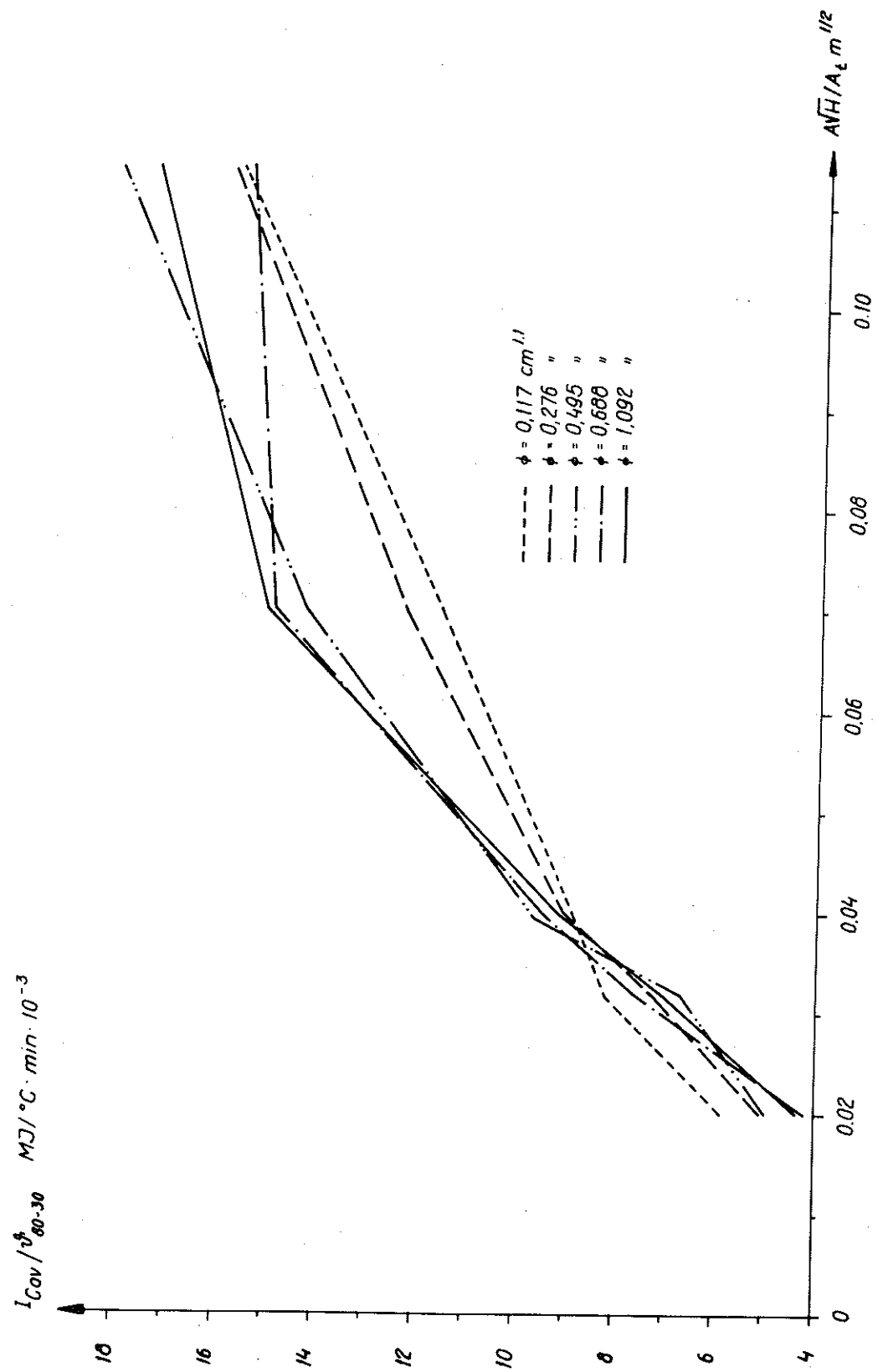

FIG 24 The relation calculated from the obtained test results between $I_{Cav}/\vartheta^4_{80-30}$ and the opening factor, $A\sqrt{H}/A_t$, of the fire cell with five different values for the porosity factor ϕ. Fire load q = 35 MJ/m^2 of the enclosing surface.

5. SIZE OF THE FIRE LOAD.

In the previous section results of tests which purely illustrate the influence of variations in porosity factor of the fire load and opening factor of the fire cell on the characteristics of the fire process have been described and analyzed. In these tests the size of the fire load, q, stick thickness belonging to the fire load and thermal properties of the enclosing structures of the fire cell have been kept constant.

In the present section, a test series which gives complementary information on the influence of the variations in the size of the fire load for certain combinations of the values of the porosity- and opening factors, is described. As for the influence of the stick thickness, b, and thermal properties of the enclosing structures, the corresponding complementary analysis is performed in sections 6 and 7 respectively.

5.1 Introductory discussion. Test characteristics.

From the investigations reported in the literature, it is known that an increase of the size of the fire load at otherwise constant conditions, results in a growth of the combustion rate defined as the weight decrease of the fire load per unit time. To begin with, this growth is linear and later decreases continously resulting in a maximum combustion rate for a certain value of the fire load. For further increase of the size of the fire load beyond this characteristic value, instead the fire duration grows thereafter approximately proportional to this increase. The characteristic value of the fire load corresponding to the maximum value of the combustion rate increases with increasing opening factor for the fire cell and depends also on the porosity factor of the fire load and the stick thickness. For a fire load which is larger than the characteristic value, the fire process is conventionally ventilation controlled, in which the weight decrease of the fire load per unit time depends mainly on the rate of penetration of the fire from the exposed surface of the wooden sticks.

In the fire tests according to the standard fire curve, this penetration rate in the beams have been shown to be approximately constant and of the order of magnitude of 0.5-0.7 mm per min for wood of the type redwood, c.f., for example, Tenning (1961) and CTH:s Document No. 274 (1962). The values are related to beam cross sections with the smallest lateral dimension of 60 mm or more and should therefore be modified when discussing their application for the stick thickness actual in the present case. Compare also what has been stated in this connection in Section 4.2. Values of the penetration rate of the fire depends further on, for example, the shape of the cross section and penetration direction of the char layer with respect to the wood grain, Ragowski (1970).

The penetration rate depends further, to a considerable degree, on the thermal conditions around the burning wooden beam, which is illustrated in FIG 25 a) and b), Knublauch (1972). For 5 cm thick redwood plates exposed to fire in 30 minutes, FIG 25 a) represents the fire process described by the gas temperature-time curve $\vartheta = 18 + 345\ \lg(\frac{8t}{a} + 1)$, where a has assumed values between 0.25 and 6 and where ϑ indicates the temperature according to the standard curve for a = 1. The combustion depths, Δd, were measured and shown in FIG 25 b). In agreement with the above mentioned circumstanses, the penetration rate of the fire, influenced by thermal conditions according to the standard curve, is of the order of magnitude of 0.5 mm per min increasing to 1 mm per min when the influence is the strongest.

The influence of different types of fire process on the combustion rate, briefly described above is illustrated in FIG 26 which gives the results obtained for full-scale tests when the fire load is in the form of wooden stick piles, Heselden (1968). In the tests the combustion rate was primarily studied for large window openings and for variations in the size of the fire load and its distribution in the fire cell. The figure shows the experimentally obtained relation between the mean combustion rate, R_{80-30}, and the air flow factor $A\sqrt{H}$ ($m^{5/2}$), alternatively the opening factor $A\sqrt{H}/A_t$ ($m^{1/2}$) for every fuel quantity referred to the floor area of the fire cell. From the figure it is observed that, except for the test with the

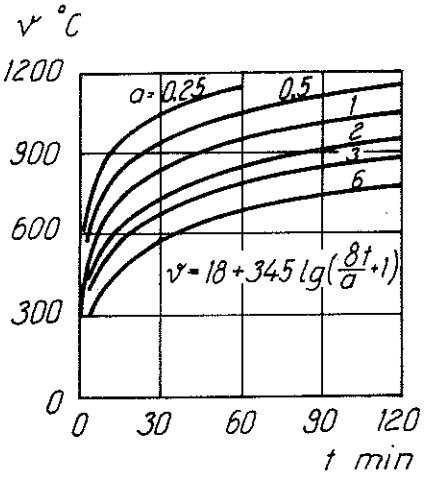

a)

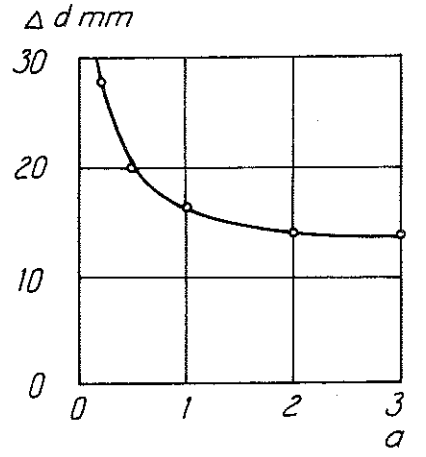

b)

FIG 25 The measured combustion depth, Δd, when 5 cm thick redwood plates are exposed to fire in 30 minutes, FIG 25 b), the fire process being described by the gas temperature-time curve $\vartheta = 18 + 345\ \lg(8t/a + 1)$, FIG 25 a), where a has assumed values between 0.25 and 6 and where ϑ indicates the temperature according to the standard curve for a = 1.

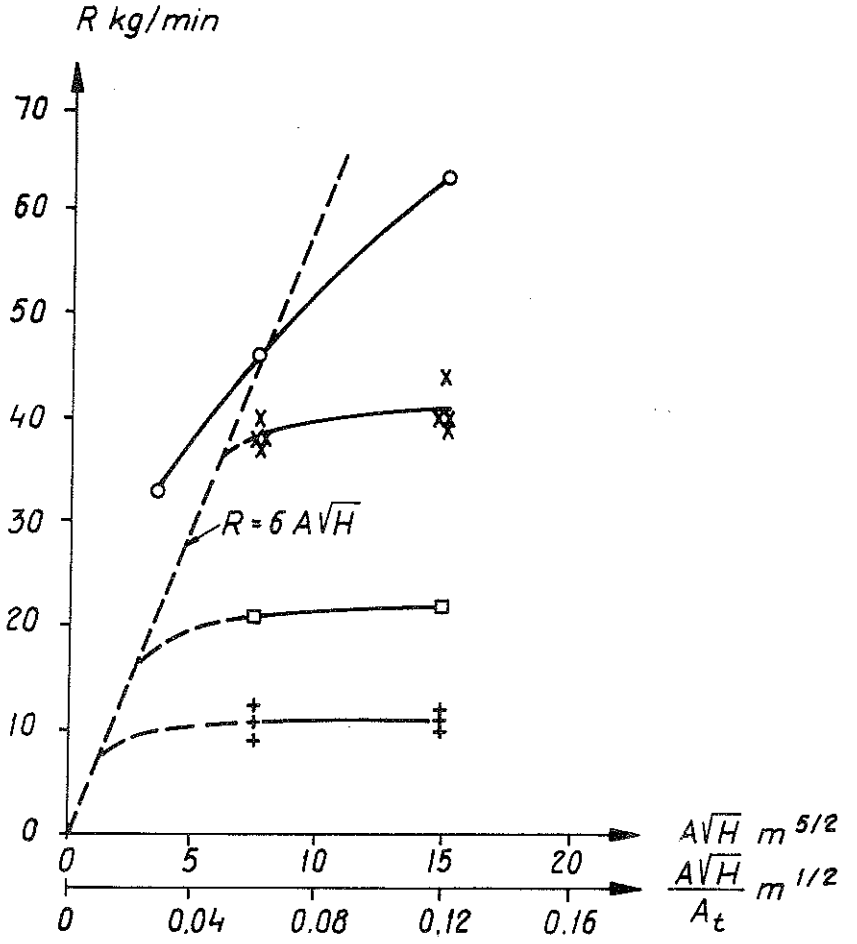

Symbol	Fire load kg/m²
○	60
x	30
□	15
+	7.5

FIG 26 The relation experimentally obtained for full-scale tests between the mean combustion rate, R_{80-30} (kg/min) and the air flow factor, $A\sqrt{H}$ ($m^{5/2}$) or alternatively the opening factor, $A\sqrt{H}/A_t$ ($m^{1/2}$) for varying fire load which is referred to the floor are of the fire cell.

largest fuel quantity, all the fires have been fuel bed controlled, which follows from the fact that an increase of the window area does not give any corresponding increase in the combustion rate for the respective fire load. For the largest fire load studied, the ventilation controlled fire process prevails for both of the lower values of the opening factor while for the higher value of the air flow factor, a transition is seen towards a fuel bed controlled process.

As mentioned before, for a given fire cell, it is true that the combustion rate increases, with increasing fuel quantity, to a maximum value at which the fire process becomes ventilation controlled. Likewise, the fire gas temperature also increases to a maximum value ϑ_{max}. A further increase of the fuel quantity does not result in any considerable change of the combustion rate. The effect instead, becomes an approximately proportional increase in fire duration. The maximum value of the fire gas temperature also increases further up to an upper limiting value, implying a stationary heat flow through the openings of the fire cell and the enclosing structures.

This fact is indicated in FIG 27 which indicates the maximum fire gas temperature, ϑ_{max}, as a function of fuel quantity registered by Ödeen (1968) in full-scale tests. The figure summarizes the results from three test series corresponding to three different values for the air quantity, G, which has been supplied to the fire cell per unit time, through a fan arrangement. Alternatively, the figure can be looked at as one, summarizing the results from three test series performed in three fire cells with different opening factors. From the figure, it is observed that, for both of the test series with air flow values of G = 1.0 and 2.0 m^3/s, the limiting values of the maximum value of the fire gas temperature, ϑ_{max}, corresponding to the stationary heat flow have almost been reached with the largest fuel quantity described. For the lowest air flow value G = 0.7 m^3/s, the described results from the test series confirm the successively damped growth in the maximum value of the fire gas temperature, ϑ_{max}, with increasing fuel quantity. For this air flow value, the asymptotic value of ϑ_{max} corresponding to the stationary heat flow

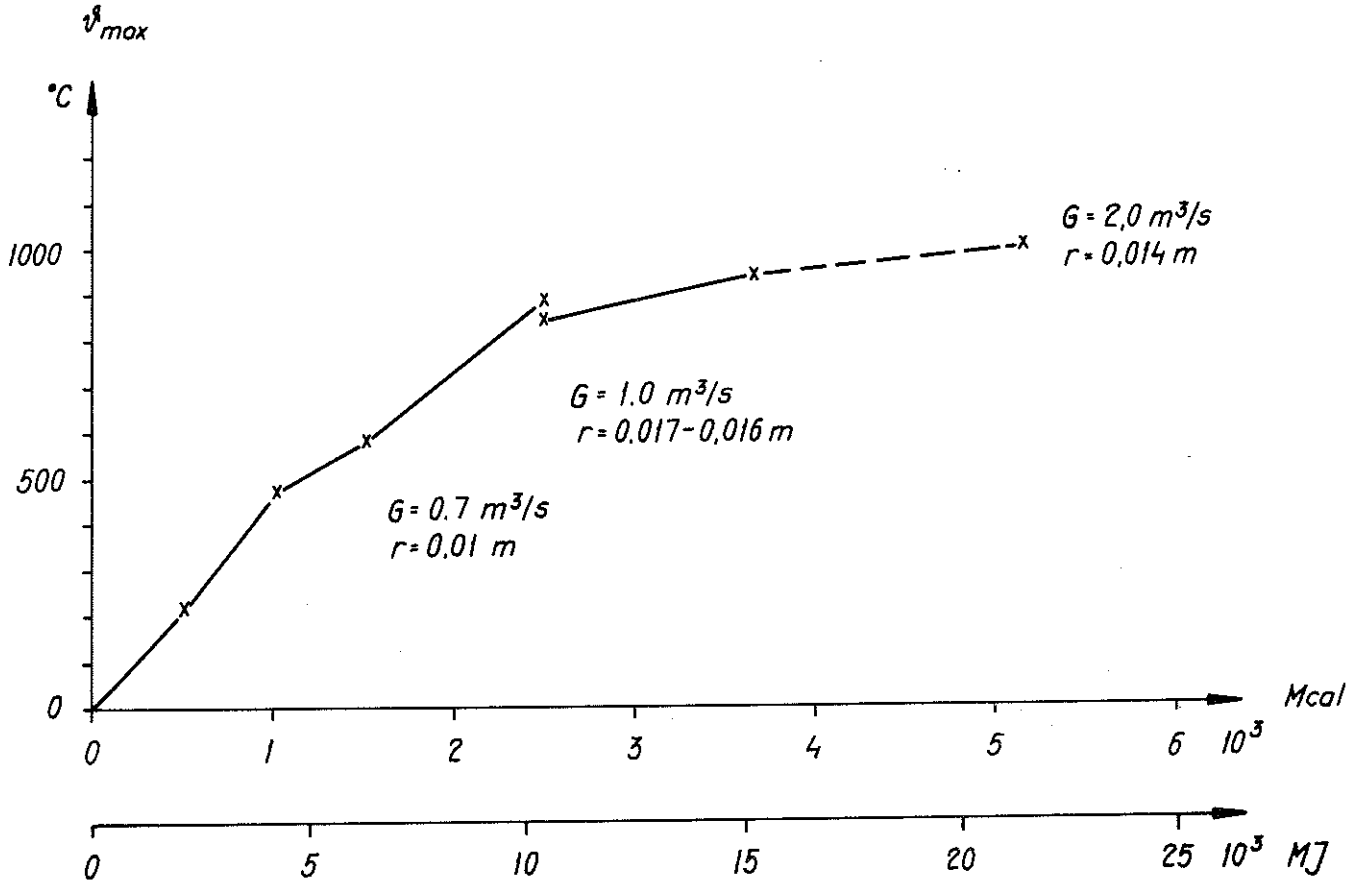

FIG 27 The influence of varying fuel quantity on the maximum gas temperature, ϑ_{max} (°C), obtained during the fire process. G indicates the quantity of combustion air (m^3/s) supplied through a fan arrangement. Volume of the fire cell is 46 m^3, the total internal enclosing surface of the fire cell being A_t = 79 m^2. The enclosing structures consist of 20 cm concrete.

is first reached when the fuel quantity is considerably larger than those used in the test series. In the test series, the size gradation of the fuel, expressed by the hydraulic radius r = volume/exposed surface, has not been kept constant. This fact does not, however, affect the fundamental conclusions arrived at in the discussion.

When Magnusson-Thelandersson (1970, 1971) published their fundamental works for a theoretical determination of the heat- and mass balance equations, expressing the gas temperature-time curve of the fire process, difficulties presented themselves when applying the theory to fire load of wood fuel type due to an extremely incomplete knowledge concerning the influence of the size of the fire load and porosity factor on the combustion rate and the fire process. This condition which is functionally analyzed, in detail, in the work from 1971 necessitated a simplified treatment for an initially fuel bed controlled fire process. This simplification implies that the fire process was assumed to be ventilation controlled, satisfying the conditions concerning the total liberated energy, c.f. Equation (15). For a fire process which is actually fuel bed controlled, such an approximation renders an overestimation of the maximum fire gas temperature and an underestimation of the fire duration which partially acts as a compensating factor.

Under this simplified assumtion, the design basis developed by Magnusson and Thelandersson, (1970), in the form of gas temperature-time curves for a complete fire process in fire cells with different thermal properties utilizes, as input parameters, the opening factor of the fire cell $A\sqrt{H}/A_t$ and size of the fire load, q, described as the total liberated energy in a complete combustion. In the computations, attention has been paid to the fact that the mentioned total energy is distributed over the whole fire process according to FIG 4, implying a distribution of the order of magnitude of 70-50 % on the flaming phase and 30-50 % on the glowing phase of the fire process.

On the whole, the same assumed energy distribution characterizes the gas temperature-time curves differentiated with respect to the opening factor, $A\sqrt{H}/A_t$, according to Swedish building standards 67, SBN 67, (1967), which can be chosen as the design basis mainly for

fire load of wood fuel nature. SBN 67 presents temperature-time curves only for the heating- and the flaming phases. For the cooling phase of the fire cell, the regulations render a linear temperature-time curve, corresponding to a temperature decrease of $10^{o}C$/min. The fire duration defined as the length of the heating- or flaming phase, T, is determined in SBN 67 according to the relation

$$T = \frac{qA_t}{6300\ A\sqrt{H}} \quad (h) \qquad (25)$$

where q is the fire load (MJ/m^2 surrounding area)

From a functional point of view, Equation (25) might seem to contain an incompatibility due to the fact that the fire duration, T, is coupled to the heating- or flaming phase while the fire loading, q, embraces the total energy liberated during the whole fire process. An enlargement has been, however, introduced in the denominator of the equation which indicated the mean value of the energy liberated per unit time during the heating- or flaming phase, compensating the rigorously functional high values of energy in the numerator. Equation (25), whose construction is simple for a practical application, renders accordingly the calculated fire duration, T, which is normally in good agreement with the experimental values for a ventilation controlled fire process. Applying Equation (25) to a fuel bed controlled fire process renders too low values for the fire duration. Instead, as mentioned before, assuming ventilation control for a fuel bed controlled fire process results in an overestimation of the maximum value of the fire gas temperature.

In FIG 28, the gas temperature-time curves for a complete fire process corresponding to a fire cell with the opening factor $A\sqrt{H}/A_t$ = 0.04 $m^{1/2}$ are compared partly according to Magnusson-Thelandersson and partly according to SBN 67. From the comparison, which embraces values between 25 and 500 MJ/m^2 (6 and 120 $Mcal/m^2$ of the enclosing surface) for q, it is observed that the decrease in fire gas temperature according to Magnusson-Thelandersson begins earlier than according to SBN 67. For low values of the fire load, the temperature-time curves according to SBN 67 overrate the thermal influence in relation to the more realistic temperature-time curves calculated by Magnusson-Thelandersson. For high values of the fire load, the opposite is true.

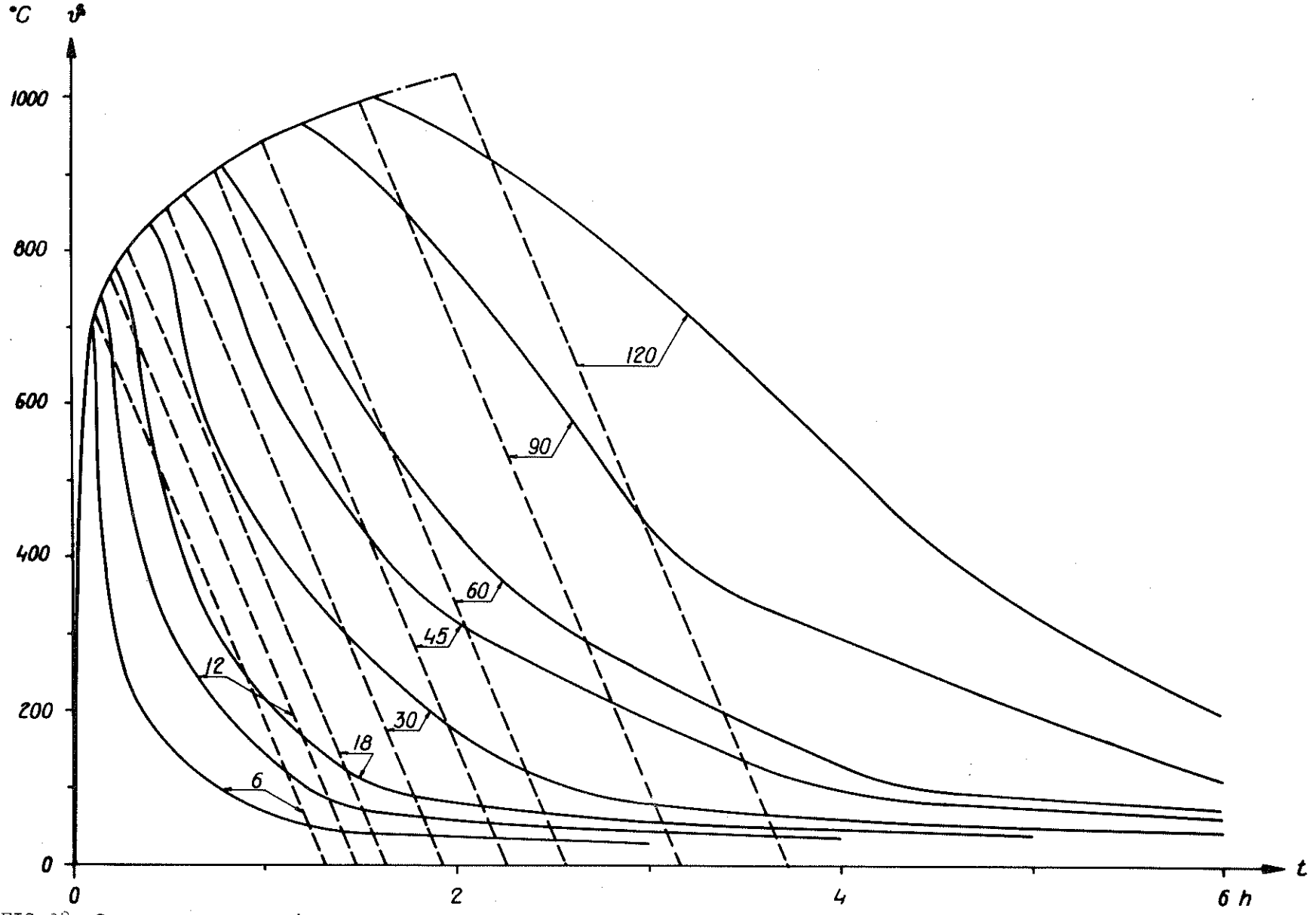

FIG 28 Gas temperature-time curves calculated by Magnusson-Thelandersson (1970), with varying fire load, q, for a fire cell with the opening factor $A\sqrt{H}/A_t = 0{,}04\ m^{1/2}$ and with enclosing structures, 20 cm thick, composed of a material with the coefficient of thermal conductivity $\lambda = 0.81\ W/m^{o}C$ and heat capacity of $\rho \cdot c_p = 1.67\ MJ/m^3\ ^{o}C$ (full line curves). The curves are compared with the corresponding curves according to SBN 67 (dashed line curves).

From this introductory discussion, based on the existing knowledge, it is observed that in fuel bed controlled fires, systematical investigations which can give increased information primarily on the influence of variations in the properties of a fire load (size, porosity factor, stick thickness) on the characteristics of the fire process, have a high degree of priority. As an integral part of such investigations, in the following, an experimental model study which has been undertaken in order to determine the dependence of joint variations in the size of the fire load and opening factor of the fire cell, on the fire process, is described and analyzed. The influence on the fire process arising from variations in the porosity of the fire load has been discussed previously in Section 4 and will complementarily be also discussed in this section while the influence of variations in the thickness of the sticks composing the fire load is illustrated in Section 6.

The test series has been performed in a cubical model fire cell with the internal lateral dimension of 750 mm, provided with one window opening, the enclosing structures being composed of 10 mm asbestos disk and 1.5 mm steel sheet as regarded from inside. In order to be able to link the investigation with the results described in the previous section, the same values of the opening factor, that is $A\sqrt{H}/A_t$ = 0.020, 0.032, 0.040, 0.070, and 0.114 $m^{1/2}$, have been studied in the test series. For all the opening factors, three values of the fire load were chosen, namely 17.5, 52.5 and 87.5 MJ/m^2 of the enclosing surface, corresponding to 1, 3, and 5 kg wood per m^2 of the enclosing surface, to be combined with the value q = 35 MJ/ /m^2 of enclosing surface, discussed in the previous section. For the middle-sized window opening with $A\sqrt{H}/A_t$ = 0.040 $m^{1/2}$, the extent of the investigation was supplemented by the fire load value of 70.0 MJ per m^2 of the enclosing surface, motivated by the fact that the fire process corresponding to this opening factor has a gas temperature-time curve which lies in the neighbourhood of that prescribed according to standards, for fire testing of building parts needed for the sake of classification, c.f., for example, Pettersson-Ödeen (1968). For all the combinations of the opening factor and size of the fire load discussed, the value of $\phi \approx 0.5$ $cm^{1.1}$ was chosen for the porosity factor. In order to extend the applicability of the results the opening factor $A\sqrt{H}/A_t$ = 0.040 $m^{1/2}$

was supplemented with two further values of the porosity factor, namely $\phi \approx 0.1$ and $\phi \approx 1.0$ $cm^{1.1}$ corresponding to a rather compact and an open wooden stick pile respectively.

5.2 Analysis of the experimental results.

By applying the calculation method briefly referred to in section 2, the energy-time curve corresponding to the respective test have been determined and described in FIG 29-35. Based on the relations given by these figures, magnitudes characterizing the fire process corresponding to those summarized in section 4, have been calculated and described in TAB III, cf. FIG 18 for the notations used.

In the following the magnitudes described in FIG 29-35 and in TAB III are discussed. The discussion is concentrated on the term I_{Cmax} which according to FIG 18 represents the maximum value of the energy liberated per unit time. In the discussion, the relation between this magnitude and the conventional mean combustion rate, R_{80-30}, during the active phase of the fire process, related to the weight decrease per unit time, is briefly analysed. At the same time the corresponding relation between the energy magnitudes I_{Cd} and I_{Cav} on one side and R_{80-30} on the other, are touched upon. Furthermore, the influence of the distribution of the fuel in the fire cell on the fire process is schematically discussed. The other fire process characteristics summarized in TAB III are only discussed as illustrations.

The discussion is partially carried out with the concepts ventilation controlled and fuel bed controlled fire respectively. A schematical definition of the concepts is therefore necessary in this connection while a more detailed analysis of these concepts has naturally been deemed to belong to the comprehensive result summary in section 8.

For a given shape of the fire cell and a given opening factor, $A\sqrt{H}/A_t$, an increase of the fuel quantity, M, or the fire load, q, results in a successively increasing mean combustion rate R_{80-30} up to a level at which R_{80-30} is approximately independent of the variations in the fuel quantity, M, FIG 36 a). This level varies

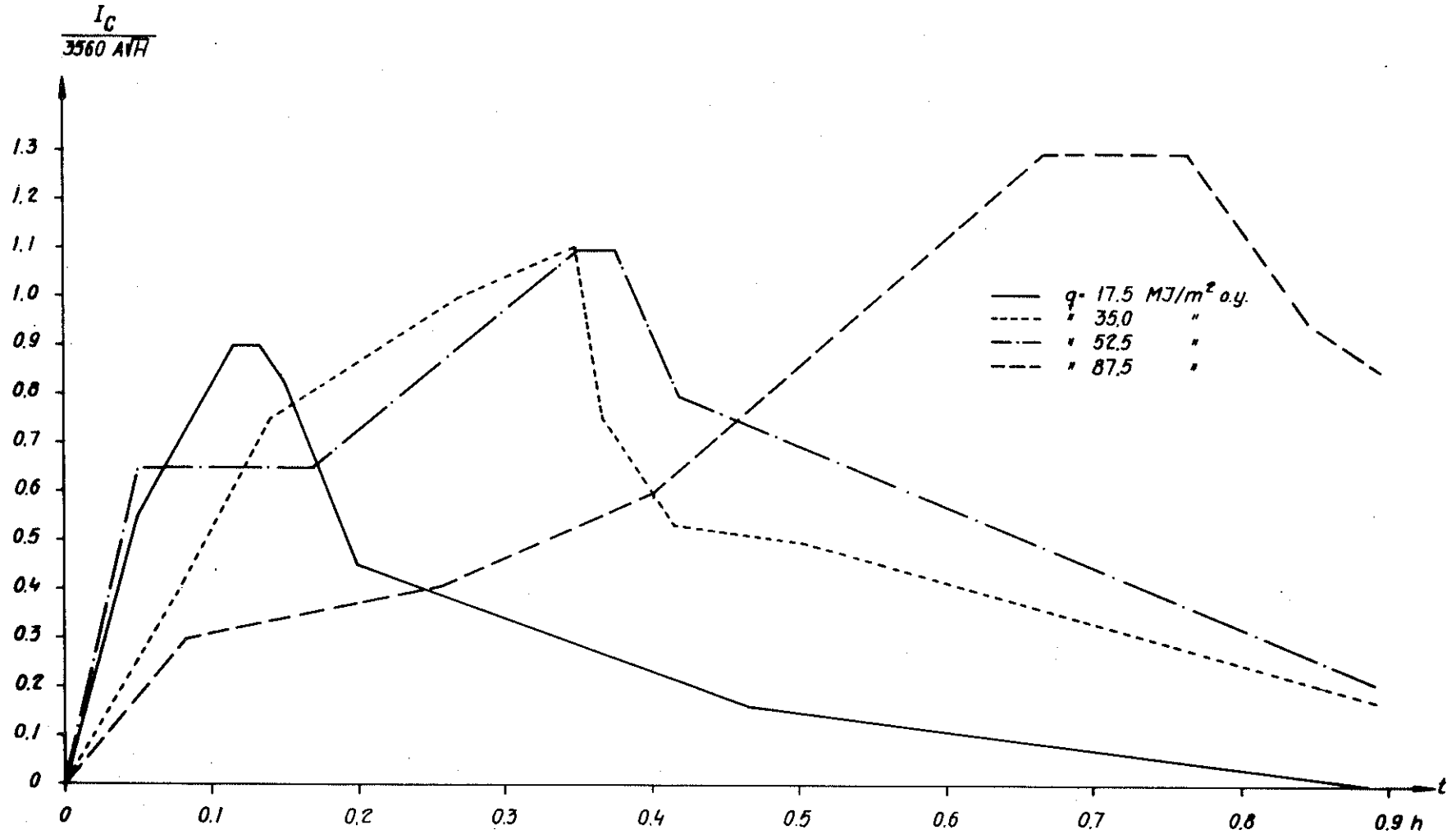

FIG 29 The theoretically calculated energy-time curve of the energy developed during the fire process for varying fire load, q, (MJ/square meter of the enclosing surface). Opening factor, $A\sqrt{H}/A_t$ = 0.020 $m^{1/2}$, porosity factor, $\phi \approx 0.5$ $cm^{1.1}$. The enclosing structures of the fire cell are composed of 10 mm asbestos disk having a density of 1020 kg/m^3 and 1.5 mm steel sheet.

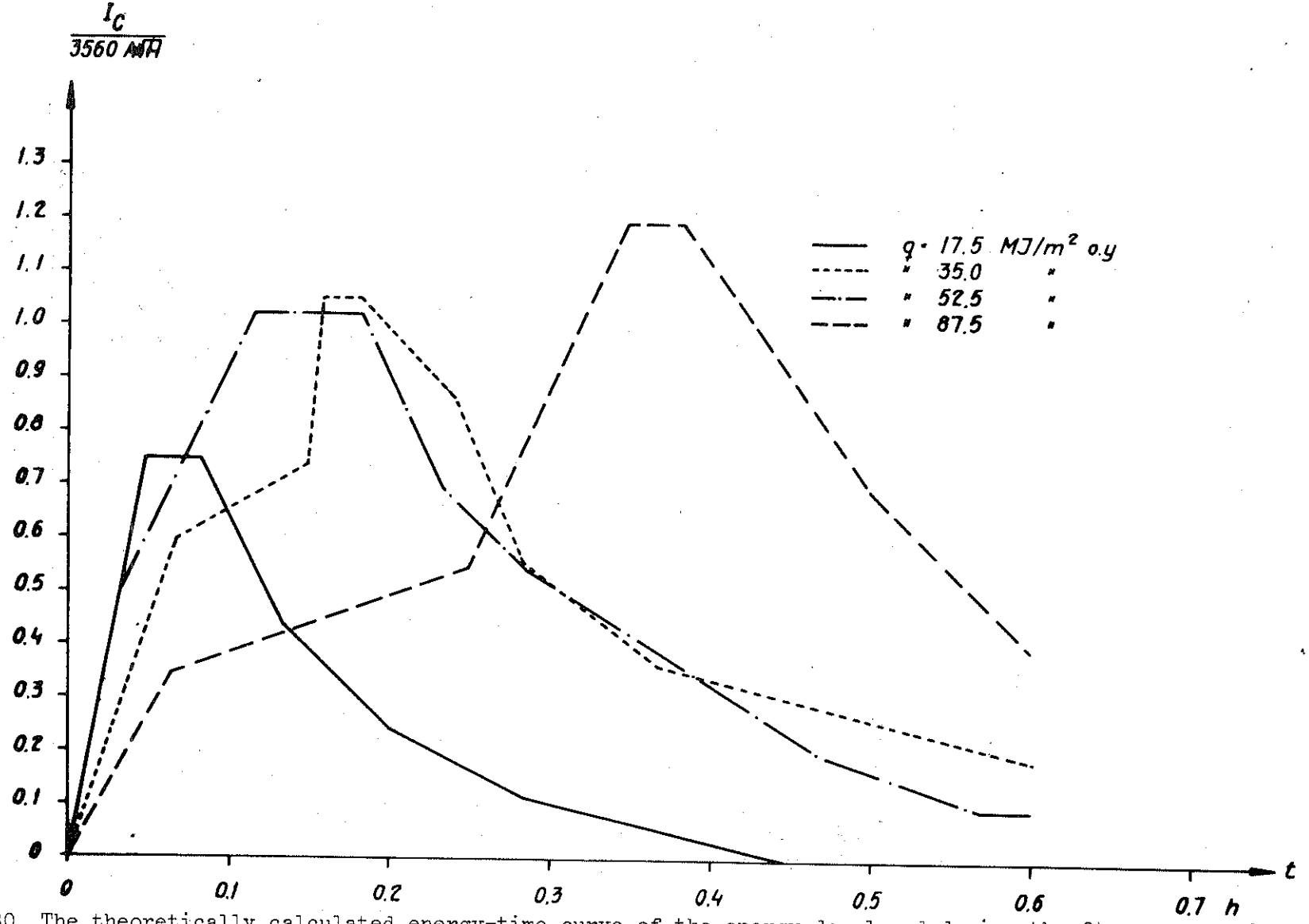

FIG 30 The theoretically calculated energy-time curve of the energy developed during the fire process for varying fire load, q (MJ/square meter of the enclosing surface). Opening factor, $A\sqrt{H}/A_t = 0.032\ m^{1/2}$, porosity factor $\phi \approx 0.5\ cm^{1.1}$. The enclosing structures of the fire cell are composed of 10 mm asbestos disk having a density of 1020 kg/m^3 and 1.5 mm steel sheet.

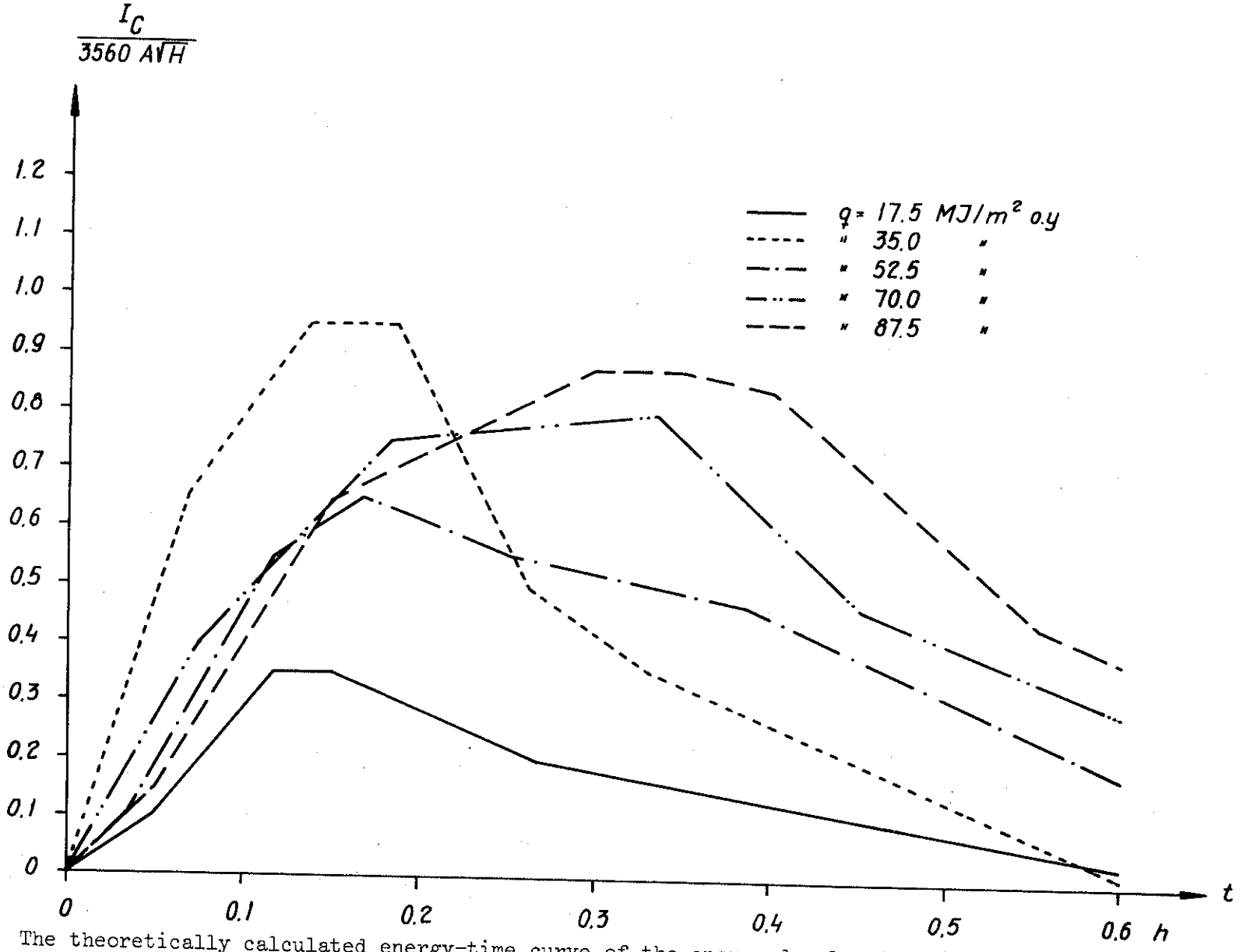

FIG 31 The theoretically calculated energy-time curve of the energy developed during the fire process for varying fire load, q (MJ/square meter of the enclosing surface. Opening factor, $A\sqrt{H}/A_t$ = 0.040 $m^{1/2}$, porosity factor, $\phi \approx 0.1\ cm^{1.1}$. The enclosing structures of the fire cell are composed of 10 mm asbestos disk having a density of 1020 kg/m^3 and 1.5 mm steel sheet.

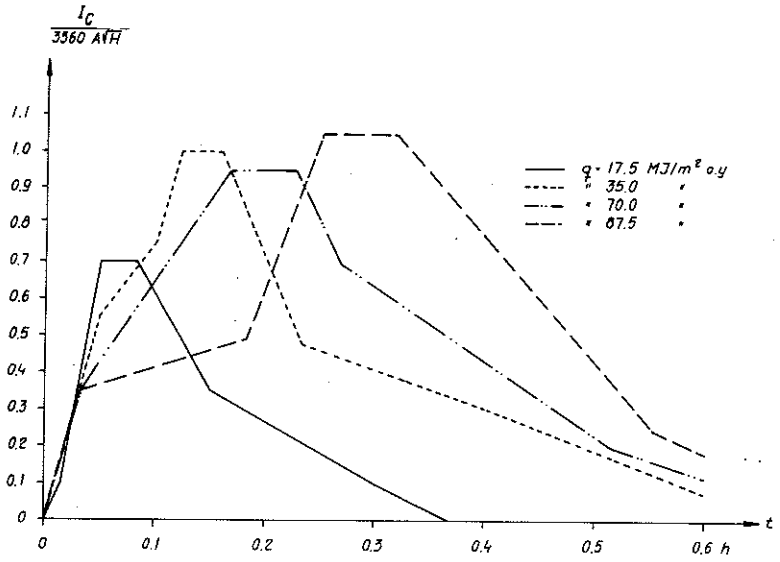

FIG 32 The theoretically calculated energy-time curve of the energy developed during the fire process for varying fire load, q (MJ/square meter of the enclosing surface). Opening factor, $A\sqrt{H}/A_t$ = 0.040 $m^{1/2}$, porosity factor, $\phi \approx 0.5$ $cm^{1.1}$. The enclosing structures of the fire cell are composed of 10 mm asbestos disk having a density of 1020 kg/m^3 and 1.5 mm steel sheet.

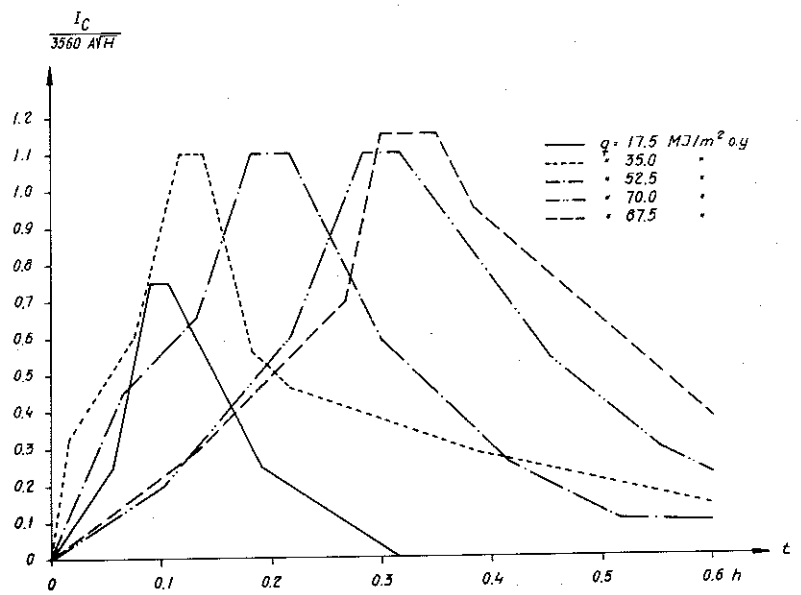

FIG 33 The theoretically calculated energy-time curve of the energy developed during the fire process for varying fire load, q (MJ/square meter of the enclosing surface). Opening factor, $A\sqrt{H}/A_t$ = 0.040 $m^{1/2}$, porosity factor $\phi \approx 1.0$ $cm^{1.1}$. The enclosing structures of the fire cell are composed of 10 mm asbestos disk having a density of 1020 kg/m^3 and 1.5 mm steel sheet.

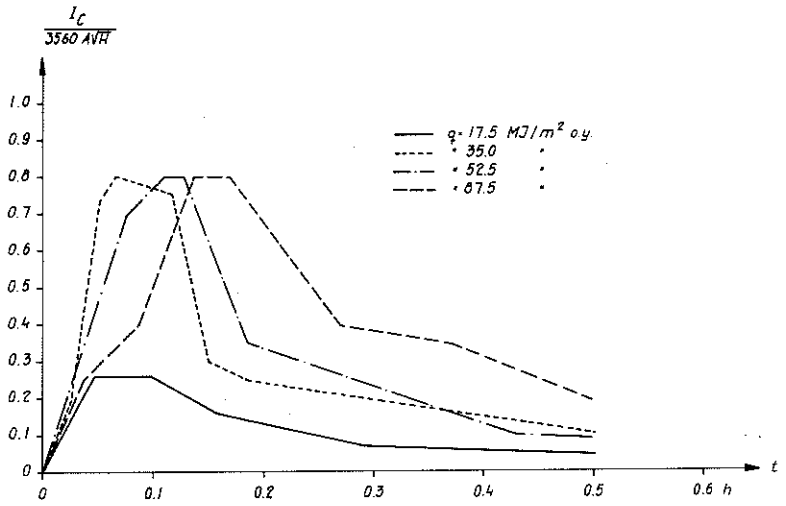

FIG 34 The theoretically calculated energy-time curve of the energy developed during the fire process for varying fire load, q (MJ/square meter of the enclosing surface). Opening factor $A\sqrt{H}/A_t$ = 0.070 $m^{1/2}$, porosity factor, $\phi \approx 0.5$ $cm^{1.1}$. The enclosing structures of the fire cell are composed of 10 mm asbestos disk having a density of 1020 kg/m^3 and 1.5 mm steel sheet.

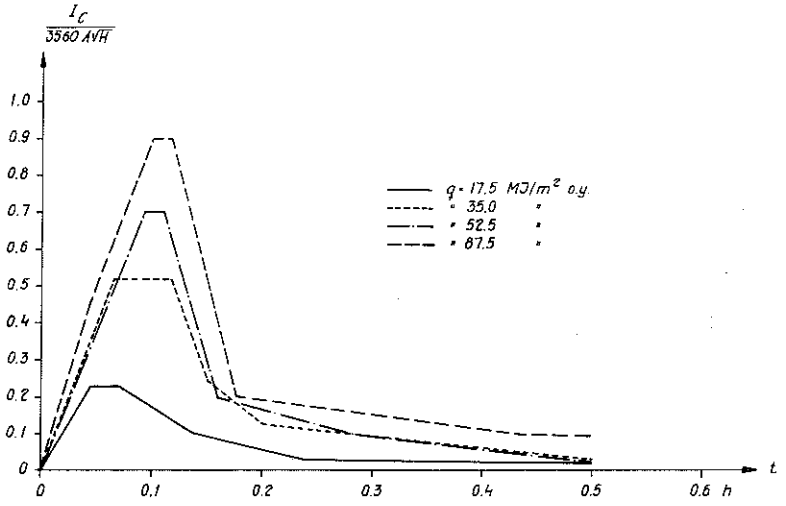

FIG 35 The theoretically calculated energy-time curve of the energy developed during the fire process for varying fire load, q (MJ/square meter of the enclosing surface). Opening factor, $A\sqrt{H}/A_t$ = 0.114 $m^{1/2}$, porosity factor, $\phi \approx 0.5$ $cm^{1.1}$. The enclosing structures of the fire cell are composed of 10 mm asbestos disk having a density of 1020 kg/m^3 and 1.5 mm steel sheet.

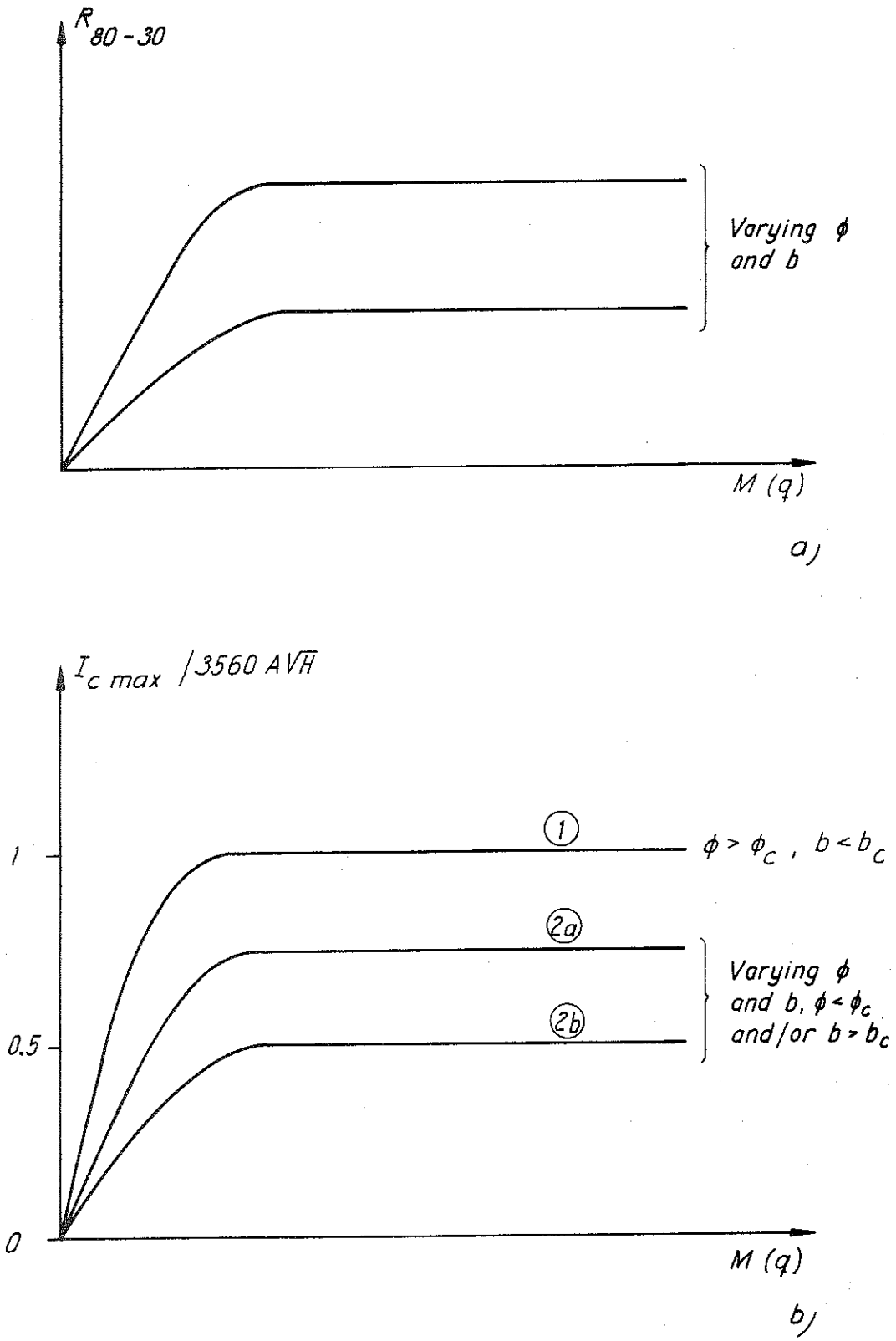

FIG 36 The fundamental relation between, on one side, the weight decrease per unit time, R_{80-30} or alternatively the maximum energy liberated per unit time, I_{Cmax} and on the other side, the fuel quantity, M, or the fire load, q.

TAB. III Characteristics and primary values with several magnitudes summarized for tests embracing a study of the influence of varying fire load and opening factor on the fire process.

$\frac{A\sqrt{H}}{A_t}$	ϕ	q_{teor}	q	$\frac{Q_a}{\varphi A\sqrt{H}}$	$R = 330A\sqrt{H}$	R_{80-30}	I_{Cmax}	t_m	I_{Cm}	t_r	I_{Cr}	R_r	$W_r = \frac{I_{Cr}}{R_r}$	t_d
$m^{1/2}$	$cm^{1,1}$	MJ/m^2 o.y.	MJ/m^2 o.y.		kg/h	kg/h	MJ/h	h	MJ/h	h	MJ/h	kg/h	MJ/kg	h
(1)	(2)	(3)	(4)	(5)	(6)	(7)	(8)	(9)	(10)	(11)	(12)	(13)	(14)	(15)
0.020	0.479	17.5	17.1	1.0	22.3	21.1	216	0.125	133	0.170	151	17.26	8.7	0.095
0.020	0.495	35.0	35.3	1.0	22.3	27.1	252	0.309	159	0.365	178	16.02	11.1	0.203
0.020	0.451	52.5	48.5	1.0	22.3	25.1	264	0.362	176	0.413	184	19.82	9.3	0.173
0.020	0.504	87.5	88.3	1.0	22.3	31.8	312	0.717	156	0.842	175	19.86	8.8	0.297
0.032	0.479	17.5	14.0	1.0	35.6	22.2	288	0.066	180	0.115	216	19.92	10.8	0.078
0.032	0.495	35.0	37.3	1.0	35.6	37.1	403	0.171	216	0.253	265	24.85	10.7	0.101
0.032	0.451	52.5	46.7	1.0	35.6	57.5	392	0.151	270	0.223	301	37.59	8.0	0.146
0.032	0.504	87.5	79.6	1.0	35.6	50.3	461	0.366	299	0.453	250	33.25	7.5	0.150
0.040	0.096	17.5	14.3	1.0	44.6	13.9	168	0.134	84	0.220	110	10.82	10.2	0.127
0.040	0.479	17.5	15.6	1.0	44.6	25.5	336	0.112	111	0.161	166	15.50	10.7	0.075
0.040	1.056	17.5	14.8	1.0	44.6	19.9	360	0.100	144	0.141	194	15.33	12.7	0.062
0.040	0.117	35.0	37.1	1.0	44.6	27.1	456	0.163	301	0.229	336	23.94	14.0	0.154
0.040	0.495	35.0	37.5	1.0	44.6	43.5	480	0.140	285	0.193	327	30.57	10.7	0.093
0.040	1.092	35.0	38.0	1.0	44.6	51.2	528	0.127	289	0.160	330	37.38	8.8	0.066
0.040	0.098	52.5	42.2	1.0	44.6	31.3	312	0.167	169	0.350	220	21.23	10.4	0.183
0.040	0.451	52.5	42.8	1.0	44.6	61.9	504	—	—	—	—	—	—	—
0.040	1.056	52.5	52.2	1.0	44.6	53.0	528	0.200	272	0.262	321	36.74	8.7	0.108
0.040	0.106	70.0	64.7	1.0	44.6	42.1	370	0.242	242	0.411	289	27.79	10.4	0.281
0.040	0.489	70.0	64.7	1.0	44.6	62.3	456	0.196	294	0.265	327	43.28	7.6	0.151
0.040	0.988	70.0	63.3	1.0	44.6	50.9	528	0.300	211	0.382	268	30.46	8.8	0.135
0.040	0.096	87.5	75.3	1.0	44.6	42.7	422	0.325	266	0.471	305	29.03	10.5	0.314
0.040	0.504	87.5	79.4	1.0	44.6	55.3	504	0.283	265	0.394	320	37.74	8.5	0.176
0.040	0.865	87.5	86.9	1.0	44.6	65.3	552	0.325	217	0.417	277	38.07	7.3	0.139
0.070	0.479	17.5	17.3	0.8	77.9	22.4	219	0.075	145	0.135	172	20.79	8.3	0.100
0.070	0.495	35.0	40.5	0.8	77.9	66.0	673	0.067	340	0.128	481	48.75	9.9	0.084
0.070	0.451	52.5	56.3	0.8	77.9	75.7	673	0.116	417	0.151	462	57.80	8.0	0.087
0.070	0.504	87.5	94.6	0.8	77.9	96.1	673	0.151	357	0.217	434	76.38	5.7	0.108
0.114	0.479	17.5	16.8	0.7	127.0	27.7	315	0.053	197	0.097	237	26.66	8.9	0.068
0.114	0.495	35.0	37.9	0.7	127.0	59.3	712	0.092	453	0.133	523	42.97	12.2	0.083
0.114	0.451	52.5	53.7	0.7	127.0	91.3	958	0.100	520	0.125	593	68.02	8.7	0.056
0.114	0.504	87.5	89.2	0.7	127.0	134.0	1232	0.109	710	0.135	791	111.58	7.1	0.063

I_{Cd}	R_d	$W_d=\frac{I_{Cd}}{R_d}$	t_1	t_2	t_g	I_{Cg}	R_g	$W_g=\frac{I_{Cg}}{R_g}$	I_{Cav}	W_{av}	ϑ_{80-30}	$\frac{R_{80-30}}{\vartheta_{80-30}}$	$\frac{I_{Cav}}{\theta_{80-30}}$	Försök nr
MJ/h	kg/h	MJ/kg	h	h	h	MJ/h	kg/h	MJ/kg	MJ/h	MJ/kg	°C	kg/°C·h	MJ/°C·h	
(16)	(17)	(18)	(19)	(20)	(21)	(22)	(23)	(24)	(25)	(26)	(27)	(28)	(29)	(30)
196	10.35	18.9	0.030	0.237	0.722	44	0.50	88.0	166	7.86	489	0.043	0.34	BB4
240	22.17	10.8	0.066	0.422	0.740	72	1.25	57.6	218	8.05	724	0.037	0.30	C49
236	19.35	12.2	0.205	0.427	1.658	52	0.70	74.3	185	7.39	605	0.041	0.31	BB16
287	6.01	47.7	0.154	0.679	2.432	61	0.12	508.3	134	4.21	515	0.062	0.26	BB10
267	19.10	14.0	0.043	0.125	0.338	66	1.21	54.5	262	11.81	538	0.041	0.49	BB40
370	24.61	15.0	0.045	0.137	0.605	95	1.45	65.6	304	8.19	747	0.050	0.40	C38
366	36.16	10.1	0.082	0.215	2.560	35	0.25	140.0	331	5.76	699	0.082	0.47	BB33
239	19.23	12.4	0.080	0.180	3.060	50	0.10	500.0	194	3.85	548	0.092	0.35	BB46
152	9.97	15.3	0.097	0.268	0.415	57	0.89	64.0	131	9.48	305	0.046	0.43	BB56
313	20.39	15.4	0.036	0.139	0.250	100	2.09	47.8	302	11.86	543	0.047	0.55	BB58
322	19.36	16.6	0.030	0.082	0.175	99	4.01	24.7	295	14.79	542	0.037	0.54	BB60
418	25.92	16.1	0.047	0.196	0.378	125	4.36	28.6	418	15.40	775	0.035	0.53	C31
453	39.49	11.5	0.037	0.251	0.474	131	2.73	48.0	427	9.82	732	0.059	0.58	C27
485	40.71	11.9	0.026	0.244	0.631	118	2.10	56.2	398	7.78	716	0.071	0.55	C23
361	24.79	14.6	0.140	0.258	0.882	73	0.80	91.3	258	8.24	545	0.058	0.47	BB50
–	–	–	–	–	–	–	–	–	–	–	–	–	–	BB52
483	30.48	15.8	0.055	0.147	2.169	42	0.21	200.0	304	5.72	586	0.090	0.52	BB54
351	37.39	9.4	0.112	0.277	1.947	50	0.55	90.9	352	8.36	724	0.059	0.48	BB68
421	40.98	10.3	0.070	0.141	3.204	41	0.31	132.3	338	5.43	678	0.092	0.50	BB70
480	31.53	15.2	0.068	0.185	3.300	34	0.17	200.0	288	5.66	575	0.089	0.50	BB72
384	28.26	13.6	0.087	0.263	1.463	74	0.58	127.6	344	8.06	698	0.061	0.49	BB62
465	31.70	14.7	0.077	0.242	2.691	52	0.16	325.0	277	5.01	548	0.101	0.50	BB64
499	35.44	14.1	0.108	0.216	2.603	68	0.34	200.0	263	4.02	503	0.130	0.52	BB66
198	17.46	11.4	0.068	0.201	0.779	45	0.67	67.2	190	8.48	323	0.070	0.59	BB76
631	59.61	10.6	0.014	0.165	0.606	122	2.54	47.9	647	9.81	753	0.088	0.86	C16
615	54.92	11.2	0.026	0.177	1.678	70	0.67	104.5	524	6.93	737	0.103	0.71	BB82
615	61.83	9.9	0.050	0.270	3.504	64	0.48	133.3	446	4.64	634	0.152	0.70	BB94
289	22.71	12.7	0.021	0.086	0.909	35	0.72	48.6	286	10.33	340	0.082	0.84	BB112
676	52.31	12.9	0.016	0.067	0.464	120	3.36	35.7	698	11.77	641	0.142	1.09	C7
875	72.04	12.1	0.018	0.062	2.590	40	0.71	56.4	735	8.05	685	0.133	1.07	BB106
1122	93.46	12.0	0.019	0.038	1.958	97	1.09	88.9	799	5.96	773	0.173	1.03	BB118

with the porosity factor, ϕ, of the fire load q and the stick thickness, b. Conventionally a fire process is defined as ventilation controlled if the mean combustion rate, R_{80-30}, is independent of the variations in the fuel quantity, M, irrespective of the R_{80-30}-level at which this is valid. For lower values of the fuel quantity, M, than those corresponding to the above-mentioned R_{80-30}-levels, the fire process is denoted as fuel bed controlled. For a more differentiated characterization of the fire process, c.f. Section 8.

With the maximum energy per unit time, I_{Cmax}, as the decisive parameter analogous concept definitions can, on the whole, be applied, cf. FIG 36 b). With a given shape of the fire cell, the maximum energy, I_{Cmax}, is approximately independent of the properties of the fire load beyond a certain fuel quantity, M, and for a porosity factor, ϕ, and a stick thickness, b, which are larger than a certain characteristic value, ϕ_c, and smaller than a characteristic value b_c respectively. On this occasion, the fire process can be strictly defined as ventilation controlled. The corresponding I_{Cmax}-level is characterized by the relation $I_{Cmax}/3560\ A\sqrt{H} \approx 1$. In the other cases I_{Cmax} is dependent of the properties of the fire load and is therefore fuel bed controlled. For $\phi > \phi_c$ and $b < b_c$ (curve (1) in FIG 36 b)) I_{Cmax} varies only approximately with fuel quantity, M, or fire load, q, within the fuel bed controlled range of the fire process. For $\phi < \phi_c$ and/or $b > b_c$, I_{Cmax} is, for low values of the fuel quantity, M, dependent of both the size of the fire load, q, and its porosity factor, ϕ, and stick thickness, b. With increasing fuel quantity, M, I_{Cmax} reaches a limiting value whose level varies with the porosity factor of the fire load, ϕ, and stick thickness, b. For these levels (curves (2a) and (2b) in FIG 36 b)) I_{Cmax} is approximately independent of the size of the fire load, q. In the following discussion, relating the fire process to the magnitude I_{Cmax}, a fire is defined as ventilation controlled only if the level $I_{Cmax}/3560\ A\sqrt{H} \approx 1$ is reached. In this concept ventilation controlled fire has also been used previously in the brief discussion in section 4. In all the other cases the fire process is defined as fuel bed controlled irrespective of whether one or several fire load characterizing parameters are acting.

With the energy magnitudes I_{Cd} and I_{Cav} as decisive parameters, concept definitions related to those applied for R_{80-30} seems to be the most practical. This implies that a fire process is defined as ventilation controlled if I_{Cd} and I_{Cav} have reached such a level that the magnitudes are independent of the variations in the size of the fire load irrespective of the I_{Cd}- or I_{Cav}-level for which this is true. In the other cases the fire process is fuel bed controlled by definition.

With these introductory concept definitions as the background, in the following, the fire process characterizing magnitudes described in FIG 29-35 and in TAB III are discussed.

For the maximum energy, I_{Cmax}, the following can be established. For both of the lowest opening factors, $A\sqrt{H}/A_t$ = 0.020 and 0.032 $m^{1/2}$ in FIG 29 and 30, the obtained I_C-t curves exhibit a somewhat irregular relation. This fact is expecially striking for the opening factor $A\sqrt{H}/A_t$ = 0.020 $m^{1/2}$. On the whole the maximum energy I_{Cmax} increases with increasing fire load, q. In these cases the I_{Cmax}-level indicates a fuel bed controlled process for both of the opening factors with the lowest q = 17.5 MJ/m^2 of the enclosing surface, while for the other described fire loads the process is almost ventilation controlled. A heavy shifting towards a slower fire process development with increasing fire load, q, is noteworthy, especially for the lowest opening factor. The established facts which are further substantiated by the data summarized in TAB III verify the relation mentioned in the previous section, namely that the characteristics of the fire process for fire cells having small window openings are extremely complicated with a large number of influencing agents which at present are very incompletely dealt with. It is interesting to note the results of the tests performed by Thomas-Heselden-Law (1967) by which they have found out that when a wood piece is placed in an incombustible atmosphere such as nitrogen, it disintegrates with almost the same rate which is true for combustion in the open air, when exposed to radiation.

In the FIG 31-33 which for the opening factor $A\sqrt{H}/A_t$ = 0.040 $m^{1/2}$ illustrate the influence of a varying porosity factor, ϕ, of the

fire load the relation obtained in the previous section is verified, namely that the changes in the porosity factor, ϕ, within the range $\phi \gtrsim 0.5$ cm$^{1.1}$ do not considerably affect the energy-time curve of the fire process. According to FIG 32 and 33, the fire process is, within this ϕ-range ventilation controlled with the opening factor $A\sqrt{H}/A_t = 0.040$ m$^{1/2}$ and for $q \geq 35$ MJ/m^2 of the enclosing surface. For the lowest investigated fire load $q = 17.5$ MJ/m^2 of the enclosing surface the fire process is, on the contrary, fuel bed controlled with a value for $I_{Cmax}/3560\ A\sqrt{H}$ amounting to approximately 0.7. Within the porosity factor range $\phi < 0.5$ cm$^{1.1}$, a decrease of the ϕ-value results in a successively slower fire process and a lower energy development during the flaming phase, which is illustrated by FIG 31 and 32 for comparison. For the porosity factor $\phi \approx 0.1$ cm$^{1.1}$ and with the opening factor, $A\sqrt{H}/A_t = 0.040$ m$^{1/2}$, the fire process is fuel bed controlled for all the values of the fire load studied. Moreover, for this low porosity factor the general picture of the fire process is less unique than that for porosity factors within the range $\phi \gtrsim 0.5$ cm$^{1.1}$.

For the opening factor $A\sqrt{H}/A_t = 0.07$ m$^{1/2}$, the obtained energy-time curves in FIG 34 illustrate a fire process which is of the fuel bed controlled type for all the values of the fire load studied within the range $q = 17.5 - 87.5$ MJ/m^2 of the enclosing surface. With increasing fire load, q, the maximum energy, I_{Cmax}, increases up to the level $I_{Cmax}/3560\ A\sqrt{H} \approx 0.8$ which is already reached for the fire load $q = 35$ MJ/m^2 of the enclosing surface. At this level, which is related to the porosity factor $\phi \approx 0.5$ cm$^{1.1}$, the maximum energy is almost independent of the variations in the size of the fire load. However, this level most probably varies with such parameters as porosity factor and stick thickness which is indicated by FIG 32 and 33 for the opening factor $A\sqrt{H}/A_t = 0.040$ m$^{1/2}$. For the opening factor $A\sqrt{H}/A_t = 0.114$ m$^{1/2}$ the energy-time curves described in FIG 35 constantly exhibit a fuel bed controlled process. With increasing fire load, q, the maximum energy I_{Cmax} increase continuously without upper limiting level reaching its value, within the investigated fire load range of $q = 17.5 - 87.5$ MJ/m^2 of the enclosing surface.

A summary of the maximum energy, I_{Cmax}, obtained from FIG 29-35 and TAB III, as a function of the opening factor, $A\sqrt{H}/A_t$, and fire load, q, with the porosity factor $\phi \approx 0.5$ cm$^{1.1}$ results in the graphical relations described in FIG 37. From these relations it is observed that within the opening factor range of $A\sqrt{H}/A_t = 0.02 - 0.07$ m$^{1/2}$, $I_{Cmax}/3560\ A\sqrt{H}$ is rather slightly dependent of the variations in the size of the fire load, q, for $q \geq 35$ MJ/m^2 of the enclosing surface. For the same fire load range, that is $q \geq 35$ MJ/m^2 of the enclosing surface, the variation of $I_{Cmax}/3560\ A\sqrt{H}$ with the size of the fire load, q, is however significant for the opening factor $A\sqrt{H}/A_t > 0.07$ m$^{1/2}$. This dependence increases with increasing opening factor. For the fire loading $q < 35$ MJ/m^2 of the enclosing surface, FIG 37 gives a considerable variation in $I_{Cmax}/3560\ A\sqrt{H}$ with the fire load, q, within the whole range studied for the opening factor. If $I_{Cmax}/3560\ A\sqrt{H} \geq 1$ is chosen as the criterium for a ventilation controlled fire process, it is seen from FIG 37 that such a type of fire process, strictly speaking, existed in the described test series only within the range $A\sqrt{H}/A_t \leq 0.04$ m$^{1/2}$, $q \geq 35$ MJ/m^2 of the enclosing surface.

With the largest studied opening factor, $A\sqrt{H}/A_t = 0.114$ m$^{1/2}$, for which the investigated fire process has constantly been fuel bed controlled, the fire process characteristics can be estimated to lie close to conditions prevailing for the fire in the open air with the differences which can be caused by variations in the flow of the combustion air and smoke gases through the wooden stick pile in both cases. Cf. FIG 38 which for this opening factor and for the porosity factor $\phi \approx 0.5$ cm$^{1.1}$ shows the variations in $I_{Cmax}/3560\ A\sqrt{H}$ with the fire load , q.

From a comparison between the different energy-time curves in FIG 29-35, it is observed that the rate of development of the fire process varies considerably. For a closer illustration of this fact, the time interval, t_m, from ignition to the mean time for I_{Cmax} reaching its maximum value is summarized in FIG 39, as a function of the opening factor $A\sqrt{H}/A_t$ and the fire load, q, with the porosity factor $\phi \approx 0.5$ cm$^{1.1}$. From this summary it follows that the dependence of t_m-s on the size of the fire load is very great with small values of the opening factor $A\sqrt{H}/A_t$. This depen-

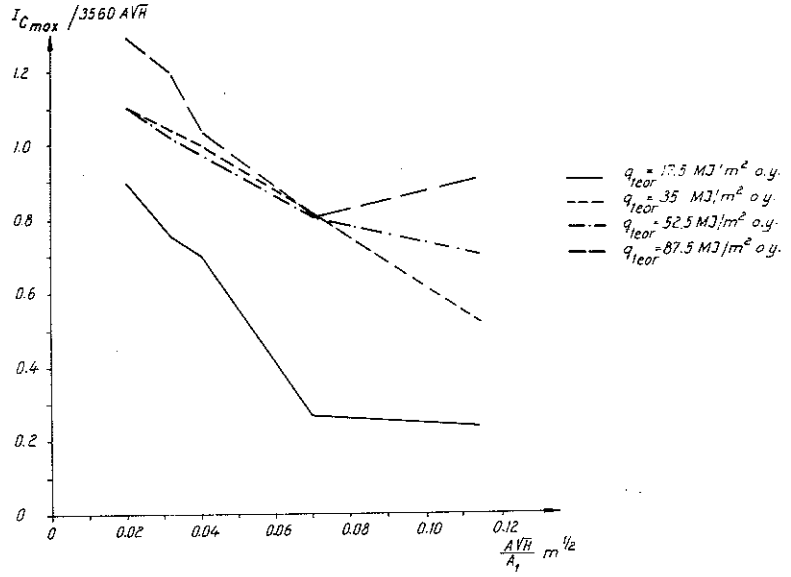

FIG 37 The relation calculated from the obtained test results between the maximum energy liberated per unit time, I_{Cmax}, and the opening factor of the fire cell, $A\sqrt{H}/A_t$, for four different values of the fire load, q. Porosity factor of the fuel $\phi \approx 0.5$ $cm^{1.1}$. The enclosing structures of the fire cell are composed of 10 mm asbestos disk having a density of 1020 kg/m^3 and 1.5 mm steel sheet.

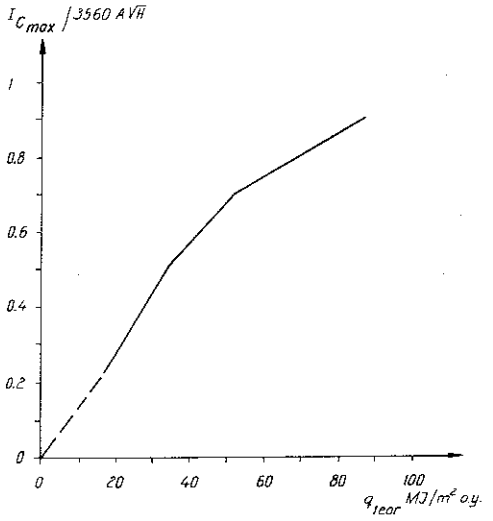

FIG 38 The relation calculated from the obtained test results between the maximum energy liberated per unit time, I_{Cmax}, and the fire load, q. Opening factor $A\sqrt{H}/A_t$ = 0.114 $m^{1/2}$, porosity factor of the fuel $\phi \approx 0.5$ $cm^{1.1}$. The enclosing structures of the fire cell are composed of 10 mm asbestos disk having a density of 1020 kg/m^3 and 1.5 mm steel sheet.

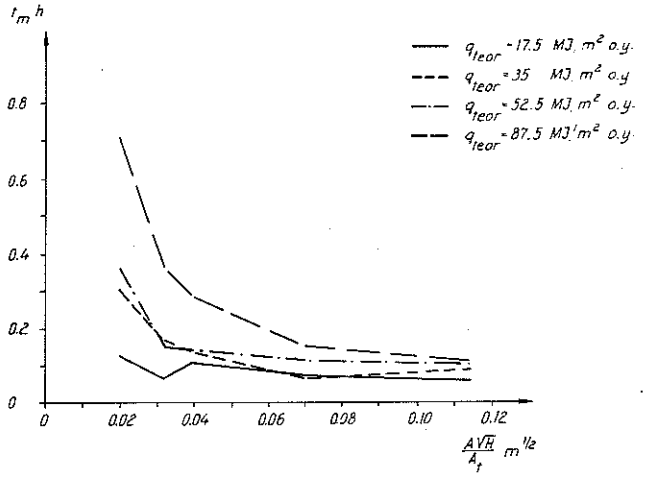

FIG 39 The relation calculated from the test results between the time magnitude, t_m (cf FIG 18) and the opening factor of the fire cell, $A\sqrt{H}/A_t$, for four different values of the fire load q_{theor}. The porosity factor $\phi \approx 0.5$ $cm^{1.1}$. The enclosing structures of the fire cell are composed of 10 mm asbestos disk having a density of 1020 kg/m^3 and 1.5 mm steel sheet.

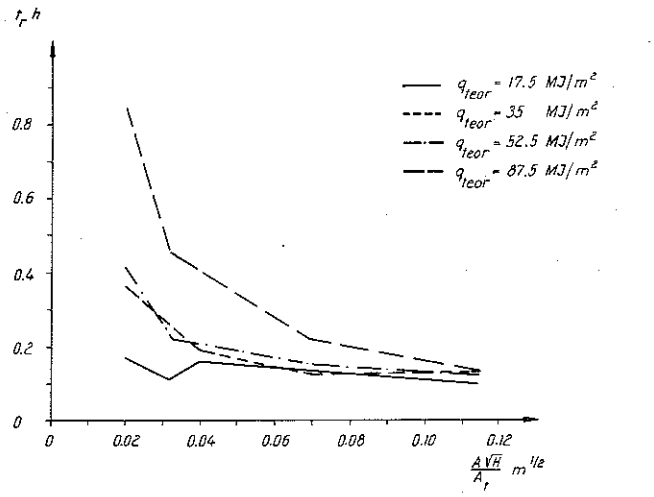

FIG 40 The relation calculated from the obtained test results between the time magnitude, t_r, and the opening factor of the fire cell, $A\sqrt{H}/A_t$, for four different values of the fire load q_{theor}. Porosity factor of the fuel $\phi \approx 0.5$ $cm^{1.1}$. The enclosing structures of the fire cell are composed of 10 mm asbestos disk having a density of 1020 kg/m^3 and 1.5 mm steel sheet.

dence decreases with increasing opening factor and from $A\sqrt{H}/A_t \approx$ $\approx 0.07\ m^{1/2}$ becomes of less practical significance considering the precision level relevant in design applications. With very small values of the fire load, $q = 17.5\ MJ/m^2$ of the enclosing surface, the time interval, t_m, is according to FIG 39 almost independent of the variations in the opening factor.

As a further complementary illustration of variations in the rate of development of the fire process, the dependence of the t_r-s interval on the opening factor $A\sqrt{H}/A_t$ and the fire load q with the porosity factor $\phi \approx 0.5\ cm^{1.1}$, is summarized in FIG 40, Here, t_r embraces the time interval from ignition to the time corresponding to $0.75\ I_{Cmax}$ on the descending part of the energy-time curve, cf. FIG 18. Essentially, the same fundamental relations are true for t_r as those established above for the time interval t_m.

In a comparison with the energy-time curves developed and applied by Magnusson-Thelandersson (1970) as shown in FIG 4 and 37, it is observed that in the works by Magnusson-Thelandersson, the level of the maximum energy is generally overestimated for small values of the fire load and within the opening factor range of $A\sqrt{H}/A_t \gtrsim$ $\gtrsim 0.04\ m^{1/2}$ for fire loadings $q \gtrsim 35\ MJ/m^2$ of the enclosing surface. For large opening factors, $A\sqrt{H}/A_t = 0.10 - 0.12\ m^{1/2}$, this overestimation increases with decreasing fire load q. With a very small opening factor, $A\sqrt{H}/A_t = 0.02\ m^{1/2}$, the design procedure given and applied by Magnusson-Thelandersson implies a certain underestimation of the level for I_{Cmax}, which is mostly marked for large values of the fire load.

An estimation of the above-mentioned over- and underestimations in the level of the maximum energy, I_{Cmax}, should be coordinated with a complementary comparison between the experimentally obtained results and the data used by Magnusson-Thelandersson for some critical time interval, that is either t_m or t_r. Here, this comparison is chosen to be based on t_r, which in Magnusson-Thelandersson's case corresponds to the time 1.25 T where T is determined by Eq. (25), cf. even FIG 4. For this reason, the curves described in FIG 41 have been calculated for the time 1.25 T as a

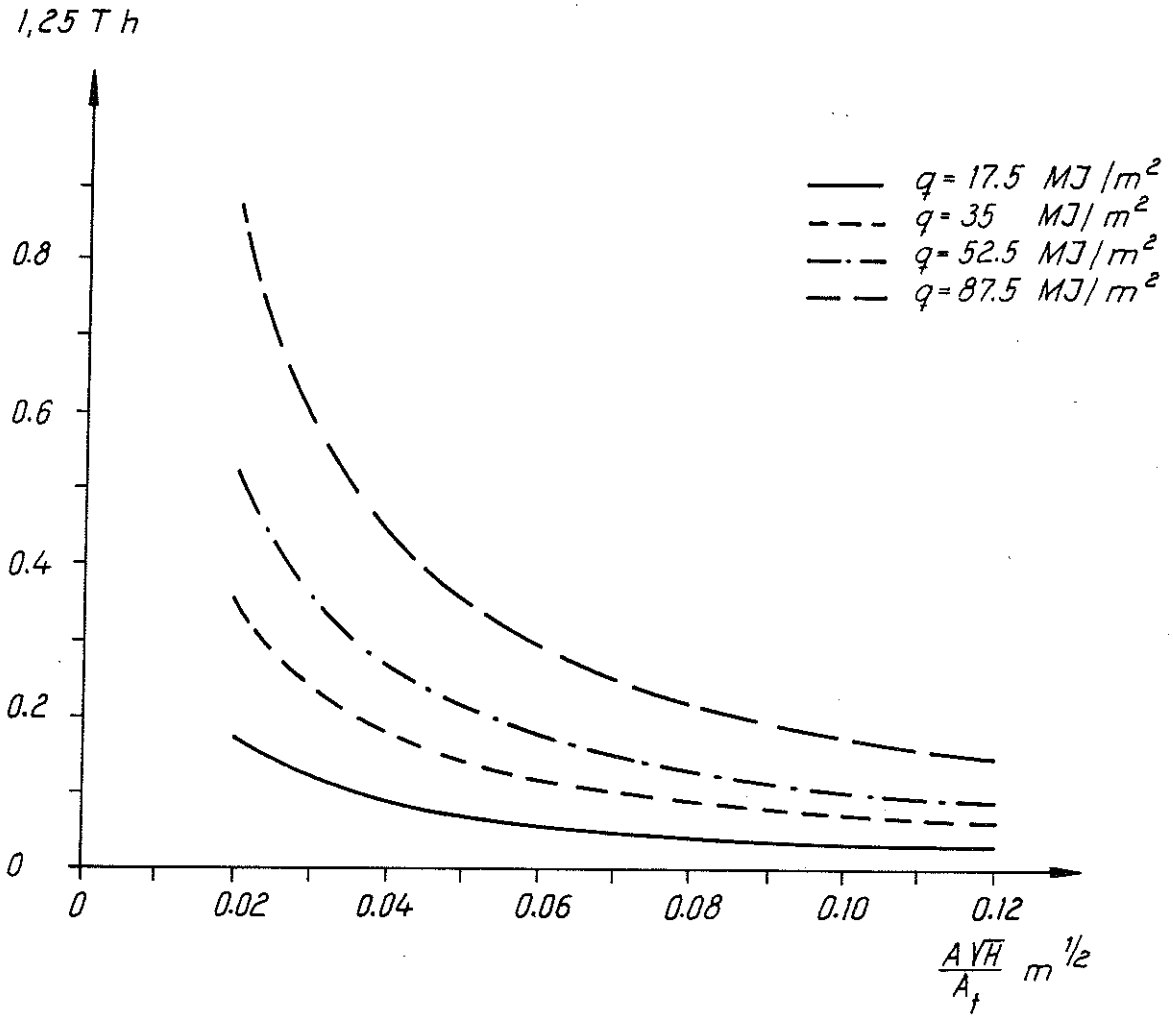

FIG 41 The relation calculated from Eq. (25) for the time magnitude 1.25 T ≈ t_r as a function of the opening factor, $A\sqrt{H}/A_t$, and size of the fire load q.

function of the opening factor $A\sqrt{H}/A_t$ and the fire load q. A direct comparison between FIG 40 and 41 shows that for the highest value of the fire load studied, q = 87.5 MJ/m^2 of the enclosing surface, both of the magnitudes t_r and 1.25 T are in good agreement within the whole range of the opening factor described. The influence of the above established over- and underestimations of I_{Cmax} on the fire process is therefore unmodified for this level of fire load. For a fire process which is genuinely ventilation controlled - cf. FIG 37 - the agreement between the theoretical magnitude 1.25 T and the experimentally obtained t_r is further good. For the lowest analyzed fire load, q = 17.5 MJ/m^2 of the enclosing surface, the time magnitude, 1.25 T, applied by Magnusson-Thelandersson is considerably smaller than the corresponding experimentally obtained time magnitude, t_r, for the range $A\sqrt{H}/A_t \approx 0.03$ m$^{1/2}$ which with respect to the fire process acts towards a compensation of the overestimation in the maximum energy, I_{Cmax}, which is here the case in Magnusson-Thelandersson's analysis. For the interjacent values of the fire load, the characteristics are interpolations of those established for the highest and the lowest fire loads.

The trends, which have been discussed above and which have been arrived at on the basis of theoretically calculated energy-time curves based on experiments, principally agree with, for instance, the results from full scale tests, Heselden (1968), which have been referred to in Section 5.1.

In the present section, alternative parameters for the combustion rate - R_{80-30}, I_{Cmax}, I_{Cd}, I_{Cav} - determining whether a fire process is fuel bed controlled or ventilation controlled, have been mentioned as an introduction. Brief definitions have also been introduced for both types of the fire process when applying the different parameters for the combustion rate. Based on the test results summarized in TAB III, these alternative methods are exemplified in the following for a characterization of a fire process for comparative purposes.

With respect to the type of a fire process, the discussion carried out above, pertaining to the maximum energy liberated per unit time, I_{Cmax}, can be summarized according to TAB IV, column 3 in which F denotes a fuel bed controlled and V a ventilation control-

TAB. IV Characterization of the tests summarized in TAB. III, with respect to fuel bed controlled (F) and ventilation controlled (V) fire processes with different magnitudes, I_{Cmax}, R_{80-30}, I_{Cd} and I_{Cav} as decisive parameters.

$\frac{A\sqrt{H}}{A_t}$	q_{teor}	I_{Cmax}	R_{80-30}	I_{Cd}	I_{Cav}
$m^{1/2}$	MJ/m^2 o.y.	MJ/h	kg/h	MJ/h	MJ/h
(1)	(2)	(3)	(4)	(5)	(6)
0.020	17.5	F	F	F, V	F, V
	35	V	F (V)	V	V
	52.5	V	F (V)	V	V
	87.5	V	F (V)	V	V
0.032	17.5	F	F	F	F, V
	35	V	F (V)	V	V
	52.5	V	V	V	V
	87.5	V	V	V	V
0.040	17.5	F	F	F	F
	35	V	F (V)	V	V
	52.5	V	V	—	—
	70	V	V	V	V
	87.5	V	V	V	V
0.070	17.5	F	F	F	F
	35	F	F	V	V
	52.5	F	F (V)	V	V
	87.5	F	F (V)	V	V
0.114	17.5	F	F	F	F
	35	F	F	F	F, V
	52.5	F	F	F	F, V
	87.5	F	V	F	F, V

led fire process - cf. also FIG 37.

With reference to the alternative parameter, that is to say the mean combustion rate, R_{80-30}, related to the weight decrease of the fire load per unit time, a fire process is conventionally defined as ventilation controlled if the mean combustion rate, R_{80-30}, with a given shape of the fire cell is independent of the variations in the fuel quantity, M, or the size of the fire load, q, FIG 36 a). With a successive increase of the fire load, q, the R_{80-30}-level corresponding to a ventilation controlled process is reached for a certain characteristic value of the fire load. For a lower value of the fire load, the fire process is, by difinition, fuel bed controlled. For fire loads above the characteristic value, it is natural to describe the fire process as ventilation controlled even if the mean combustion rate falls below the previously mentioned R_{80-30}-level with increasing fire load.

With such a definition, the experimental R_{80-30}-values described in TAB III, column 7, lead to a fire process characterization as in TAB IV, column 4, where the notations are without parenthesis. From this table it is observed that differences in relation to the corresponding characterization of the energy parameter, I_{Cmax}, exist for the fire load range $q \gtrsim 35$ MJ/m^2 of the enclosing surface with the opening factor $A\sqrt{H}/A_t = 0.020$ m$^{1/2}$, for the fire load $q = 35$ MJ/m^2 of the enclosing surface with the opening factors $A\sqrt{H}/A_t$ = = 0.032 and 0.040 m$^{1/2}$, and for the fire load $q = 87.5$ MJ/m^2 of the enclosing surface with $A\sqrt{H}/A_t = 0.114$ m$^{1/2}$. If the definition of the fire process based on the mean combustion rate is modified so that a fire process is described as ventilation controlled if

$$R_{80-30} \geq R_1 = 5.5\, A\sqrt{H} \quad \text{(kg wood/min)} \tag{26}$$

Cf. Eq. 14 and TAB III, column 6, then the fire process characterization is changed according to the given notations inside parentheses in TAB IV, column 4. Thereby, agreement with the characterization based on the energy magnitude, I_{Cmax}, is improved for the three lowest values of the opening factor $A\sqrt{H}/A_t = 0.020$, 0.032 and 0.040 m$^{1/2}$. At the same time, new deviations are however introduced for high values of the fire load with the opening factor

$A\sqrt{H}/A_t = 0.070$.

With the energy magnitudes I_{Cd} and I_{Cav} as decisive parameters for determination of the type of the fire process, it is, as mentioned earlier, natural to apply the same difinitions as when the mean combustion rate R_{80-30} is decisive. With increasing fire load, q, in addition to a given shape of the fire cell, a level is reached for I_{Cd} and I_{Cav} which is characterized by the fact that the respective energy magnitude is almost uninfluenced by the variations in the size of the fire load. This level is reached for a certain characteristic fire load. For lower values of the fire load, the fire process is fuel bed controlled while for higher values the process is ventilation controlled.

With such a definition, TAB III, columns 16 and 25 gives a fire process characterization according to TAB IV, columns 5 and 6, for the actual test series, cf. also FIG 42 and 43. The notation (F, V) herein means that the type of the fire process is difficult to estimate in relation to fuel bed controlled (F) or ventilation controlled (V) conditions. Excluding the cases which are difficult to characterize and choosing I_{Cd} and I_{Cav} as the basis of the described test series results in TAB IV give a consistent description of the type of the fire process. In comparison with the description based on the energy magnitude I_{Cmax}, deviations are obtained with I_{Cd} and I_{Cav} as decisive parameters for the fire load range $q \approx 35$ MJ/m^2 of the enclosing surface with the opening factor $A\sqrt{H}/A_t = 0.070$ m$^{1/2}$.

Further alternatives characterizing the fire process are, for instance, I_{Cm} and I_{Cr}, that is the mean value of the energy liberated per unit time during the time intervals t_m and t_r respectively. These magnitudes are illustrated in FIG 44 and 45 as functions of the opening factor, $A\sqrt{H}/A_t$, and the fire load, q. Principially, this complementary description does not contribute to anything new as far as the analysis of the type of fire process concerned why further comments have been deemed to be unnecessary.

From the above discussion it is observed that a characterization of the type of the fire process, in certain cases, depends on

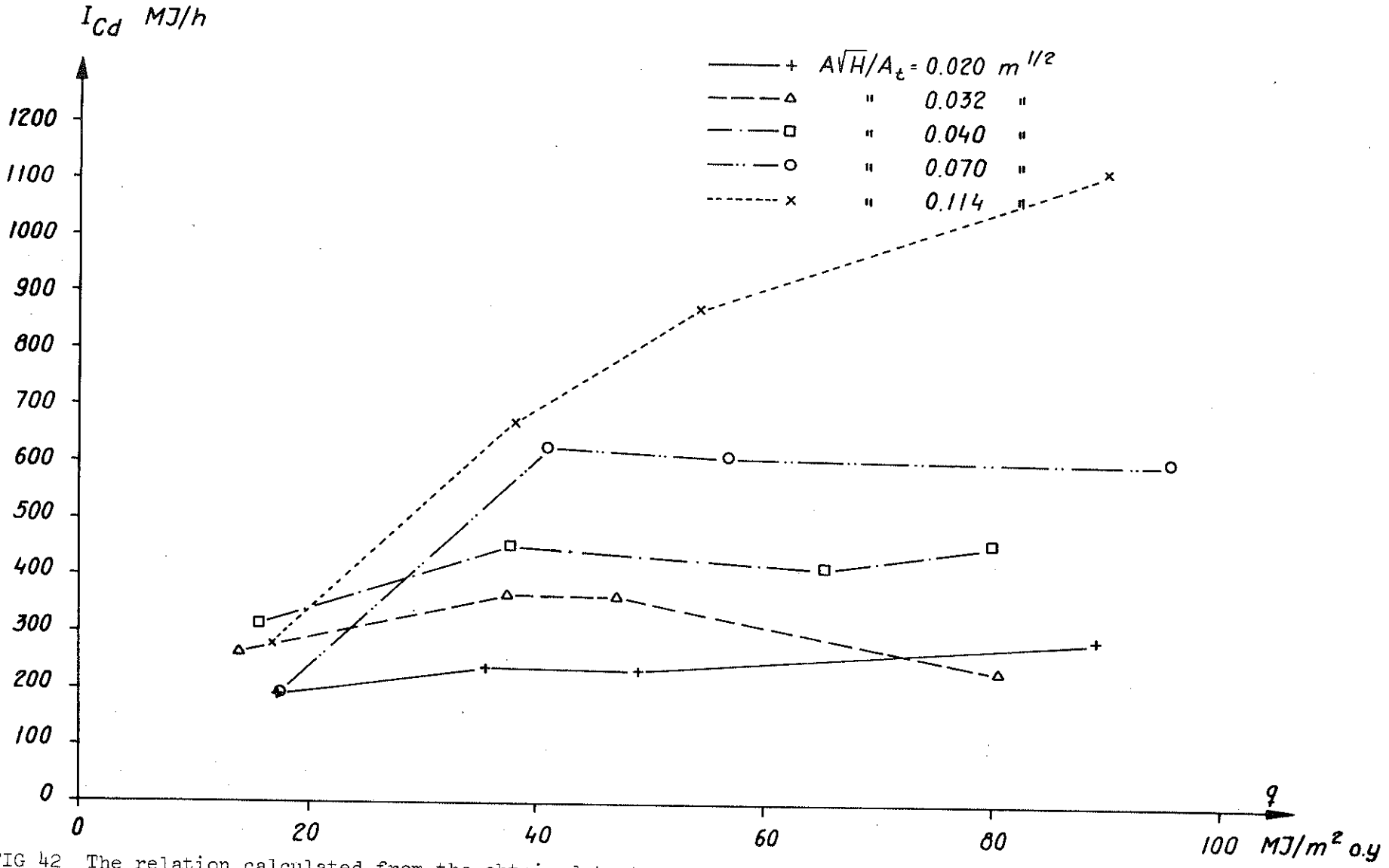

FIG 42 The relation calculated from the obtained test results between I_{Cd} (MJ/h) and the fire load, q (MJ/square meter of the enclosing surface) for varying opening factor, $A\sqrt{H}/A_t$ ($m^{1/2}$). The porosity factor, $\phi \approx 0.5$ $cm^{1.1}$. The enclosing structures of the fire cell are composed of 10 mm asbestos disk having a density of 1020 kg/m^3 and 1.5 mm steel sheet.

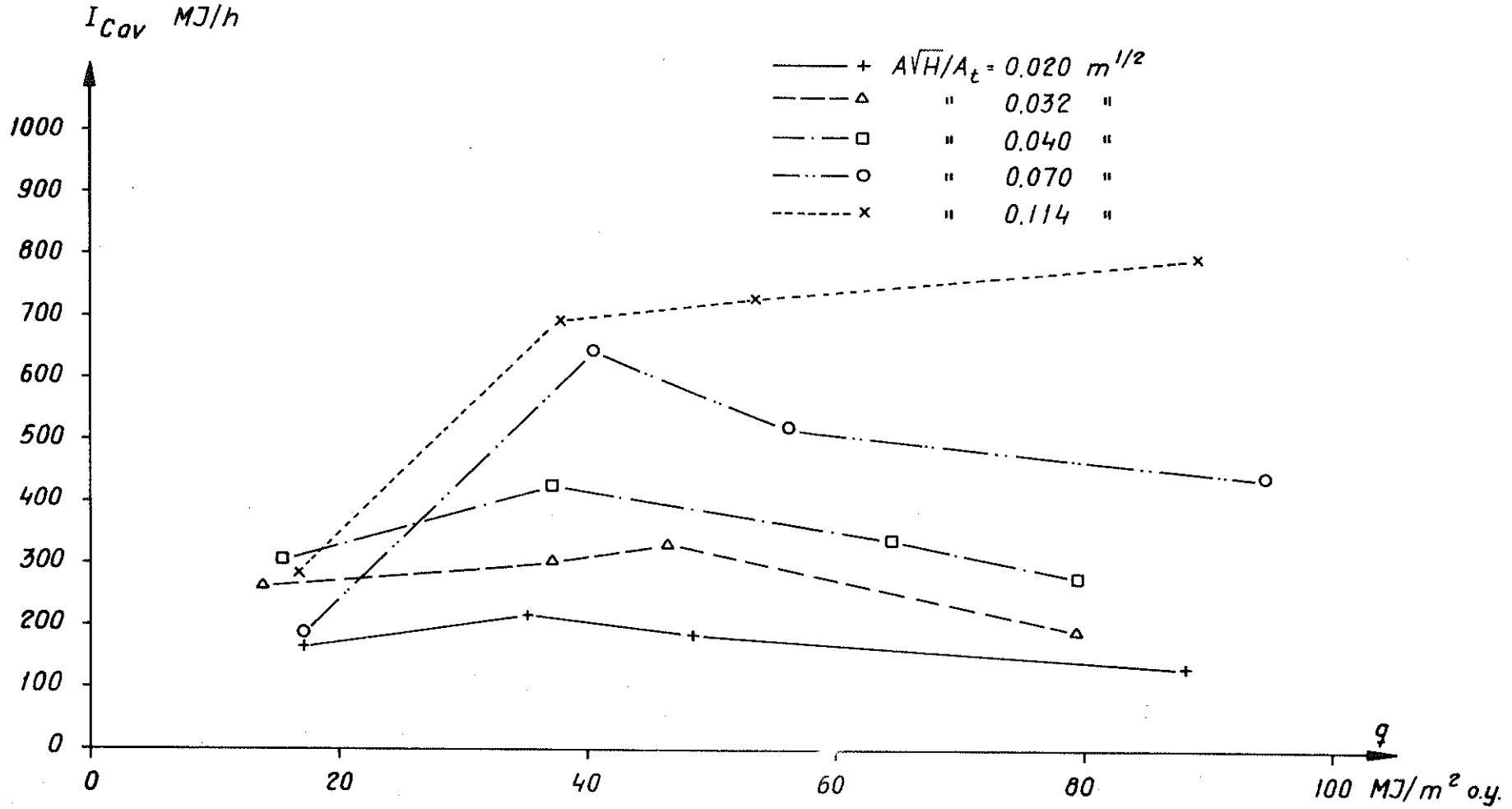

FIG 43 The relation calculated from the obtained test results between the mean value of the released energy, I_{Cav} (MJ/h) and the fire load, q (MJ/square meter of the enclosing surface) for varying opening factor, $A\sqrt{H}/A_t$ ($m^{1/2}$). Porosity factor, $\phi \approx 0.5$ $cm^{1.1}$. The enclosing structures of the fire cell are composed of 10 mm asbestos disk having a density of 1020 kg/m^3 and 1.5 mm steel sheet.

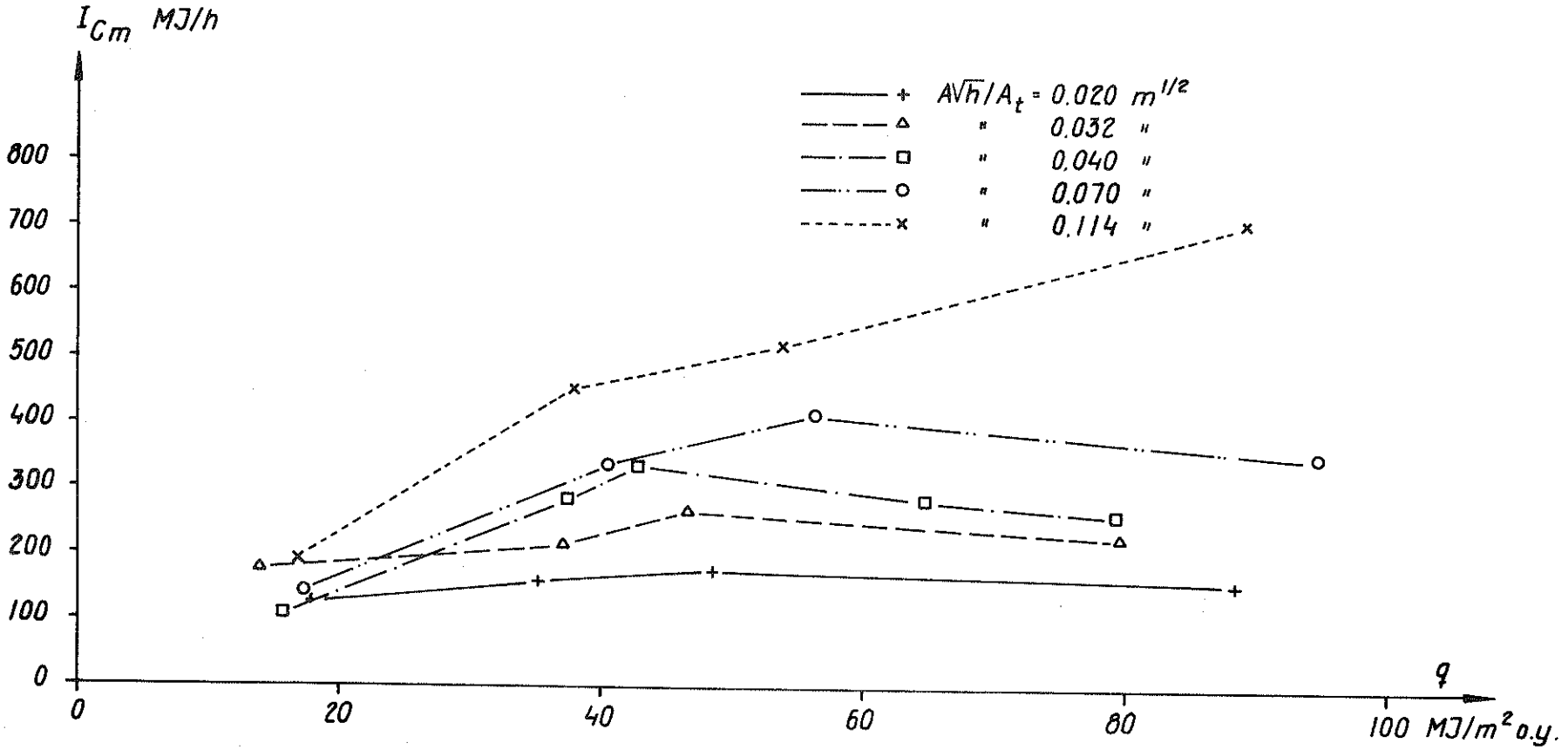

FIG 44 The relation calculated from the obtained test results between I_{Cm} (MJ/h) and the fire load, q (MJ/square meter of the enclosing surface) for varying opening factor, $A\sqrt{H}/A_t$ ($m^{1/2}$). The porosity factor $\phi \approx 0.5$ $cm^{1.1}$. The enclosing structures of the fire cell are composed of 10 mm asbestos disk having a density of 1020 kg/m^3 and 1.5 mm steel sheet.

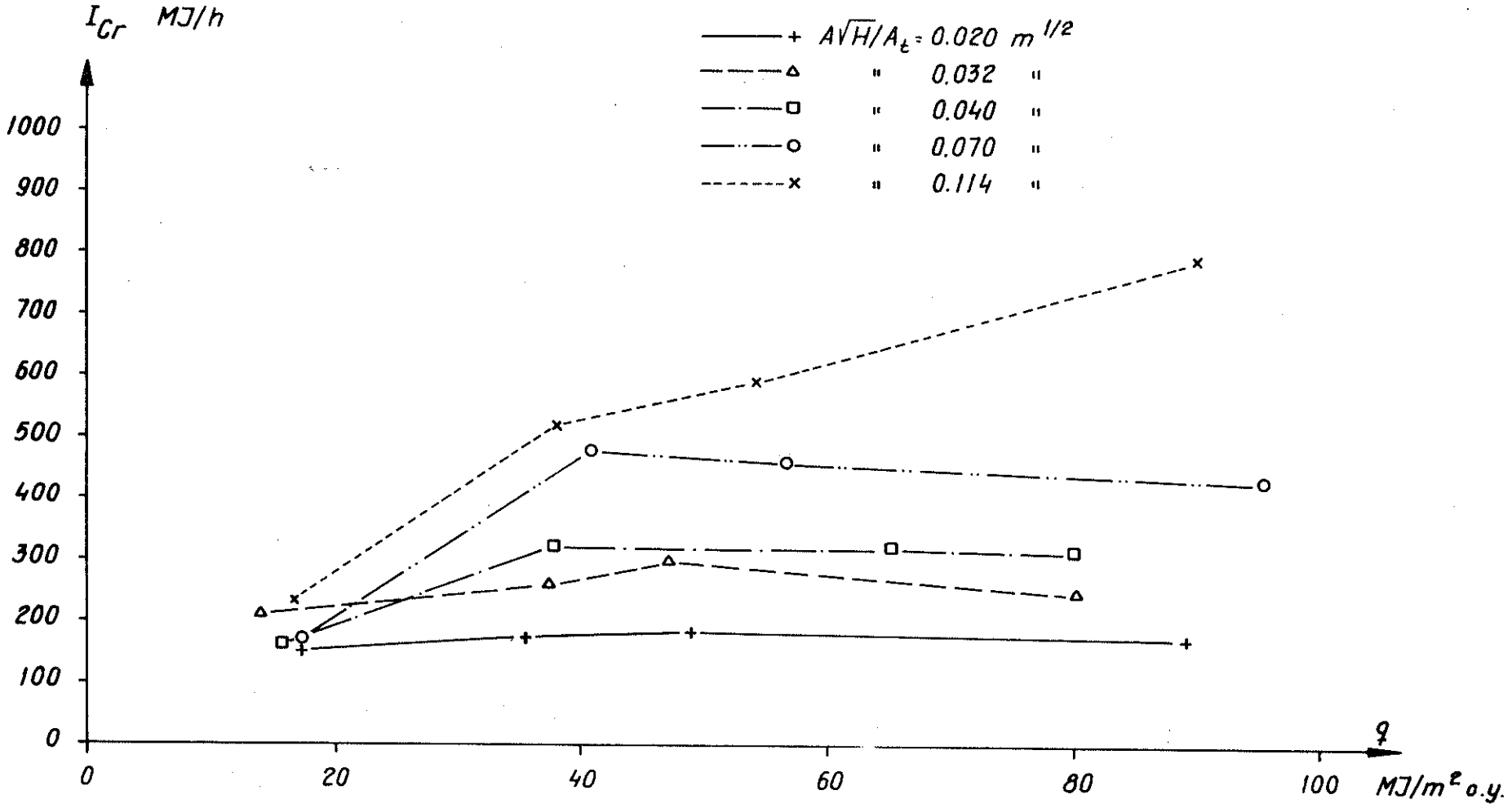

FIG 45 The relation calculated from the obtained test results between I_{Cr} (MJ/h) and the fire load, q (MJ/square meter of the enclosing surface) for varying opening factor, $A\sqrt{H}/A_t$ ($m^{1/2}$). The porosity factor, $\phi \approx 0.5$ $cm^{1.1}$. The enclosing structures of the fire cell are composed of 10 mm asbestos disk having a density of 1020 kg/m^3 and 1.5 mm steel sheet.

which parameter is used as the decisive one, with respect to the combustion rate or the energy liberated per unit time. Among the studied parameters, generally those which describe the liberated energy per unit time are preferred to the more conventionally used parameter that is, the combustion rate stated as the weight decrease per unit time, due to the fact that the first mentioned parameters constitute a primary information basis for calculation of the characteristics of a fire process by heat- and mass balance equations. Among the energy parameters, the maximum value of the energy liberated per unit time, I_{Cmax}, has the substantial advantage that it makes a more differentiated description of the type of the fire process possible, which will be closely discussed in section 8.

In this connection, a substantial influence with varying fire load, which is difficult to understand, is the distribution of the fuel in the fire cell, illustrated in FIG 46, where in a) a large fire load with a high wooden stick pile occupying the major part of the volume of the fire cell is shown and in b) a small fire load with a low wooden stick pile resulting in a considerable free air volume between the pile and the ceiling of the fire cell is illustrated.

The non-negligible influence of the distribution of the fuel in the fire cell on the fire process accentuates the difficulty of finding a relation on one side between conditions prevailing in real fires with fire load composed of different furniture and equipments and on the other side the conditions prevailing in pure fires with well defined wooden stick piles.

The primary reason that the fire process studies described in the literature have predominantly been performed with fire load in the form of wooden stick piles is the goal to achieve as well-defined and as controllable test conditions as possible and thus increase reproducibility of the tests and facilitate the rather far-reaching comparisons between the test results obtained at different laboratories. Real fire loads in the form of different furniture and equipment units are however characterized by combustion properties which may vary within wide limits. This results, for example, in

the fact that in translation of the test results, a high wooden stick pile does not necessarily correspond to a compact real furniture and vice versa. This fact accentuates the difficulty of transferring the conditions prevailing during tests with wooden stick piles, for a given type of fire cell, to have a general validity in a practical application with real fire load components composed of furniture, textile goods etc. Further factors which make the translation complicated and which can influence a fire process under real conditions are, for instance, floor-, wall- and ceiling coverings.

In the following, some of the differences existing, on one side, with a large fire load in the form of a high wooden stick pile (FIG 46 a)) and on the other side a small fire load in the form of a low wooden stick pile (FIG 46 b)) are briefly discussed, Lundin-Fäldt (1968).

For wood fuel the main combustion takes place by different carbon compounds being formed, here denoted by C (=carbon) for simplicity, and which therefore constitute the most important combustible components of the fire process. Therefore, the primary combustion with air (oxygen gas, O_2) will take place in the lower part of the wooden stick pile for which the following relation is true

$$C + O_2 \rightleftharpoons CO_2 \qquad (27)$$

Thus in the corresponding lower part of the fire cell, carbon dioxide, CO_2, is predominantly formed. Equilibrium should however be maintained between carbon monoxide, CO, and carbon dioxide, CO_2, which due to existence of oxygen excess implies that the following dissociation equilibrium should be true

$$CO_2 \rightleftharpoons CO + 1/2\ O_2 \qquad (28)$$

The equilibrium is thus shifted to the left which also persists at elevated temperatures.

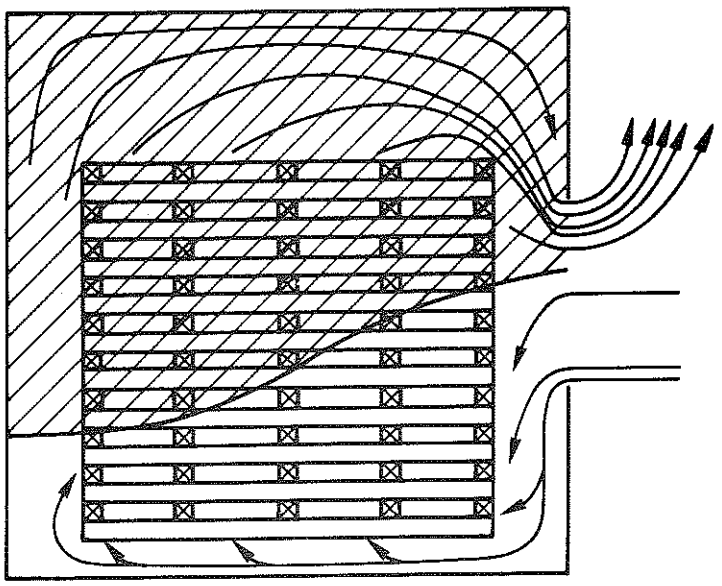

a.)

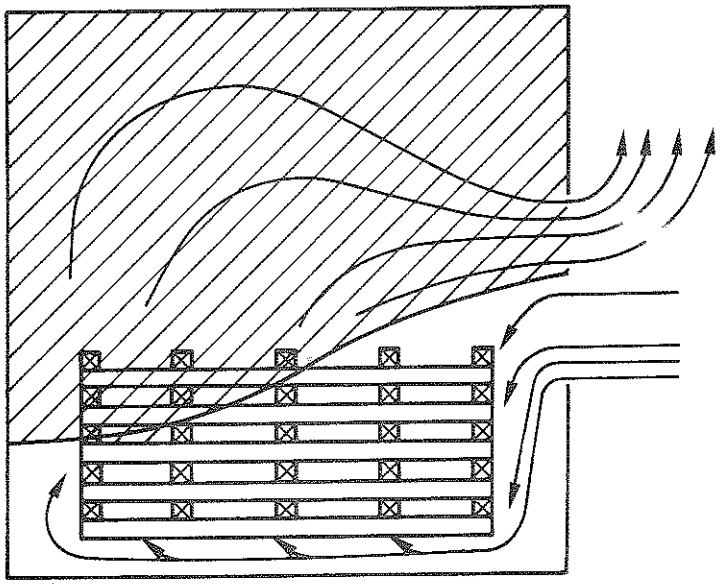

b.)

= oxygen deficit = the range for the generatorgas equilibrium

FIG 46 Principle sketch of two separate forms of a wooden stick pile illustrating in a) a high and in b) a low value for the fire load. The range for the oxygen deficit within which the generator-gas equilibrium should be maintained is also sketched in the figures.

A combustion process according to Eq (27) gives rise to a strongly exothermal reaction, implying that a considerable heat energy is developed. Therefore, with a wooden stick pile formed according to FIG 46 b), elevated temperatures are developed in the upper free space of the fire cell.

With a wooden stick pile formed according to FIG 46 a), that is a high and rather compact pile, the elevated heat development at the lower part of the pile gives rise to a considerable heat transport upwards which in combination with the prevailing elevated temperatures results in the fact that the carbon dioxide gas coming from the bottom is converted according to a new equilibrium, called generator gas equilibrium stated by the following relation

$$CO_2 + C \rightleftharpoons 2\ CO \qquad (29)$$

Depending on the actual temperature level, the carbon dioxide in the upper internal part of the pile is more or less converted to carbon monoxide. On this occasion a temperature dependence as in TAB V is true. From the table it is observed that at a temperature in the vicinity of 1000°C, the CO_2 gases flowing upwards will almost thoroughly be transformed to carbon monoxide gas. Consequently, the equilibrium according to Eq (29) will hold true with oxygen deficit and fuel excess - a condition which prevails in the upper internal part of the pile, since the oxygen flowing to the fire cell will be used up in the lower part primarily exposed.

The discussed influence of varying shape of the wooden stick pile on the fire process, corresponding to varying size of the fire load is confirmed by the magnitudes described in TAB III. As an example, the exothermal reaction for a pile shaped according to FIG 46 b) with elevated temperatures in the upper part of the fire cell, can be observed from the characteristics belonging to the mean temperature of the flaming phase, ϑ_{80-30}, in column 27. Apart from the lowest fire load, q = 17.5 MJ/m^2 of the enclosing surface, which in most cases has been to little to give a fully developed fire at the prevailing conditions, the mean temperature, with some exceptions, decreases with increasing fire load or pile height, which is in agreement with the expected conditions according to the discussion carried out. This is not, however, true

TAB. V Illustration of the CO_2 - CO equilibrium at different temperature levels for the reaktion $C + CO_2 \rightleftharpoons 2\ CO$.

Temperature °C	CO_2 vol-%	CO vol-%
450	98	2
500	95	5
600	77	23
700	42	58
800	10	90
900	3	97
950	1.5	98.5

for the values ϑ_{80-30} corresponding to the largest opening factor, $A\sqrt{H}/A_t = 0.114\ m^{1/2}$, in which case they increase with increasing fire load. This deviation can be explained by the fact that with such a large window opening, the neutral plane adjusts itself, for the air quantity flowing in and out, so high in the opening that an oxygen excess is obtained within major part of the wooden stick pile, resulting in a combustion process according to FIG 46 b), even for a large value of the fire load.

Besides the conclusions drawn previously concerning the different energy- and time characteristics for the fire process, it is further observed from TAB III, that after the maximum value of energy liberated per unit time, I_{Cmax}, is reached, the curve declines rather rapidly and thereafter is successively retarded going over to a flat part with a low energy level. This fact is illustrated by the time magnitudes t_1, t_2 and t_g in the columns 19, 20 and 21 respectively, which for the descending part of the energy-time curve state the time period from 0.75 I_{Cmax} to 0.5 I_{Cmax}, from 0.75 I_{Cmax} to 0.25 I_{Cmax} and from 0.75 I_{Cmax} to the zero-energy level respectively, cf. FIG 18.

In FIG 47-49, the values of the three time magnitudes t_1, t_2 and t_3 calculated from the obtained test results are summarized as a function of the opening factor, $A\sqrt{H}/A_t$, and the size of the fire load, q. The values are true for the porosity factor $\phi \approx 0.5\ cm^{1.1}$. The described relations show a dependence of the time periods t_1 and t_2 on the opening factor and the size of the fire load, which is principally in agreement with the corresponding condition for the time periods t_m and t_r previously analyzed in FIG 39 and 40. The conclusions reached at are, on the whole, also true for the time periods t_1 and t_2. From FIG 40, 47 and 48 the following simple, approximate relations are obtained as rough estimations

$$t_2 \approx t_r \tag{30}$$

$$t_1 = (1/3 - 1/4)\ t_2 \tag{31}$$

For the time period, t_g, the values summarized in FIG 49 render a less precision than what is the case for the other time magnitu-

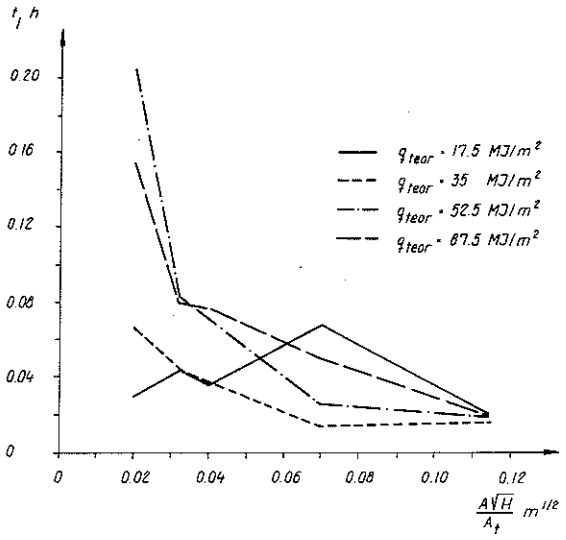

FIG 47 The relation calculated from the obtained test results between the time magnitude t_1 (cf FIG 18) and the opening factor of the fire cell $A\sqrt{H}/A_t$ for four different values of the fire load q_{theor}. Porosity factor $\phi \approx 0.5$ $cm^{1.1}$. The enclosing structures of the fire cell are composed of 10 mm asbestos disk having a density of 1020 kg/m^3 and 1.5 mm steel sheet.

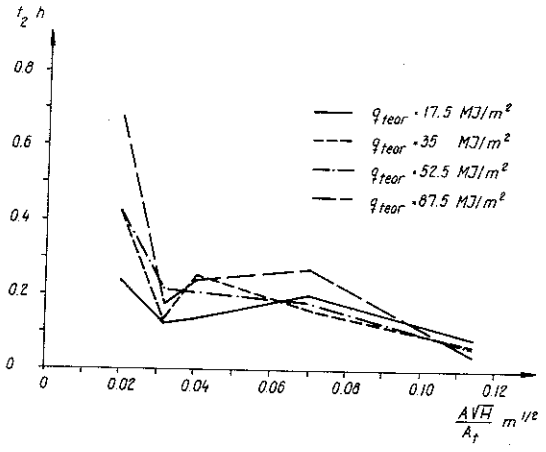

FIG 48 The relation calculated from the obtained test results between the time magnitude t_2 (cf FIG 18) and the opening factor of the fire cell $A\sqrt{H}/A_t$, for four different values of the fire load q_{theor}. Porosity factor $\phi \approx 0.5$ $cm^{1.1}$. The enclosing structures of the fire cell are composed of 10 mm asbestos disk having a density of 1020 kg/m^3 and 1.5 mm steel sheet.

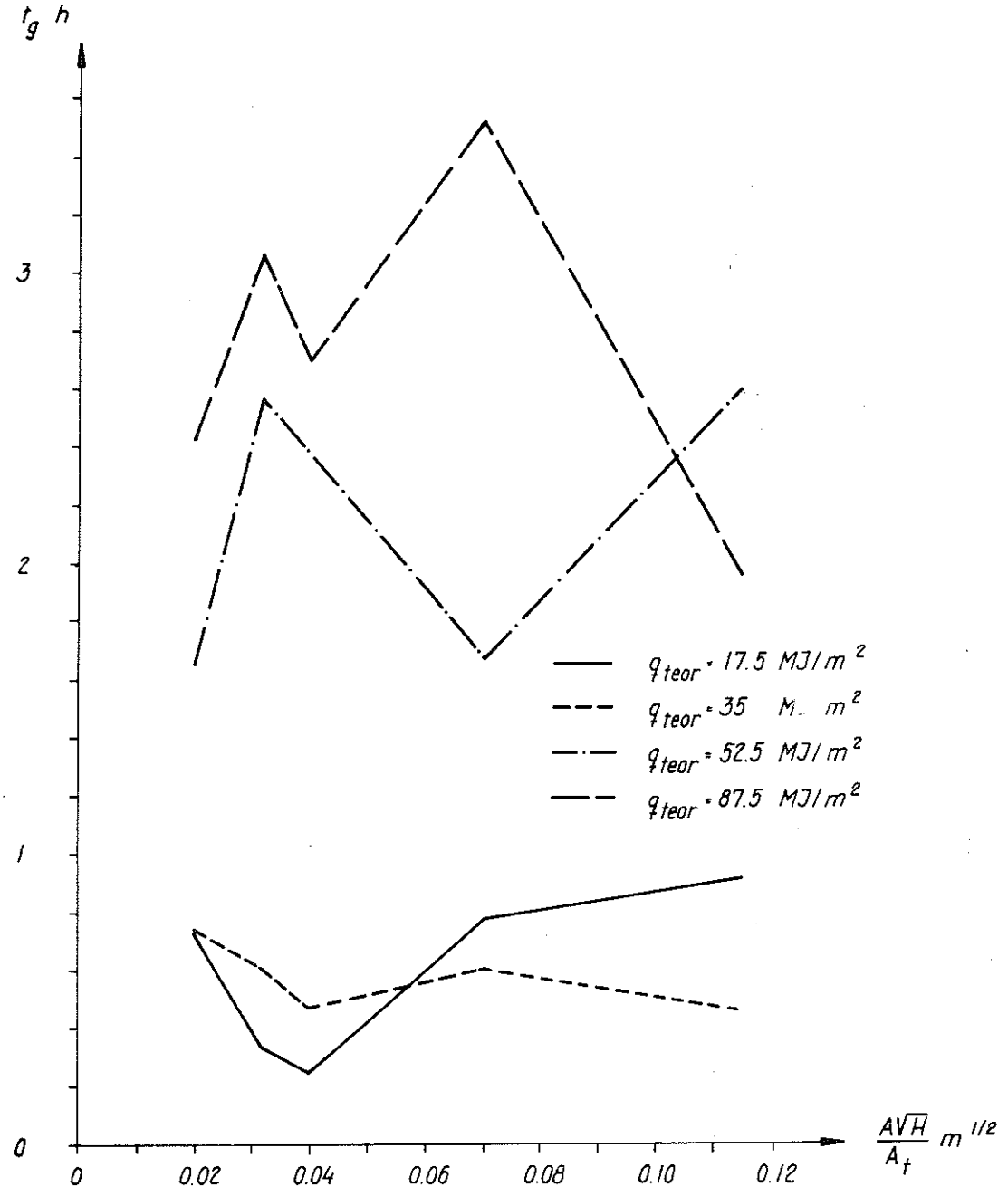

FIG 49 The relation calculated from the obtained test results between the time magnitude t_g (cf FIG 18) and the opening factor of the fire cell, $A\sqrt{H}/A_t$, for four different values of the fire load q_{theor}. Porosity factor $\phi \approx 0.5$ cm$^{1.1}$. The enclosing structures of the fire cell are composed of 10 mm asbestos disk having a density of 1020 kg/m^3 and 1.5 mm steel sheet.

des. With respect to the fact that the practical determination of the time magnitude, t_g, according to FIG 18, with fulfillment of the energy conditions according to Eq (15), has been done through extrapolation of the I_C-t curve within a flat part of the curve, the obtained poor precision for the time period t_g is natural. The consequence of applying this procedure is not significant, since an incorrect t_g-value chosen within reasonable limits has very little influence in a theoretical determination of the gas temperature-time curve of the fire process by heat- and mass balance equation of the fire cell. On the whole, FIG 49 states that the time period, t_g, increases with increasing value of the fire load, q, while the influence of the variations in the opening factor of the fire cell, $A\sqrt{H}/A_t$, can be deemed to be insignificant.

Finally, the gas flow, Q, of the fire process, that is the quantity of hot fire gases flowing out through the window opening of the fire cell per unit time, will be mentioned. This magnitude is described in TAB III, column 5, in the form of $Q_a/\varphi A\sqrt{H}$, cf. Eqs (11) and (12). From the table it is observed that for the opening factor within the range $A\sqrt{H}/A_t = 0.020 - 0.040\ m^{1/2}$, this gas flow quotient is unity. Therefore, within this range, Eq (11) is true for the gas flow, Q, implying that the gas flow can be calculated with satisfactory precision ignoring the vertical acceleration of the flow in the window opening. This relation is not however true for both of the largest opening factors $A\sqrt{H}/A_t = 0.070$ and $0.114\ m^{1/2}$ which is indicated in TAB III by the fact that the values of gas flow quotient are clearly less than 1, 0.8 and 0.7 respectively. The conclusion is thoroughly in agreement with the facts obtained in the previous section.

Through an approximate analysis according to Magnusson-Thelandersson (1971), an approximate relation has been derived in the previous section, Eq (24 a), which renders a direct proportionality between the gas flow, Q, or Q_a and the quotient I_{Cav}/ϑ_g where ϑ_g is the fire gas temperature. In order to illustrate this approximate relation, the gas flow, Q, related to the gas flow $(Q_a)_{A\sqrt{H}/A_t = 0.04}$ with the opening factor $A\sqrt{H}/A_t = 0.04\ m^{1/2}$ is described in FIG 50 as a function of the quotient $I_{Cav}/\vartheta_{80-30}$ according to the test results summarized in TAB III, columns 5 and 29. In the figure a

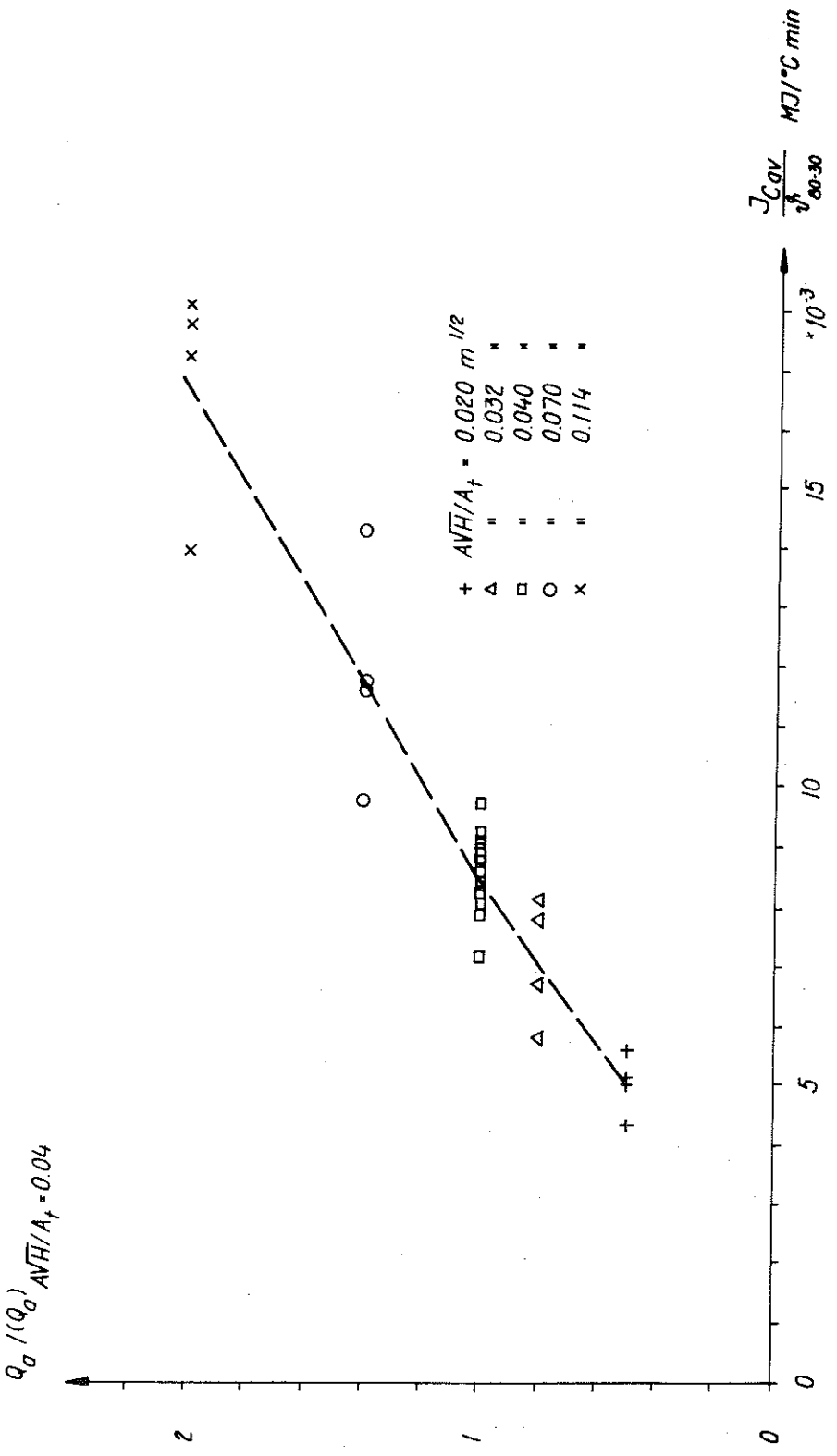

FIG 50 The relation determined from the obtained test results in TAB III, columns 5 and 29, between the gas flow Q_a related to the gas flow $(Q_a)_{A\sqrt{H}/A_t = 0.04}$ for the opening factor $A\sqrt{H}/A_t = 0.04\ m^{1/2}$ and the ratio $I_{Cav}/\vartheta_{80-30}$.

dashed line has been inserted which joins the mean values of the test results belonging to each group and which well confirms the approximate relation according to Eq (24 a). Determination of the coefficient from FIG 50 combined with application of Eq (11) for the gas flow $(Q_a)_{A\sqrt{H}/A_t = 0.04}$ results in the expression

$$Q_a = 0.005 \varphi A_t \frac{I_{Cav}}{\vartheta_{80-30}} \qquad (32)$$

where Q_a is in kg/min, φ in kg/min · $m^{5/2}$, A_t in m^2 and $I_{Cav}/\vartheta_{80-30}$ in MJ/°C · min · 10^3. The proportionality factor φ is almost independent of temperatures above 300°C, that is within the range which is ordinarily actual for fire. The proportionality factor varies somewhat with the combustion rate and is about 330 kg/min · $m^{5/2}$ for the combustion rate 0 and about 360 kg/min · $m^{5/2}$ for the maximum combustion rate. Thus Eq (32) can approximately be written in the following form

$$Q_a = 1.7 A_t \frac{I_{Cav}}{\vartheta_{80-30}} \qquad (32a)$$

From FIG 50 it is observed that the gas flow Q_a besides varying with the quotient $I_{Cav}/\vartheta_{80-30}$ also varies with the size of the fire load. This variation is not however decisive in an ordinary practical application. From the values corresponding to the opening factor $A\sqrt{H}/A_t = 0.040\ m^{1/2}$ it is further observed from TAB III that no significant dependence on the porosity factor, ϕ, appears to exist, cf. TAB II, column 29 for further details.

For the functional relationship between $I_{Cav}/\vartheta_{80-30}$ and opening factor of the fire cell, $A\sqrt{H}/A_t$, the test results according to TAB III, column 29, finally confirm the discussion carried out previously in section 4 in connection with FIG 24.

6. STICK THICKNESS OF THE FIRE LOAD.

6.1 Introductory discussion. Test characteristics.

With respect to the properties of the fire load, the influence of the variations in the porosity factor, ϕ, and size of the fire load, q, on the fire process, have been previously analyzed in Sections 4 and 5. The analysis holds true for a geometrically pure and uniquely defined fire load in the form of a wood crib according to FIG 10.

From the model tests performed by Gross (1962) concerning the flaming phase characteristics of a wood crib for fire in the open air, it is observed that the combustion rate, R, besides depending on the porosity factor of the fire load, also depends on the thickness, b, of the individual stick, c.f. FIG 11. In the result description of Gross, the complementary influence of the thickness, b, of the wood crib is taken into consideration through a scale modified combustion rate. This description is verified for a thickness variation within the range b = 1.6 - 91.5 mm.

A transition from fire in the open air to fire in a closed compartment with window opening results in modifications with respect to gas flow conditions and characteristics of the combustion process which have been closely discussed in earlier sections. These modifications are not of such a nature that they can principally change the dicisive parameters as far as a detailed description of the fire load is concerned. Thus, for a fire load in the form of a wooden crib according to FIG 10 in a closed fire cell with window opening, the three parameters

size of the fire load, q,
the porosity factor, ϕ, and
the stick thickness, b

can be presumed to be sufficient for an approximate description with respect to properties of the fire process relevant in this connection. For this purpose it is obvious that the side conditions requiring constant material properties and constant initial humidity for the wood fuel, should be fulfilled.

The estimation made is supported by Thomas-Heselden's report (1972) concerning an international test series, performed within CIB's sphere of activity, to study a fully developed fire process in a fire cell in the model scale. In this report, the variables used for a fire load in the form of a wood crib include fire load density, fuel thickness, and fuel spacing. The variable fuel spacing is stated as linearly proportional with fuel thickness. The values investigated for the fuel thickness consist of 10, 20, and 40 mm and for the fuel spacing of 1/3, 1, and 3 times the stick thickness. Within the variation range embraced by the test series, the test results render the following for the variable fuel thickness:

a) A negligible influence on the mean combustion rate for all the window openings studied,

b) A quantitative influence on the mean value of the fire gas temperature, ϑ_{80-30}, amounting to approximately 5 % for a small opening factor, while the influence is almost negligible for a large opening factor, and

c) A quantitative influence on the radiation intensity in the window openings amounting to about 5 % for a small opening factor and about 35 % for a large opening factor.

In a fire process which is of the fuel bed controlled type, the combustion rate should, in the light of discussions carried out in earlier sections, increase with decreasing stick thickness at approximately unchanged size, q, and porosity factor, ϕ, for the fire load. This conclusion follows from the fact that the exposed surface of the fire load at constant fire load volume is inversely proportional with the stick thickness, b, and that the penetration rate of the fire from the exposed surface of the wooden sticks can be assumed to be approximately constant.

At constant total weight, M, for the fire load and constant rate, v_i, for penetration of the fire from exposed surface of the fire load, the combustion rate, R_c, stated as the weight decrease per unit time, will decrease linearly with the time, t, for a fire load in the form of long sticks with square cross sectional area having the lateral dimension of b. This fact is illustrated in FIG 51,

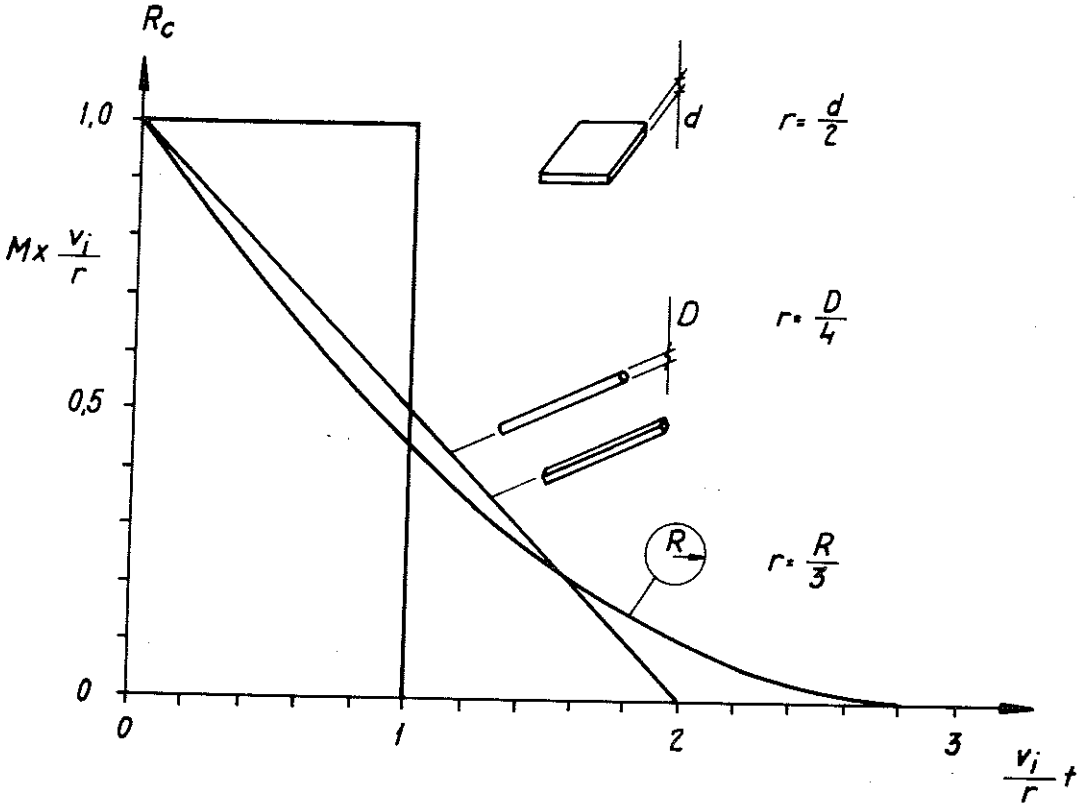

FIG 51 The variation of the combustion rate, R_C, with time, t, for varying lath shape, assuming that the penetration rate of the fire from the exposed surface of the fire load is constant.

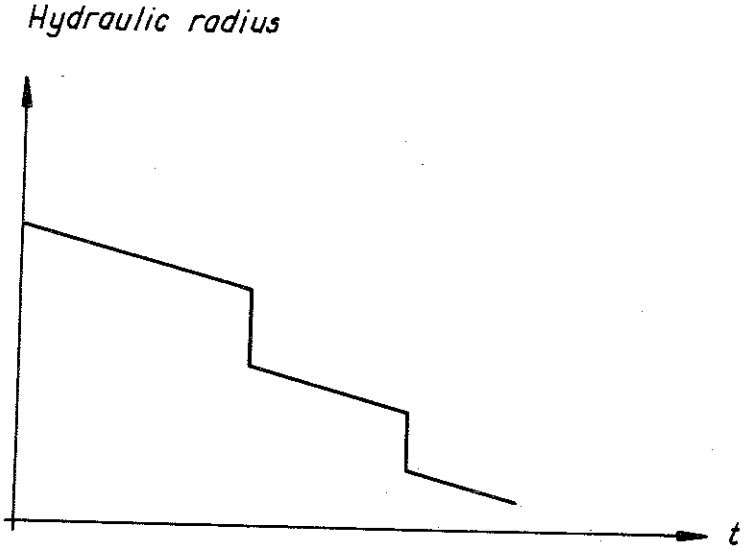

FIG 52 The variation of the hydraulic radius of the furniture such as wardrobes during the fire process.

taken from Ödeen (1963), in which the combustion rate, R_C, is given as a function of the dimensionless magnitude $v_i \cdot t/r$. In this expression, r is the so called hydraulic radious, that is the ratio between the original volume and the initially exposed surface of the fire load. The same relation with the combustion rate, R_C, decreasing linearly with the time, t, is also true for a fire load in the form of long cylindrical wooden bars. For fire load in the form of wooden disks, uni- or bilaterally exposed to fire, the same simplified assumption renders a constant combustion rate, R_C. Finally, FIG 51 also indicates the application of the mentioned assumption on a fire load composed of spherical wooden elements with a combustion rate, R_C, which decreases slower than a linear decrease.

From what has been stated before, it is observed that shape and initial size of the elements of the fire load can be expected to have a non-negligible influence of the properties of the fire process with fuel bed controlled fires. Such a circumstance significantly complicates a translation of the results from studies on fire processes with pure fire loading of the type wood cribs, to their application to realistic fire load occuring in practice, such as furniture, textiles, coverings etc. Further complications may arise with fire load components which during a fire process may change in element shape of hydraulic radius, r, in an abrupt manner, c.f. FIG 52. Examples on such fire load components are wardrobes and cupboards with equipments for which the hydraulic radious is abruptly changed when the doors have burnt through. Another example is the component bookshelf with books for which the hydraulic radious can change several times by repeated collapsing effects. In its initial form, the bookshelf with carefully arranged books has a hydraulic radius with a well-defined magnitude, while successive collapsing effects result in a fire load shape which has similarities with an irregular wooden stick pile.

In a ventilation controlled fire with a given fire cell and air supply and with approximately unchanged values for the fuel quantity and porosity factor, the exposed surface of the wooden sticks will increase and at the same time the amount of air per unit area which is available for the combustion of the wood will decrease

when the stick thickness, b, or the hydraulic radius, r, decreases for a fire load in the form of a regular wood crib according to FIG 10. This circumstance results in the fact that the total burning surface increases. The resulting influence is however reduced due to the fact that the combustion intensity at the same time decreases as a consequence of the decreased available air quantity per unit area of the fuel. Variations in the stick thickness, b, of a wood crib or the hydraulic radius, r, can therefore be expected to have a rather insignificant influence on the combustion rate and gas temperature of the fire process with ventilation controlled fires.

The described circumstances are illustrated in FIG 53 which indicates the relation determined, with full scale tests, between the maximum fire gas temperature, ϑ_{max}, and the hydraulic radius, r, of the fire load. The figure summarizes the results from three part series, characterized by the values given in the figure for the total fuel quantity, M, and the air quantity, G, which is supplied to the fire cell per unit time, through the fan system. The fire load in the tests consisted of timber with a somewhat irregular piling. The given curves show that for every known combination of the fuel quantity, M, and the supplied air flow, G, there is a corresponding maximum value for the hydraulic radius, r, above which the maximum temperature, ϑ_{max}, substantially decreases due to an incomplete flaming.

In the light of what has been mentioned above, a complementary investigation dealing with the question of how the characteristics of the fire process are influenced by the variations in the stick thickness of a regular wooden crib, seems to be urgent. Such a complementary investigation should be given such a form that together with the test series described in the previous section it covers, as thoroughly as possible, the most important variation ranges for the related parameters opening factor, $A\sqrt{H}/A_t$, of the fire cell in addition to the size of the fire load, q, porosity factor, ϕ, and the stick thickness, b, for a fire load in the form of a regular wooden crib according to FIG 10. With the results from such systematical investigations and through a reasonable number of fire pro-

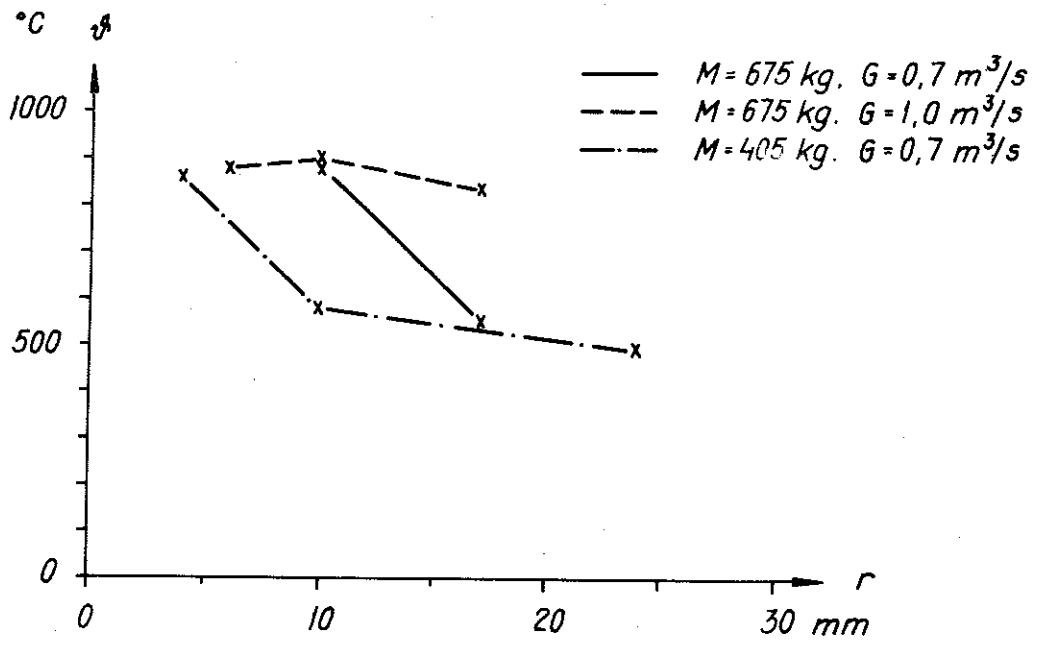

FIG 53 The influence of varying hydraulic radius, r (mm), on the maximum gas temperature, ϑ_{max} (°C), obtained during the fire process. G indicates the quantity of combustion air (m^3/s) supplied per unit time through a fan arrangement and M the total fuel quantity (kg). Volume of the fire cell is 46 m^3, the total internal enclosing surface of the fire cell being A_t = 79 m^2. The enclosing structures consist of 20 cm concrete.

cess tests, practically representative and realistic fire loads could be calibrated and referred to fire load of well-defined type of wood crib using, for instance, equivalent porosity factor and equivalent stick thickness or hydraulic radius. Through such calibration attempts, the future changes in the type of realistic fire loads should successively be able to be taken into consideration after additional studies with rather little loss in time and money.

In the following, a test series studying the combined influence of the porosity factor of the fire load with fire load consisting of wood cribs according to FIG 10, is described. In the test series it has been tried to choose such an opening factor, $A\sqrt{H}/A_t$, that both ventilation- and fuel bed controlled fire processes become analyzed, which has resulted in comparative studies for both of the opening factors 0.04 and 0.114 $m^{1/2}$. With respect to the size of the fire compartment, five lateral dimensions were estimated to give a representativt picture of the influence of the stick thickness on the fire process and thus the dimensions b = 10, 12.5, 25, 40, and 50 mm were chosen. Considering the results obtained in Section 4, three values of the porosity factor were believed to be suitable, namely ϕ = 0.1, 0.5 and 1.0 $cm^{1.1}$, corresponding to a compact, a "normal" and an open crib. However, in a test series built up in this manner, certain tests had to be omitted partly because the actual constellation n - N - L for the desired ϕ-value could not be obtained and partly because the crib corresponding to the porosity factor with small lateral dimensions for the sticks could not be accommodated in the fire cell. For all the tests it has been tried to have a constant fire load of q_{theor} = 52.5 MJ/m^2 of the enclosing surface.

6.2 Analysis of the experimental results.

Through application of the calculation procedure, briefly referred to in Section 2, the energy-time curve, corresponding to respective tests have been determined and described in FIG 54-60. Based on the relations given in the figures, the fire process characterizing magnitudes corresponding to those summarized in Section 4, have been calculated and described in Table VI, c.f. FIG 18 for the app-

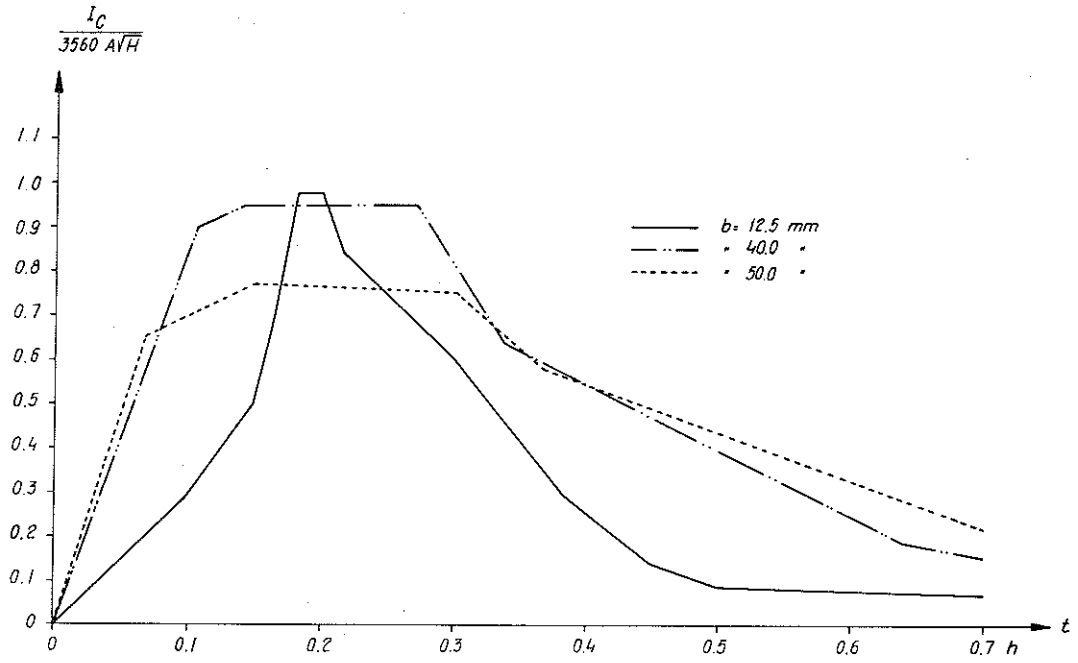

FIG 54 Theoretically calculated energy-time curve of the energy developed during the fire process with varying stick thickness, b (mm). Opening factor $A\sqrt{H}/A_t$ = 0.040 $m^{1/2}$, porosity factor $\phi \approx 0.5$ $cm^{1.1}$. The enclosing structures of the fire cell are composed of 10 mm asbestos disk having a density of 1020 kg/m^3 and 1.5 mm steel sheet.

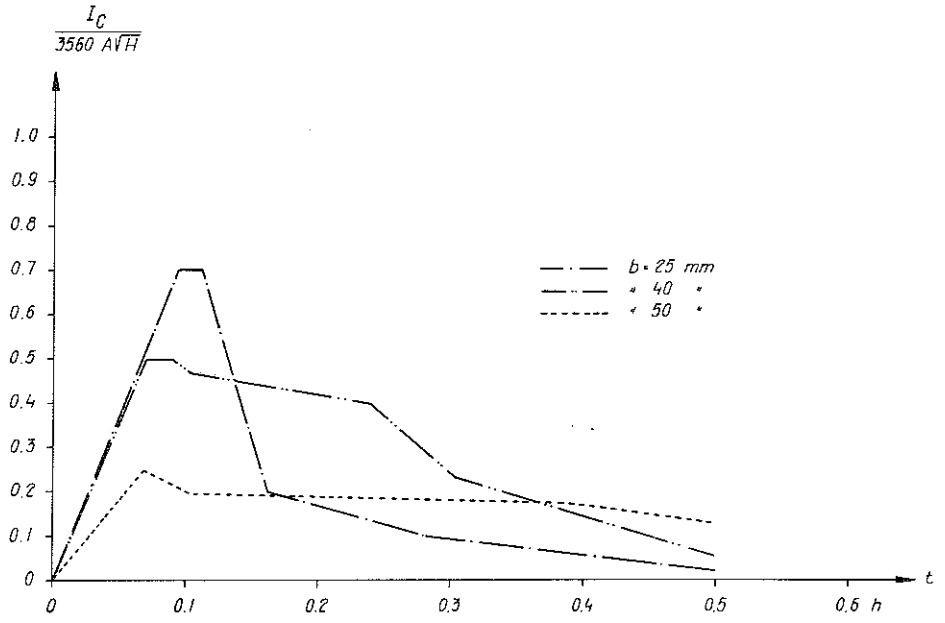

FIG 55 Theoretically calculated energy-time curve of the energy developed during the fire process with varying stick thickness, b (mm). Opening factor $A\sqrt{H}/A_t$ = 0.114 $m^{1/2}$, porosity factor $\phi \approx 0.5$ $cm^{1.1}$. The enclosing structures of the fire cell are composed of 10 mm asbestos disk having a density of 1020 kg/m^3 and 1.5 mm steel sheet.

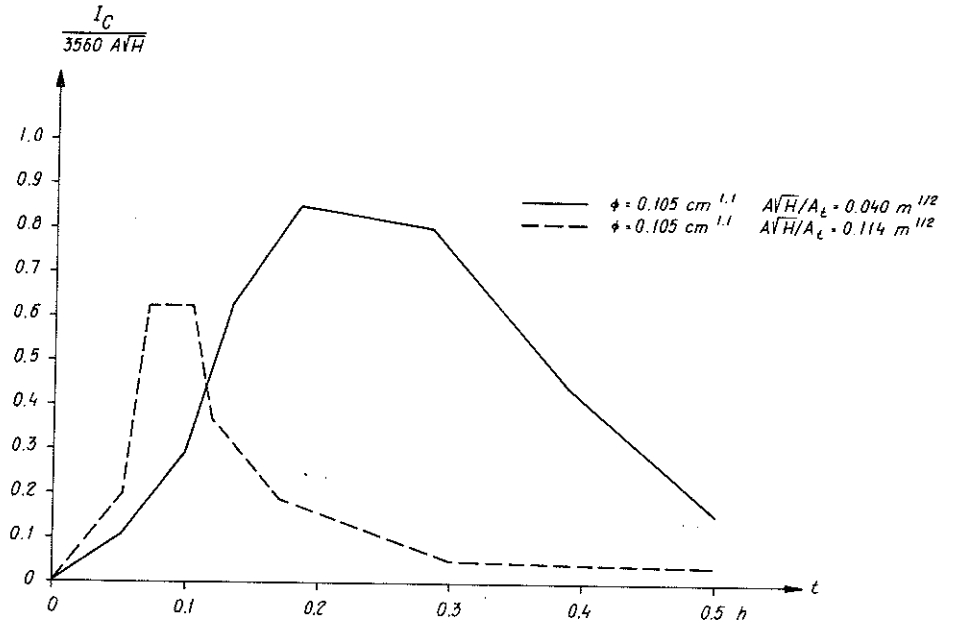

FIG 56 Theoretically calculated energy-time curve of the energy developed during the fire process with the constant stick thickness, b = 10 mm. Opening factor $A\sqrt{H}/A_t$ = 0.040 and 0.114 $m^{1/2}$ respectively. The enclosing structures of the fire cell are composed of 10 mm asbestos disk having a density of 1020 kg/m^3 and 1.5 mm steel sheet.

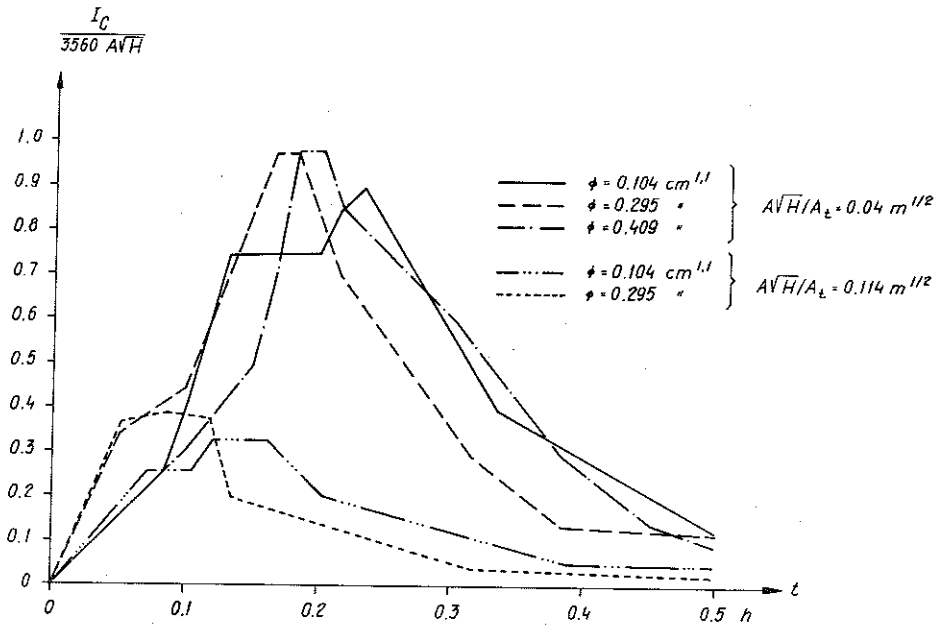

FIG 57 Theoretically calculated energy-time curve of the energy developed during the fire process with varying porosity factor but a constant stick thickness, b = 12.5 mm. Opening factor $A\sqrt{H}/A_t$ = 0.040 and 0.114 $m^{1/2}$ respectively. The enclosing structures of the fire cell are composed of 10 mm asbestos disk having a density of 1020 kg/m^3 and 1.5 mm steel sheet.

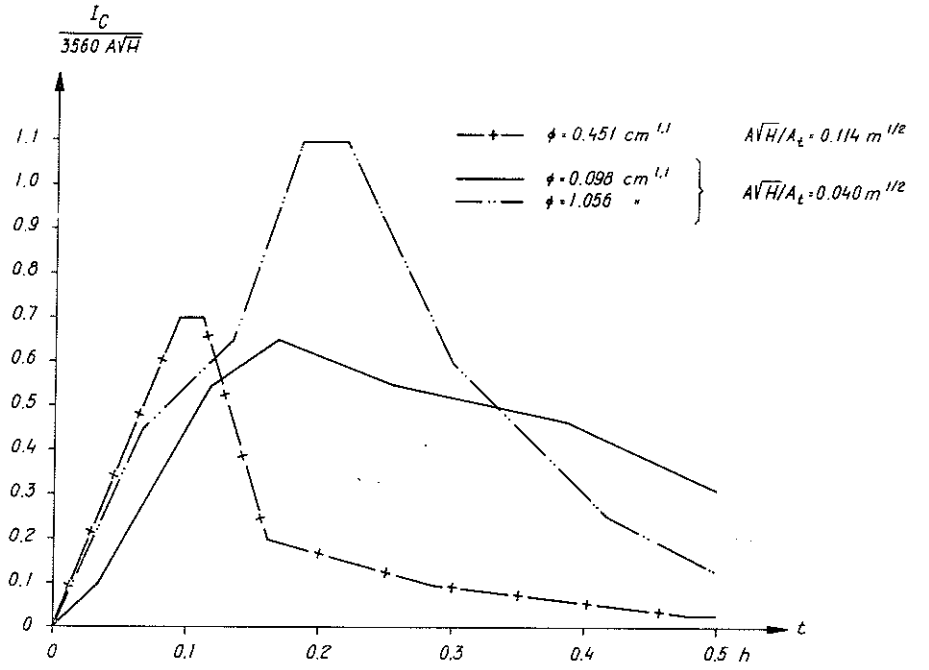

FIG 58 Theoretically calculated energy-time curve of the energy developed during the fire process with varying porosity factor ϕ ($cm^{1.1}$) but a constant stick thickness, b = 25 mm. Opening factor $A\sqrt{H}/A_t$ = 0.040 and 0.114 $m^{1/2}$ respectively. The enclosing structures of the fire cell are composed of 10 mm asbestos disk having a density of 1020 kg/m^3 and 1.5 mm steel sheet.

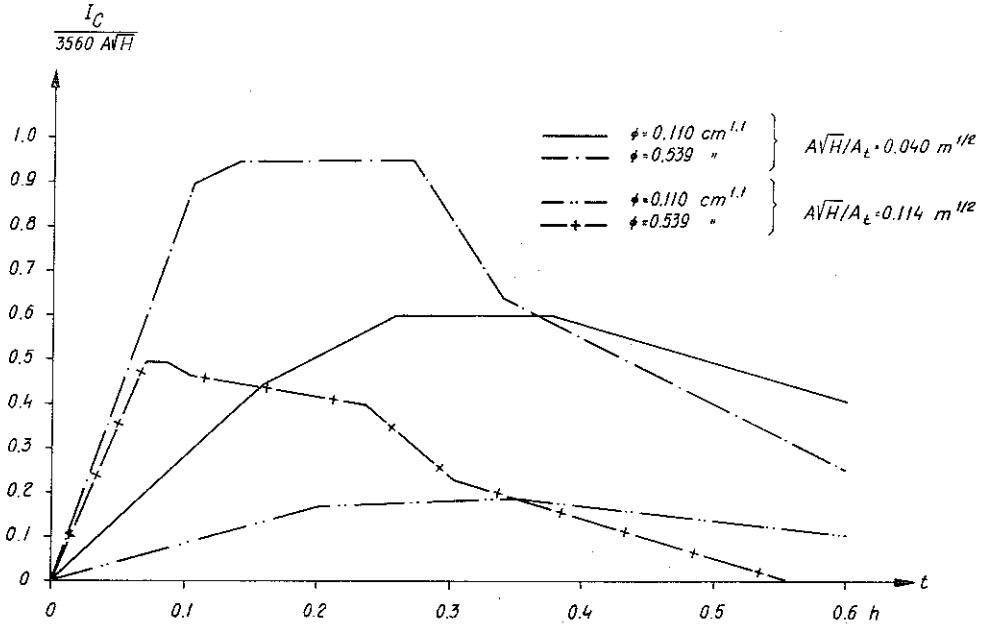

FIG 59 Theoretically calculated energy-time curve of the energy developed during the fire process with varying porosity factor ϕ ($cm^{1.1}$) but a constant stick thickness, b = 40 mm. Opening factor $A\sqrt{H}/A_t$ = 0.040 and 0.114 $m^{1/2}$ respectively. The enclosing structures of the fire cell are composed of 10 mm asbestos disk having a density of 1020 kg/m^3 and 1.5 mm steel sheet.

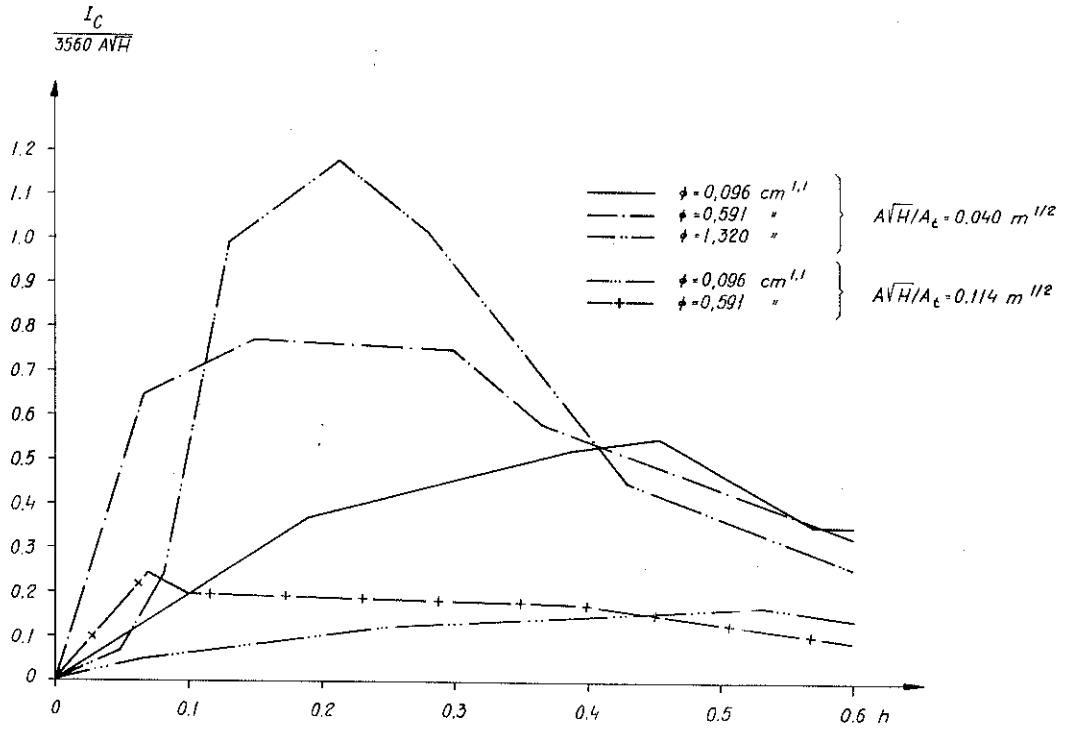

FIG. 60 Theoretically calculated energy-time curve of the energy developed during the fire process with varying porosity factor, ϕ ($cm^{1.1}$) but a constant stick thickness, b = 50 mm. Opening factor, $A\sqrt{H}/A_t$ = 0.040 $m^{1/2}$ respectively. The enclosing structures of the fire cell are composed of 10 mm asbestos disk having a density of 1020 kg/m^3 and 1.5 mm steel sheet.

TAB. VI Characteristics and primary values with several magnitudes summarized for tests embracing a study of the influence of varying stick thickness of the fuel on the fire process.

$\frac{A\sqrt{H}}{A_t}$	b	ϕ	q_{teor}	q	$\frac{Q_a}{\varphi A\sqrt{H}}$	$R = 330A\sqrt{H}$	R_{80-30}	I_{Cmax}	t_m	I_{Cm}	t_r	I_{Cr}	R_r	$W_r = \frac{I_{Cr}}{R_r}$	t_d	I_{Cd}
$m^{1/2}$	mm	$cm^{1.1}$	MJ/m^2o.y.	MJ/m^2o.y.		kg/h	kg/h	MJ/h	h	MJ/h	h	MJ/h	kg/h	MJ/kg	(h)	MJ/h
(1)	(2)	(3)	(4)	(5)	(6)	(7)	(8)	(9)	(10)	(11)	(12)	(13)	(14)	(15)	(16)	(17)
0.040	10	0.105	52.5	57.6	1.0	44.6	50.2	398	0.233	230	0.334	264	31.66	8.3	0.202	372
	12.5	0.104	52.5	52.6	1.0	44.6	51.4	432	0.283	193	0.329	219	29.34	7.5	0.153	374
	12.5	0.295	52.5	43.8	1.0	44.6	56.7	470	0.175	233	0.212	266	37.97	7.0	0.076	425
	12.5	0.409	52.5	49.0	1.0	44.6	60.1	470	0.192	169	0.255	229	35.17	6.5	0.087	416
	25	0.098	52.5	42.2	1.0	44.6	31.3	312	0.167	169	0.350	220	21.23	10.4	0.183	361
	25	0.451	52.5	42.8	-	44.6	61.9	504	-	-	-	-	-	-	-	-
	25	1.056	52.5	52.2	1.0	44.6	53.0	528	0.200	272	0.262	321	36.74	8.7	0.108	483
	40	0.110	52.5	57.6	1.0	44.6	28.1	288	0.308	189	0.540	220	18.84	11.7	0.390	263
	40	0.539	52.5	59.7	1.0	44.6	45.2	456	0.207	259	0.325	312	26.67	11.7	0.241	435
	50	0.096	52.5	49.5	1.0	44.6	18.7	264	0.451	169	0.535	178	15.29	11.6	0.295	233
	50	0.591	52.5	57.6	1.0	44.6	31.0	365	0.225	295	0.375	313	26.39	11.8	0.317	345
	50	1.320	52.5	57.8	1.0	44.6	40.6	566	0.216	286	0.333	338	27.41	12.3	0.207	471
0.114	10	0.105	52.5	52.5	0.7	127.0	151.2	862	0.083	342	0.110	460	79.41	5.8	0.048	828
	12.5	0.104	52.5	56.5	0.7	127.0	74.0	452	0.137	290	0.184	323	53.83	6.0	0.120	405
	12.5	0.295	52.5	55.9	0.7	127.0	110.9	534	0.083	360	0.125	411	81.02	5.1	0.086	506
	25	0.451	52.5	53.7	0.7	127.0	91.3	958	0.100	520	0.125	593	68.02	8.7	0.056	875
	40	0.110	52.5	59.6	0.7	127.0	31.0	246	0.259	207	0.484	219	20.93	10.5	0.399	230
	40	0.539	52.5	58.7	0.7	127.0	42.8	684	0.076	387	0.241	535	38.69	13.8	0.191	608
	50	0.096	52.5	52.6	0.7	127.0	21.2	233	0.533	152	0.638	163	15.70	10.4	0.331	205
	50	0.591	52.5	56.5	0.7	127.0	23.4	342	0.067	168	0.242	245	27.78	8.8	0.191	277

R_d	$W_d = \frac{I_{Cd}}{R_d}$	t_1	t_2	t_g	I_{Cg}	R_g	$W_g = \frac{I_{Cg}}{R_g}$	I_{Cav}	W_{av}	ϑ_{80-30}	$\frac{R_{80-30}}{\vartheta_{80-30}}$	$\frac{I_{Cav}}{80-30}$	Försök nr
kg/h	MJ/kg	h	h	h	MJ/h	kg/h	MJ/kg	MJ/h	MJ/kg	°C	kg/°C·h	MJ/°C·h	
(18)	(19)	(20)	(21)	(22)	(23)	(24)	(25)	(26)	(27)	(28)	(29)	(30)	(31)
33,49	11.1	0.063	0.144	2.239	46	0.21	219.0	328	6.52	620	0.081	0.53	BB 133
36.75	10.2	0.048	0.160	2.591	40	0.17	235.3	303	5.90	555	0.092	0.54	BB 134
28.46	14.9	0.056	0.125	1.885	48	0.19	252.6	237	4.18	483	0.118	0.49	BB 132
18.21	22.8	0.077	0.151	3.158	33	0.14	235.7	176	2.94	396	0.152	0.44	BB 135
24.79	14.6	0.140	0.258	0.882	73	0.80	91.3	258	8.24	545	0.058	0.47	BB 50
–	–	–	–	–	–	–	–	–	–	–	–	–	BB 52
30.48	15.8	0.055	0.147	2.169	42	0.21	200.0	304	5.72	586	0.091	0.52	BB 54
17.99	14.6	0.174	0.348	0.977	73	0.90	81.1	258	9.19	556	0.050	0.46	BB 130
34.11	12.8	0.125	0.283	0.638	124	1.87	66.3	446	9.87	837	0.054	0.53	BB 131
14.23	16.4	0.271	0.478	0.623	113	2.12	53.3	202	10.84	461	0.041	0.44	BB 127
26.03	13.2	0.178	0.356	0.576	130	2.02	64.3	357	11.51	718	0.043	0.49	BB 128
36.18	13.0	0.063	0.237	0.497	162	3.95	41.0	529	13.05	957	0.043	0.55	BB 129
85.27	9.7	0.022	0.088	2.480	50	0.54	92.6	722	4.78	570	0.265	1.27	BB 126
57.55	7.0	0.059	0.159	2.905	44	0.33	133.3	375	5.07	440	0.168	0.85	BB 125
82.81	6.1	0.014	0.125	3.914	34	0.15	226.7	473	4.27	492	0.226	0.96	BB 124
72.04	12.1	0.018	0.062	2.590	40	0.71	56.3	735	8.05	685	0.133	1.07	BB 106
21.47	10.7	0.150	0.815	1.480	71	0.89	79.8	223	7.21	319	0.097	0.70	BB 136
36.51	16.6	0.051	0.176	0.315	207	6.15	33.6	625	14.61	673	0.064	0.93	BB 137
13.95	14.7	0.137	0.350	1.972	42	0.57	73.7	181	8.53	266	0.080	0.68	BB 121
25.27	10.9	0.280	0.576	1.232	104	3.35	31.0	272	11.64	370	0.063	0.73	BB 122

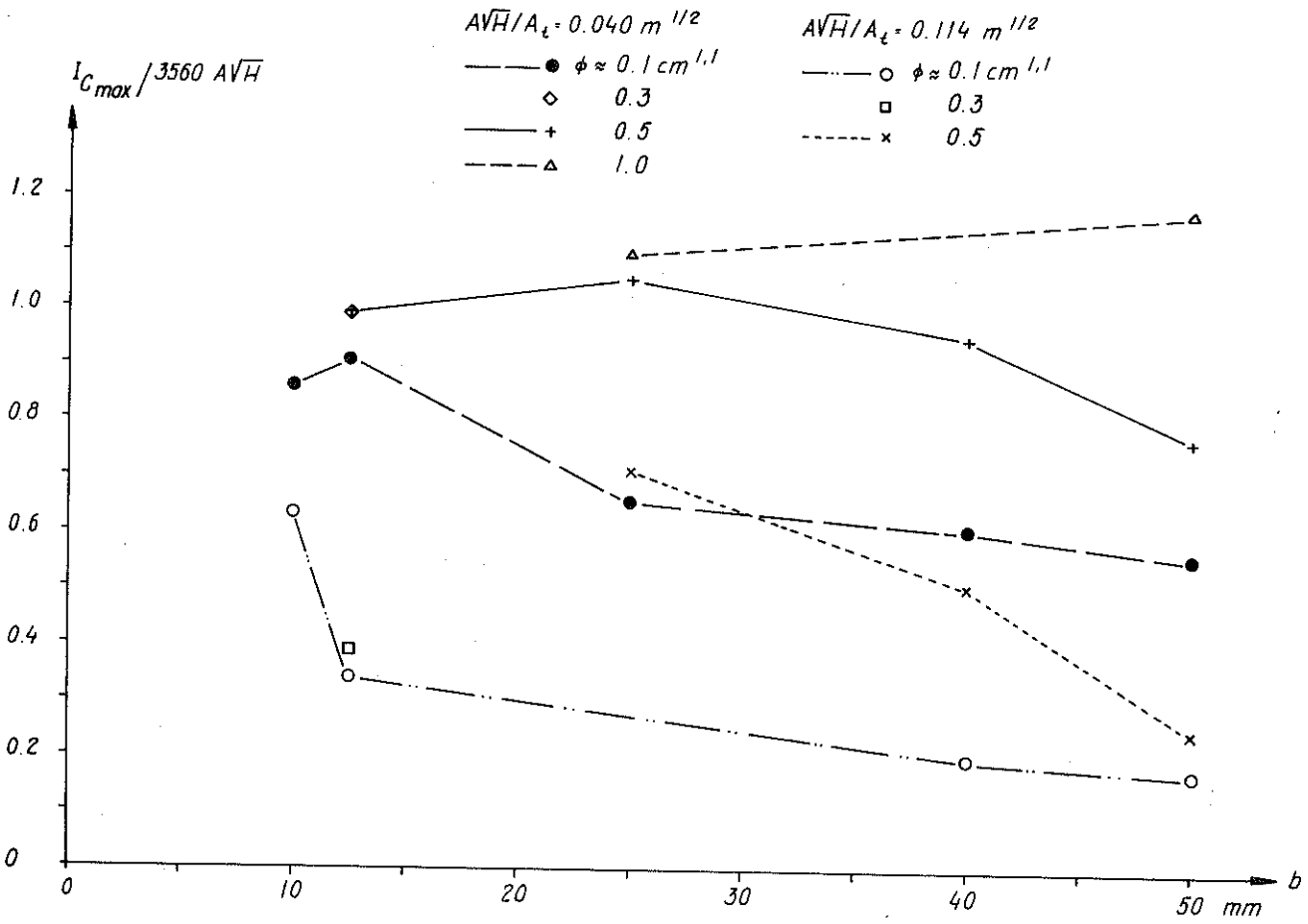

FIG 61 The relation determined from the experimental results between the maximum energy liberated per unit time, I_{Cmax}, and the stick thickness, b, of the fire load with varying porosity- and opening factor. The enclosing structures of the fire cell are composed of 10 mm asbestos disk having a density of 1020 kg/m^3 and 1.5 mm steel sheet.

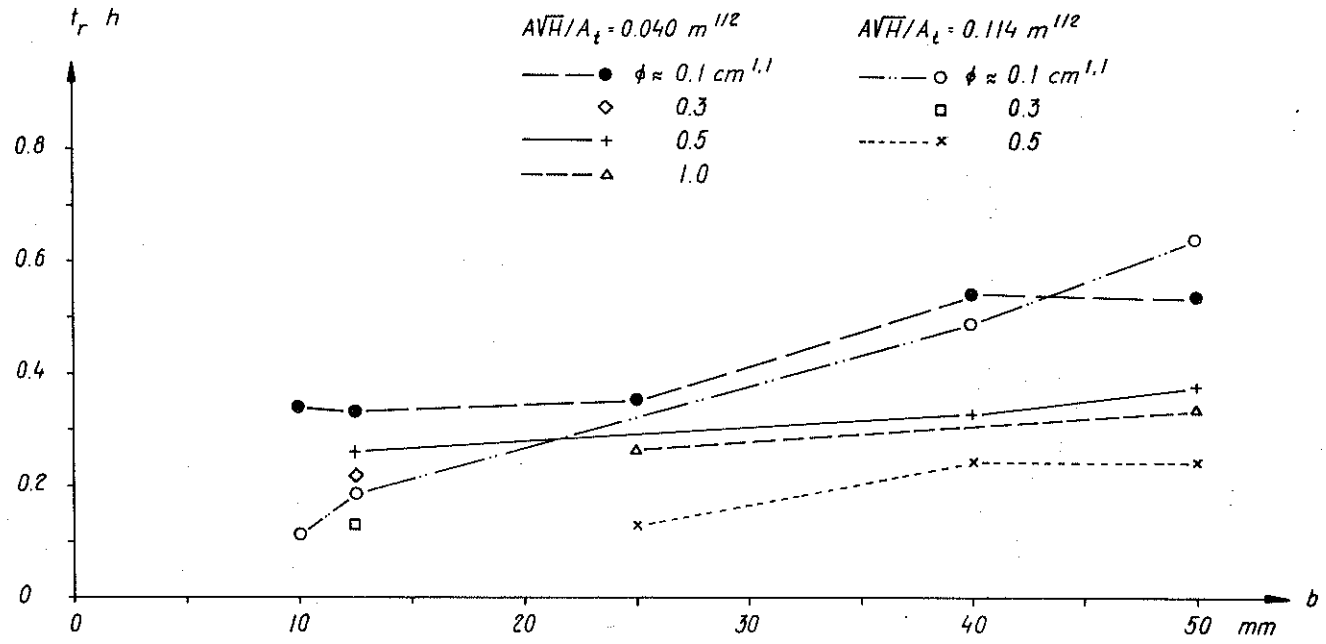

FIG 62 The relation calculated from the obtained test results between the time magnitude, t_r, and the stick thickness, b, of the fire load with varying porosity- and opening factor. The enclosing structures of the fire cell are composed of 10 mm asbestos disk having a density of 1020 kg/m^3 and 1.5 mm steel sheet.

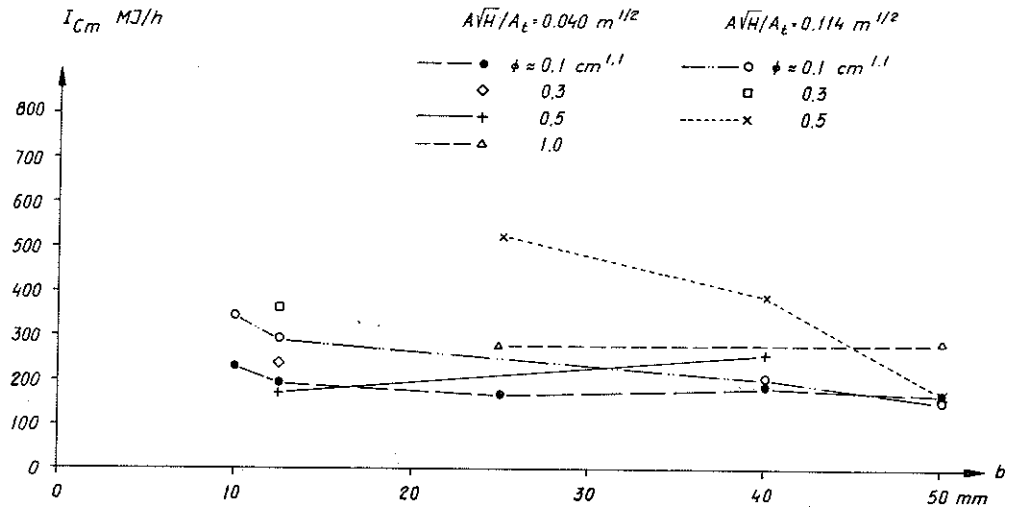

FIG 63 The relation calculated from the obtained test results between I_{Cm} (MJ/h) and stick thickness of the fuel, b (mm), with varying porosity- and opening factors. The enclosing structures of the fire cell are composed of 10 mm asbestos disk having a density of 1020 kg/m^3 and 1.5 mm steel sheet.

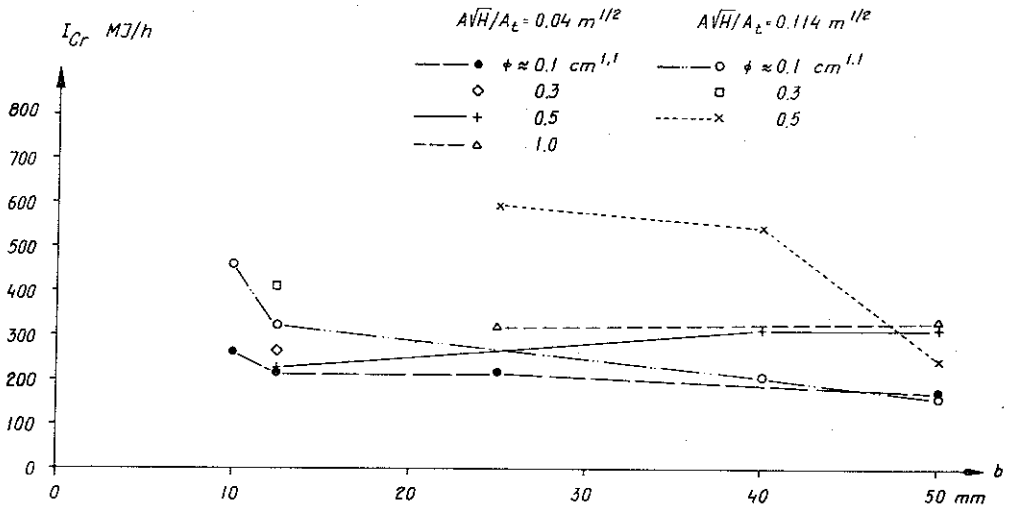

FIG 64 The relation calculated from the obtained test results between I_{Cr} (MJ/h) and stick thickness of the fuel, b (mm), with varying porosity- and opening factors. The enclosing structures of the fire cell are composed of 10 mm asbestos disk having a density of 1020 kg/m^3 and 1.5 mm steel sheet.

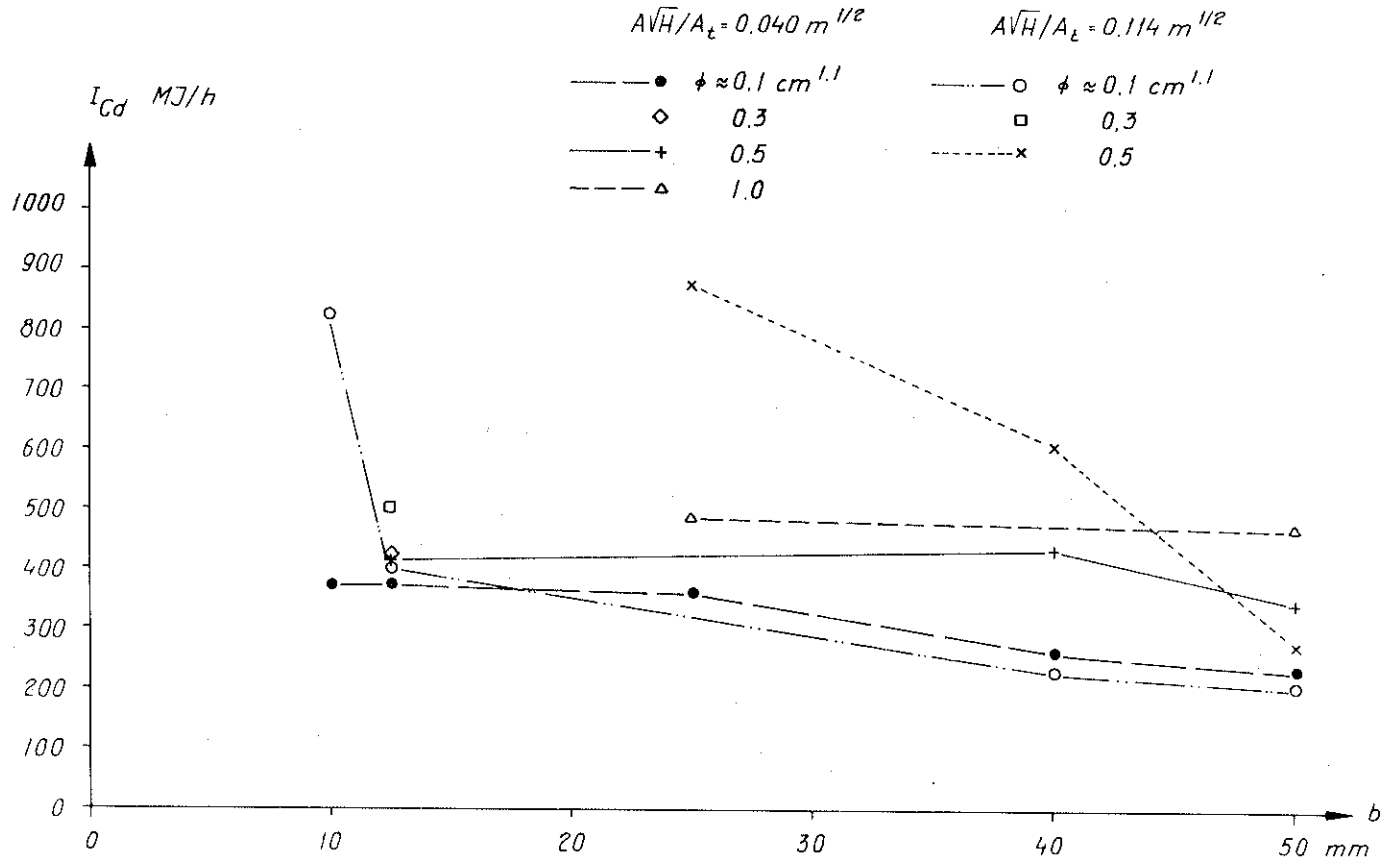

FIG 65 The relation calculated from the obtained test results between I_{Cd} (MJ/h) and stick thickness of the fuel, b (mm), with varying porosity and opening factors. The enclosing structures of the fire cell are composed of 10 mm asbestos disk having a density of 1020 kg/m^3 and 1.5 mm steel sheet.

lied notations. As a complementary information the energy magnitudes I_{Cmax}, I_{Cm}, I_{Cr}, and I_{Cd} have been summarized in FIG 61 and 63-65 as functions of the stick thickness, b, of the fire load, with varying porosity factor, ϕ, and opening factor $A\sqrt{H}/A_t$. Analogously, the time period, t_r, is summarized in FIG 62 with relation to the same variables b, ϕ, and $A\sqrt{H}/A_t$.

In the following the described results are briefly analyzed. The statements made in this analysis should be considered in the light of the essential background that for all the tests there is an approximately constant fire load of $q_{theor} = 52.5$ MJ/m^2 of the enclosing surface.

From FIG 61 and the corresponding results from FIG 54-60 plus Table VI, column 9, the following statement can be made about the maximum energy liberated per unit time, I_{Cmax}, during the fire process.

With the terminology defined in Section 5.2, ventilation controlled fire process - $I_{Cmax}/3560\ A\sqrt{H} \approx 1$ - has, strictly speaking, existed at the opening factor $A\ H/A_t = 0.040$ m$^{1/2}$ for the porosity factor $\phi \approx 1.0$ cm$^{1.1}$, within the whole studied variation range of the stick thickness, b, and for the porosity factor $\phi \approx 0.5$ cm$^{1.1}$ within the thickness range of b < 30 mm. The few tests performed for the combination $A\sqrt{H}/A_t = 0.040$ m$^{1/2}$, $\phi \approx 0.3$ cm$^{1.1}$, render a ventilation controlled fire process for the stick thickness b = 12.5 mm. For the lowest studied value of the porosity factor ϕ 0.1 cm$^{1.1}$ corresponding to a compact crib, the described results according to FIG 61, possibly indicate a ventilation controlled fire process for the stick thickness b < 5-10 mm with the opening factor $A\sqrt{H}/A_t$ = = 0.040 m$^{1/2}$. An analogous indication can also be observed from FIG 61 for the porosity factors $\phi \approx 0.1$ and 0.5 cm$^{1.1}$ with the opening factor $A\sqrt{H}/A_t = 0.114$ m$^{1/2}$, that is, a possible ventilation controlled fire process for very small stick thickness, b, having an estimated order of magnitude of 5 mm or less. For all the other tests described in this section the fire process has been of the fuel bed controlled type.

In agreement with what has been established in the previous sections, a decrease of the porosity factor, ϕ, at otherwise approximately unchanged conditions results in a decrease in the maximum released energy, I_{Cmax}. For the stick thickness $b \lesssim 25$ mm this decrease in I_{Cmax} predominantly takes place within the porosity factor range of $\phi \lesssim 0.5$ cm$^{1.1}$. For larger stick thicknesses, b, variations in the porosity factor, ϕ, results also in a substantial influence on the maximum energy, I_{Cmax}, within the variation range $0.5 \lesssim \phi \lesssim 1.0$ cm$^{1.1}$. For a given porosity factor, ϕ, and a given stick thickness, b, $I_{Cmax}/3560\ A\sqrt{H}$, according to FIG. 61, is always lower with the opening factor $A\sqrt{H}/A_t = 0.114$ m$^{1/2}$ than with the opening factor $A\sqrt{H}/A_t = 0.040$ m$^{1/2}$ which is in agreement with the conditions found in the previous sections, c.f., for instance, FIG. 37. Aside from the combination $A\sqrt{H}/A_t = 0.04$ m$^{1/2}$, $\phi \approx 1.0$ cm$^{1.1}$, the curves described in FIG. 61 exhibit a falling tendency for the maximum energy, I_{Cmax}, with increasing stick thickness, b. The curves indicate that the results which have been presented in the previous sections and which have all been related to the stick thickness b = 25 mm can, with acceptable presicion, be expanded to be generally valid for the stick thickness range $20 \lesssim b \lesssim 30$ mm. For such combinations of the opening factor, $A\sqrt{H}/A_t$, and the porosity factor, ϕ, wich give a ventilation controlled type of fire process, the results obtained for the stick thickness b = 25 mm, according to FIG. 61, seem to be able to be expanded to an approximate applicability within the significantly larger stick thickness range of $10 \lesssim b \lesssim 40$ mm.

The I_{Cmax}-values summarized in FIG. 61 are generally true for an approximately constant fire load, $q_{theor} = 52.5$ MJ/m^2 of the enclosing surface. It can, therefore, be expected that a reduction in the maximum energy, I_{Cmax}, through decreased porosity factor and/or increased stick thickness, b, is matched by a corresponding increase in fire duration. Such a relation is verified by FIG. 62 in which the relation between the time magnitude t_r - the time interval from ignition to the time corresponding to $0.75\ I_{Cmax}$ on the descending part of the energy-time curve - and the stick thickness, b, of the fire load at varying porosity- and opening factors, is illustrated by the obtained test results. The figure also confirms the previously described relation that, at otherwise constant conditions, an increase of the opening factor, $A\sqrt{H}/A_t$, results in a decrease of the

fire duration, c.f., for instance, FIG. 40.

As a complement, the three energy magnitudes I_{Cm}, I_{Cr}, and I_{Cd} defined according to Section 4.2 are summarized in FIG. 63-65. From the figures it is observed that the three magnitudes generally exhibit consistent characteristics. A decrease of the porosity factor, ϕ, results in a decrease of the energy liberated per unit time for I_{Cm}, I_{Cr}, and I_{Cd}, similar to that for I_{Cmax}. Minor disturbances in this trend can, however, be observed for small and large stick thicknesses. The relation for I_{Cmax}, that is, a generally reduced energy level with increasing stick thickness, b, is less pronounced for the energy magnitudes I_{Cm}, I_{Cr}, and I_{Cd} and thus specially at the lower opening factor, $A\sqrt{H}/A_t = 0.040\ m^{1/2}$. In the light of the influence of the variations in the opening factor, $A\sqrt{H}/A_t$, the curves in FIG. 63-65 confirm the relation established in the previous sections, that the mean energies I_{Cm}, I_{Cr}, and I_{Cd} as well as the maximum energy I_{Cmax}, increase with increasing opening factor, c.f., for instance, FIG. 20-22, 42, 44, and 45. However, within the described variation range, this relation is disturbed for large stick thicknesses, b > 40-45 mm.

For the mean energies I_{Cm}, I_{Cr}, and I_{Cd} it is true, in the same manner as for I_{Cmax}, that the corresponding time periods t_m, t_r, and t_d - columns 10, 12, and 16 in Table VI - increase with decreasing energy level and vice versa assuming an approximately constant fire load. Essentially the same relation characterizes also the time period t_1, that is the time interval between the times corresponding to 0.75 I_{Cmax} and 0.5 I_{Cmax} on the descending part of the energy-time curve, which expresses how fast the energy-time curve falls - c.f. FIG. 66 and column 20, Table VI in combination with FIG. 62.

With a small stick thickness, b, the variations in the porosity factor, ϕ, have very little influence on the energy-time curve of the fire process, which, in this case, is verified for both the opening factor $A\sqrt{H}/A_t = 0.040\ m^{1/2}$ and the opening factor $A\sqrt{H}/A_t = 0.114\ m^{1/2}$, by the relation obtained with the stick thickness b = 12.5 mm according to FIG. 57. This relation is further verified by the magnitudes I_{Cmax}, I_{Cm}, I_{Cr}, and I_{Cd} according to columns 9, 11,

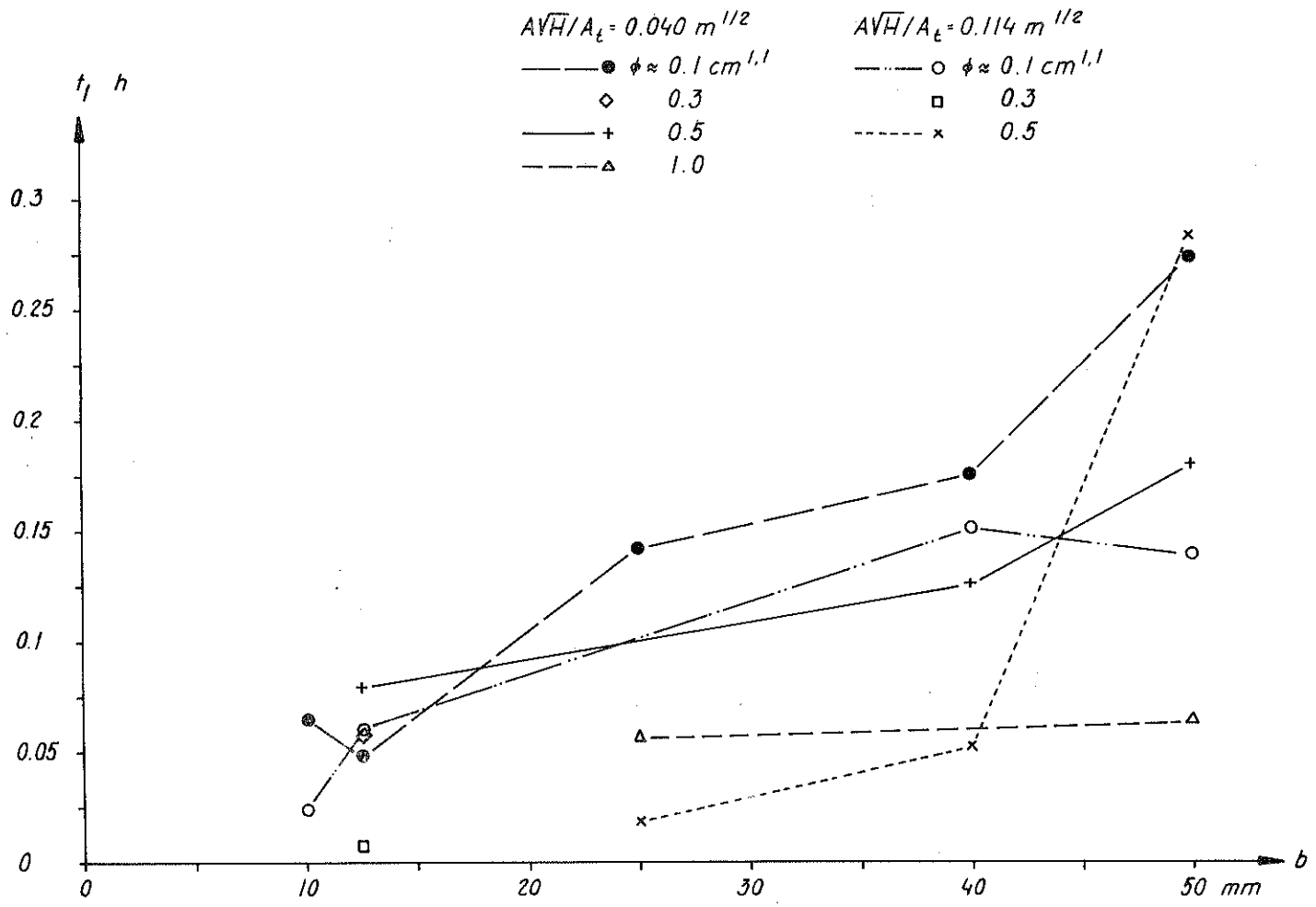

FIG 66 The relation calculated from the obtained test results between the time magnitude, t_1, and the stick thickness, b, of the fire load with varying porosity- and opening factor. The enclosing structures of the fire cell are composed of 10 mm asbestos disk having a density of 1020 kg/m^3 and 1.5 mm steel sheet.

13, and 17 plus FIG. 61 and 63-65. This circumstance could be explained by the fact that the higher the porosity factor is chosen at a small stick thickness, the higher the crib would become. The influence of increased distance between sticks on the fire process is counteracted partly by the fact that the free air-filled space above the crib decreases giving an accentuated combustion with oxygen deficit and partly by the fact that with a high crib, the lower parts only insignificantly get exposed to the radiation from the flames in the upper part of the fire cell. Thus no combustion-increasing effect on the crib is obtained, since the temperature inside the crib is higher than the air-filled space situated above, which is also established by Harmathy (1972). Variations in the porosity factor, ϕ, are, however, significant for the fire process with larger stick thicknesses which is illustrated by FIG. 59 and 60 for the stick thickness b = 40 and 50 mm respectively. From these figures it is observed that a low ϕ-value gives rise to a low, rather flat energy-time curve while a high ϕ-value results in a more concentrated and much higher maximum energy value with time. This circumstance is explained by the fact that an increase in the porosity factor at a large stick thickness does not have any significant influence on the height of the crib at the same time as the space between the sticks increases so that both the oxygen passage and radiation exposure by the flames are facilitated.

Finally comments are made on the magnitudes belonging to the cooling phase of the fire process, that is the mean value of the combustion rate, R_g, mean value of the energy liberated per unit time I_{Cg} and the heat value $W_g = I_{Cg}/R_g$, all belonging to the time interval, t_g, which regarded from the time corresponding to 0.75 I_{Cmax} on the descending part of the energy-time curve, embraces the total cooling phase according to FIG. 18. The three magnitudes are described in columns 24, 23, and 25 respectively and the time interval, t_g, is described in column 22 Table VI.

From the described values it is observed that the total energy $t_g \cdot I_{Cg}$, liberated during the time interval, t_g, has a rather moderate variation with the opening factor, $A\sqrt{H}/A$, the porosity factor, ϕ, and the stick thickness, b. For all the factors together the mean value of the total energy amounts to 94.7 MJ and by division into

groups with respect to the opening factor, $A\sqrt{H}/A_t$, and the stick thickness, b, then Table VII is true for the corresponding mean values. The table shows a tendency towards increased total liberated energy during the cooling phase, with increasing opening factor, $A\sqrt{H}/A_t$, and decreasing stick thickness, b.

For the mean combustion rate, R_g, of the cooling phase column 24, Table VI and FIG. 67 generally show an increasing trend with increased stick thickness, b, and with increasing porosity factor, ϕ. This trend appears to be somewhat diffuse which should primarily be regarded as a consequence of the fact that the experimental basis does not allow any higher degree of precision in a theoretical evaluation of the cooling phase of the fire process. This fact is also reflected in a summary of the mean value $W_g = I_{Cg}/R_g$ belonging to the cooling phase, according to FIG. 68, based on column 25, Table VI. In conformity with what has been established in previous sections, FIG. 68 renders a heat value, W_g, which is always very high, the reason being a combination of high liberated radiation energy and a very slow weight decrease of the fire load during the cooling phase, t_g. As a general trend, the figure shows a marked decrease in the heat value, W_g, with increasing stick thickness, b. This trend is more obvious for the lower opening factor $A\sqrt{H}/A_t$ = 0.040 than for the higher one $A\sqrt{H}/A_t$ = 0.114 $m^{1/2}$. The obtained variations of the combustion rate, R_g, and the heat value, W_g, with the stick thickness, b, could be explained by the fact that at the onset of the cooling phase, t_g, using slender sticks, the remaining fuel is mainly composed of burning pieces while the portion of the product of completely burnt sticks, that is "ashes" is small which gives a high heat value per kg of the remaining fuel. With large dimensions, the length of the flaming phase of the fire process increases which implies that with an approximately constant penetration rate through the timber a good buring depth is obtained resulting in the fact that the external parts of the sticks would be burnt completely before the internal parts are turned into flames. Thus, when the cooling phase begins the portion of the completely burnt products is larger than what is true for the more slender sticks and consequently a lower heat value is obtained for the cooling phase.

$A\sqrt{H}/A_t = 0.040\ m^{1/2}$		$A\sqrt{H}/A_t = 0.114\ m^{1/2}$	
84.8 MJ		108.2 MJ	
b = 10, 12.5 mm	b = 40, 50 mm	b = 10, 12.5 mm	b = 40, 50 mm
100.3 MJ	75.2 MJ	128.3 MJ	94.2 MJ

TAB. VII Mean value of the liberated energy, $I_{Cg} \times t_g$, during the cooling phase, t_g, with division into groups with respect to the opening factor, $A\sqrt{H}/A_t$, and the stick thickness.

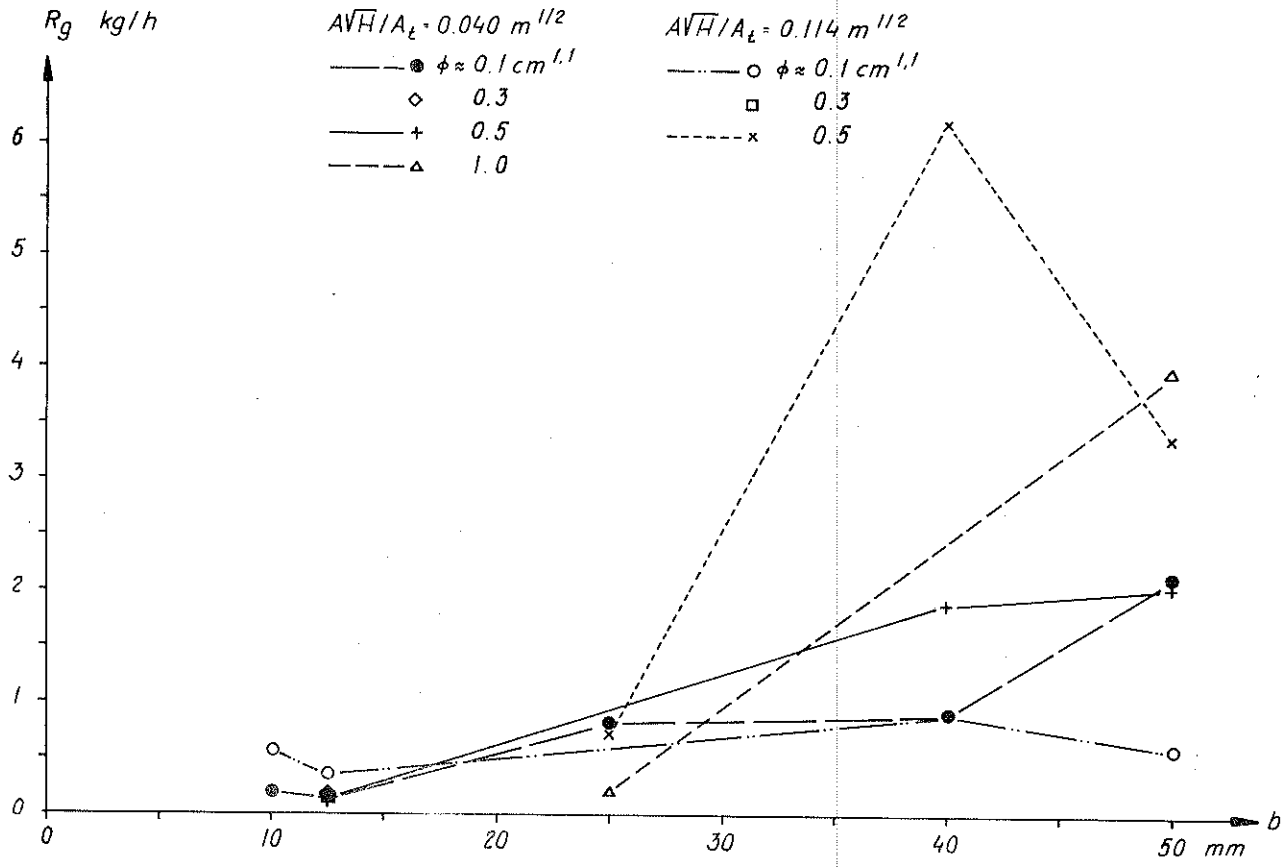

FIG 67 The experimentally determined relation between the mean combustion rate, R_g, of the cooling phase and the stick thickness, b, of the fire load with varying porosity- and opening factor. The enclosing structures of the fire cell are composed of 10 mm asbestos disk having a density of 1020 kg/m^3 and 1.5 mm steel sheet.

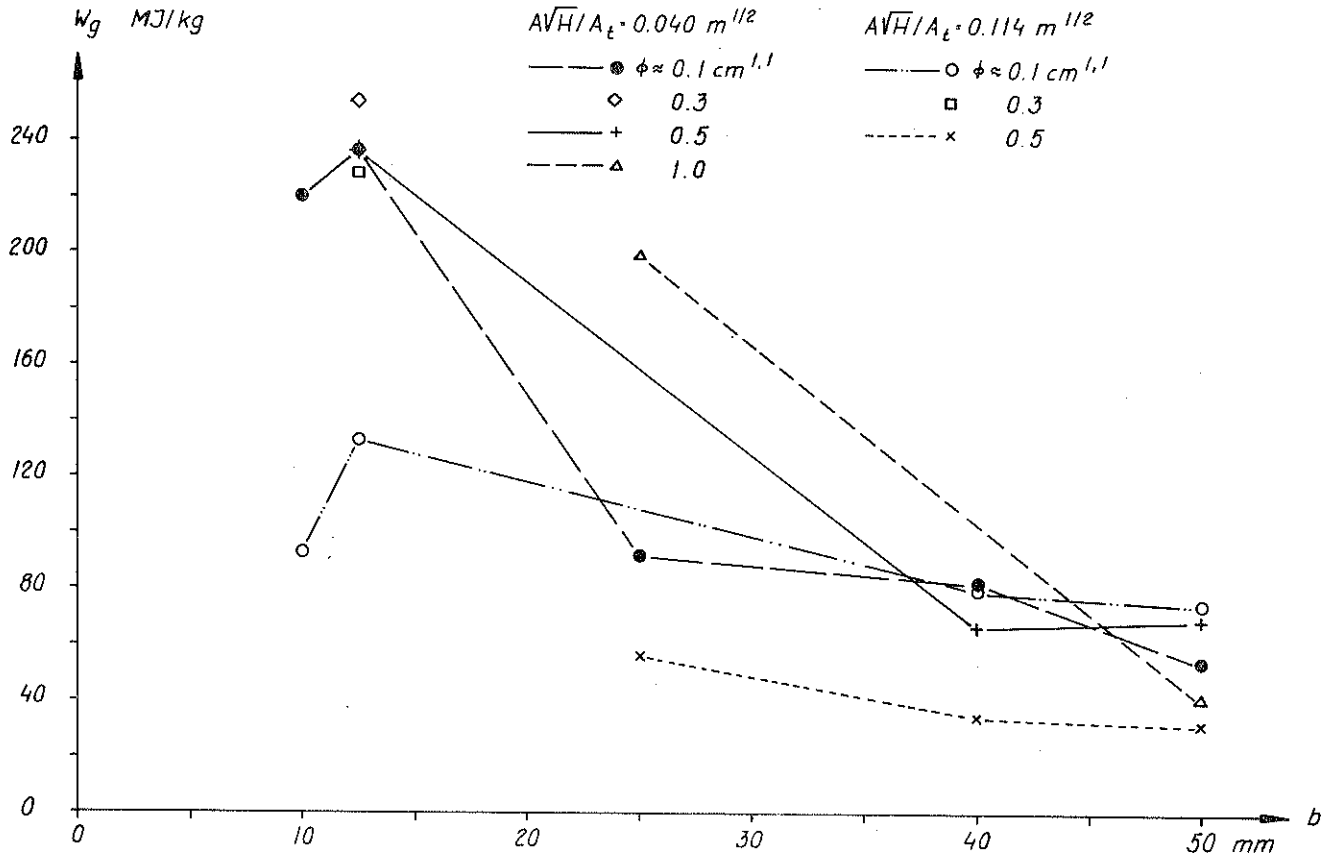

FIG 68 The relation determined from the experimental results between the mean heat value, $W_g = I_{Cg}/R_g$, of the cooling phase and the stick thickness, b, of the fire load with varying porosity- and opening factor. The enclosing structures of the fire cell are composed of 10 mm asbestos disk having a density of 1020 kg/m^3 and 1.5 mm steel sheet.

7. THERMAL PROPERTIES OF THE ENCLOSING STRUCTURES OF THE FIRE CELL.

7.1 Introductory discussion. Test characteristics.

Changes in the thermal properties of the enclosing structures of a fire cell, directly influence the term I_W in energy balance of the fire cell, Equation (1). With a given value for the energy, I_C, released by combustion of the fire load, a change of the term I_W influences the other terms of the energy balance and thus also the gas temperature-time curve, ϑ_g-t, of the fire process.

This condition has been theoretically studied by Ödeen (1963) and Magnusson-Thelandersson (1970), using the heat- and mass balance equations of the fire cell. For an illustration of the order of magnitude of the influence of the variations in the thermal properties of the enclosing structures on the gas temperature, FIG. 69 shows gas temperature-time curves calculated by Magnusson-Thelandersson (1970), which are true for a fire load of $q = 250$ MJ/m^2 of the enclosing surface in a fire cell with the opening factor $A\sqrt{H}/A_t = 0.040$ m$^{1/2}$ for 8 different shapes of the enclosing structures. At otherwise unchanged conditions, the figure gives a substantially higher gas temperature, ϑ_g, for a strongly heat insulated enclosing structure of light-weight concrete (type C) than for a poorly heat insulated enclosing structure of thin steel sheet (type F). For the latter type of enclosing structure, variations in the resulting emissivity, according to the figure, gives a strong influence on the gas temperature. For fire cells with heat insulated enclosing structures, this influence is, however, ordinarily of minor practical importance.

In the mentioned works by Ödeen (1963) and Magnusson-Thelandersson (1970) the authors assume a time variation for the heat quantity released per unit time, I_C, which is not affected by the changes in the thermal properties of the enclosing structures of the fire cell. Unfortunately, there is no description of any experimental results in the literature which gives the basis for an estimation of the precision in such an assumption. On the whole, literature concerning experimental investigations of the influence of changes in the properties of the enclosing structures on different characteristics of the fire process, is extremely scarce. A complementary test series

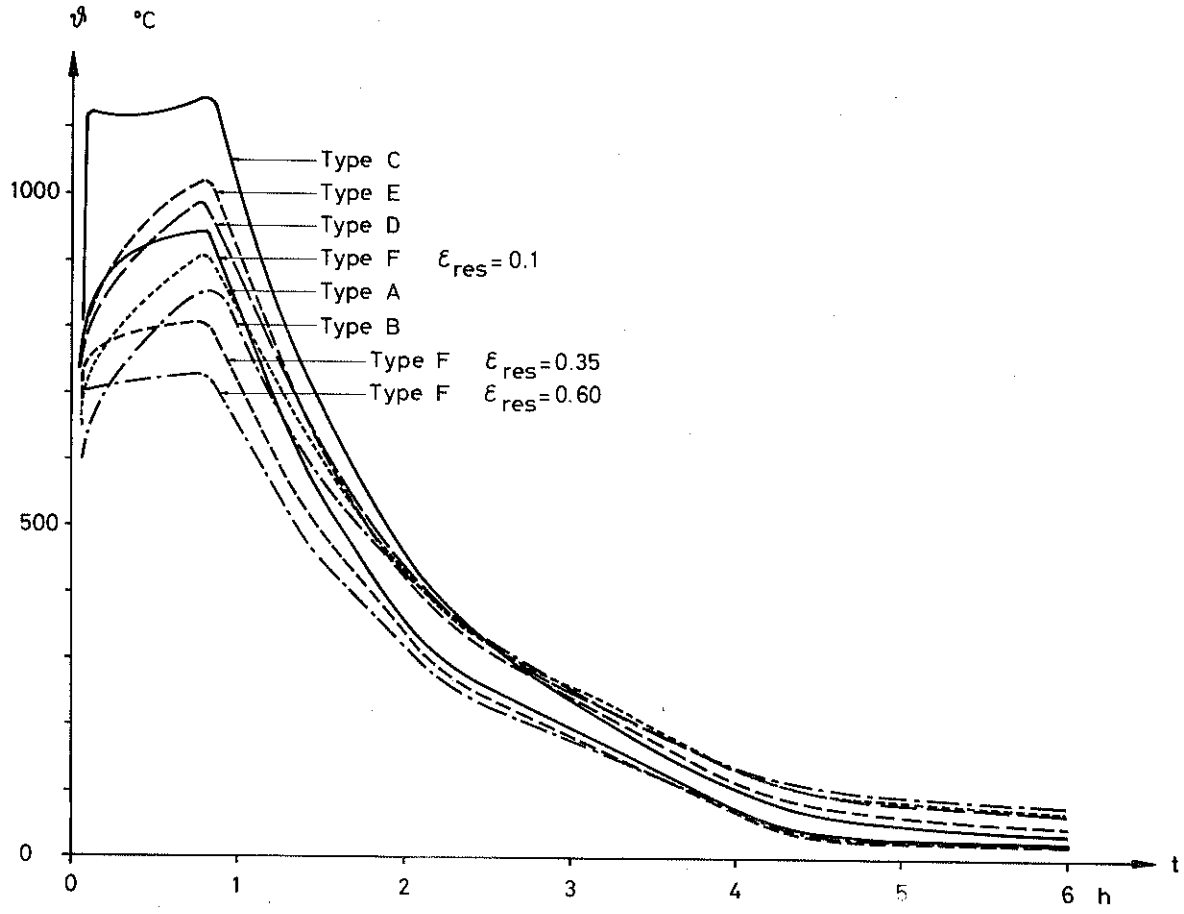

FIG. 69 Gas temperature-time curves, ϑ_g - t, calculated by heat- and mass balance equations of the fire cell with 8 different forms for the enclosing structures of the fire cell. Fire load q = 250 MJ/square m of the enclosing surface, opening factor, $A\sqrt{H}/A_t$ = 0.04 $m^{1/2}$. Among the different alternatives for the enclosing structures, type B denotes concrete, type C light weight concrete with a density of γ = 500 kg/m^3 and type F 2 mm steel sheet in the ceiling and walls plus concrete in the floor.

dealing with the fire load in the form of a regular wood cribs according to FIG. 10 has thus been deemed to be necessary and has also been performed with a comparative study for the following three types of enclosing structures which observed from the external surface inwards have the following components:

a) 1.5 mm steel sheet
b) 1.5 mm steel sheet + 10 mm asbestos disk with the density of 1020 kg/m^3
c) 1.5 mm steel sheet + 125 mm light-weight concrete with the density of 500 kg/m^3.

The three types mentioned here represent a poorly heat insulated, a moderately heat insulated and a strongly heat insulated construction respectively.

In order to relate the results to the ones described in the previous sections, the same values of the opening factor, that is $A\sqrt{H}/A_t$ = 0.020, 0.032, 0.040, 0.070 and 0.114 $m^{1/2}$, and the same value of the fire load q = 35.0 MJ/m^2 of the enclosing surface corresponding to 2 kg wood/m^2 are maintained in the experiments. For the stated combination wall construction - opening factor a porosity factor of $\phi \approx$ 0.5 $cm^{1.1}$ was chosen. In order to somewhat expand the applicability of the test series, the well-insulated construction, that is alternative c) mentioned above, with the intermediate opening factor $A\sqrt{H}/A_t$ = 0.040 was completed with four further values of the porosity factor ϕ, namely ϕ = 0.04, 0.3, 0.7, and 1.1 $cm^{1.1}$ through which a broader insight into the subject was obtained by a direct comparison with the values obtained for alternative b), steel sheet + asbestos disk, described in Section 4.

7.2 Analysis of the experimental results

By applying the calculation procedure briefly referred to in Section 2, the energy-time curves corresponding to the respective tests have been determined and described in FIG. 70-73. Based on the relations obtained from the figures, the fire process characterizing parameters corresponding to those summarized in Section 4 have been determined and described in Table VIII, c.f. FIG. 18 for the applied notations. As a complement, the energy magnitudes I_{Cmax}, I_{Cm}, I_{Cr}, and I_{Cd} are summarized in FIG. 74-78 for varying opening factor, $A\sqrt{H}/A_t$, and poro-

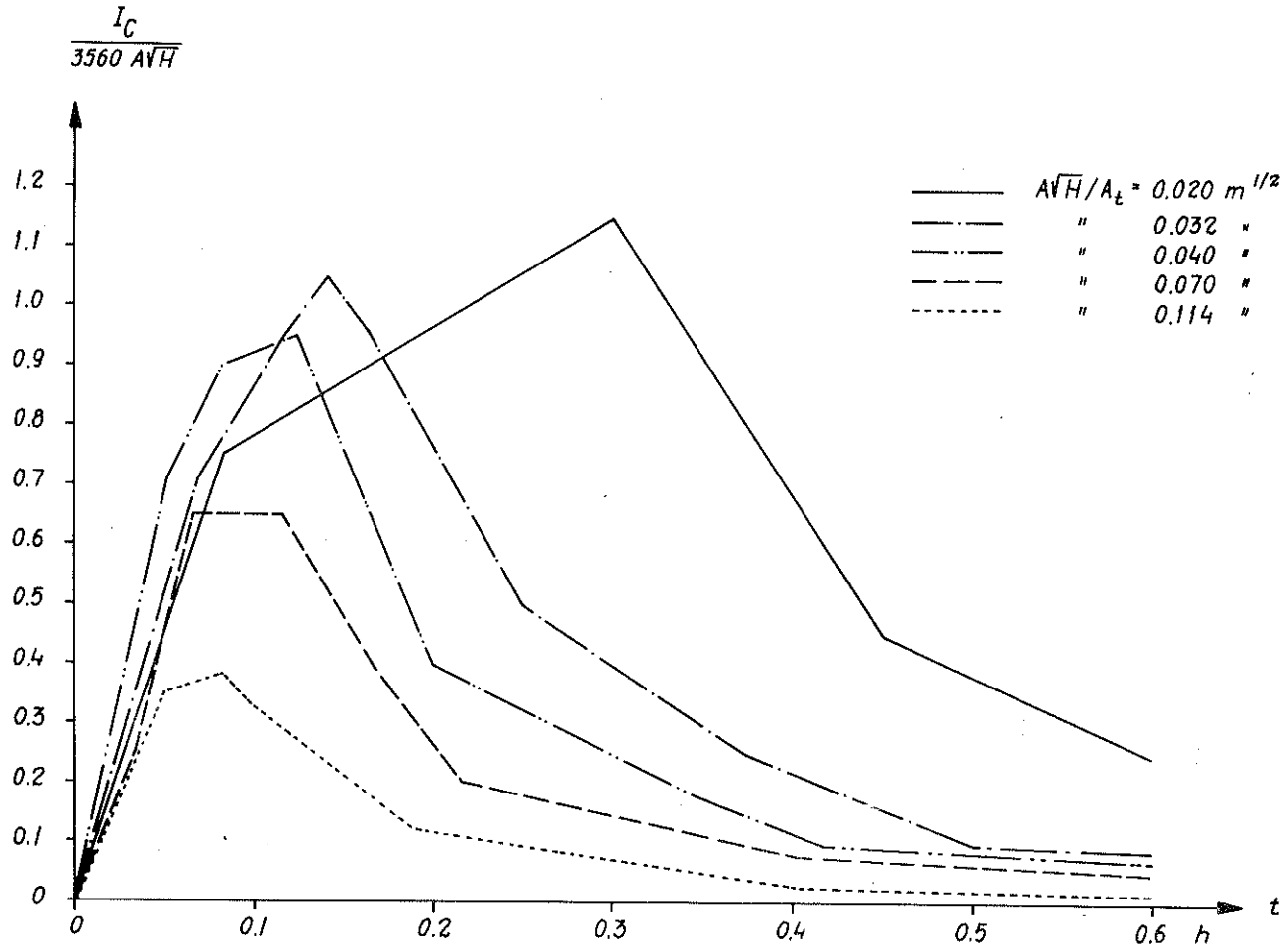

FIG 70 Theoretically calculated energy-time curve of the energy developed during the fire process with varying opening factor, $A\sqrt{H}/A_t$ ($m^{1/2}$). The enclosing structure consists of 1.5 mm steel sheet. Fire load q = 35 MJ/square meter of the enclosing surface, porosity factor ϕ = 0.495 $cm^{1.1}$.

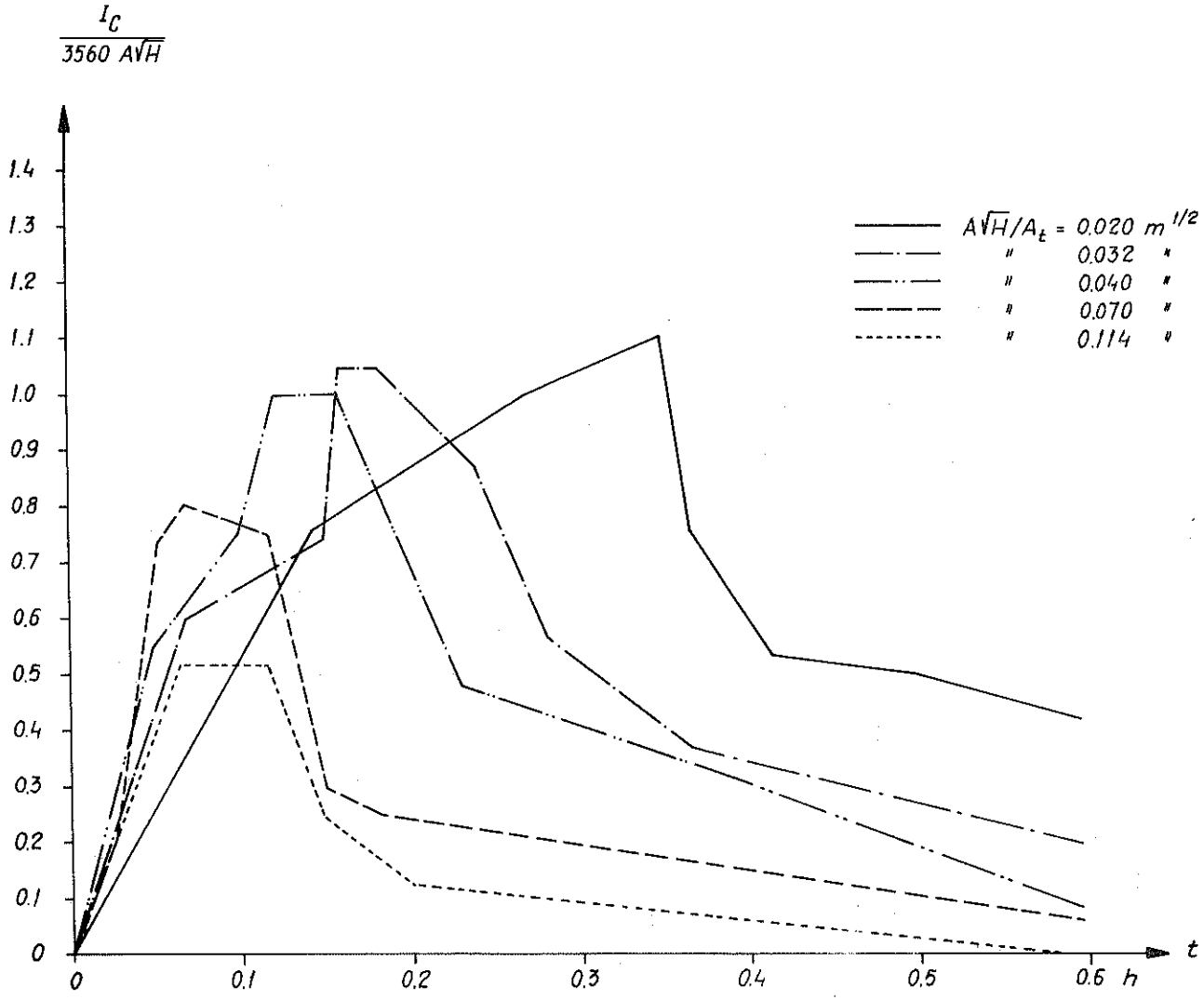

FIG 71 Theoretically calculated energy-time curve of the energy developed during the fire process with varying opening factor, $A\sqrt{H}/A_t$ ($m^{1/2}$). The enclosing structure consists of 1.5 mm steel sheet + 10 mm asbestos disk (density 1020 kg/m^3). Fire load q = 35 MJ/square meter of the enclosing surface, porosity factor ϕ = 0.495 $cm^{1.1}$.

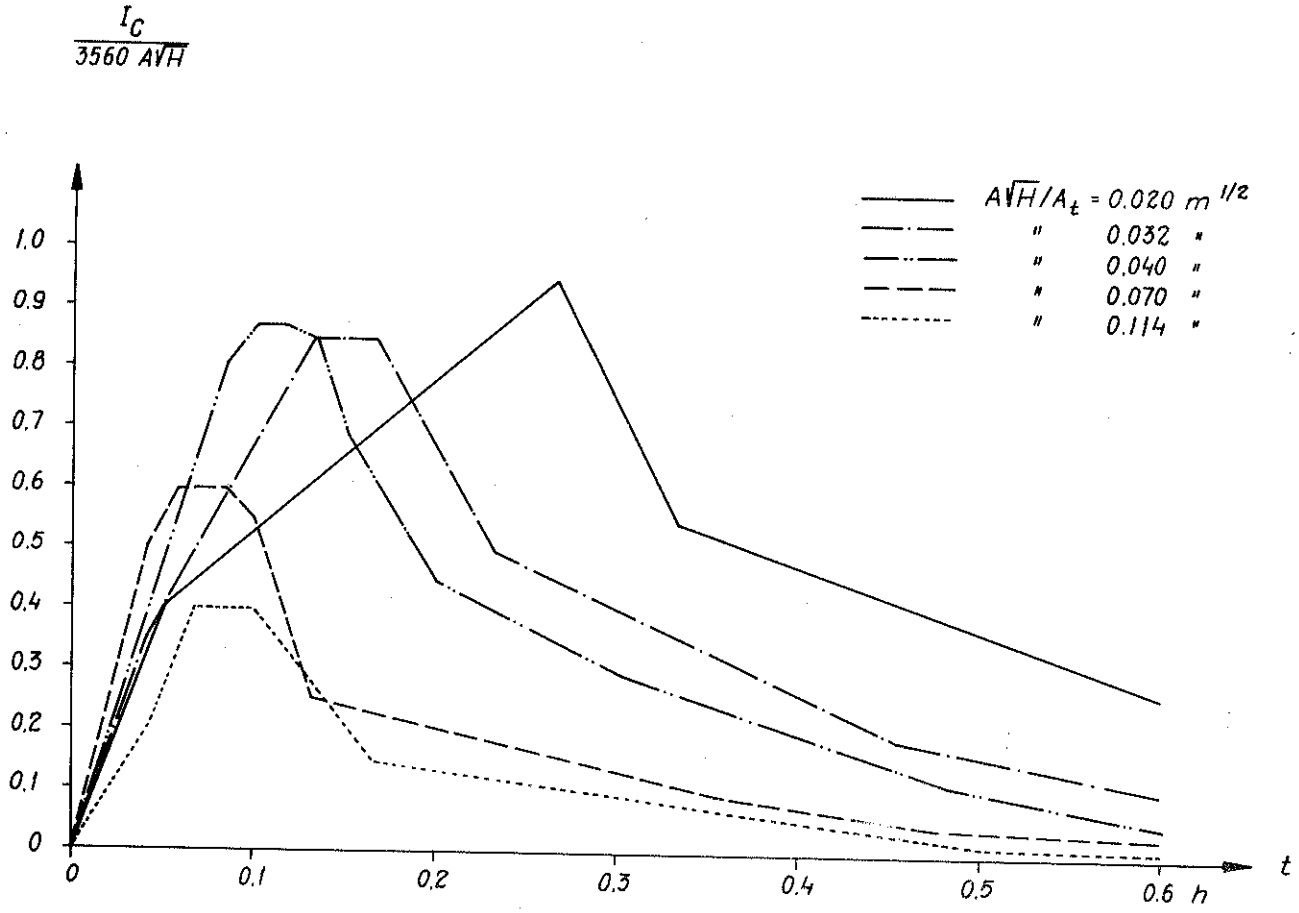

FIG 72 Theoretically calculated energy-time curve of the energy developed during the fire process with varying opening factor, $A\sqrt{H}/A_t$ ($m^{1/2}$). The enclosing structure consists of 1.5 mm steel sheet + 125 mm light weight concrete (density 500 kg/m^3). Fire load q = 35 MJ/square meter of the enclosing surface, porosity factor ϕ = 0.517 $cm^{1.1}$.

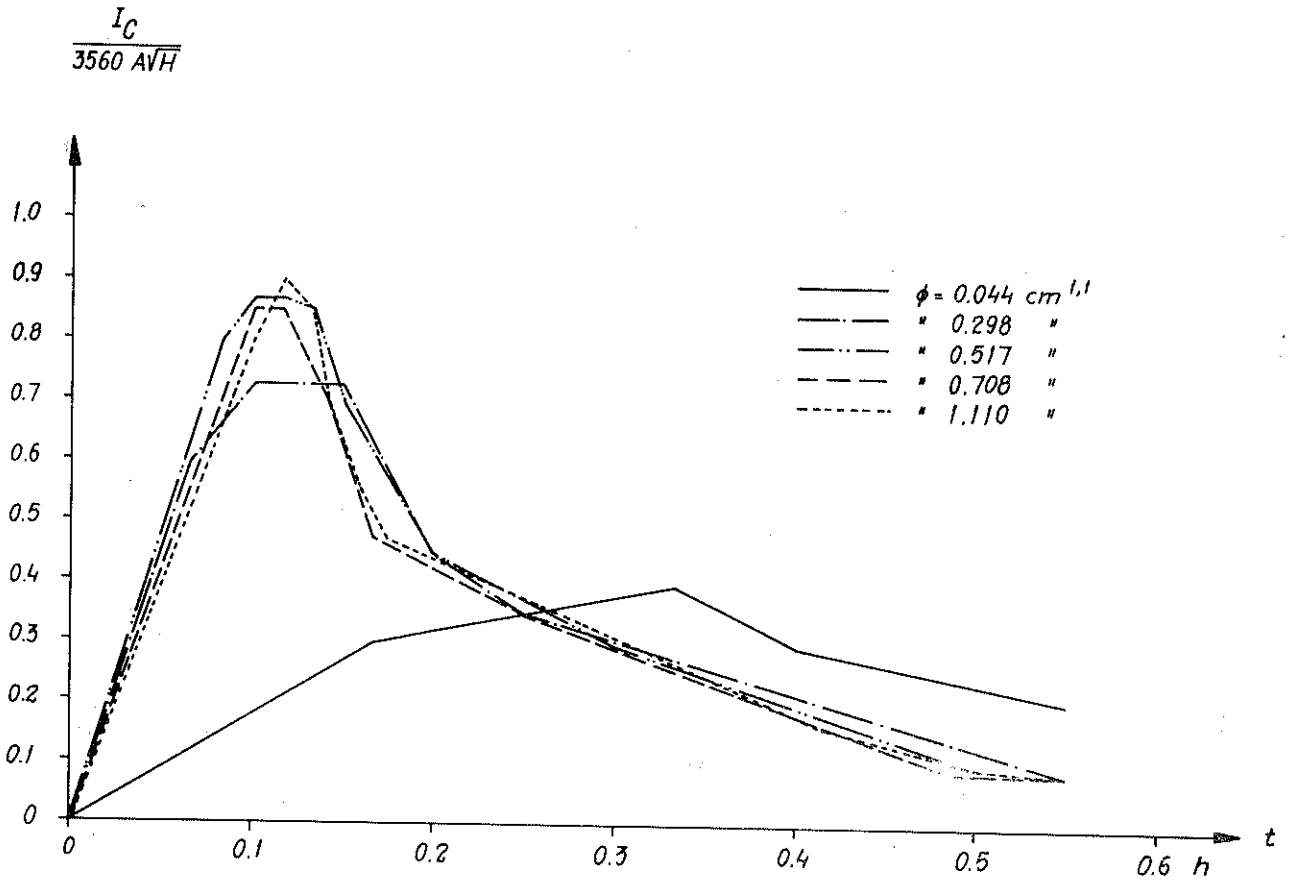

FIG 73 Theoretically calculated energy-time curve of the energy developed during the fire process with varying porosity factor, ϕ ($cm^{1.1}$). The enclosing structure consists of 1.5 mm steel sheet + 125 mm light weight concrete (density 500 kg/m^3). Opening factor, $A\sqrt{H}/A_t$ = 0.040 $m^{1/2}$, fire load q = 35 MJ/square meter of the enclosing surface.

TAB. VIII Characteristics and primary values with several magnitudes for tests embracing a study of the influence of varying thermal properties of the enclosing structures on the fire process.

Enclosing surfaces	$\frac{A\sqrt{H}}{A_t}$	ϕ	q_{theor}	q	$\frac{Q_a}{\varphi\ A\sqrt{H}}$	$R = 330A\sqrt{H}$	R_{80-30}	I_{Cmax}	t_m	I_{Cm}	t_r	I_{Cr}	R_r	$W_r = \frac{I_{Cr}}{R_r}$
	$m^{1/2}$	$cm^{1.1}$	MJ/m^2 o.y.	MJ/m^2 o.y.		kg/h	kg/h	MJ/h	h	MJ/h	h	MJ/h	kg/h	MJ/kg
(1)	(2)	(3)	(4)	(5)	(6)	(7)	(8)	(9)	(10)	(11)	(12)	(13)	(14)	(15)
1.5 mm steel sheet	0.020	0.495	35.0	35.6	1.0	22.3	23.0	276	0.300	190	0.362	199	18.20	10.9
	0.032	0.495	35.0	35.9	1.0	35.6	46.1	403	0.142	243	0.197	275	33.91	8.1
	0.040	0.495	35.0	32.8	1.0	44.6	48.7	442	0.100	286	0.160	335	37.86	8.8
	0.070	0.495	35.0	36.9	0.8	77.9	57.7	546	0.092	327	0.149	396	42.89	9.2
	0.114	0.495	35.0	36.9	0.7	127.0	53.4	520	0.083	344	0.118	376	50.77	7.4
1.5 mm steel sheet + 10 mm asbestos disk	0.020	0.495	35.0	35.3	1.0	22.3	27.1	252	0.309	159	0.365	178	16.02	11.1
	0.032	0.495	35.0	37.3	1.0	35.6	37.1	403	0.171	216	0.253	265	24.85	10.7
	0.040	0.117	35.0	37.1	1.0	44.6	27.1	456	0.163	301	0.229	336	23.94	14.0
	0.040	0.276	35.0	37.8	1.0	44.6	41.7	408	0.148	275	0.200	303	29.88	10.1
	0.040	0.495	35.0	37.5	1.0	44.6	43.5	480	0.140	285	0.193	327	30.57	10.7
	0.040	0.688	35.0	34.8	1.0	44.6	51.6	504	0.117	306	0.152	340	35.99	9.5
	0.040	1.092	35.0	38.0	1.0	44.6	51.2	528	0.127	289	0.160	330	37.38	8.8
	0.070	0.495	35.0	40.5	0.8	77.9	66.0	673	0.067	340	0.128	481	48.75	9.9
	0.114	0.495	35.0	37.9	0.7	127.0	59.3	712	0.092	453	0.133	523	42.97	12.2
1.5 mm steel sheet + 125 mm light weight concrete	0.020	0.517	35.0	37.8	1.0	22.3	30.0	228	0.267	141	0.307	148	20.46	7.2
	0.032	0.517	35.0	36.9	1.0	35.6	43.6	326	0.150	196	0.207	224	30.99	7.2
	0.040	0.044	35.0	37.7	1.0	44.6	21.2	192	0.333	120	0.400	128	15.77	8.1
	0.040	0.298	35.0	39.2	1.0	44.6	50.5	348	0.125	231	0.184	261	35.74	7.3
	0.040	0.517	35.0	38.7	1.0	44.6	58.9	418	0.108	241	0.160	287	40.94	7.0
	0.040	0.708	35.0	36.5	1.0	44.6	62.7	408	0.108	220	0.148	261	40.37	6.5
	0.040	1.110	35.0	35.8	1.0	44.6	56.0	432	0.117	222	0.144	256	41.68	6.1
	0.070	0.517	35.0	36.6	0.8	77.9	66.0	504	0.071	323	0.111	378	54.28	7.0
	0.114	0.517	35.0	36.2	0.7	127.0	63.5	547	0.083	298	0.127	370	47.24	7.8

t_d	I_{Cd}	R_d	$W_d = \frac{I_{Cd}}{R_d}$	t_1	t_2	t_g	I_{Cg}	R_g	$W_g = \frac{I_{Cg}}{R_g}$	I_{Cav}	W_{av}	ϑ_{80-30}	$\frac{R_{80-30}}{\vartheta_{80-30}}$	$\frac{I_{Cav}}{\vartheta_{80-30}}$	Försök nr
h	MJ/h	kg/h	MJ/kg	h	h	h	MJ/h	kg/h	MJ/kg	MJ/h	MJ/kg	°C	kg/°C·h	MJ/°C·h	
(16)	(17)	(18)	(19)	(20)	(21)	(22)	(23)	(24)	(25)	(26)	(27)	(28)	(29)	(30)	(31)
0.219	241	18.27	13.2	0.061	0.207	0.838	50	0.33	151.5	233	10.10	510	0.045	0.46	S 3
0.112	356	50.38	7.1	0.052	0.173	1.373	44	0.17	258.8	363	7.87	585	0.079	0.62	S 8
0.111	409	35.16	11.6	0.032	0.151	0.667	68	0.42	161.9	419	8.62	609	0.080	0.68	S 13
0.096	514	53.01	9.7	0.037	0.125	0.787	75	0.92	81.5	442	7.67	608	0.095	0.73	S 18
0.077	472	51.66	9.1	0.043	0.132	1.812	41	0.62	66.1	363	6.80	529	0.101	0.68	S 23
0.203	240	22.17	10.8	0.066	0.422	0.740	72	1.25	57.6	218	8.05	724	0.037	0.30	C 49
0.101	370	24.61	15.0	0.045	0.137	0.605	95	1.45	65.6	304	8.19	747	0.050	0.40	C 38
0.154	418	25.92	16.1	0.047	0.196	0.378	125	4.36	28.6	418	15.40	775	0.035	0.54	C 31
0.128	379	36.09	10.5	0.079	0.306	0.563	116	2.28	50.9	384	9.21	700	0.059	0.55	C 29
0.093	453	39.49	11.5	0.037	0.251	0.474	131	2.73	48.0	427	9.82	732	0.059	0.58	C 27
0.077	455	44.66	10.2	0.046	0.102	0.618	106	1.92	55.2	437	8.47	762	0.068	0.57	C 25
0.066	485	40.71	11.9	0.026	0.244	0.631	118	2.10	56.2	398	7.78	716	0.071	0.55	C 23
0.084	631	59.61	10.6	0.014	0.165	0.606	122	2.54	47.9	647	9.81	753	0.088	0.86	C 16
0.083	676	52.31	12.9	0.016	0.067	0.464	120	3.36	35.7	698	11.77	641	0.092	1.09	C 7
0.135	199	18.59	10.7	0.097	0.324	2.133	36	0.47	76.6	174	5.80	617	0.049	0.28	L 3
0.112	298	37.02	8.1	0.080	0.231	2.343	30	0.30	100.0	300	6.89	792	0.055	0.38	L 8
0.233	168	15.32	11.0	0.166	0.333	1.967	36	0.49	73.5	164	7.76	413	0.052	0.39	L 11
0.124	324	31.86	10.2	0.060	0.260	2.249	35	0.44	79.6	342	6.78	714	0.071	0.47	L 12
0.092	384	34.34	11.2	0.050	0.223	2.740	29	0.33	87.9	400	6.79	845	0.070	0.47	L 13
0.073	371	34.15	10.9	0.052	0.230	1.685	47	0.63	74.6	383	6.11	817	0.077	0.47	L 14
0.059	390	28.25	13.8	0.050	0.225	1.523	52	0.59	88.1	312	5.57	740	0.076	0.42	L 15
0.073	476	46.77	10.2	0.017	0.167	1.839	42	0.56	75.0	348	5.27	787	0.084	0.44	L 18
0.072	511	39.68	12.9	0.027	0.168	1.743	40	0.57	70.2	449	7.07	660	0.096	0.68	L 23

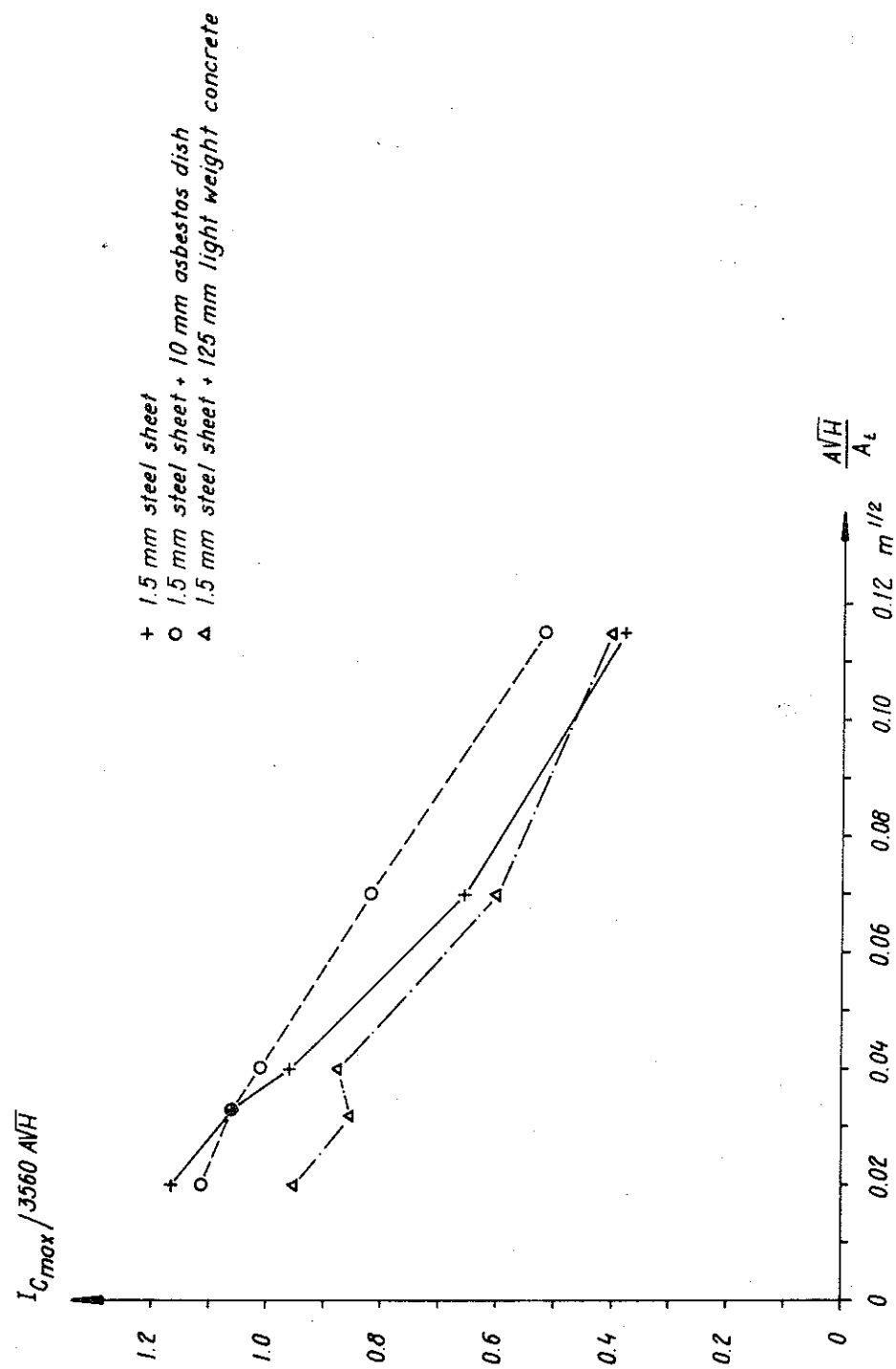

FIG. 74 The relation obtained from the experimental results between the maximum energy released per unit time, I_{Cmax}, and the opening factor, $A\sqrt{H}/A_t$, for three alternative types of enclosing structures. Fire load q_{theor} = 35.0 MJ/square m of the enclosing surface, porosity factor $\phi \approx 0.5$ $cm^{1.1}$.

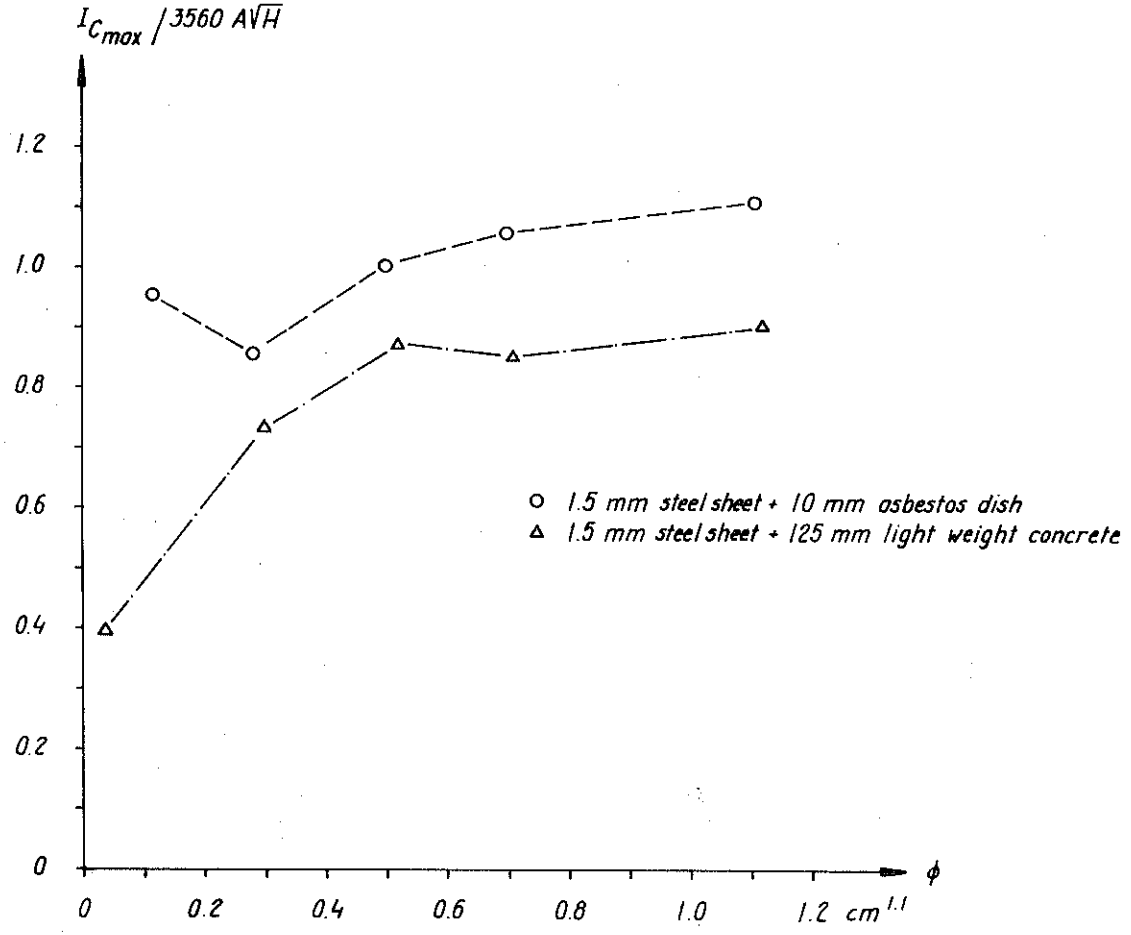

FIG. 75 The relation obtained from the experimental results between the maximum energy released per unit time, I_{Cmax}, and the porosity factor, ϕ, for two alternative types of enclosing structures. Opening factor, $A\sqrt{H}/A_t$ = 0.040 $m^{1/2}$, fire load q_{theor} = 35.0 MJ/square m of the enclosing surface.

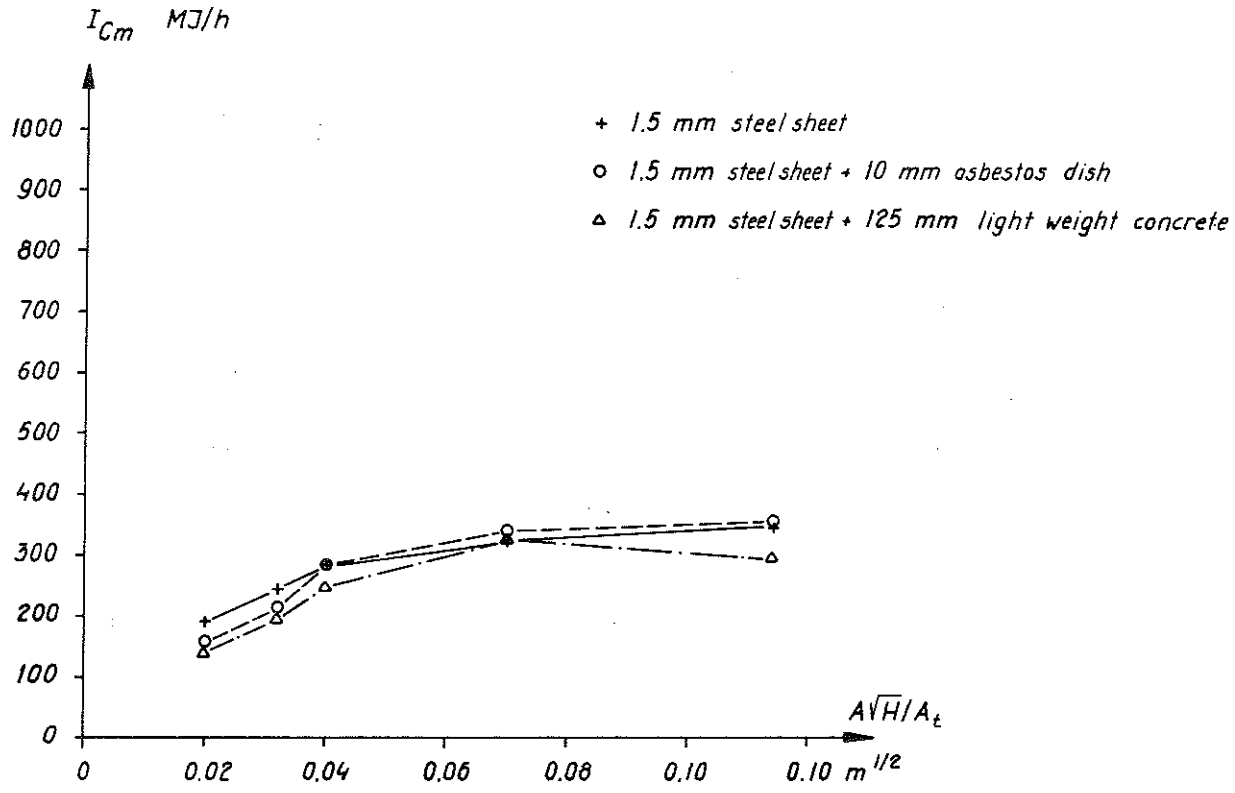

FIG 76 The relation calculated from the obtained test results between I_{Cm} (MJ/h) and the opening factor, $A\sqrt{H}/A_t$ ($m^{1/2}$) with different structural formations of the enclosing structure. Fire load q = 35 MJ/square meter of the enclosing surface, porosity factor $\phi \approx 0.5$ $cm^{1.1}$.

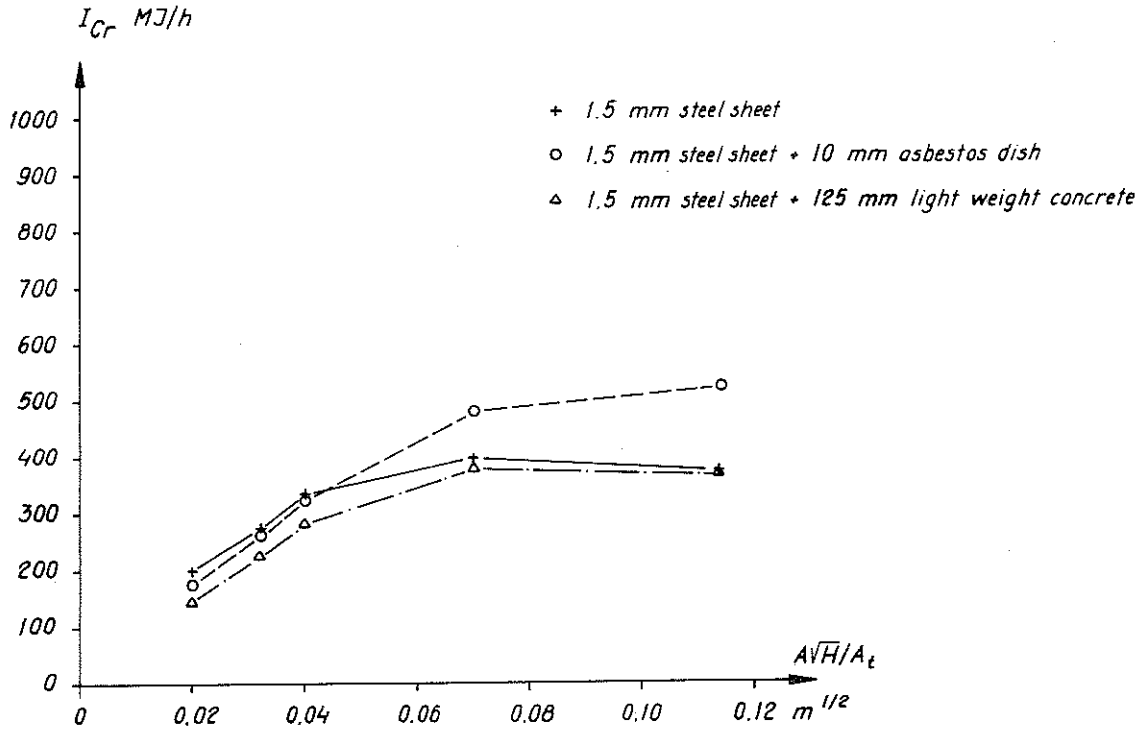

FIG 77 The relation calculated from the obtained test results between I_{Cr} (MJ/h) and the opening factor, $A\sqrt{H}/A_t$ ($m^{1/2}$) with different structural formations of the enclosing structure. Fire load q = 35 MJ/square meter of the enclosing surface, porosity factor $\phi \approx 0.5$ $cm^{1.1}$.

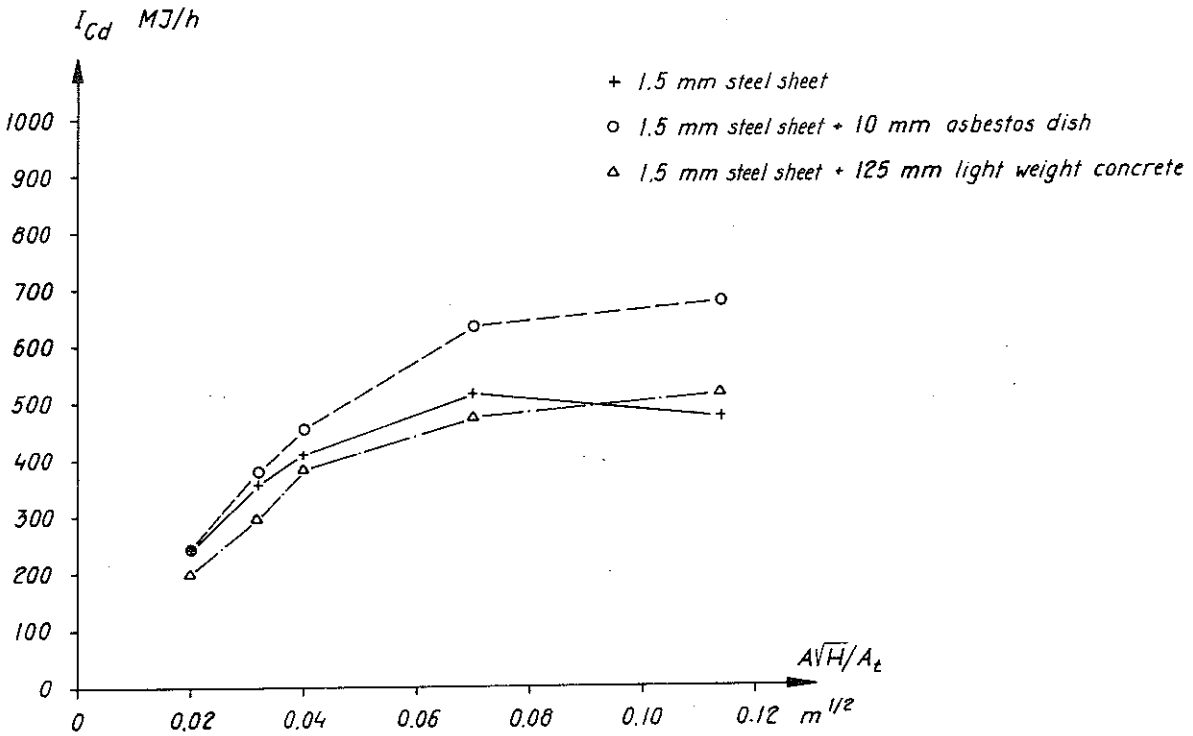

FIG 78 The relation calculated from the obtained test results between I_{Cd} (MJ/h) and the opening factor, $A\sqrt{H}/A$ ($m^{1/2}$) with different structural formations of the enclosing structure. Fire load q = 35 MJ/square meter of the enclosing surface, porosity factor $\phi \approx 0.5$ $cm^{1.1}$.

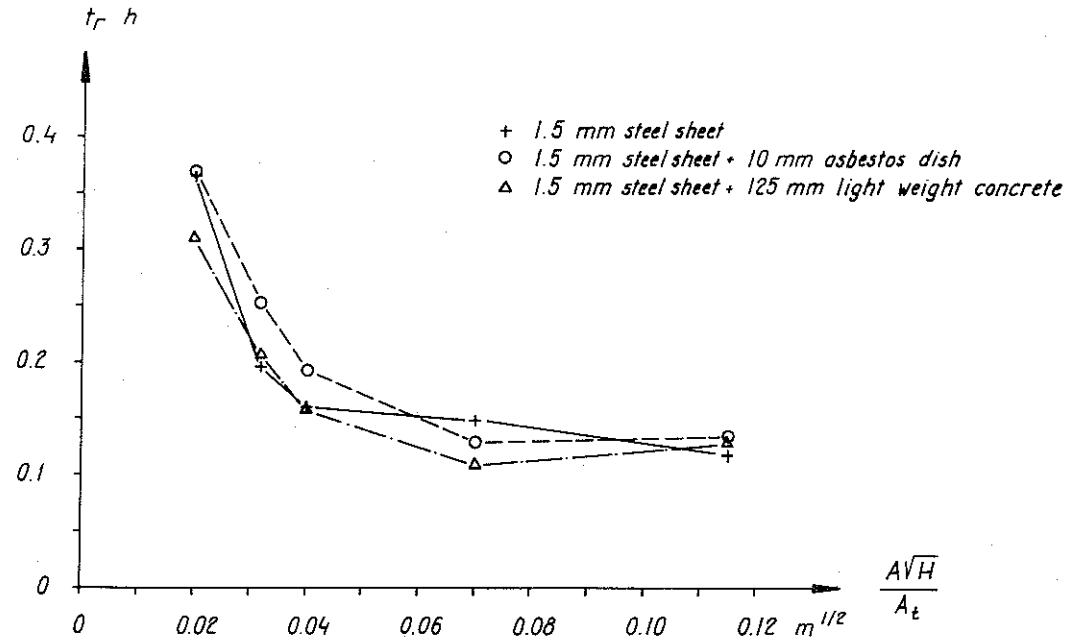

FIG. 79 The relation obtained from the test results between the time magnitude, t_r, and the opening factor, $A\sqrt{H}/A_t$, of the fire cell for three alternative types of enclosing structures. Fire load q_{theor} = 35.0 MJ/square m of the enclosing surface, porosity factor $\phi \approx 0.5$ $cm^{1.1}$.

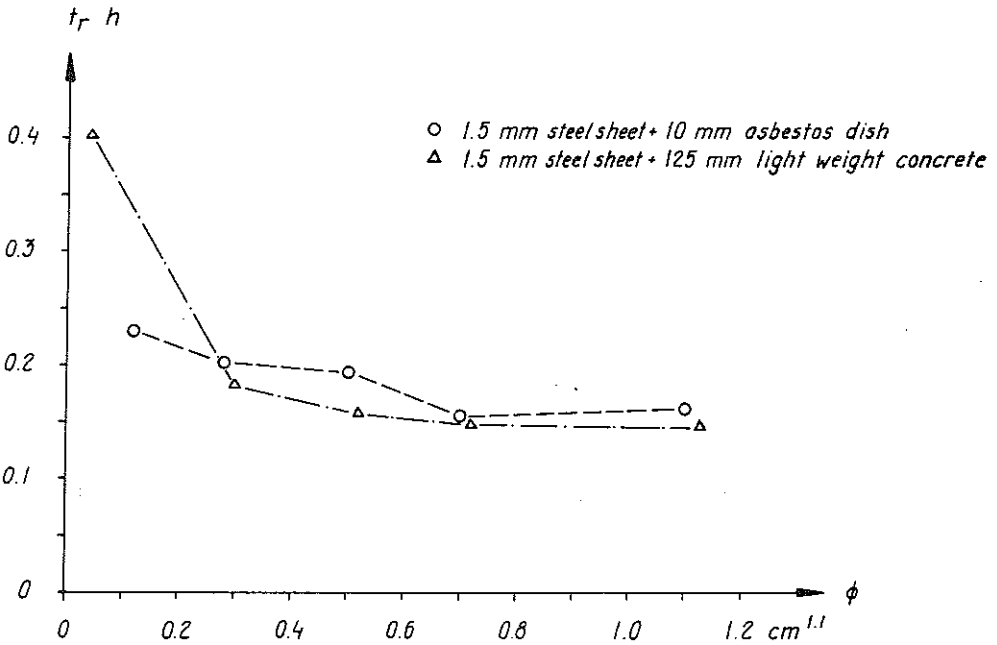

FIG. 80 The relation obtained from the test results between the time magnitude, t_r, and the porosity factor, ϕ, for two alternative types of enclosing structures. Opening factor, $A\sqrt{H}/A_t$ = 0.040 $m^{1/2}$, fire load, q_{theor} = 35.0 MJ/square m of the enclosing surface.

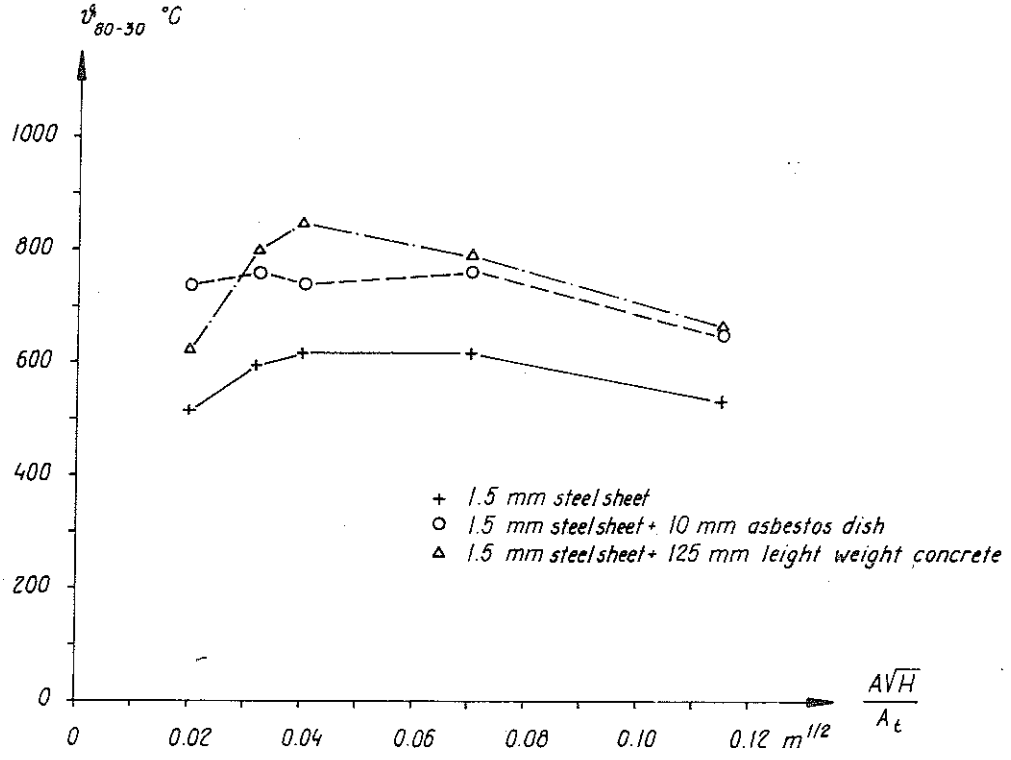

FIG. 81 The mean gas temperature, ϑ_{80-30}, as a function of the opening factor, $A\sqrt{H}/A_t$, for three alternative types of enclosing structures. Fire load, q_{theor} = 35.0 MJ/sqare m of the enclosing surface, porosity facotr, $\phi \approx 0.5$ cm$^{1.1}$.

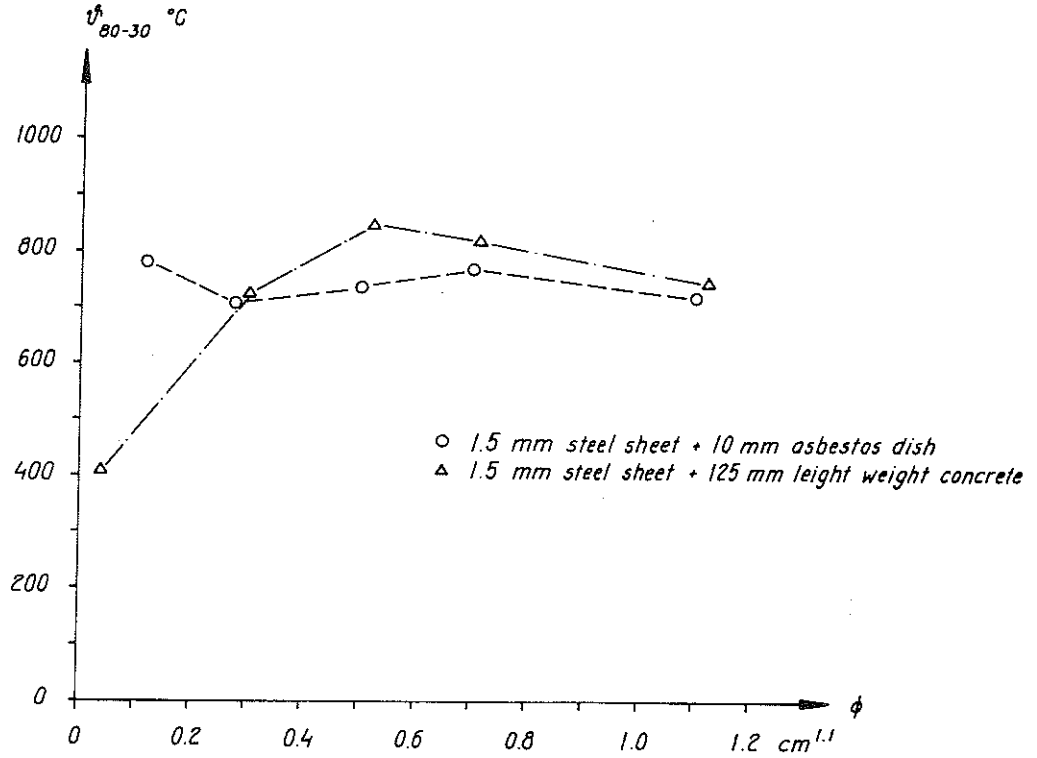

FIG. 82 The mean gas temperature, ϑ_{80-30}, as a function of the porosity factor, ϕ, for two alternative types of enclosing structures. Opening factor $A\sqrt{H}/A_t$ = 0.04 m$^{1/2}$, fire load, q_{theor} = 35.0 MJ/square m of the enclosing surface.

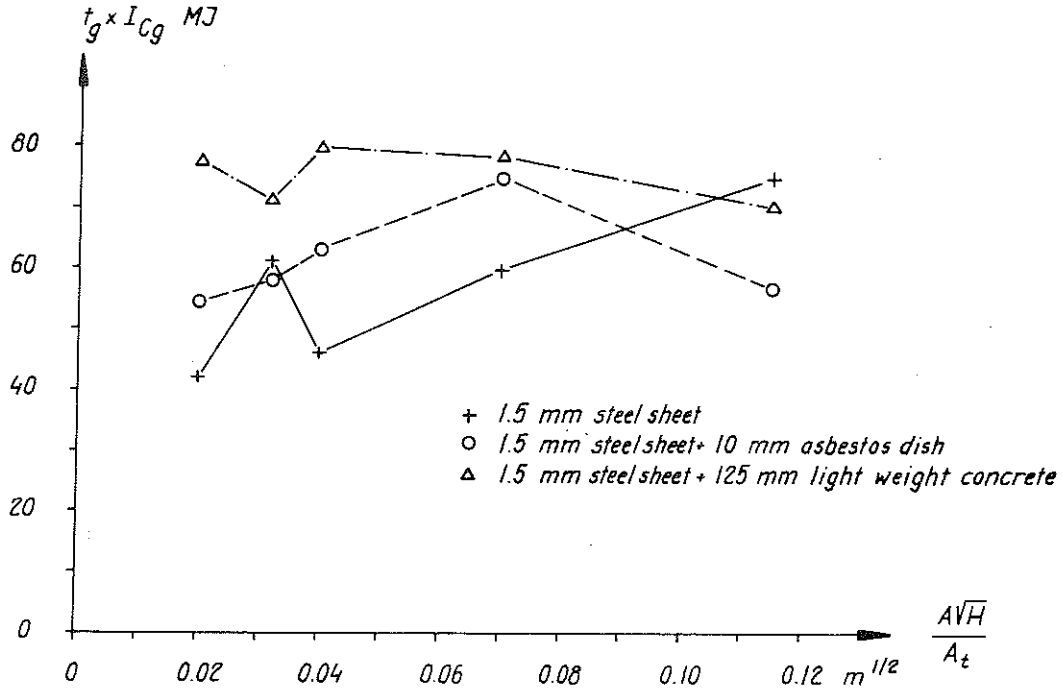

FIG. 83 The relation obtained from the experimental results between the energy magnitude, $t_g \times I_{Cg}$, and the opening factor, $A\sqrt{H}/A_t$, of the fire cell for three alternative types of enclosing structures. Fire load, q_{theor} = 35,0 MJ/square m of the enclosing surface, porosity facotr, $\phi \approx 0.5$ cm$^{1.1}$.

sity factor, ϕ, and analogously the time magnitude, t_r, is summarized in FIG. 79 and 80 as a function of the same variables. An illustration of the gas temperature of the fire cell is given in FIG. 82 and 83 by the mean gas temperature, ϑ_{80-30}. Furthermore, the energy magnitude, $t_g \times I_{Cg}$, corresponding to the cooling phase of the fire process is described in FIG. 81 as a function of the opening factor $A\sqrt{H}/A_t$. All the described results are related to an approximately constant size of the fire load $q_{theor} = 35.0$ MJ/m^2 of the enclosing surface.

In the theoretical analysis of the obtained experimental results, values of the temperature dependent coefficient of conductivity according to TAB. I have been employed as an indication of the thermal properties of the material in the enclosing structures and for the enphalpy, I, the relations given in FIG. 84 are used. In the analysis, the influence of initial humidity has been taken into consideration in an approximate manner. For every material type - asbestos, light-weight concrete - the same initial humidity has been assumed in every test in a part series. For fire cells with enclosing structures of asbestos disk, the influence of such an assumption is practically negligible in all the tests. For fire cells with enclosing structures of light-weight concrete, the corresponding influence is greater. It has been characteristical within the part series that the light-weight concrete members have been changed for every new opening factor. In the first test for an opening factor a moisture ratio of about 23 % was maintained and in the last test the moisture ratio was 8 %, calculated on the basis of the dry unit weight. The prevailing variations in the moisture ratio has been estimated to have no influence on the conclusions drawn in the following.

As far as the influence of variations in the opening factor, $A\sqrt{H}/A_t$, and porosity factor, ϕ, on the energy-time curve and corresponding energy manitudes I_{Cmax}, I_{Cm}, I_{Cr}, and I_{Cd} is concerned, the experimental and analytical results described in Table VIII and FIG. 70-78 verify those obtained in the previous sections. On the whole, it is generally true that the energy characteristics are rather insignificantly influenced by the great variations in the thermal properties of the enclosing structures embraced by the test series. The only exception from this rule is the described results for very

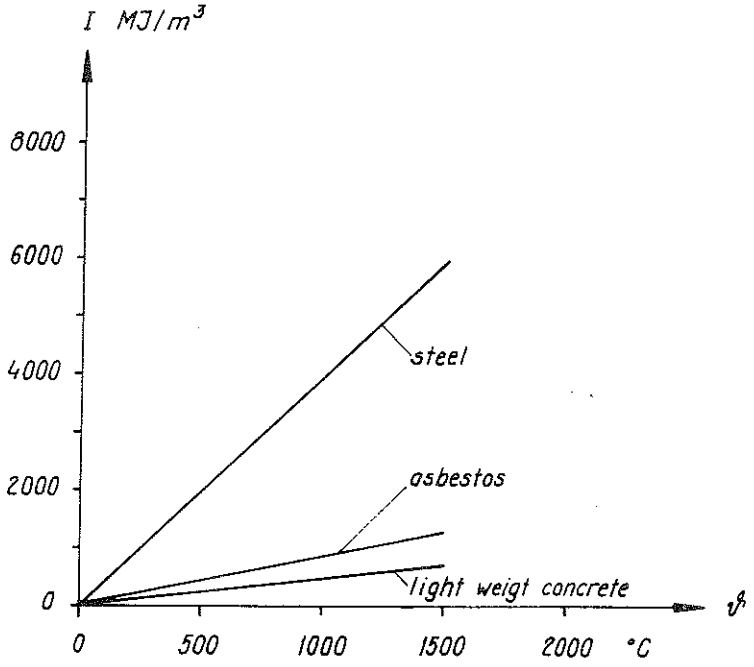

FIG. 84 The relation used in the analysis between the enthalpy, I, and the temperature, ϑ, for steel sheet, asbestos disk with a density of 1020 kg/m^3, and light weight concrete with a density of 500 kg/m^3.

small values of the porosity factor, ϕ, according to FIG. 75. This deviation can possibly be explained by the highly irregular conditions prevailing during the fire process with fire load having an extremely low porosity factor. Generally, the obtained results render a higher value for the energy released per unit time, I_C, with enclosing structures of steel sheet + asbestos than with enclosing structures of steel sheet + light-weight concrete. For the third type of the enclosing structures investigated, that is 1.5 mm steel sheet, the obtained I_C-values are close to those for the alternative steel sheet + asbestos with small opening factors and close to those for the alternative steel sheet + light-weight concrete with large opening factors. A somewhat irregular picture is presented by the energy magnitude I_{Cm}, FIG. 76 which can be explained by the fact that the influence of variations in the thermal properties of the enclosing structures is insignificant for this magnitude and is of the same order of magnitude of the error made when reproducing the test series.

The relations established above for the described energy magnitudes are also essentially true for the time magnitudes of the energy-time curve according to Table VIII, columns 10, 12, 16, 20, 21, 22 and specially FIG. 79 and 80 as far as the fundamental time magnitude, t_r, of the heating phase is concerned. A deviating and somewhat heterogenous picture is presented by the time magnitude t_g which describes the total length of the cooling phase. In spite of the strong shifting tendency of the results, it can uniquely be concluded from Table VIII, column 22, that a fire cell with well heat insulated enclosing structures - steel sheet + light-weight concrete - has a significantly longer cooling phase than the other two fire alternatives. From FIG. 81 it is observed that the total energy, $t_g \times I_{Cg}$, liberated during the cooling phase is approximately independent of the variations in the thermal properties of the enclosing structures. This conclusion has been drawn in the light of the rather large errors technically arising when evaluating the time magnitude t_g.

To sum up, it can thus be established that the thermal properties of the enclosing structures of the fire cell can be allowed to vary within wide limits without any decisive influence on the fundamental

energy- and time magnitudes of the fire process in practical design. Consequently, in practical calculation of the gas temperature-time curve of the fire process by heat- and mass balance equations, this influence can ordinarily be neglected, as far as the liberated energy per unit time, I_C, in the energy Equation (1) is concerned. With unchanged term, I_C, in Equation (1), an increase in the heat insulating capacity of the enclosing structures results in a decrease of the term I_W and a simultaneous increase of the terms I_L and I_R and thereby also an increase in the fire gas temperature, ϑ_g. This fact is verified by measured values for the mean value of the fire gas temperature during the active phase of the fire, ϑ_{80-30}, described in Table VIII, column 28, and in FIG. 82 and 83. The rather small difference in the fire gas temperature for both of the fire cell types with enclosing structures steel + light-weight concrete and steel + asbestos, might appear surprising. The explanation possibly lies in the fact that for the first-mentioned type the heat insulating capacity is substantially reduced by an ordinarily high percentage of initial moisture which demands a significant heat supply for its evaporation and consequently resulting in an increase of the term I_W in the energy balance equation and a simultaneous reduction of the fire gas temperature ϑ_g.

8. COMPREHENSIVE ANALYSIS. A BASICAL OUTLINE FOR THEORETICAL DETERMINATION OF THE FIRE PROCESS CHARACTERISTICS.

Results from tests, which for fires in closed compartments with one window opening purely illustrate the influence of variations in the porosity of the fire load, Section 4, size of the fire load, Section 5, stick thickness of the fire load, Section 6, thermal properties of the enclosing structures, Section 7, and opening factor of the fire cell, Sections 4-7, on the fire process characteristics, have been described and analyzed in the previous sections. In the present section an attempt is made to do a comprehensive analysis of the obtained results with the chief objective of giving a basical outline for the time curve, I_C - t, of the energy liberated per unit time as a function of the mentioned influences for a fire load of the type wood cribs. Through such a basis, a background is provided for a differentiated theoretical analysis of the gas temperature-time of the complete fire process at both ventilation- and fuel bed controlled conditions, using the method given by Magnusson-Thelandersson (1970, 1971), see also Section 2. Access to differentiated gas temperature-time curves, determined in this manner, for fire processes with fire load of wood cribs makes calibration of realistic fire load in the form of furniture, textile goods and other equipments for primarily usual types of fire cells in daily life possible by a reasonably limited number of full-scale tests, for instance by equivalent values for the main characteristics of a wood crib. Thereby, in a practical fire technological design, the usually favourable conditions of the fire exposure in fuel bed controlled processes could be taken into consideration, which, at present, is not possible due to insufficient knowledge. Similarly, a comprehensive analysis and schematization of the results, as described before, gives a more detailed and as far as the combustion technique is concerned, a sounder basis for a description of the conditions corresponding to fuel bed - and ventilation controlled fire processes.

8.1 The criteria given in the literature for different types of fire processes. General demands on the basis for fire process calculations.

On appearence of the published works by Magnusson-Thelandersson (1970, 1971) for a theoretical determination of the gas temperature of the fully developed fire process, the application to fuel bed controlled fire processes, as mentioned before, got complicated owing to the great insufficency of knowledge on the influence of variations in the size of the fire load and porosity factor on the combustion rate. This circumstance necessitated a simplified treatment of fuel bed controlled processes characterized by a general assumption of ventilation controlled conditions with the conditions for the total released energy according to Equation (15) being satisfied. For fire processes which are actually fuel bed controlled, this approximation renders an overestimation of the maximum fire gas temperature and an underestimation of the fire duration which partly acts as a compensating factor.

The design basis, described by Magnusson-Thelandersson (1970), in the form of gas temperature-time curves for fully developed fire processes in fire cells with different thermal properties for the enclosing structures has the opening factor, $A\sqrt{H}/A_t$, of the fire cell and size of the fire load, q, defined as the total energy released per unit area of the enclosing surface, A_t, in a complete combustion, as input parameters. Alternatively the fire duration, T, determined through the opening factor, $A\sqrt{H}/A_t$, and the fire load, q, is used instead of the fire load, q, according to Equation (25), C.f. the corresponding comments on page 72. In calculation of the design basis, attention has been paid to the fact that the total energy, in reality, is distributed over the fire process according to FIG. 4 with an order of magnitude of 70-50 % on the flaming phase and 30-50 % on the cooling phase.

Thus, for a given type of fire cell, the design procedure employed by Magnusson-Thelandersson (1970) using their own method, takes the influencing parameters opening factor, $A\sqrt{H}/A_t$, and size of the fire load, q, into consideration whereas no attention is paid to the

other significant, fire process characterizing factors influencing the fire process. The authors are aware of this limitation which is discussed, in detail, in the work by Magnusson-Thelandersson (1971). The applied simplification should be regarded in the light of the fact that the opening factor, $A\sqrt{H}/A_t$, and the size of the fire load, q, are usually among the decisive parameters and that the existing knowledge at the time of appearance of the works did not allow a more far-reaching and differentiated treatment. For practical circumstances, Magnusson-Thelandersson's method applied to ventilation controlled fire processes, gives a sufficiently accurate description of a realistic fire exposure. However, a direct use of the design procedure applied to fuel bed controlled fire processes can result in significant overestimations, specially for such structures as non insulated or lightly insulated steel constructions in fires of short duration.

As mentioned before, Magnusson-Thelandersson have discussed the conditions for fuel bed and ventilation controlled fire processes and the application of their method in both cases, in their report from 1971. In this connection, these conditions are given in an approximate and extremely simplified mathematical form. Based on the results from full-scale tests published in the literature taken from many sources including a report of Butcher-Bedford-Fardell (1968), Ödeen (1968) and Ehm-Arnault (1969), Magnusson-Thelandersson calculated the relation between $R_{80-30}/A\sqrt{H}$ and $M/(rA\sqrt{H})$ in addition to the relation between $R_{80-30}/A\sqrt{H}$ and $M/A\sqrt{H}$, given i FIG. 85 and 86 where M denotes the total fuel quantity in kg wood equivalent as far as the heat value is concerned and r the hydraulic radius, that is the ratio between the initial volume and the initially exposed surface of the fire load. The summarized values exhibit a significant dispersion. It should, however, be observed that the values from Ödeen's full-scale tests which most obviously fall outside the trend of the summary refer to fire processes with unnatural ventilation, that is a ventilation imposed through a fan system. From the straight line inserted in the figure where horizontal lines correspond to ventilation controlled and inclined lines to fuel bed controlled process the following approximate conditions are obtained for fuel bed controlled fires:

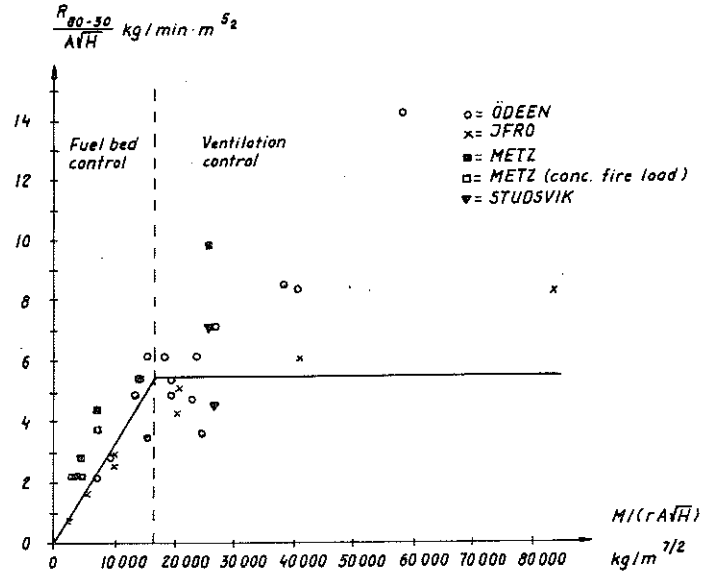

FIG 85 The experimentally obtained relation between $R_{80-30}/A\sqrt{H}$ and $M/(r\ A\sqrt{H})$ from full-scale tests performed at different research stations.

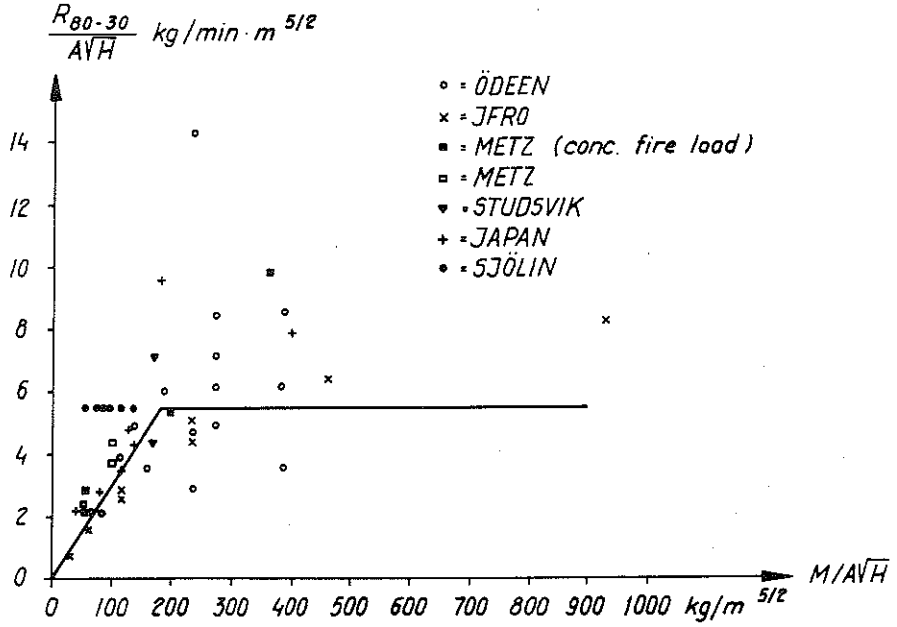

FIG 86 The experimentally obtained relation between $R_{80-30}/A\sqrt{H}$ and $M/A\sqrt{H}$ from full-scale tests performed at different research stations.

$$M/A\sqrt{H} < 175 \text{ kg/m}^{5/2} \tag{33}$$

or alternatively

$$M/(rA\sqrt{H}) \leq 17000 \text{ kg/m}^{7/2} \tag{34}$$

It should, however, be emphasized that these relations are based on the mean combustion rate, R_{80-30}, indicating the weight decrease of the fuel per unit time, as the decisive combustion parameter.

In this connection a paper published by Harmathy (1972, I, II) is further of special interest in which the main characteristics of the flaming phase are primarily treated for fire processes in fire cells. The presentation is concentrated on fire loads of the type wood cribs, which are described by the total fuel quantity, M, and the initially fire exposed surface, A_s. In the paper, the methods presented in the literature for fire process calculations by means of heat- and mass balance equations of the fire cell - Kawagoe-Sekine (1963), Ödeen (1963), Kawagoe (1967) and Magnusson-Thelandersson (1970) - are discussed and a greatly simplified alternative method is presented for calculation of the temperature-time curve of the flaming phase. Unfortunately Magnusson-Thelandersson´s publication from 1971 does not seem to be known for Harmathy which has partly resulted in the fact that Magnusson-Thelandersson´s method from 1970 for fire process calculations is incorrectly discussed in application cases not intended for and partly that many viewpoints and conclusions which are given out to be new have already been published in Magnusson-Thelandersson´s work from 1971.

For the mean combustion rate, R_{80-30}, of the flaming phase, Harmathy describes, with a ventilation controlled process, the relation analogous to Equation (14)

$$R_{80-30} = 0.0236\ \Phi \tag{35}$$

where

Φ is a ventilation parameter having the same dimension as the mean combustion rate, R_{80-30}, and defined by the expression

$$\Phi = \rho_a \sqrt{g} \cdot A\sqrt{H} \qquad (36)$$

where

ρ_a is the air density and g the gravitational acceleration. With ρ_a = 1.29 kg/m^3 and g = 9.8 m/s^2 Equations (35) and (36) are equivalent to Equation (14) with the constant k = 5.7 kg/min · m$^{5/2}$.

Based on the results, described in the literature, from model- and full-scale tests with fire load of wood cribs, Harmathy has determined the relation between the ratios R_{80-30}/A_s and Φ/A_s by which the graphical representation according to FIG. 87 has been obtained. The experimental data given in FIG. 87 are characterized by a significant dispersion, but in spite of this fact a ventilation controlled region described by an inclined line and a fuel bed controlled one indicated by a horizontal line can be obviously observed. The former line is described by Equation (35) and the latter line which, accordingly, indicates the mean combustion rate in fuel bed controlled conditions, by

$$R_{80-30} = 0.0062\ A_s \qquad (37)$$

Comparing Equations (35) and (37) the relation

$$\Phi/A_s = 0.263\ \text{kg/m}^2 \cdot \text{s} \qquad (38)$$

is obtained for the critical point between both types of fire processes with fire in a closed fire call having window openings and a fire load of the type wood cribs.

The relation (38) can be alternatively rewritten in the form $M/(r \cdot A\sqrt{H})$ whereby a value, for the critical point, of the order of magnitude of 12 000 kg/m$^{7/2}$ is obtained, as compared with the value given by Magnusson-Thelandersson amounting to 17 000 kg/m$^{7/2}$, c.f. Equation (34). These values should be regarded in the light of the significant dispersion in the test results prevailing in the procedure applied. In reality these two types of fire processes are not distinguished from each other by a sharp limit but instead by a critical range.

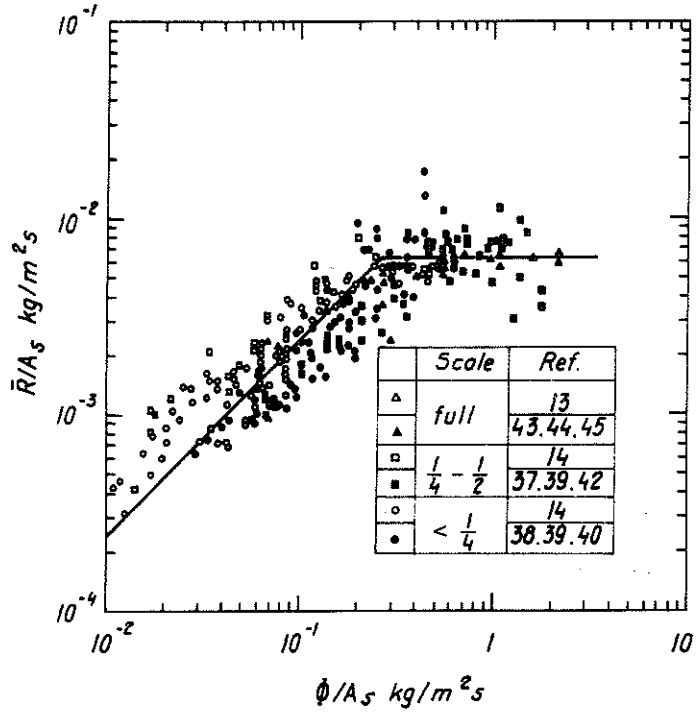

FIG. 87 The relation R_{80-30}/A_s between the mean combustion rate, R_{80-30}, during the flaming phase and the initially exposed fuel surface, A_s, related to the relation Φ/A_s between the ventilation parameter, Φ, and the initially exposed fuel surface, A_s. Summary according to Harmathy (1972), based on the results from compartment fires in model- and full scale described in the literature, using fire load of regular wood cribs.

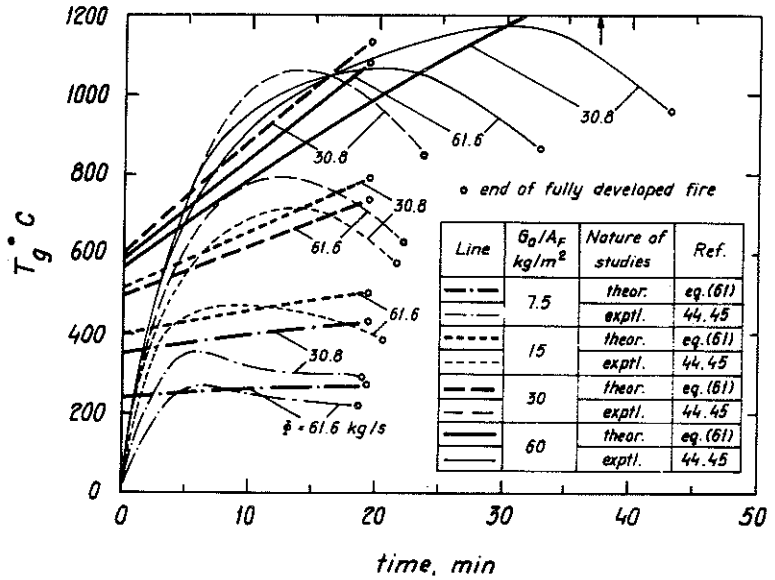

FIG. 88 Comparison between gas temperature-time curves obtained by full-scale tests using fire load of wood cribs and those determined according to the approximate method (straight lines) proposed by Harmathy (1972).

The greatly simplified approximate method presented by Harmathy for determination of the gas temperature-time curve during the flaming phase of the fire process gives straight lines as results illustrated in FIG. 88 in comparison with curves obtained through full-scale tests. The following objections can be made against this procedure.

In the initial phase of the fire, the presented approximate method gives an instantaneous temperature rise whereafter the temperature-time curve of the flaming phase is composed of a straight line. Even if the calculated mean temperature lies in an approximately correct level, the straight line gives a too rough description of the real fire process to be accepted as the design basis. In particular, the instantaneous temperature rise and the corresponding significant deviation from the real temperature curve during the initial phase of the fire can give rise to a greatly overestimated fire exposure for such structures as non-insulated and lightly insulated steel constructions.

In the procedure, the properties of the fire load is described solely by the size and the initially fire exposed fuel surface, A_s, which is an insufficient characterization and possibly gives the explanation to the significant dispersion in results with the applied procedure according to FIG. 87. For a wood crib, further significant influencing factors for the fire load are the free horizontal surface for vertical air flow through the pile, the so called chimney area, A_v, the thickness, b, of the individual stick and height of the pile in relation to the geometry of the fire cell, expressed in Gross' porosity factor by the number of the layers, N, of the wood crib - c.f. Equation (17) and FIG. 11. Consequences of the greatly simplified treatment by Harmathy is, for instance, illustrated by the conditions found for tests C9 and C3. In both of these tests the size of the fire load has been the same, $q_{theor} = 35$ MJ/m^2 of the enclosing surface and the initially fire exposed fuel surface, A_s, has deviated only by approximately 13 %. Furthermore the opening factor of the fire cell has been the same in both tests, $A\sqrt{H}/A_t = 0.114$ m$^{1/2}$. Variations in the other properties of the fire load gives a large difference in the values of the porosity factor, ϕ, amounting to 0.117 cm$^{1.1}$ for the test C9 and 0.688 cm$^{1.1}$ for the test C3 and a significant difference in the fire gas temperature, ϑ_{80-30}, of the

flaming phase amounting to 448°C for the test C9 and 704°C for the test C3.

An insufficiently differentiated description of the properties of the fire load according to Harmathy results in further great difficulties for calibration of realistic fire loads such as furniture, textile goods and other equipments by means of fire loads in the form of regular wood cribs. Thereby the possibility of a more detailed survey of practically representative fire processes, through a combination of a few full-scale tests having realistic fire load, and results from systematically planned test series in model scale with reasonable cost, using fire load of the type wood cribs, which is the case if these model scale test series had been performed with an accurate description of the fire load is excluded.

In short, it can accordingly be established that a calibrating basis for practically representative fire processes obtained through fire process studies in model scale with pure fire loads in the form of wood cribs should fulfill the primary requirement of an accurate and complete fire load description as far as possible, for instance by means of the size, q, porosity factor, ϕ, and stick thickness, b, or alternatively by the size, q, the initially exposed surface, A_s, chimney area for the vertical air flow through the pile, A_v, stick thickness, b, and height of the pile in relation to the geometry of the fire cell. The basis obtained through fire process studies should further be such that it has a direct relation to heat- and mass balance equations of the fire cell and that it can facilitate a differentiated calculation of, for instance, the temperature-time curve of a fully developed fire process with variations in part properties of the fire load, opening factor of the fire cell and thermal characteristics of the enclosing structures. The basis should in a differentiated manner cover different types of fire processes, both ventilation controlled and fuel bed controlled.

8.2 Derivation of criteria based on the released energy for different types of fire processes.

The criteria referred to in the previous section, for ventilation controlled and fuel bed controlled fire processes - Equations (33), (34) and (38) - are generally based on the mean combustion rate, R_{80-30}, of the flaming phase represented by the weight decrease of the fuel per unit time, as the decisive parameter. A fire process is thus defined as ventilation controlled, if R_{80-30} is proportional with the air flow factor $A\sqrt{H}$ or the ventilation parameter, Φ, and at the same time being approximately independent of the properties of the fire load - fuel quantity, M, and hydraulic radius, r, according to the discussion by Magnusson-Thelandersson (1971) and of the initially exposed fuel surface, A_s, according to the discussion by Harmathy (1972). A fire process is defined as fuel bed controlled, if R_{80-30} is proportional with the initially exposed fuel surface or with the fire load magnitude M/r - alternatively the fuel quantity, M, at a higher degree of approximation - and at the same time being independent of the air flow factor, $A\sqrt{H}$, or the ventilation parameter, Φ. In a detailed application these definitions, using fire load of wood cribs, result in a transition from fuel bed controlled to ventilation controlled fire process which with a given fire cell varies with the porosity factor, ϕ, of the fire load and stick thickness, b, - c.f. FIG. 36 a and the corresponding comments.

As mentioned in the previous sections, the energy released per unit time, I_C, is a more direct basical magnitude as the basis for fire process calculations by heat- and mass balance equations of the fire cell, than the combustion rate, R_{80-30}. For this reason - and also from the point of view of combustion technic - a magnitude characterizing the released energy, I_C, is to be preferred to the combustion rate, R_{80-30}, as the decisive parameter in criteria for different types of fire processes. As shown in Section 5.2, the magnitude maximum energy released per unit time, described in the dimensionless form $I_{Cmax}/3560\ A\sqrt{H}$, offers the best possibility for a unique and differentiated definition of the type of the fire process. By this parameter, the fire process can strictly be defined as ventilation controlled if with a given shape of the fire cell the maximum

energy, I_{Cmax}, is approximately independent of the variations in the properties of the fire load - c.f. FIG. 36 b, Curve (1). With fire load in the form of regular wood cribs, this condition is fulfilled within a range above a certain fuel quantity, M, and for a porosity factor, ϕ, which is larger than a certain characteristic value, ϕ_c, and a stick thickness b less than a certain characteristic value, b_c. Thereby the criterium for a ventilation controlled fire process is that

$$I_{Cmax}/3560\ A\sqrt{H} \approx 1 \qquad (39)$$

In other cases, I_{Cmax}, for a given shape of the fire cell, depends on the variations in one or several properties of the fire load and the fire process is accordingly of the fuel bed controlled type. For $\phi > \phi_c$ and $b < b_c$, the maximum energy released per unit time, I_{Cmax}, is approximately dependent of only the variations in the fuel quantity, M, or size of the fire load, q. For $\phi < \phi_c$ and/or $b > b_c$ using small fuel quantities, M, the maximum energy, I_{Cmax}, varies with both the size of the fire load, q, its porosity factor, ϕ, and stick thickness b. When the fuel quantity increases, I_{Cmax} reaches an approximate limiting value with a level which depends on the porosity factor, ϕ, of the fire load and stick thickness, b. At each such a level - Curves (2a) and (2b) in FIG. 36 b - I_{Cmax} is approximately independent of the variations in the fuel quantity, M, or the size of the fire load, q.

With a presentation according to FIG. 36 b, four different types of ranges can accordingly be distinguished in relation to the fire load properties influencing the maximum energy released per unit time, I_{Cmax}. For $\phi > \phi_c$ and $b < b_c$, I_{Cmax} is approximately independent of the changes in the properties of the fire load within a range where the fuel quantity, M, is larger than a certain characteristic value, M_{cl} which, strictly speaking implies a ventilation controlled fire process with $I_{Cmax}/3560\ A\sqrt{H} \approx 1$. For $\phi > \phi_c$, $b < b_c$ and $M < M_{cl}$, I_{Cmax} varies with the fuel quantity, M, or the size of the fire load, q, and is almost independent of the porosity factor, ϕ, of the fire load and the stick thickness, b. For $\phi < \phi_c$ and/or $b > b_c$, I_{Cmax} varies with the porosity factor, ϕ, and the stick thickness, b, according to Curve (2a) and (2b) in FIG. 36 b, and at the same time is almost in-

dependent of the changes in the size of the fire load, q, for the fuel quantity, M, which is larger than a certain characteristic value, M_{c2}. Finally, for $\phi < \phi_c$ and/or $b > b_c$ and $M < M_{c2}$, I_{Cmax} depends on all the three properties of the fire load - the size, q, the porosity factor, ϕ, and the stick thickness, b. For the three latter types of ranges it is generally true that $I_{Cmax}/3560\ A\sqrt{H} < 1$ with the consequence that the fire process, with varying number of properties for the fire load, is fuel bed controlled.

In the light of what has been mentioned, a modification of the criteria proposed by Harmathy (1972) and Magnusson-Thelandersson (1971), for fuel bed- and ventilation controlled fire processes through the exchange of the mean combustion rate, R_{80-30} with the maximum energy released per unit time, I_{Cmax}, is of vital interest. For this reason, the relation between the magnitudes I_{Cmax}/A_s and $A\sqrt{H}/A_s$ determined from the results of the model fire studies described in Sections 4-7 with fire load of regular wood cribs, is summarized in FIG. 89.

Considered in the light of logarithmically graduated axes in FIG. 87 and linearly graduated axes in FIG. 89, the summary in FIG. 89, exhibits less dispersion compared with the corresponding summary published by Harmathy (1972) by using R_{80-30}, instead of the energy magnitude, I_{Cmax}, as the decisive parameter in FIG. 87. The main reason to this is that the values described in FIG. 89 are taken from tests which have been performed by the same test apparatus under unique and well defined conditions while the values in FIG. 87 include results from tests performed at different scales and in different laboratories with greater variations in the test conditions.

Using the values in FIG. 89, an inclined line can, with a rough approximation, be inserted according to the figure, describing a ventilation controlled fire process with I_{Cmax} determined by the relation

$$I_{Cmax} = 3500\ A\sqrt{H}\ \ MJ/h \tag{40}$$

A horizontal line can also be inserted describing a fuel bed controlled fire process with I_{Cmax} determined according to the expression

$$I_{Cmax} = 300\ A_s\ \ MJ/h \tag{41}$$

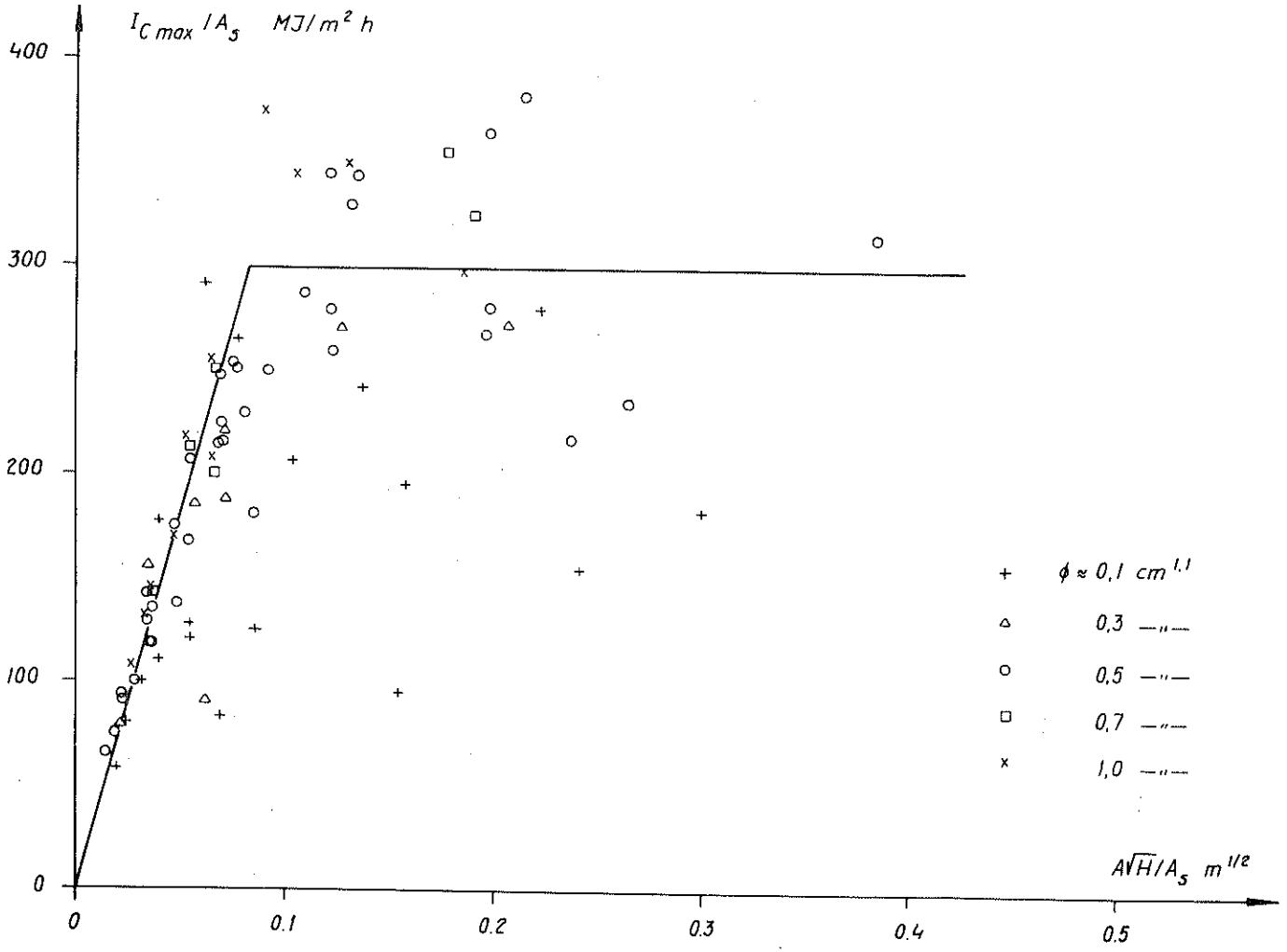

FIG. 89 The relation, calculated from the results of model tests performed by the author, between I_{Cmax}/A_s and $A\sqrt{H}/A_s$, where A_s is the initially exposed fuel surface. The fire load is in the form of a regular wood cribs. The inserted straight lines are described by Equations (40) and (41).

Thereby, the transitional point between a ventilation controlled and a fuel bed controlled is determined by the relation

$$A\sqrt{H}/A_s = 0.086\ m^{1/2} \tag{42}$$

Recalculated by the technic introduced by Harmathy (1972) - Equation (38) - Equation (42) gives

$$\Phi/A_s = 0.35\ kg/m^2 \cdot s \tag{43}$$

to be compared with the value 0.263 $kg/m^2 \cdot s$ determined by Harmathy.

From the summary described in FIG. 89 it is observed that the test results exhibit a rather slight dispersion within the ventilation controlled range up to $A\sqrt{H}/A_s \approx 0.05\ m^{1/2}$. Thus, within this subrange, the maximum energy released per unit time is decisively determined by the air flow factor according to Equation (40), the influence of the variations in the properties of the fire load being practically negligible. However, within the fuel bed controlled range the dispersion in the test results is significant which proves that within this range, many more properties of the fire load than the initially exposed surface, A_s, have a substantial influence on the characteristics of the fire process. Within the intermediate range $0.05 < A\sqrt{H}/A_s < 0.086\ m^{1/2}$ which can be interpreted as a transition between ventilation controlled and fuel bed controlled fire processes, the air flow factor, $A\sqrt{H}$, together with the differentiated properties of the fire load - size, q, porosity factor, ϕ, and stick thickness, b - constitute the decisive influencing factors. This transitional range stands out as the most complicated as far as the combustion technic is concerned.

Alternatively, the initially exposed surface, A_s, of the fire load can be taken into consideration by a description which, with the same degree of simplification, characterizes the fire load through the magnitude M/r, where M is the total fuel weight or energy content and r is the hydraulic radius of the fire load. With this modification and considering the technic described by Magnusson-Thelandersson (1971), the relation between the magnitudes $I_{Cmax}/3560\ A\sqrt{H}$ and $M/rA\sqrt{H}$ determined by the results from model fire studies described in Sec-

tions 4-7 with fire load in the form of regular wood cribs, is summarized in FIG. 90. Compared with the description in FIG. 89, the summary according to FIG. 90 gives visually a general impression of less dispersion for the values calculated from the test results. In lesser extent, this circumstance is due to the fact that variations in the density of the fire load has been taken into consideration in FIG. 90 which is not the case with the FIG. 89. Differences in the visual impression between FIG. 89 and 90 are mainly explained by different description technics for the same test results with the use of the same variables, that is, the air flow factor, $A\sqrt{H}$, and the initially exposed fuel surface, A_s or M/r which is proportional with these variables.

With an approximation which is reasonable for ordinary practical applications, the test results summarized in FIG. 90 can be inserted on three successive strainght lines, describing three different ranges with respect to the type of the fire process. Within the range $M/rA\sqrt{H} < 75000$ MJ/m$^{7/2}$ a fuel bed controlled fire process prevails and within the range $M/rA\sqrt{H} > 150000$ MJ/m$^{7/2}$ there is a ventilation controlled fire process.. The range $75000 < M/rA\sqrt{H} < 150000$ MJ/m$^{7/2}$ constitutes the transitional range between the two chief types of fire processes. The straight lines give the corresponding relation for the maximum energy released per unit time, I_{Cmax}, as follows

a) $$I_{Cmax} = 0.0367\ M/r \quad MJ/h \tag{44}$$

for fuel bed controlled fire process, that is for $M/rA\sqrt{H} < 75000$ MJ/m$^{7/2}$

b) $$I_{Cmax} = 0.0108\ M/r + 1940\ A\sqrt{H} \quad MJ/h \tag{45}$$

for the transitional zone between fuel bed- and ventilation controlled fire process, that is for $75000 < M/rA\sqrt{H} < 150000$ MJ/m$^{7/2}$.

c) $$I_{Cmax} = 3560\ A\sqrt{H} \quad MJ/h \tag{46}$$

for a ventilation controlled fire process, that is

$M/rA\sqrt{H} > 150000$ MJ/m$^{7/2}$

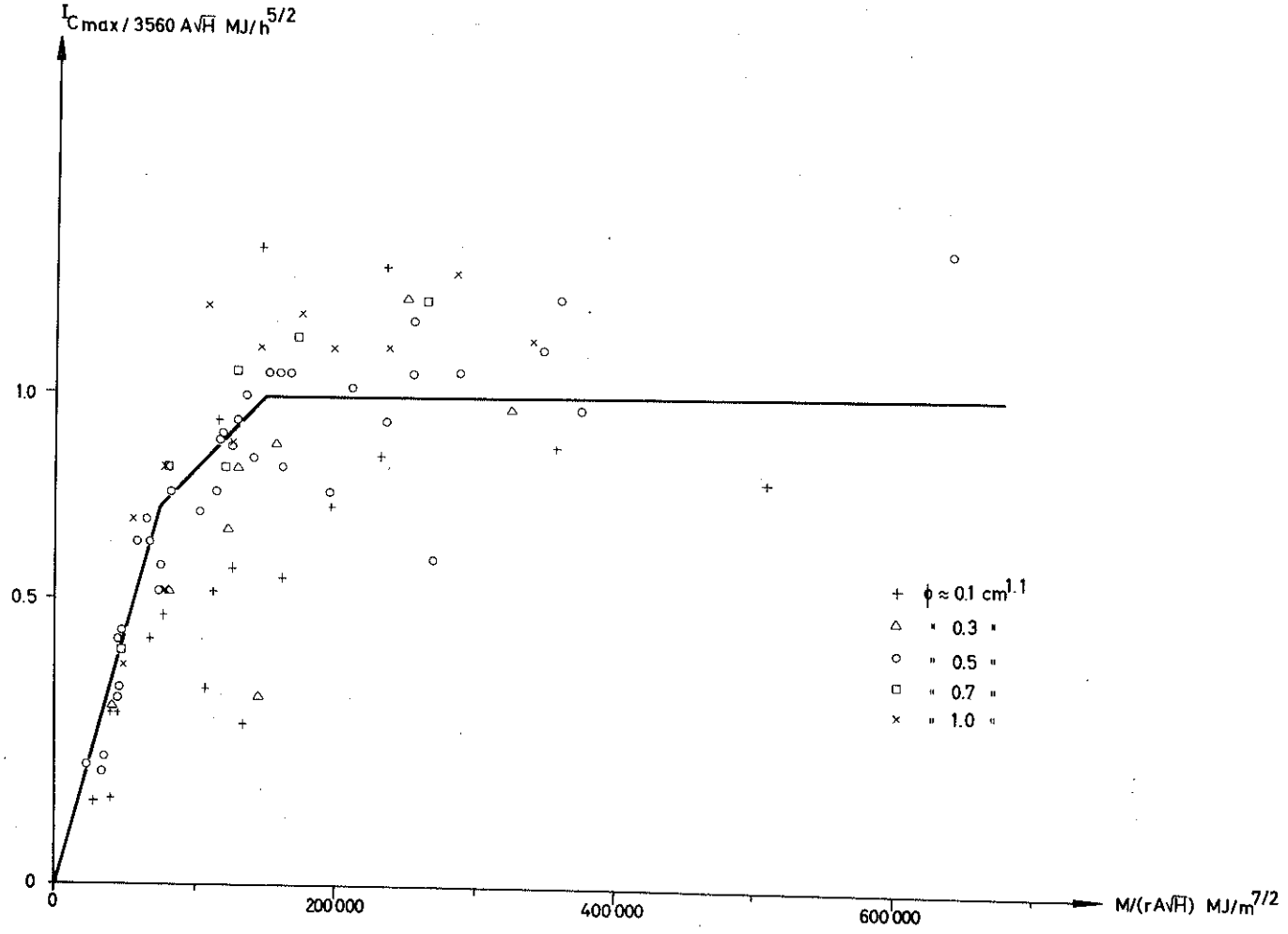

FIG. 90 The relation, calculated from the results of model tests performed by the author, between $I_{Cmax}/3560\ A\sqrt{H}$ and $M/(rA\sqrt{H})$, where M is the total energy content of the fuel. The fire load is in the form of a regular wood cribs. The inserted straight lines are described by Equations (44) - (46).

In spite of the broad variation range for the studied parameters in the test series, the dispersion in the test results using Equations (44) - (46) is rather moderate. Primarily the largest deviations correspond to tests with a low porosity factor, ϕ, and a small stick thickness, b, which can be taken into consideration in a more general application. Furthermore, it should be established that most of the points which, in a ventilation controlled fire process, deviate from and exceed the value $I_{Cmax} = 3560\ A\sqrt{H}$ MJ/h arise from tests performed with both of the lower opening factors $A\sqrt{H}/A_t = 0.02$ and $0.032\ m^{1/2}$ respectively. In a design for a ventilation controlled fire process according to equation (46), a magnified value should therefore be given to the maximum energy released per unit time, I_{Cmax}, with lower values of the opening factor. For the opening factor $A\sqrt{H}/A_t = 0.02\ m^{1/2}$, the magnifying factor is estimated to amount to 1.2 which thereafter decreases linearly with increasing opening factor and assumes the value 1.0 for the opening factor $A\sqrt{H}/A_t = 0.04\ m^{1/2}$.

According to the summary in FIG. 90 and Equations (45) and (46), the $M/rA\sqrt{H}$ - value above which the fire process is of the ventilation controlled type is $M/rA\sqrt{H} = 150000\ MJ/m^{7/2}$. If, in agreement with what has been applied in the previous section, it is assumed that heat value of wood during the most active period of the flaming phase is 10.78 MJ/kg, then the given $M/rA\sqrt{H}$ - value recalculated to an equivalent quantity of wood, as far as the heat value is concerned, corresponds to $M/rA\sqrt{H} = 14000\ kg/m^{7/2}$. This value is in good agreement with the value $M/rA\sqrt{H} = 17000\ kg/m^{7/2}$ obtained by Magnusson-Thelandersson (1971), with full scale tests, according to Equations (34).

As an explanation to the significant dispersion in the test results according to FIG. 87, 89 and 90, it has been mentioned above that the initially exposed fuel surface, A_s, or the equivalent magnitude M/r are insufficient parameters for a satisfactory characterization of the fire load as far as the range for a fuel bed controlled fire process or the transitional zone between ventilation- and fuel bed controlled fire processes are concerned. A refined summary of the test results, described in Sections 4-7, with respect to all the influencing factors of the fire load - fuel quantity, M, porosity factor, ϕ, and the stick thickness b - is therefore of interest. Such a result

summary is presented in FIG. 91, in which corrections with respect to the variations in porosity factor, ϕ, and the stick thickness, b, have been introduced in an approximate manner, related to the trends found for the influence of these parameters in the previous sections. The maximum energy released per unit time, I_{Cmax}, is illustrated on the vertical axis under the form

$$\frac{I_{Cmax}}{3560\ A\sqrt{H}} \sqrt{\frac{\phi_{0.5}}{\phi}}$$

where $A\sqrt{H}$ ($m^{5/2}$) is the air flow factor, ϕ the actual porosity factor and $\phi_{0.5}$ the porosity factor value of 0.5 $cm^{1.1}$. Since it has been established in the previous sections that variations in the porosity factor have little influence in ventilation controlled fire processes, and that variations of ϕ in the interval $0.5 < \phi < 1.1$ $cm^{1.1}$ have only marginal effects on these studied parameters, the ratio $\phi_{0.5}/\phi$ has been assigned the value 1 although in FIG. 91 for the opening factor $A\sqrt{H}/A_t \leq 0.04$ $m^{1/2}$ and also for $\phi \geq 0.5$ $cm^{1.1}$. Within the range $0.04 \leq A\sqrt{H}/A_t \leq 0.07$ $m^{1/2}$, ϕ is determined by linear interpolation, that is from the Equation:

$$\phi = \frac{1}{3}(7\phi_{0.5} - 4\phi_v) - \frac{(A\sqrt{H}/A_t)}{0.03}(\phi_{0.5} - \phi_v)$$

where ϕ_v is the real value of the porosity factor. The Equation is true for $\phi_v \leq 0.5$ $cm^{1.1}$. For $\phi_v > 0.5$ $cm^{1.1}$, ϕ is replaced by 0.5 $cm^{1.1}$. The magnitude

$$\frac{M}{A\sqrt{H}} \left(\frac{b_{25}}{b}\right)$$

is illustrated on the horizontal axis. In this expression M(MJ) indicates the total fuel quantity, b the actual stick thickness and b_{25} the stick thickness 25 mm which is true for most of the tests described here. However, due to the trends found in the results the stick thickness, b, has been assigned with the real value only for $b > 25$ mm while for $b \leq 25$ mm the ratio b_{25}/b has been substituted by 1.

Compared with the corresponding, less differentiated result summary in FIG. 90, the description according to FIG. 91 gives a significant lesser dispersion in the results for the fuel bed controlled range of the fire process and for the transitional zone between the venti-

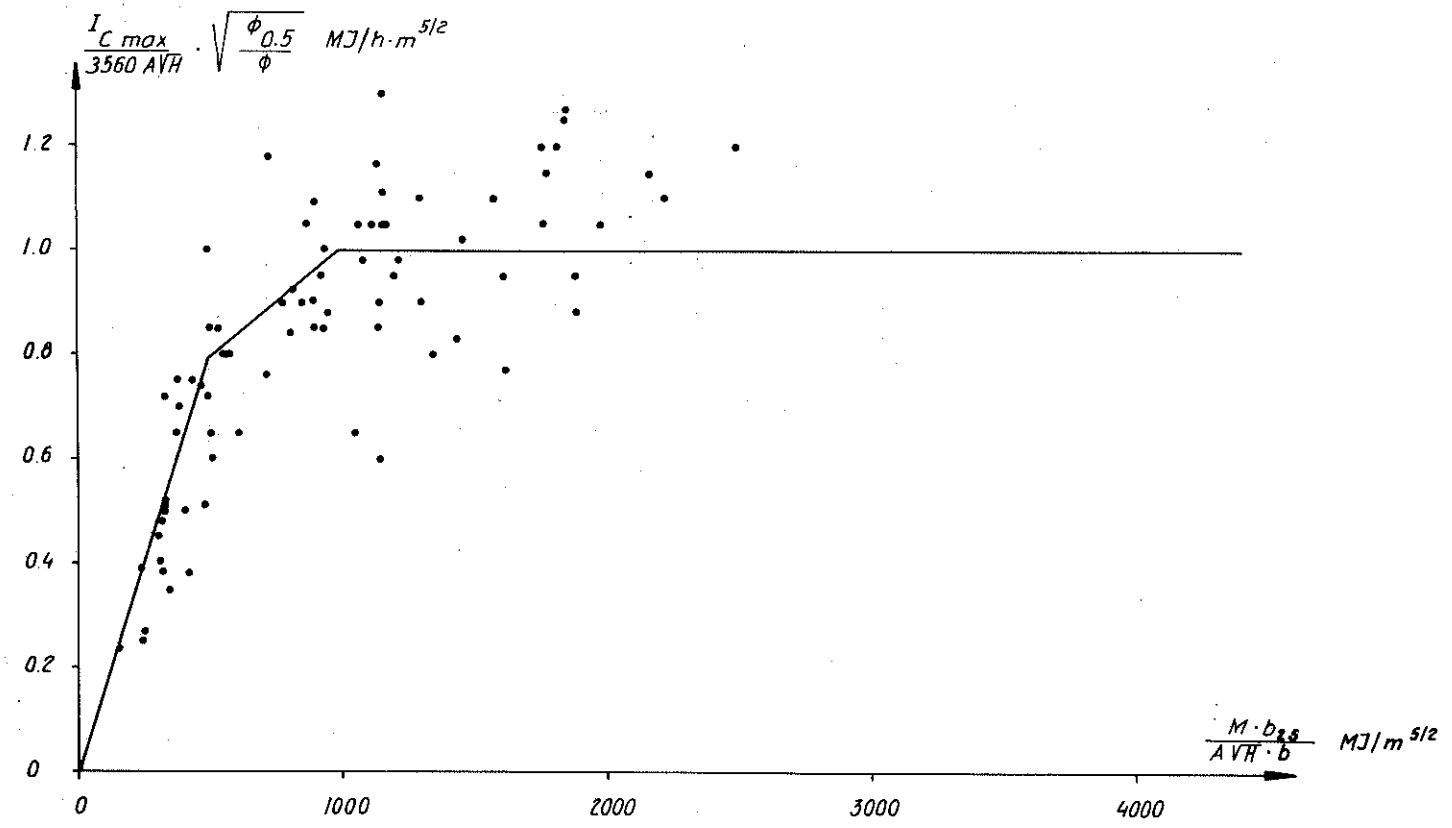

FIG. 91 The relation, calculated from the results of model tests performed by the author between $I_{Cmax}/3560\ A\sqrt{H}$ and $M \cdot b_{25}/A\sqrt{H} \cdot b$. According to the texts certain side conditions are true for the summary in the choice of $\phi_{0.25}/\phi$ and b_{25}/b. The fire load is in the form of a regular wood cribs. The inserted straight lines are described by Equations (53) - (56).

lation- and fuel bed controlled fire processes. For the ventilation controlled range of the fire process, the dispersion in the test results is approximately equivalent for the descriptions in FIG. 90 and 91 which is due to the fact that the properties of the fire process have an insignificant influence with this type of fire process. The fact that a significant dispersion remains also in a more far-reaching and differentiated summary, according to FIG. 91, emphasizes the great experimental difficulties to achieve a high degree of reproducibility with the present types of tests.

8.3 Simplified criteria for determination of the type of fire process.

From the analysis described in Section 8.2 it is observed that an increased differentiation with respect to the influencing parameters, results in summaries determined from the test results with reduced dispersion. At the same time, it can however, be established from FIG. 91 that even with a far-reaching differentiation there will be a significant dispersion in the summarized results due to great difficulties to achieve a high degree of reproducibility with these actual types of investigations. As a natural development of the discussion presented in Section 8.2, this circumstance leads to the necessity of a study dealing with the consequences of one or several influencing parameters being neglected when determining the time curve of the fire process for the energy released per unit time, I_C. Such an additional study is favoured by the fact that in a highly differentiated description, there are difficulties in interpreting the results from a well-defined fire load in the form of regular wood cribs to their application in practical cases when the fire load is composed of furniture, textile goods and other equipments.

The result summaries described in the previous and the present section constitute the basis for estimating which influencing factors are decisive or insignificant. These result summaries are supplemented by FIG. 92-94 which illustrate how the maximum energy released per unit time, I_{Cmax}, is influenced by variations in the opening factor of the fire cell, $A\sqrt{H}/A_t$, size of the fire load, q, and the thermal properties of the enclosing structure of the fire cell.

Considering the whole subject-matter, it is observed that the opening

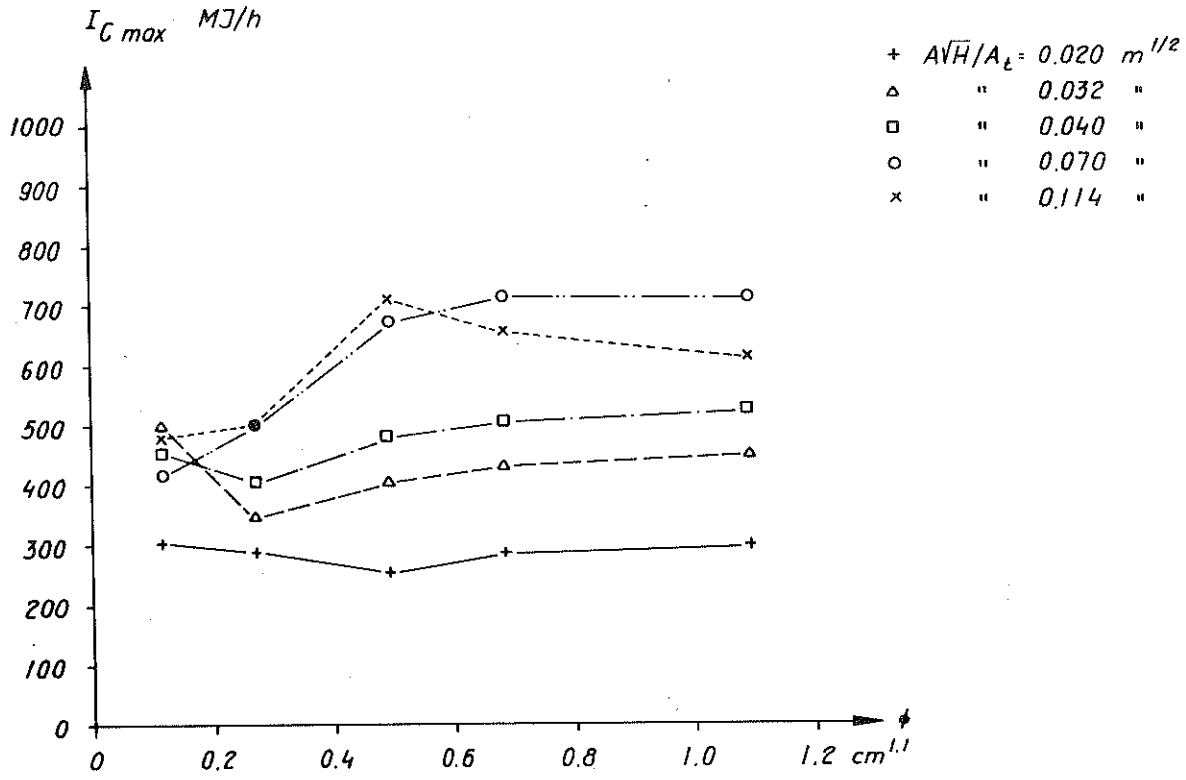

FIG. 92 The relation calculated from the obtained test results between I_{Cmax} (MJ/h) and the porosity factor, ϕ ($cm^{1.1}$), with varying opening factor $A\sqrt{H}/A_t$ ($m^{1/2}$). Fire load $q = 35$ MJ/square meter of the enclosing surface. The enclosing structures of the fire cell are composed of 10 mm asbestos disk having a density of 1020 kg/m^3 and 1.5 mm steel sheet.

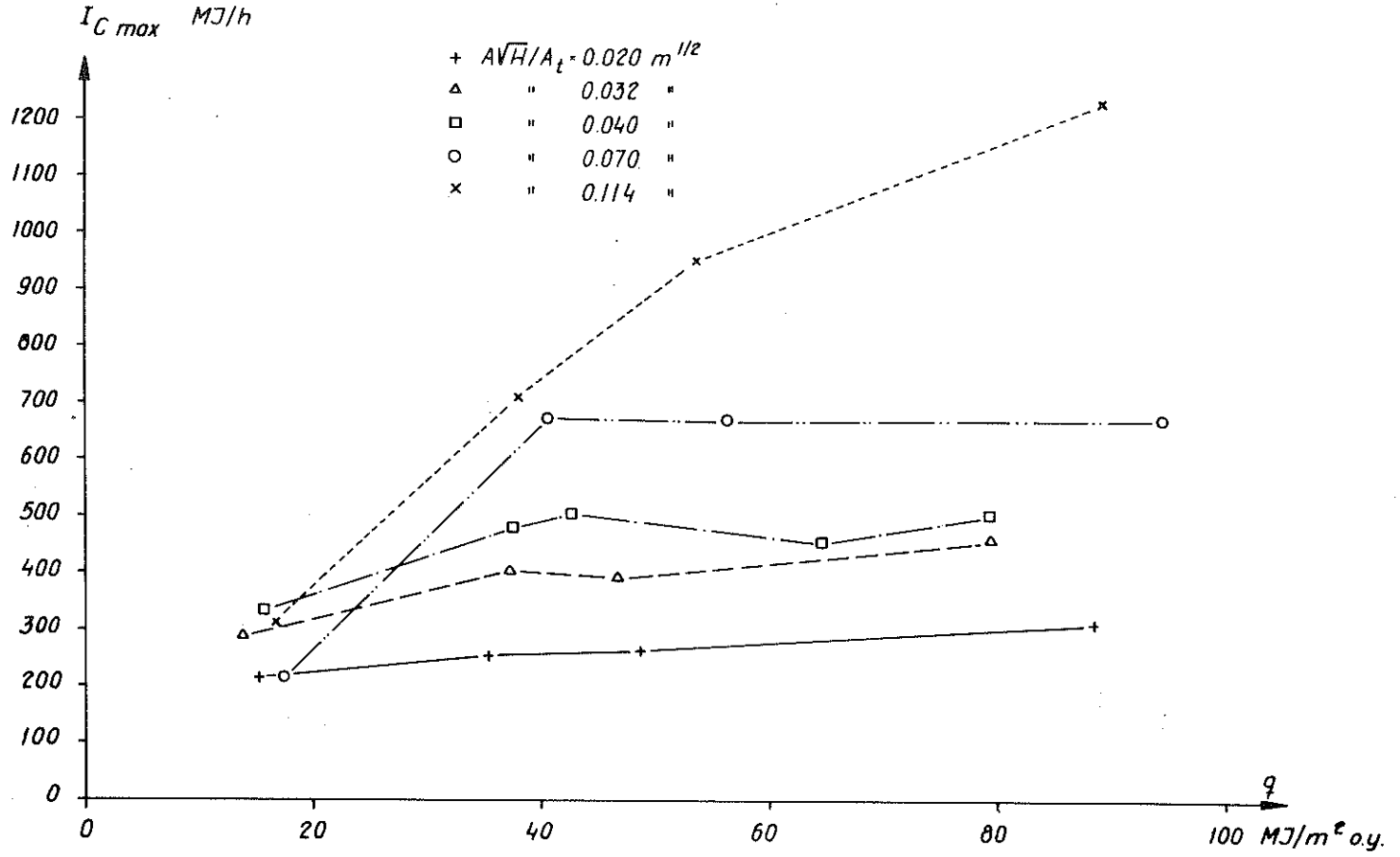

FIG. 93 The relation calculated from the obtained test results between I_{Cmax} (MJ/h) and the fire load q (MJ/square meter of the enclosing surface) with varying opening factor, $A\sqrt{H}/A_t$ ($m^{1/2}$). Porosity factor $\phi \approx 0.5 \cdot cm^{1.1}$. The enclosing structures of the fire cell are composed of 10 mm asbestos disk having a density of 1020 kg/m^3 and 1.5 mm steel sheet.

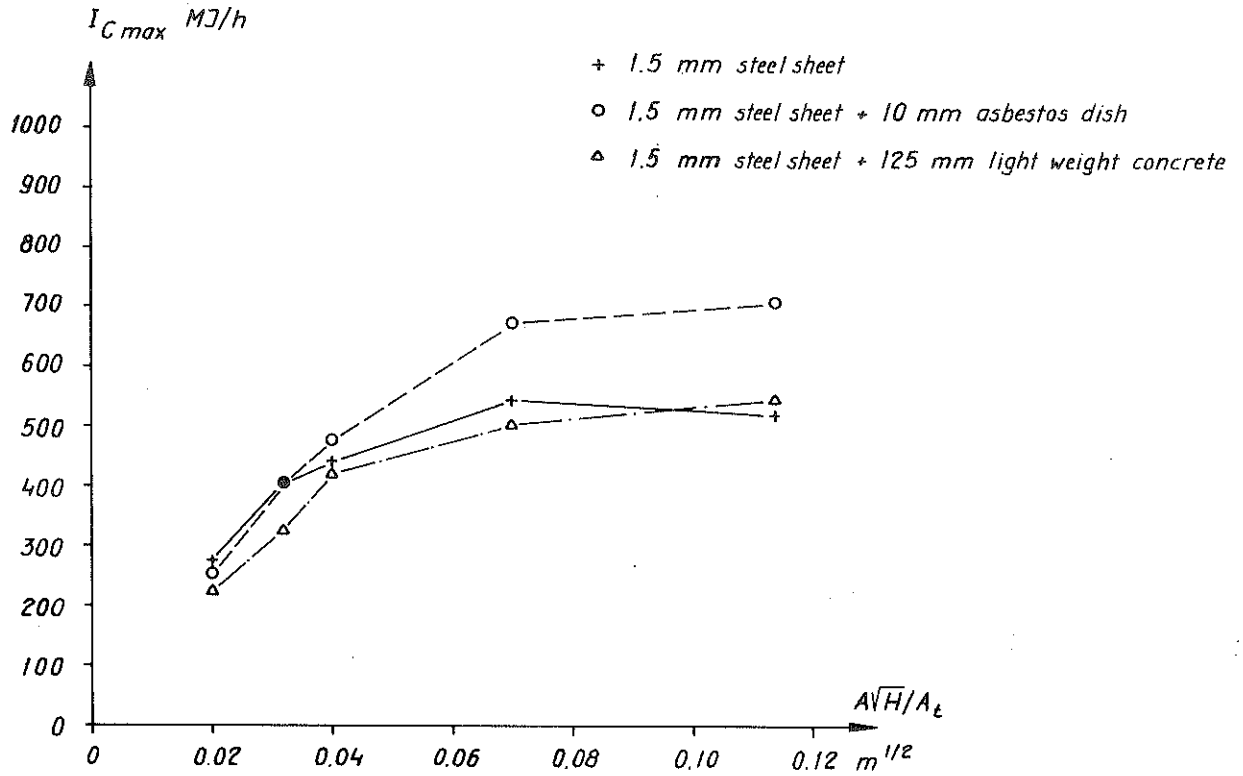

FIG. 94 The relation calculated from the obtained test results between I_{Cmax} (MJ/h) and the opening factor, $A\sqrt{H}/A_t$ ($m^{1/2}$) with some different types of enclosing structures belonging to the fire cell. Fire load q = 35 MJ/square meter of the enclosing surface, porosity factor $\phi \simeq 0.5$ $cm^{1.1}$.

factor, $A\sqrt{H}/A_t$ or alternatively air flow factor, $A\sqrt{H}$, generally belong to the group of decisive parameters. In the normal case I_{Cmax} increases in the beginning with increasing opening factor which constitutes a criterium for a ventilation controlled fire process. For a certain value of the opening factor which more or less depends on the other influencing factors, I_{Cmax} reaches a highest level which is thereafter approximately maintained with further increase of the opening factor. The fire process then turns to the fuel bed controlled type.

From what has been described before, particularly Section 5, it is further observed that the size of the fire load, q, or alternatively the total fuel quantity, M, also constitutes a decisive parameter with great influence on I_{Cmax} within the fuel bed controlled range of the fire process and within the transitional zone between ventilation- and fuel bed controlled fire processes. Together, the opening factor, $A\sqrt{H}/A_t$, or alternatively the air flow factor, $A\sqrt{H}$, and the size of the fire load, q, or alternatively the total fuel quantity, M, constitute the most significant factors influencing the energy released per unit time, I_C.

For the porosity factor ϕ, it is true that variations within the range $\phi \geq 0.5$ cm$^{1.1}$ have insignificant influence on the time curve of I_C. For this reason, it can be practical that, as a first step, limit the future discussion to the porosity factor within this range and, as a second step give brief corrections for the case $\phi < 0.5$ cm$^{1.1}$. From the analysis described in Section 6, it is further observed that the influence of variations in the stick thickness, b, of the fire load is rather insignificant for b < 30 mm; however, an exception from this rule should be made for very small stick thicknesses, which is of minor importance in a practical application. As a first step, it is therefore practical to limit the future discussion to the range b ≤ 30 mm and as a complement thereto, give guiding principles for correction when b > 30 mm. Since the described model fire studies have mainly been performed with the stick thickness b = 25 mm for the fire load, it is preferred that the first step of the future discussion is based on b = 25 mm. Relating this to FIG. 36 b the selected ϕ - and b limitations imply that the summary obtained from the first step will correspond to the Curve (1), which with $\phi > \phi_c$ and

$b < b_c$ describes fuel bed- and ventilation controlled fire processes in the rigorous sense.

As far as the influence of variations in the thermal properties of the enclosing structures of the fire cell is concerned, the results analyzed in Section 7 verify the fact that this influence is ordinarily negligible for the energy released per unit time, I_C. This influence can therefore be neglected when studying the criteria based on I_{Cmax}, for determination of the type of the fire process. However, the influence of the variations in the thermal characteristics of the enclosing structures on the gas temperature-time curve of the fire process cannot usually be neglected.

In the light of the discussion carried out before, the relation between the magnitudes $I_{Cmax}/3560\ A\sqrt{H}$ and $M/A\sqrt{H}$ determined by the results from the model fire studies described in Sections 4-7, is summarized in FIG. 95, with the limitations discussed above, that is as necessary condition for the summary the relations $\phi \gtrsim 0.5^{1.1}$ and $b = 25$ mm are true. Analogous with the discussion carried out in Section 8.2, three successive straight lines can be inserted by means of the results according to FIG. 95, which describe three different ranges with respect to the type of the fire process. The range $M/A\sqrt{H} < 500\ MJ/m^{5/2}$ embraces a fuel bed controlled fire process and the range $M/A\sqrt{H} > 1000\ MJ/m^{5/2}$ a ventilation controlled fire process. The intermediate range $500 \leq M/A\sqrt{H} \leq 1000\ MJ/m^{5/2}$ constitutes a transitional range between the two chief types of fire processes. For the maximum energy released per unit time, I_{Cmax}, the three straight lines correspond to the relations:

a) $$I_{Cmax} = 5.6\ M \quad MJ/h \tag{47}$$

for a fuel bed controlled fire process, that is for $M/A\sqrt{H} < 500\ MJ/m^{5/2}$.

b) $$I_{Cmax} = 1.52\ M + 2040\ A\sqrt{H} \quad MJ/h \tag{48}$$

for the transitional range between fuel bed- and ventilation controlled fire processes, that is for $500 \leq M/A\sqrt{H} \leq 1000\ MJ/m^{5/2}$

c) $$I_{Cmax} = 3560\ A\sqrt{H} \quad MJ/h \tag{49}$$

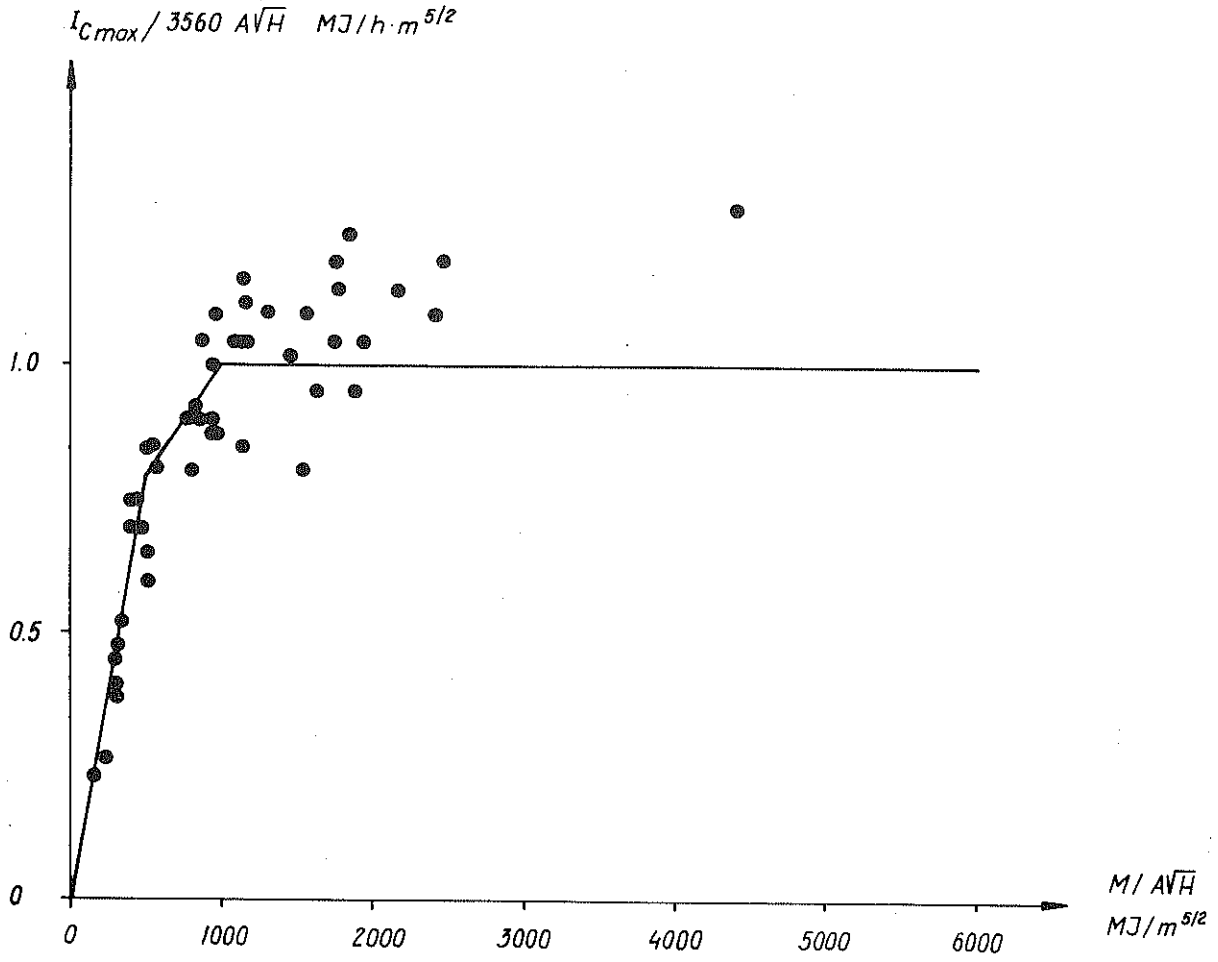

FIG. 95 The relation, calculated from the results of model tests performed by the author, between $I_{Cmax}/3560\ A\sqrt{H}$ and $M/A\sqrt{H}$, where M is the total energy content of the fuel. The inserted straight lines are described by Equations (47) - (49). The fire load is in the form of a regular wood cribs. In the summary, only the test for which the relations $\phi \gtrsim 0.5$ cm$^{1.1}$ and the stick thickness b = 25 are true, have been considered.

for a ventilation controlled fire process, that is for $M/A\sqrt{H} > 1000$ MJ/m$^{5/2}$.

The values summarized in FIG. 95 exhibit a very moderate dispersion and the deviations from the inserted polygon shaped curve are, in many cases, less than 10 %. As for precision, the result description according to the method applied in FIG. 95 is consequently superior to corresponding descriptions in Section 8.2 and in comparison with the summary of the published results in different connections presented by Harmathy (1972), FIG. 87, a better precision up to the tenth power is achieved. In estimation of the precision in the presentation according to FIG. 95, it should be noted that many of the points which, in a ventilation controlled fire process, deviate from and exceed the value $I_{Cmax} = 3560\ A\sqrt{H}$ MJ/h originate from tests performed at both of the lower opening factors $A\sqrt{H}/A_t = 0.02$ and $0.032\ m^{1/2}$ respectively, which has also been established previously in Sections 4, 5 and 7. In a design according to Equation (49) for a ventilation controlled fire process, a reasonable magnification should therefore be given to the maximum energy released per unit time, I_{Cmax}, at lower values of the opening factor. For the opening factor $A\sqrt{H}/A_t = 0.02\ m^{1/2}$ the magnifying factor is estimated to amount to 1.2 which thereafter decreases linearly with increasing opening factor and assumes the value 1 at $A\sqrt{H}/A_t = 0.04\ m^{1/2}$.

In connection with FIG. 86, the result summary in FIG. 95 is completed by describing the calculated relation between the magnitudes $I_{Cmax}/3560\ A\sqrt{H}$ and $M/A\sqrt{H}$ in FIG. 96, based on the results from full-scale tests published in the literature, performed by Kawagoe (1958), x), at Fire Research Station, JFRO (Butcher-Beford-Fardell, 1968, Heselden, 1968, and Law, 1968, Δ) in Metz (Ehm-Arnault, 1969, +), in Studsvik (Ödeen-Nordström, 1967, Pettersson-Ödeen, 1968, Ahlqvist-Thelandersson, 1968, and Ödeen, 1970, □) and by Sjölin (1970, o). Among these full-scale tests, those described by Sjölin have been performed with a practically representative fire load in the form of furniture, textile goods and other equipments while the fire load in the other tests have been composed of regular wood cribs. The polygon-shaped line for I_{Cmax} according to Equations (47) - (49), has also been inserted in the figure.

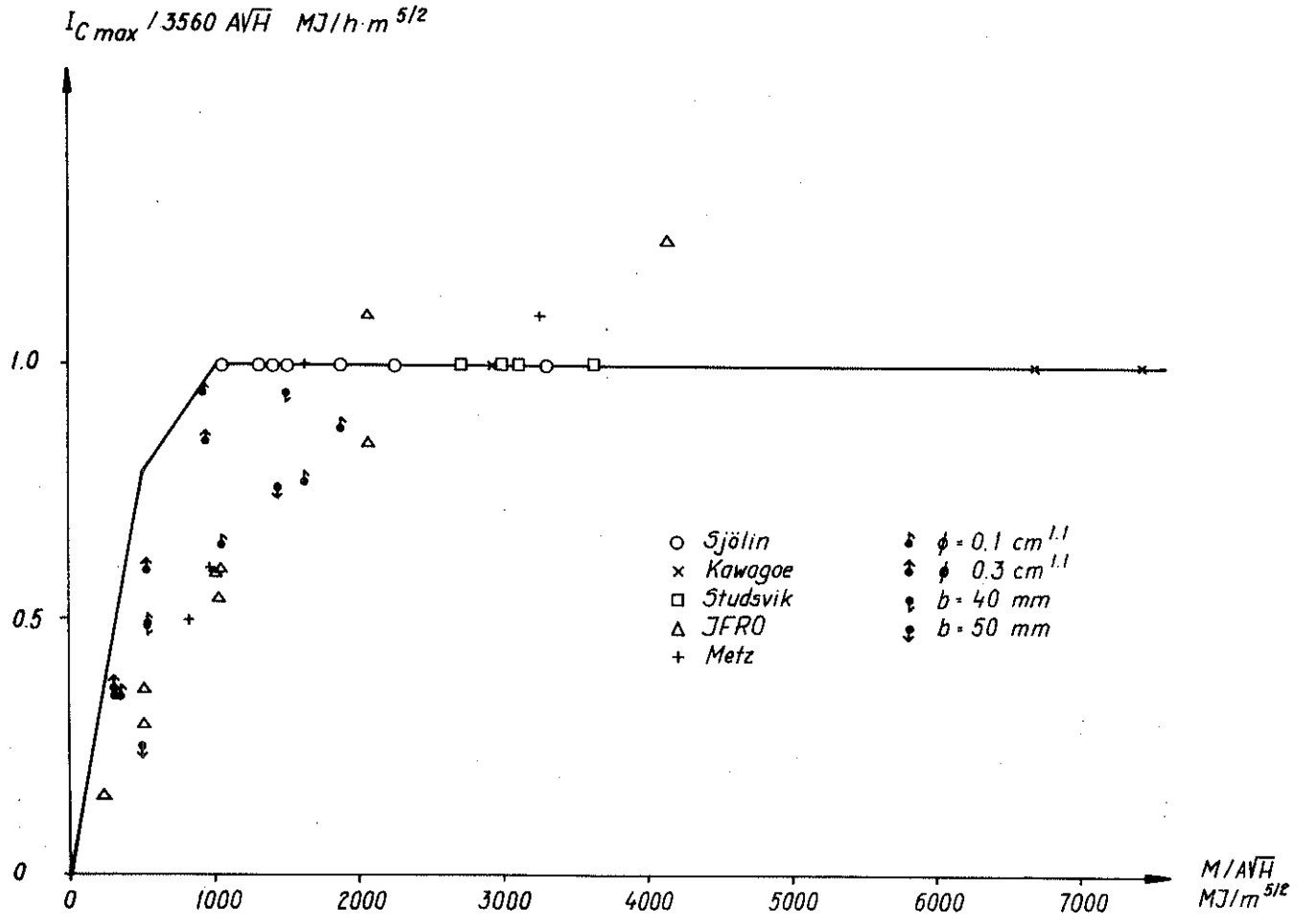

FIG. 96 The relation obtained between $I_{Cmax}/3560\ A\sqrt{H}$ and $M/A\sqrt{H}$, based on the results from full-scale tests described in the literature. Also the corresponding relation determined by model tests performed by the author, has been inserted in the figure, corresponding to the porosity factors ϕ = 0.1 and 0.3 $cm^{1.1}$ with the stick thickness b = 25 mm and to the stick thickness b = 40 mm and 50 mm with the porosity factor, $\phi \approx 0.5\ cm^{1.1}$. The inserted straight lines are described by Equations (47) - (49).

From FIG. 96 it is observed that all the full-scale tests performed by Kawagoe and Sjölin in addition to those performed in Studsvik, have been ventilation controlled in the rigorous sense. All the calculated I_{Cmax}-values fall in the vicinity of the I_{Cmax}-level according to Equation (49). For JFRO and Metz-tests it is generally true that they do not satisfy the conditions prevailing for the polygon-shaped line, that is $\phi \geq \phi_c = 0.5$ cm$^{1.1}$ and $b \leq b_c = 30$ mm which explains the fact that I_{Cmax} in these tests, is significantly lower within the fuel bed controlled and within the transitional range between ventilation- and fuel bed controlled fire processes than what is given by Equations (47) and (48) respectively. Within the ventilation controlled range of the fire process the deviations from I_{Cmax}-values according to Equation (47) are also rather moderate for I_{Cmax}-values from JFRO- and Metz-tests which is due to the fact that the variations in the properties of the fire load are less decisive in a ventilation controlled fire process.

In FIG. 96 a number of I_{Cmax}-values have also been indicated which are intended for the model fire studies reported in the present publication and correspond to the porosity factors $\phi = 0.1$ and 0.3 cm$^{1.1}$ with the stick thickness $b = 25$ mm and to stick thicknesses $b = 40$ and 50 mm with the porosity factor $\phi = 0.5$ cm$^{1.1}$. For the combination $\phi = 0.3$ cm$^{1.1}$, $b = 25$ mm, the described values indicate a practically negligible deviation from I_{Cmax} according to Equation (49) within the range $M/A\sqrt{H} > 1000$ MJ/m$^{5/2}$ and a deviation from I_{Cmax} according to Equation (47) amounting to a maximum of approximately 20 % within the range $M/A\sqrt{H} < 500$ MJ/m$^{5/2}$. For the combination $\phi = 0.1$ cm$^{1.1}$, $b = 25$ mm the corresponding deviations amount to a maximum of 35 % and 40 % respectively. Analogously, for the combination $\phi = 0.5$ cm$^{1.1}$, $b = 40$ mm, FIG. 96 gives the corresponding maximum deviations amounting to 20 % and 40 % respectively and for the combination $\phi = 0.5$ cm$^{1.1}$, $b = 50$ mm the corresponding maximum deviations are 25 % and 65 % respectively. A more differentiated illustration of the influence of variations in ϕ and b on I_{Cmax} is given by the results reported in Sections 4 and 6 - c.f., for instance, FIG. 61 and TAB. II, III and VI. The fire processes obtained for $\phi < 0.5$ cm$^{1.1}$ and $b > 30$ mm besides depending on the opening factor and size of the fire load depend also on the detailed form of the wood crib. They can, therefore, not be denoted as ventilation- or fuel bed controlled in the rigorous sense. Instead of

being devided in this manner, they can suitably be classified as combined fuel bed- and crib controlled within the range $M/A\sqrt{H} < 500$ MJ/m$^{5/2}$ combined ventilation- and crib controlled within the range $M/A\sqrt{H} >$ 1000 MJ/m$^{5/2}$ and combined ventilation-,fuel bed- and crib controlled within the transitional range $500 \leq M/A\sqrt{H} \leq 1000$ MJ/m$^{5/2}$. Related to a presentation according to FIG. 36 b, the fire processes pertain to curves of type (2a) and (2b).

8.4 Translation of the results from a fire process with fire load of wood cribs to a fire process with practically representative fire load.

The summary in FIG. 96, introduced in Section 8.3, constitutes an illustrating basis for a descussion of the possibilities to relate the results from a fire process with fire load in the form of regular wood cirbs, to the results from a fire process with practically representative fire load in the form of furniture, textile goods and other equipments. The I_{Cmax}-values indicated by o and determined by the results from full-scale tests performed by Sjölin (1970) are of special interest, since the fire load consisted of furniture and equipments representative for a flat.

As it is observed from the figure, all these tests are characterized by I_{Cmax}-values which practically coincide with the horizontal line corresponding to the rigorously ventilation controlled fire process, with the maximum energy released per unit time I_{Cmax}, determined by Equation (49). This implies that a simulation of realistic fire processes in flats can be performed by model fire studies with fire load of wood cribs provided that the piles are formed in such a manner that $\phi \geq \phi_c = 0.5$ cm$^{1.1}$ and the stick thickness $b \leq b_c = 30$ mm. Hereof, it also follows that the maximum energy released per unit time, I_{Cmax}, in realistic fires in flats, can be determined, with satisfactory precision, from Equation (47) in fuel bed controlled conditions, from Equation (49) in ventilation controlled conditions and from Equation (48) within the transitional zone between fuel bed- and ventilation controlled fire processes. For a definitive verification hereof, the tests performed by Sjölin should, however, by supplemented with some full-scale tests with realistic fire loads representative for flats

and with fire processes which fall outside the ventilation controlled range, that is when the following relations are true

$$M/A\sqrt{H} < 1000 \quad MJ/m^{5/2}$$

or

$$A\sqrt{H}/A_t > q/1000 \; m^{1/2} \qquad (50)$$

where q is the fire load expressed in MJ/m^2 of the total enclosing surface. The conclusion drawn should be regarded in the light of the fact that in Sjölin´s investigation, no compact fire load components in the form of, for instance, well-filled bookshelves with low combustion rate, have been included. This fact implies that without complementary fire process studies the conclusion is strictly applicable only to the easily combustible part of the fire load belonging to a flat which for Swedish flats is within the range q = 40 - 105 MJ/m^2 of the enclosing surface (Nilsson, 1970). This part of the fire load should, however, be decisive for the fire process in flats.

As far as the I_{Cmax}-level and the corresponding range for the type of fire process are concerned, the tests performed by Sjölin with representative and realistic fire loads for flats, give calculated I_{C-max}-values which according to FIG. 96 are quite close to the results obtained with fire load of wood cribs. This fact is esential to establish in the light of the previously found relations according to Magnusson-Thelandersson, with the combustion rate, R_{80-30}, as the decisive magnitude instead of I_{Cmax}. In a presentation based on the magnitude, R_{80-30}, Sjölin´s tests according to FIG. 86 results in a contradiction in that the tests fall within the fuel bed controlled range of the fire process, while the R_{80-30}-level corresponds to the ventilation controlled range. This circumstance strengthens the reason, mentioned in the previous sections, for using I_{Cmax} as the decisive mgnitude for a determination of the type of fire process at fires in closed compartments with window openings.

In order to relate a fire process having fire load of the type wood cribs to a fire process with practically representative fire load

in the form of furniture, textile goods and other equipments, Harmathy (1972, II) has introduced the magnitude

$$\varphi_o = A_s/G_o \quad m^2/kg \tag{51}$$

where A_s is the initially exposed surface of the fuel in m^2 and G_o the initial fuel quantity in kg. By φ_o, the condition for a fuel bed controlled fire process according to Equations (38) and (36) can be transformed to the relation analogous to Equation (50), namely

$$A\sqrt{H}/A_t = \varphi_o \cdot q/275 \quad m^{1/2} \tag{52}$$

The transformation is based on the values $\rho_a = 1.29$ kg/m^3, $g = 9.8$ m/s^2 and the nominal heat value of wood at complete combustion = 18 MJ/kg. Equations (50) and (52) become identical, if $\varphi_o = 0.275$ m^2/kg. Thus, using Harmathy's procedure, realistic fire processes in representative Swedish flats, can be related to fire processes with fire load of wood cribs, if the condition $\varphi_o = 0.275$ m^2/kg is generally satisfied. This φ_o-value is within the variation range $0.1 < \varphi_o < 0.4$ m^2/kg which is given by Harmathy for conventional furnishment.

The exemplary analysis above illustrates how differentiated results obtained by model fire studies can be transformed to a description of realistic fire processes with practically representative fire load in the form furniture, textile goods and other equipments in fires arising in flats, after some calibrating full-scale tests. The translation parameters are composed of equivalent porosity factor, ϕ_e, and equivalent stick thickness, b_e, or equivalent parameters. Systematically performed calibrating tests in full scale with realistic fire load for common fire cells such as offices, schools, hospitals, stores etc. have a high degree of priority.

8.5 Brief design basis for the time curve of the energy released per unit time in a complete fire process.

The model fire studies, described in Sections 4-7, dealing with the maximum energy released per unit time and the determination of the type of fire process based on this magnitude, is summarized in Sections 8.2 and 8.3. The summary is based on tests with fire load in the form of wood cribs. In FIG. 96, this description is supplemented by I_{Cmax}-values determined by the results of full-scale tests described in the literature, in which the fire load has been of the type wood cribs and in the form of furniture, textile goods and other equipments.

Equations (40) and (41) give I_{Cmax} for ventilation controlled and fuel bed controlled fire processes respectively, with the air flow factor, $A\sqrt{H}$, and the initially exposed surface of the fuel, A_s, as parameters. The transitional points between both types of the fire processes is determined by Equation (42). The description summarized by these relations is, by form, similar to that introduced by Harmathy (1972) which is based on the mean combustion rate, R_{80-30}, of the flaming phase expressed by weight decrease per unit time, instead of having the maximum energy, I_{Cmax}, as the decisive magnitude.

A somewhat more refined result summary is given by Equations (44) - (46), which differentiate the maximum energy released per unit time, I_{Cmax}, with respect to fuel bed controlled fire process, ventilation controlled fire process and the transitional zone between these two chief types of fire processes. The parameters are composed of the air flow factor, $A\sqrt{H}$, and the ratio M/r between the total energy content of the fuel, M, and the initial hydraulic radius, r, of the fuel. Since the magnitude M/r is directly proportional to the initially exposed fuel surface, A_s, the descriptions according to Equations (40) - (41) and (44) - (46) become equivalent with respect to the influencing parameters.

Among the result descriptions presented, the summary according to FIG. 91 is the most differentiated one, in which the total energy content of the fuel, M, porosity factor, ϕ, and the stick thickness, b, are taken into consideration when dealing with the properties of

the fire load. Thereby, the following I_{Cmax}-relations correspond to the polygon-shaped line inserted in the figure through calculated I_{Cmax}-values.

a) $$I_{Cmax} = 5.6\ M \sqrt{\frac{\phi}{\phi_{0.5}}}\ \left(\frac{b_{25}}{b}\right)\ \text{MJ/h} \qquad (53)$$

for the fuel bed controlled range of the fire process, that is for $Mb_{25}/A\sqrt{H} \cdot b < 500\ \text{MJ/m}^{5/2}$.

b) $$I_{Cmax} = \left(1.52\ M\ \frac{b_{25}}{b} + 2040\ A\sqrt{H}\right) \sqrt{\frac{\phi}{\phi_{0.5}}}\ \text{MJ/h} \qquad (54)$$

for the transitional range between fuel bed- and ventilation controlled fire processes, that is for $500 \leq Mb_{25}/A\sqrt{H} \cdot b \leq 1000\ \text{MJ/m}^{5/2}$.

c) $$I_{Cmax} = 3560\ A\sqrt{H} \sqrt{\frac{\phi}{\phi_{0.5}}}\ \text{MJ/h} \qquad (55)$$

for the ventilation controlled range of the fire process, that is for $Mb_{25}/A\sqrt{H} \cdot b > 1000\ \text{MJ/m}^{5/2}$.

The following side conditions are true for application of the relations. If the opening factor $A\sqrt{H}/A_t < 0.04\ \text{m}^{1/2}$, the real porosity factor, ϕ, is replaced by $\phi_{0.5} = 0.5\ \text{cm}^{1.1}$, all through. If the opening factor, $A\sqrt{H}/A_t > 0.07\ \text{m}^{1/2}$, ϕ assumes the real value within the range $\phi \leq 0.5\ \text{cm}^{1.1}$ while the real ϕ is substituted by $\phi_{0.5} = 0.5\ \text{cm}^{1.1}$ for $\phi > 0.5\ \text{cm}^{1.1}$. Within the range $0.04 \leq A\sqrt{H}/A_t \leq 0.07\ \text{m}^{1/2}$, ϕ is determined by linear interpolation, that is from the Equation:

$$\phi = \frac{1}{3}\left(7\phi_{0.5} - 4\phi_v\right) - \frac{A\sqrt{H}/A_t}{0.03}\left(\phi_{0.5} - \phi_v\right) \qquad (56)$$

where ϕ_v is the real value of the porosity factor. The Equation is true for $\phi_v \leq 0.5\ \text{cm}^{1.1}$. For $\phi_v > 0.5\ \text{cm}^{1.1}$, ϕ is replaced by $0.5\ \text{cm}^{1.1}$. As for the stick thickness, b, real value is used if $b \geq b_{25} = 25$ mm while b is replaced by 25 mm for real $b < 25$ mm. The application of the relations is experimentally verified only up to $b \approx 50$ mm.

Assuming $\phi/\phi_{0.5} = 1$ and $b/b_{25} = 1$, the simplified I_{Cmax}-expressions according to Equations (47) - (49) are obtained which together describe fire processes that are either fuel bed-or ventilation con-

trolled in the regorous sense. Therby, with fuel bed controlled conditions the maximum energy, I_{Cmax}, is determined by the total energy content of the fuel, M, alone and with ventilation controlled conditions by the air flow factor, $A\sqrt{H}$, alone. Within the transitional range between the two chief types of fire processes, the maximum energy, I_{Cmax}, is determined by the magnitudes M and $A\sqrt{H}$ in combination. Fuel bed- or ventilation controlled fire processes, in the rigorous sence, exist for the porosity factor $\phi \geq 0.5$ $cm^{1.1}$ and the stick thickness $b \leq 30$ mm, with a precision which is satisfactory for practical use. For porosity factors and stick thicknesses outside these variation ranges, the fire process besides being influenced by the air flow factor, $A\sqrt{H}$, and the total heat content of the fuel, M, is also influenced by the other properties of the fire load.

For all the I_{Cmax}-relations briefly mentioned above, the I_{Cmax}-values should be magnified if the opening factor $A\sqrt{H}/A_t < 0.04$ $m^{1/2}$. The value of the correcting multiplicator employed should be 1.2 for $A\sqrt{H}/A_t = 0.02$ $m^{1/2}$ and should thereafter decrease linearly with increasing opening factor and assume the value 1 for $A\sqrt{H}/A_t = 0.04$ $m^{1/2}$.

In order to be able to draw the time curve of the energy released per unit time, I_C, the maximum energy, I_{Cmax}, as above, should be supplemented by a basis which facilitates a determination of a number of characteristical time magnitudes, defined through FIG. 18. Ordinarily a satisfactory precision can be achieved if the time magnitudes t_r, t_d, t_1 and t_2 are given.

For the time magnitude, t_r, which indicates the time from ignition to the time corresponding to $I_C = 0.75\ I_{Cmax}$ on the descending part of the energy-time curve, the analysis in Section 5.2 gives the approximate relation

$$t_r = 1.25\ T \qquad (57)$$

in a ventilation controlled fire process with the porosity factor $\phi \approx 0.5$ $cm^{1.1}$ - c.f. FIG. 40 and 41. In this relation T indicates the fire duration determined by Equation (25). In a fuel bed controlled fire process, Equation (57) gives a t_r-value which is lower than the real one. A t_r-value determined by Equation (57), with acceptable

precision in ordinary practical applications, can be derived in the following manner.

A combination of Equations (25), (46) and (57) which all assume ventilation controlled conditions in the rigorous sense, gives the relation

$$t_r = 1.25\ T = \frac{1.25\ q\ A_t}{6300\ A\sqrt{H}} = \frac{0.7\ q\ A_t}{3560\ A\sqrt{H}}$$

or the expression

$$t_r = \frac{0.7\ q\ A_t}{I_{Cmax}} \tag{58}$$

Under this form, a determination of t_r can be extended to fuel bed controlled fire processes. Lower real I_{Cmax}-values, approximately give the prolongation in t_r, which is caused by a transition from ventilation controlled to fuel bed controlled conditions, for a given fuel quantity.

For the time magnitude t_d, which indicates the time interval between the times corresponding to $I_C = 0.75\ I_{Cmax}$ on the ascending and descending parts of the energy-time curve, an elaboration of the values described in TAB. II, III and VI gives the approximate relation

$$t_d/t_r = 0.55\left[1 + 11(A\sqrt{H}/A_t - 0.08)(\phi - 0.4)\right] \tag{59}$$

The application of the relation is limited to the experimentally investigated variation ranges, that is for the opening factor $A\sqrt{H}/A_t \lesssim 0.12\ m^{1/2}$ and for the porosity factor $\phi \lesssim 1.1\ cm^{1.1}$. For $A\sqrt{H}/A_t > 0.12$, the values corresponding to $A\sqrt{H}/A_t = 0.12\ m^{1/2}$ can roughly be used.

For the time magnitudes t_1 and t_2, which, according to FIG. 18, describe the descending part of the energy-time curve between the interval ($I_C = 0.75\ I_{Cmax}$, $I_C = 0.5\ I_{Cmax}$) and ($I_C = 0.75\ I_{Cmax}$, $I_C = 0.25\ I_{Cmax}$) respectively, the analysis presented in Section 5.2, verifies the following two approximate expressions - c.f. Equations (30) and (31)

$$t_2 \approx t_r \tag{60}$$

$$t_1 \approx 0.3\ t_2 \tag{61}$$

The following energy condition should be added to the basis, summarized above, for a determination of the level for the maximum energy released per unit time, I_{Cmax}, and of the time magnitudes t_r, t_d, t_1 and t_2 – c.f. Equation (15)

$$\int_0^{t_g} I_C dt = M \tag{62}$$

where M is the total heat content of the fuel expressed in MJ. This condition determines the terminal part of the I_C - t curve, through the time magnitude t_g according to FIG. 18.

As a complement, it is moreover true that the gas flow, Q, can be determined by Equation (11) for $A\sqrt{H}/A_t \leq 0.04\ m^{1/2}$ where the vertical acceleration of the flow in the window opening need not be taken into consideration. However, for larger values of the opening factor, this vertical acceleration should be taken into consideration which results in the fact that the gas flow, Q_a, should be determined by Equation (12) in which C assumes the values 0.8 and 0.7 for the opening factors $A\sqrt{H}/A_t = 0.07$ and $0.114\ m^{1/2}$ respectively. Alternatively, the gas flow, Q, or Q_a can be calculated by the approximate relation according to Equation (32) or (32a), within the whole variation range of the opening factor, $A\sqrt{H}/A_t$.

A determination of the time curve of a complete fire process for the energy released per unit time, I_C, is facilitated through the basis summarized above, with a precision which is acceptable in ordinary cases. The determination can be carried out with a rather far-reached differentiation for pure fire load in the form of regular wooden cribs, wherein the opening factor of the fire cell, $A\sqrt{H}/A_t$, size of the fire load, q, porosity factor, ϕ, and stick thickness, b, should be taken into consideration. By determining the equivalent porosity factor, ϕ_e, and equivalent stick thickness, b_e, for main fire load components, through systematically performed, complementary calibrating tests, the corresponding differentiation should be possible for practically representative fire load in the form of furniture, textile goods and

and other equipments.

8.6 Comparative illustration of the energy- and gas temperature-time curves for different types of fire processes.

In Section 8.5 a brief basis is given for determining the time curve of a complete fire process, for the energy released per unit time, I_C, using fire load of regular wood cribs, with a precision which is satisfactory for ordinary practical cases. For this type of fire load, the basis facilitates a theoretical calculation of the gas temperature-time curve of the complete fire process by the heat- and mass balance equations of the fire cell according to Section 2, with varying opening factor, $A\sqrt{H}/A_t$, thermal properties of the enclosing structures of the fire cell, size of the fire load, q, porosity factor, ϕ, of the fire load and stick thickness, b, of the fire load. Systematical calculations as such, result in a design basis which in practical applications could be used for fire load in the form of furniture, textile goods and other equipments through the equivalent porosity factor, ϕ_e, and the equivalent stick thickness, b_e.

A systematical design basis of the above mentioned type, in the form of differentiated gas temperature-time curves for a complete fire process will be published in some other connection. The presentation here is limited to an illustration of the time curve for the released energy per unit time, I_C - t and the gas temperature time, ϑ_g - t, corresponding to the chief types of fire processes defined in Section 8.3, namely ventilation- and fuel bed controlled fire processes in the rigorous sense, and crib controlled fire process. All the subvariants according to Section 8.3 (combined fuel bed- and crib controlled, combined ventilation- and crib controlled and combined ventilation-, fuel bed- and crib controlled processes) are summarized by the designition crib controlled.

The illustration is carried out for a fire cell with the opening factor $A\sqrt{H}/A_t = 0.08\ m^{1/2}$ and with the enclosing structures, 200 mm thick, composed of a material with the coefficient of thermal conductivity of $\lambda = 0.81\ W/m^{\circ}C$ and the heat capacity of $c \cdot \gamma = 1.67\ MJ/m^3\ ^{\circ}C$. This fire cell agrees with type A in Magnusson-Thelandersson (1970),

with respect to the thermal properties of the enclosing structures.

As far as the relation between the maximum value for the energy released per unit time, I_{Cmax}, and the magnitude, $M/A\sqrt{H}$, is concerned, the basical curves employed for the illustration assume the existence of a fire load in the form of wood cribs and a summary of the obtained results according to Equations (53) - (56). The stick thickness, b, of the fire load is generally assumed to be $b \leq 25$ mm, that is $b/b_{25} = 1$. The basical curves are described in FIG. 97. For the porosity factor $\phi \geq 0.5$ cm$^{1.1}$, Curve (I) describes a fuel bed- or ventilation controlled fire process in the rigorous sense, while Curves (II) and (III) describe crib controlled fire processes corresponding to the porosity factors $\phi = 0.25$ and $\phi = 0.09$ cm$^{1.1}$ respectively. As a consequence of this assumption, if $b/b_{25} = 1$ then the three polygon-shaped basic curves acquire their deflection points for identical $M/A\sqrt{H}$-values, namely $M/A\sqrt{H} = 500$ and 1000 MJ/m$^{5/2}$, c.f. Equations (53) - (55). In FIG. 97 a curve branch (IA) marked by dashed lines has also been inserted, which can be considered as a prolongation of the horizontal line $I_{Cmax}/A\sqrt{H} = 3560$ MJ/h, corresponding to a rigorously ventilation controlled fire process, within the fuel bed controlled range and which is thus related to the discussion according to Magnusson-Thelandersson (1970), based on a ventilation controlled fire process as the general assumption.

The $M/A\sqrt{H}$-values, for which the gas temperature-time curve corresponding to a complete fire process has been determined in the illustrating discussion, are marked by points on the basical curves. The folfowing fire load corresponds to these values, denoted by C MJ/m$^{5/2}$, with the opening factor $A\sqrt{H}/A_t = 0.08$ m$^{1/2}$:

$$q = C \frac{A\sqrt{H}}{A_t} = 0.08\ C \text{ MJ/m}^2 \qquad (63)$$

In a ventilation controlled fire process in the rigorous sense -- Curve (I) for $M/A\sqrt{H} > 1000$ MJ/m$^{5/2}$ - the $M/A\sqrt{H}$-values marked by points can alternatively be related to the fire duration, T, according to Equation (25) which gives the expression

$$T = \frac{C}{6300} \text{ h} \qquad (64)$$

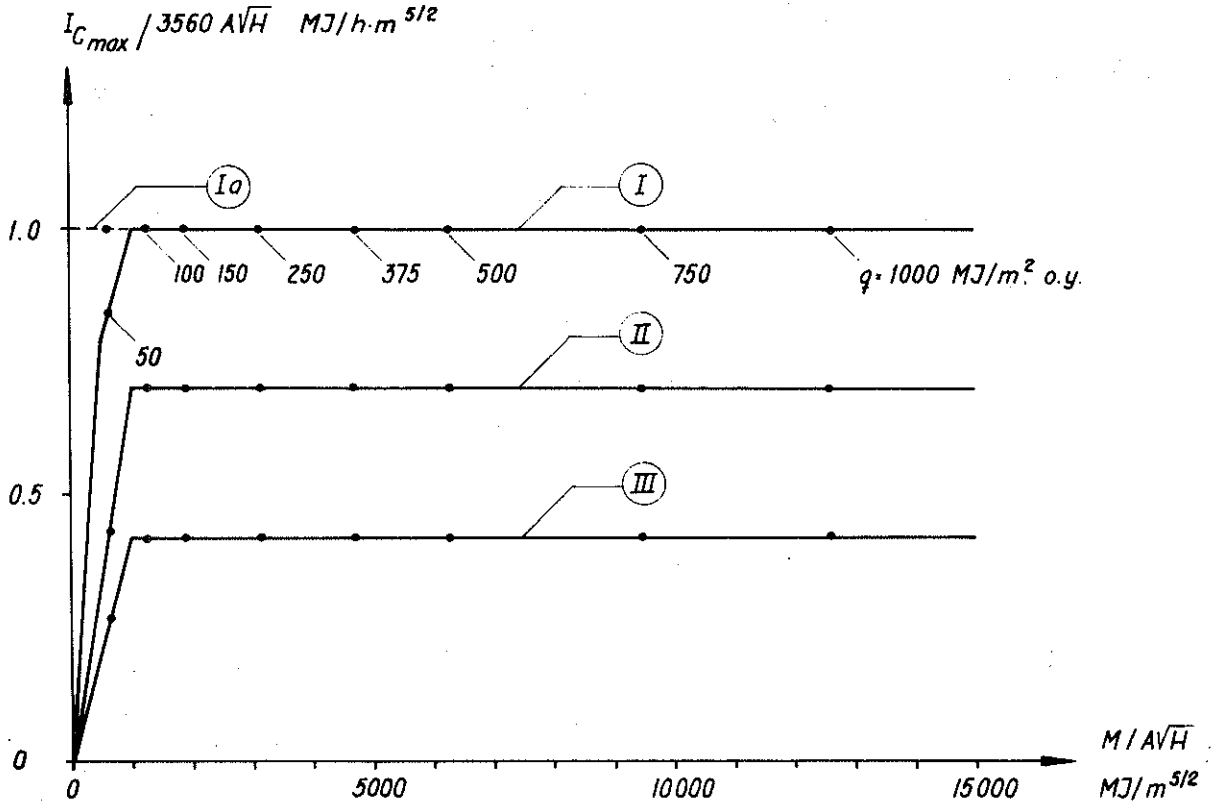

FIG. 97 Illustration of the assumed relation, for different shapes of the fire load, Curves (I) - (III), between I_{Cmax} and $M/A\sqrt{H}$. The curves assume a stick thickness $b \leq 25$ mm, that is $b/b_{25} = 1$. Further, for Curve (I) the porosity factor of $\phi \geq 0.5$ cm$^{1.1}$ is true, for Curve (II) $\phi = 0.25$ cm$^{1.1}$ and for Curve (III) $\phi = 0.09$ cm$^{1.1}$. The dashed curve (I_a) indicates the maximum energy level assumed by Magnusson-Thelandersson (1970) under the assumption of general ventilation control. In connection with the introduced values of the fire load, q, marked by points on the curves, the opening factor is $A\sqrt{H}/A_t = 0.08$ m$^{1/2}$.

From Curve (I) and Equation (63) it is observed that, a ventilation controlled fire in the rigorous sense, exists if the porosity factor of the fire loading $\phi \geq 0.5$ cm$^{1.1}$ and if at the same time, the fire load $q > 80$ MJ/m^2 for the selected opening factor $A\sqrt{H}/A_t = 0.08$ m$^{1/2}$. For the porosity factor $\phi \geq 0.5$ cm$^{1.1}$ and the fire load $q < 40$ MJ/m^2, the fire process is fuel bed controlled in the rigorous sense, while for the porosity factor $\phi > 0.5$ cm$^{1.1}$ and the fire load $40 \leq q \leq 80$ MJ/m^2, the fire process falls within the transitional zone between the rigorously fuel bed- and ventilation controlled fire processes. For porosity factor $\phi < 0.5$ cm$^{1.1}$, the fire process is of the type crib controlled with subvariants according to Section 8.3.

With the I_{Cmax}-level according to FIG. 97 and the time magnitudes, t_r, t_d, t_1, t_2 and t_g determined by Equations (58) - (62), the complete time curve for the energy released per unit time, I_C, can be drawn with a precision, which is satisfactory in ordinary practical applications. An example of this is given in FIG. 98 a and 98 b for the I_C - t curves corresponding to the basic curves (I), (II), and (III) according to FIG. 97 for $M/A\sqrt{H} = 630$ and 6300 MJ/m$^{5/2}$ or alternatively $q = 50$ and 500 respectively. As a complement, the I_C - t curve, corresponding to the basic curve (Ia), which according to Magnusson-Thelandersson (1970) generally assumes a ventilation controlled fire process in the rigorous sense, is also described in FIG. 98 for the fire load $q = 50$ MJ/m^2, at which a realistic fire process is fuel bed controlled, the I_C - t curves corresponding to basic curves (I) and (Ia) deviate from each other. For the fire load $q = 500$ MJ/m^2 a realistic fire process is however ventilation controlled, and consequently the basic curves (I) and (Ia) give coinciding I_C - t relations. From the I_C - t curves illustrated in FIG. 98, it is generally observed that a reduced level for the maximum energy released per unit time, I_{Cmax}, is followed by a slower fire development and an increased fire duration.

Based on energy-time curves, - with the basic appearance according to FIG. 98 and determined in an analogous manner - related to $M/A\sqrt{H}$ - or q-values, the corresponding gas temperature-time curves have been calculated for a complete fire process, according to Section 2, for a fire cell with the opening factor $A\sqrt{H}/A_t = 0.08$ m$^{1/2}$ and with

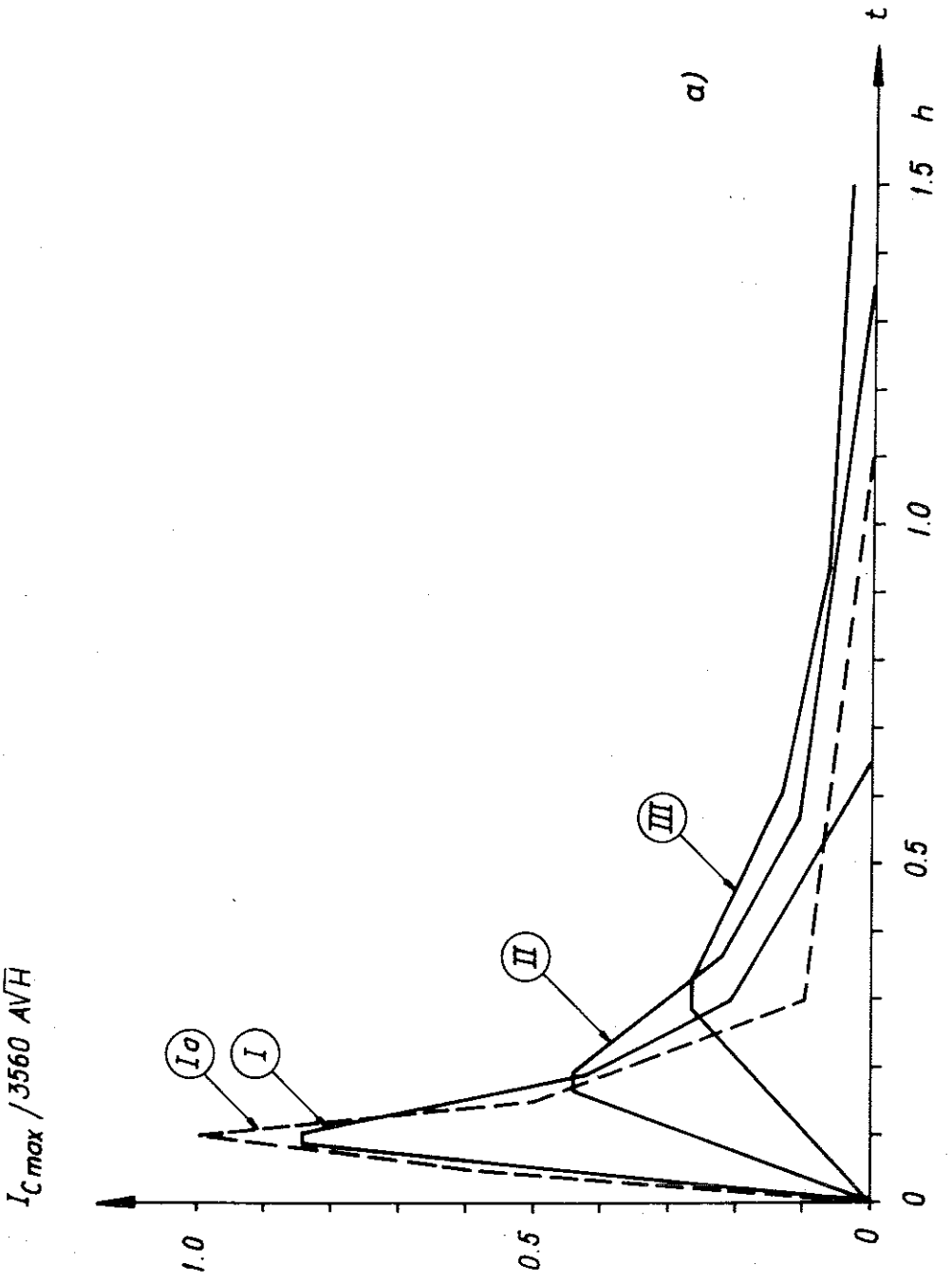
$I_{C\,max}$ / 3560 $A\sqrt{H}$
1.0
0.5
0
Ia
I
II
III
a)
t
0
0.5
1.0
1.5 h

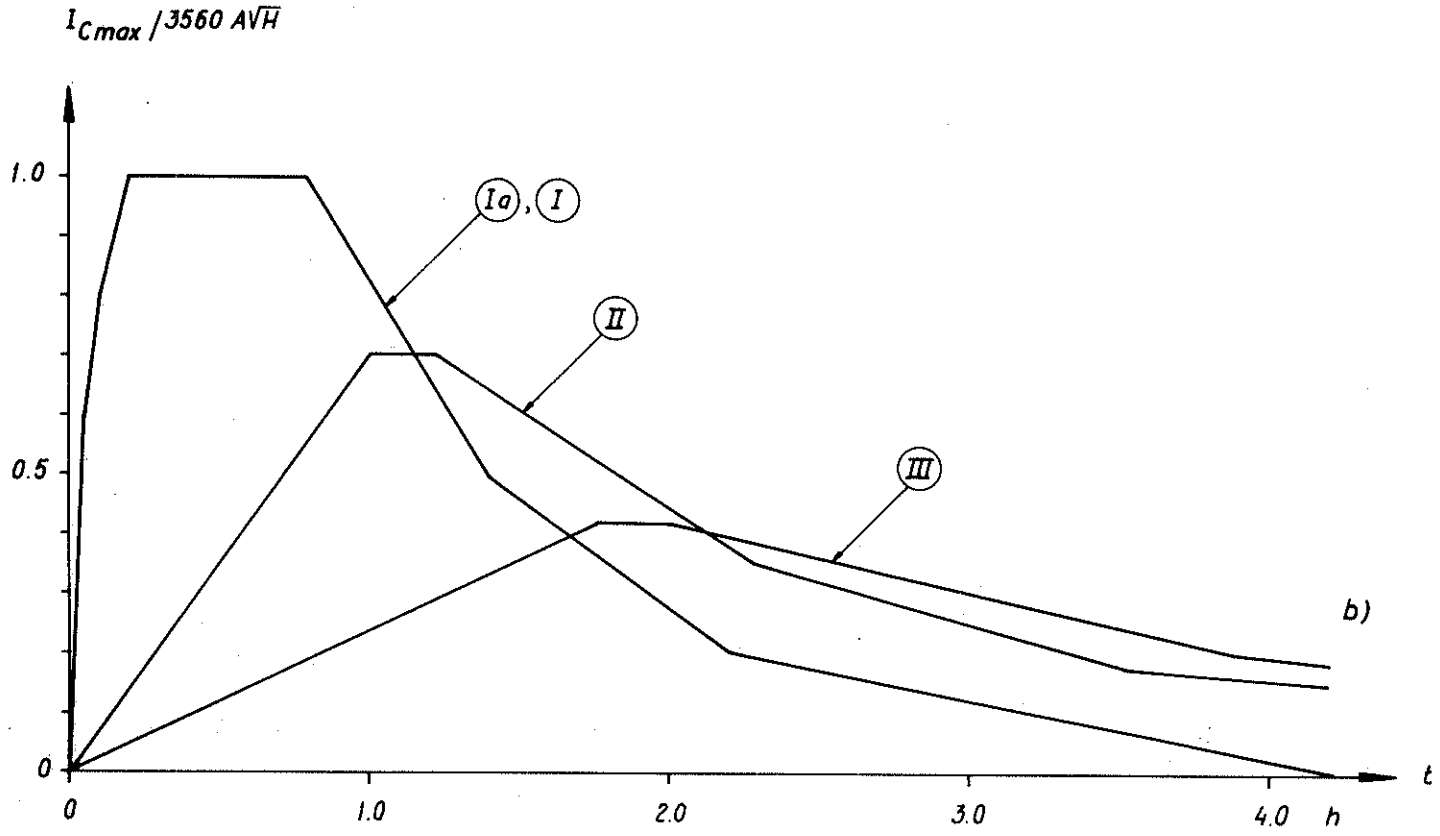

FIG. 98 The energy-time curves, determined from the relations given in Section 8.5 for $M/A\sqrt{H} = 630\ MJ/m^{5/2}$, alternatively $q = 50\ MJ/m^2$ of the enclosing surface, a, and $M = 6300\ MJ/m^{5/2}$, alternatively $q = 500\ MJ/m^2$ of the enclosing surface, b, in a fire process where the relation between I_{Cmax} and $M/A\sqrt{H}$ is described by curves (I) - (III) in FIG. 97 (—). As a complement the energy-time curve assumed by Magnusson-Thelandersson under the assumption of a generally ventilation controlled fire process is also given in the figure, c.f. FIG. 4 (---).

the enclosing structures according to the above. The value 0.8 has been used for the C-factor included in the term gas flow, Q_a, in Equation (12).

For I_{Cmax} according to FIG. 97, the results are described in FIG. 99, 100, and 101, corresponding to the basic curves (I), (II), and (III) respectively.

The gas temperature-time curves summarized in FIG. 99, are true for a rather easily combustible wood crib with the porosity factor $\phi \geq 0.5$ cm$^{1.1}$. For this case, the assumption of a generally ventilation controlled fire process, introduced by Magnusson-Thelandersson, gives a satisfactory solution of the problem for the fire load $q > 80$ MJ/m^2, within which range the fire process is really ventilation controlled in the rigorous sense. For the fire load $q = 50$ MJ/m^2, a gas temperature-time curve determined under the assumption of ventilation control, results in an overestimation of the maximum value of the fire gas temperature and a simultaneous underestimation of the fire duration. The difference obtained, is however, moderate.

On the other hand the assumption of a ventilation controlled fire process, naturally gives a poor description of the real gas temperature-time curve of a fire process which is obviously crib controlled, which fact is illustrated by FIG. 100 and 101, corresponding to the I_{Cmax}-basic curves (II) and (III) according to FIG. 97. For the fire load $q = 500$ MJ/m^2, the maximum fire gas temperature, ϑ_{max}, amounts to 1080 °C according to a calculation for a ventilation controlled fire process, while a more correct calculation by $I_C - t$ curves, denoted by (II) and (III), in FIG. 98 b, gives the value $\vartheta_{max} = 895$ °C for the porosity factor $\phi = 0.25$ cm$^{1.1}$, and the value $\vartheta_{max} = 610$ °C for the porosity factor $\phi = 0.09$ cm$^{1.1}$. For the fire load $q = 50$ MJ/m^2 the corresponding three ϑ_{max}-values amount to 935, 540 and 375 °C respectively.

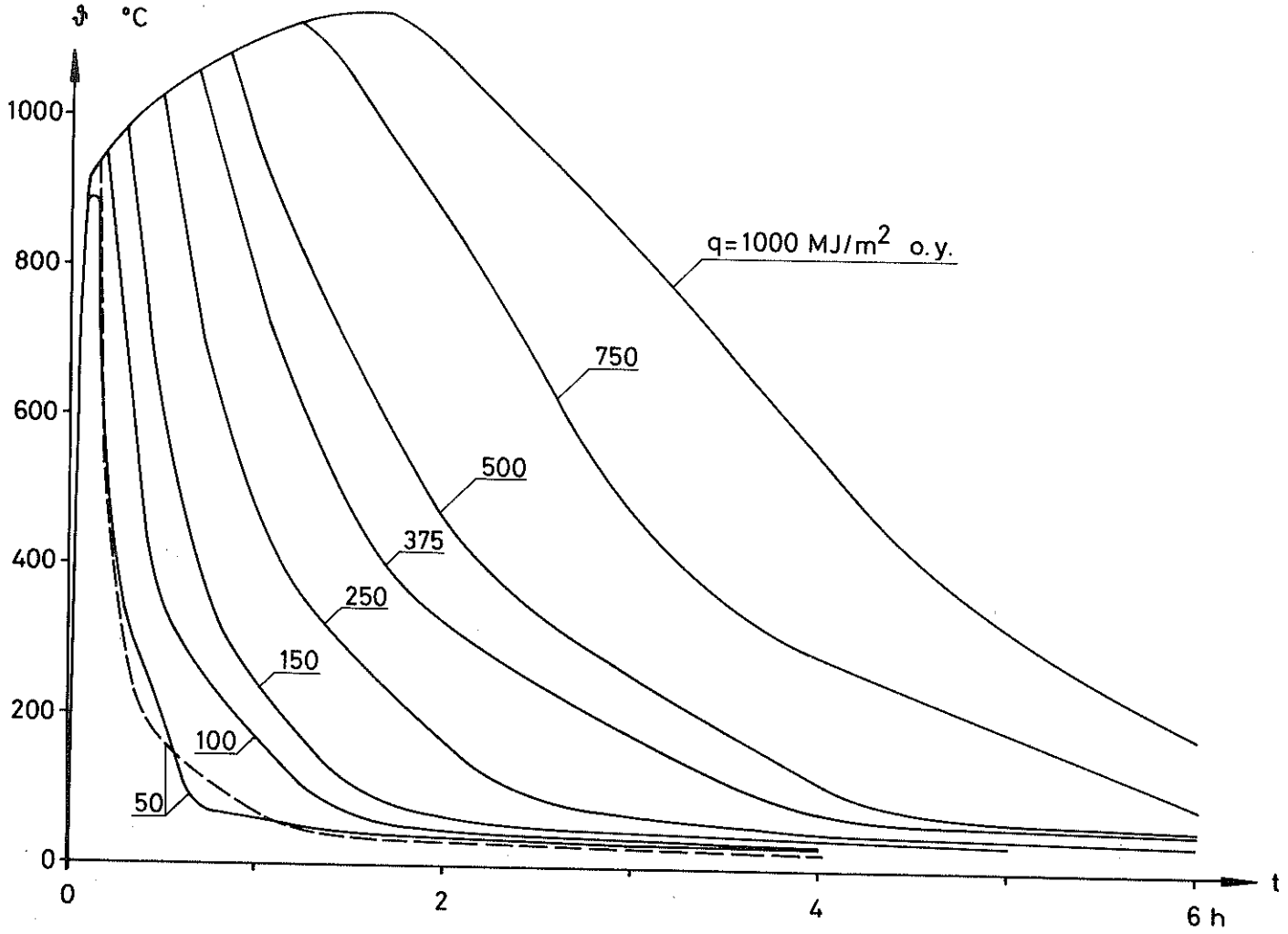

FIG. 99 The theoretically calculated gas temperature-time curves based on the energy-time curves determined according to the relation described in Section 8.5 in a fire process where the relation between I_{Cmax} and $M/A\sqrt{H}$ is described by curve (I) in FIG. 97 (—). As a complement, the corresponding gas temperature-time curves described by Magnusson-Thelandersson, calculated from the energy-time curves summarized in FIG. 4 is also given in the figure, under the assumption of a ventilation controlled fire process (- - -).

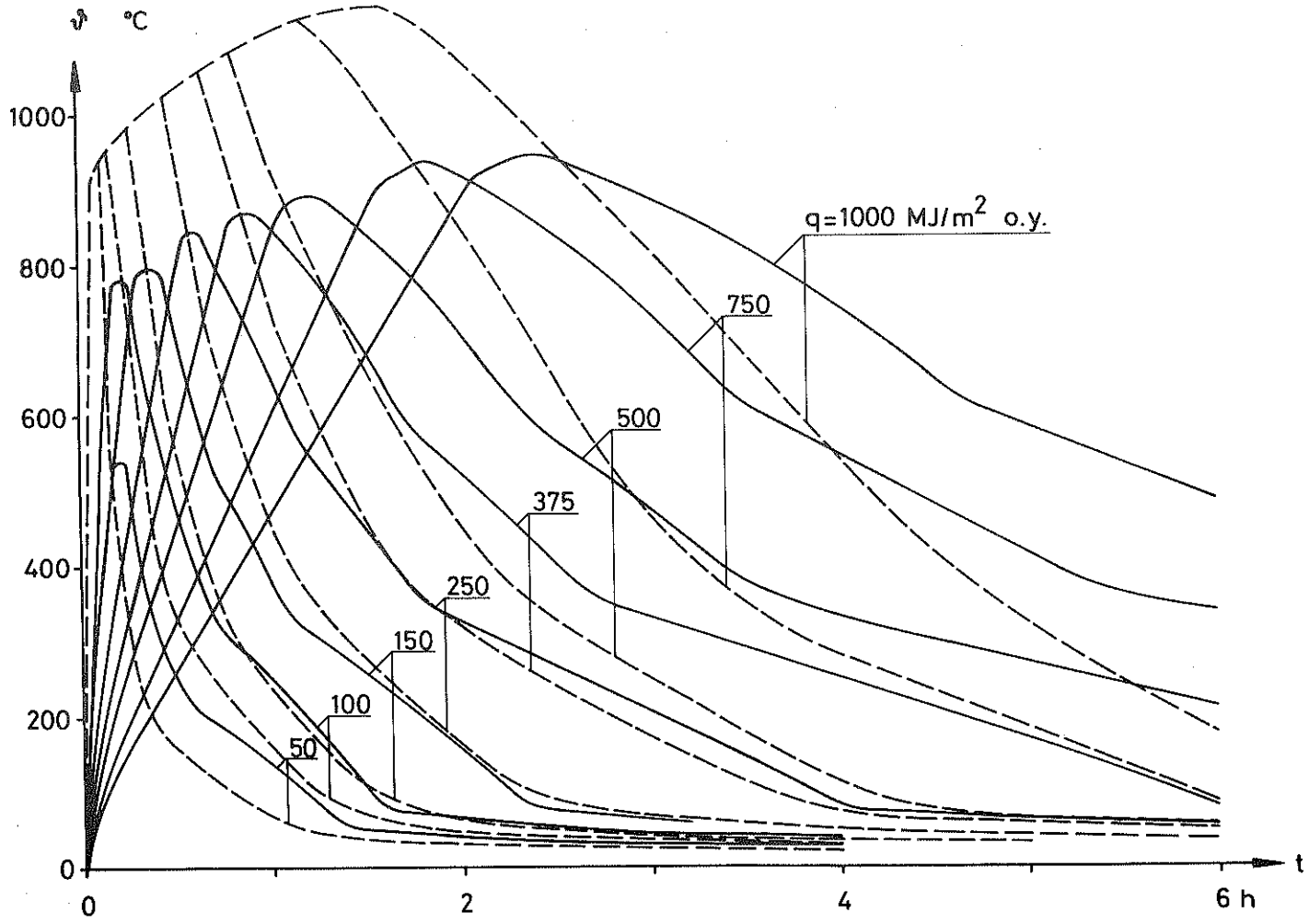

FIG. 100 The theoretically calculated gas temperature-time curves, based on the energy-time curves determined according to the relation described in Section 8.5 in a fire process where the relation between I_{Cmax} and $M/A\sqrt{H}$ is described by Curve (II) in FIG. 97 (—). As a complement, the corresponding gas temperature-time curves described by Magnusson-Thelandersson, calculated from the energy-time curves summarized in FIG. 4, is also given in the figure, under the assumption of a ventilation controlled fire process (- - - -).

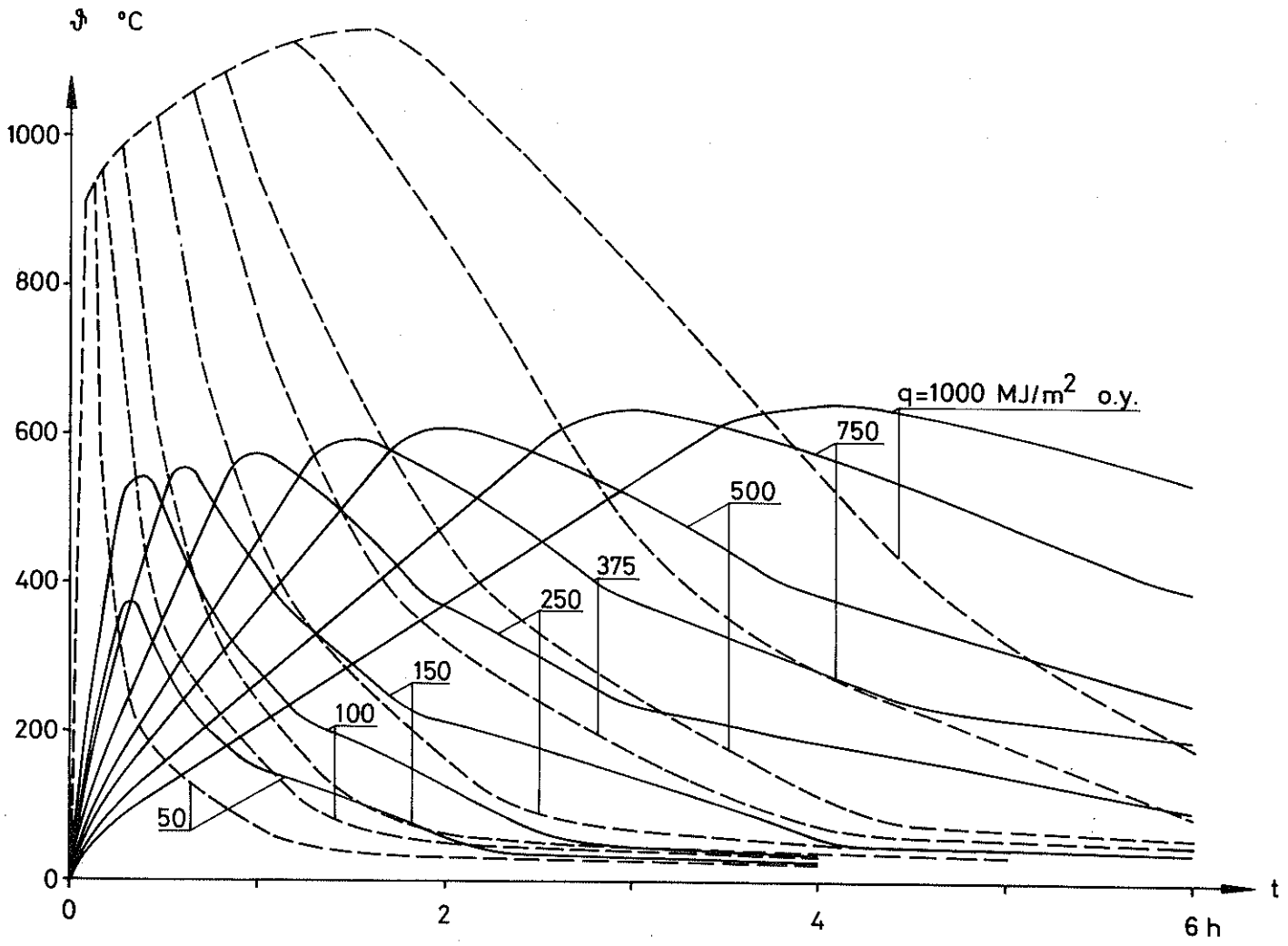

FIG. 101 The theoretically calculated gas temperature-time curves, based on the energy-time curves determined according to the relation described in Section 8.5, in a fire process where the relation between I_{Cmax} and $M/A\sqrt{H}$ is described by Curve (III) in FIG. 97 (—). As a complement, the corresponding gas temperature-time curves described by Magnusson-Thelandersson, calculated from the energy-time curves summarized in FIG. 4, is also given in the figure, under the assumption of a ventilation controlled fire process (- - -).

SUMMARY

In order to make a functionally based fire technological design of bearing and fire partitioning structures possible, a differentiated survey of the characteristics of the complete fire process in the fire cell with varying properties for the fuel and enclosing walls, floor and ceiling, is one of the primary requirements. In this case, a survey of the energy released per unit time during the fire process is fundamental for a determination of the gas temperature-time curve of the fire process. For wood fuel fires, it is, however, extremely difficult to give this energy development per unit time, since for this kind of fuel, the combustion simultaneously takes place both in the solid components and in the gases formed during the pyrolysis, in a manner which is, up to now, unexplained.

Therefore, in a test series, the influence of the characteristics of the fire cell and the size and properties of the fire load on the fire process and the energy-time curve, has been studied. For every test the energy-time curve which rendered a satisfactory agreement between the gas temperature-time curve as measured through tests and calculated through a theoretical model, was iteratively determined. The results could be systematized, so that the time curve for the energy released per unit time generally could be assumed to be approximately known, whereafter the gas temperature-time curve of the complete fire process can be calculated with varying properties for the fire cell and the quantity and form of the fuel.

Scope of the test series.

A theoretical fire technological design performed by the heat- and mass balance equations of the fire cell, presumes knowledge on the energy development of the fuel during the whole fire process. For wood fuel fires it is, however, extremely difficult to indicate this energy development per unit time, since for this type of fuel the combustion simultaneously takes place both in the solid components and in the gases formed during pyrolysis in such a way that it has hitherto been impossible to clarify. Therefore, in order to study this energy development for fires, with wood cribs as the fuel, combustion studies have been supplementet by a theoretical analysis through the heat- and mass balance equations of the fire cell, with the primary objective of determining the influence on the fire process for a wood crib in a closed fire cell having one window opening with variations in

1) the quantity of the combustible material,
2) the piling density of the fuel,
3) the thickness of the individual stick,
4) the window area of the fire cell, and

5) the thermal properties of the enclosing structures of the fire cell.

Test arrangements.

Three cubical, closed fire chambers at the model scale with one window opening and with the internal lateral dimensions measuring 500, 750 and 1000 mm respectively, were used in the tests. However, all the tests analyzed in this report refer to the tests performed in the intermediate model scale. The fire cells were covered externally by steel sheet and internally by 10 mm asbestos disk (in applicable cases is only true for point 5 above). The window opening of the fire cell was chosen in a square form and the dimensions given to this opening were such that the five different values, namely, $A\sqrt{H}/A_t$ = 0.020, 0.032, 0.040, 0.070 and 0.114 $m^{1/2}$ were obtained for the opening factor, which together cover a broad and realistic range of variation. The opening factor is defined as $A\sqrt{H}/A_t$, in which A_t (m^2) denotes the inner surface area of the walls, floor and ceiling which bound the fire cell from its surroundings, A (m^2) is the total opening area of the fire cell (windows, doors etc.) and H (m) is a weighted mean value of the heights of the openings.

The studied values for the fire load, q, which were normally composed of redwood sticks having square cross sectional areas with b = 25 mm, were q = 17.5, 35.0, 52.5, 70.0 and 87.5 MJ/square m of the enclosing surface. In order to study the influence of the thickness of the individual stick, besides the lateral dimension b = 25 mm even sticks with dimensions b = 10, 12.5, 40 and 50 mm were taken into consideration.

In order to characterize the piling density of the fuel, the porosity factor ϕ ($cm^{1.1}$) is used, defined through the relation

$$\phi = N^{0.5}\, b^{1.1}\, \frac{A_v}{A_s} \qquad (1)$$

with

$$A_s = 2nb\left\{2NL + b\left[N - n(N-1)\right]\right\} \qquad (2)$$

$$A_v = (L - nb)^2 \qquad (3)$$

In these formulas, b denotes the thickness (square cross section) and L (cm) the length of each wooden stick, n the number of sticks per layer, N the number of layers, A_s the area of all the sticks, initially exposed to the air, and A_v the free horizontal area for vertical air flow through the pile. The variation range for the porosity factor of the fire load in the investigation is 0.1 - 1.3 $cm^{1.1}$.

In order to investigate the influence of variations in the thermal properties of the enclosing structures on the fire process, the alternatives 1.5 mm steel sheet, 1.5 mm steel sheet + 10 mm asbestos disk and 1.5 mm steel sheet + 125 mm light weight concrete, were studied.

In the investigation, the combustion rate was determined, according to the experimentally developed practice, that is, by the weight loss of the fuel, the gas temperature-time curve of the fire process plus radiation and smoke intensities.

For every test, the energy-time curve which rendered a satisfactory agreement between the experimentally obtained gas temperature-time curve and that calculated through a theoretical model, was iteratively determined by the heat- and mass balance equations of the fire cell. Thereby, the energy-time curve was assumed to have a basic appearance according to FIG. 1, in which a number of magnitudes characterizing the time curve, studied here are also illustrated.

For easily combustible wood cribs characterized by $\phi \gtrsim 0.5$ $cm^{1.1}$ and b < 30 mm, an upper value, based on the summarized results was obtained for the maximum heat development I_{Cmax}, where the relation between this magnitude, the fuel quantity, M, and the air flow factor, $A\sqrt{H}$, is given by FIG. 2. Three different ranges can be distinguished in the figure, namely

a) a fuel bed controlled range of the fire process for $M/A\sqrt{H} < 500$ $MJ/m^{5/2}$, where

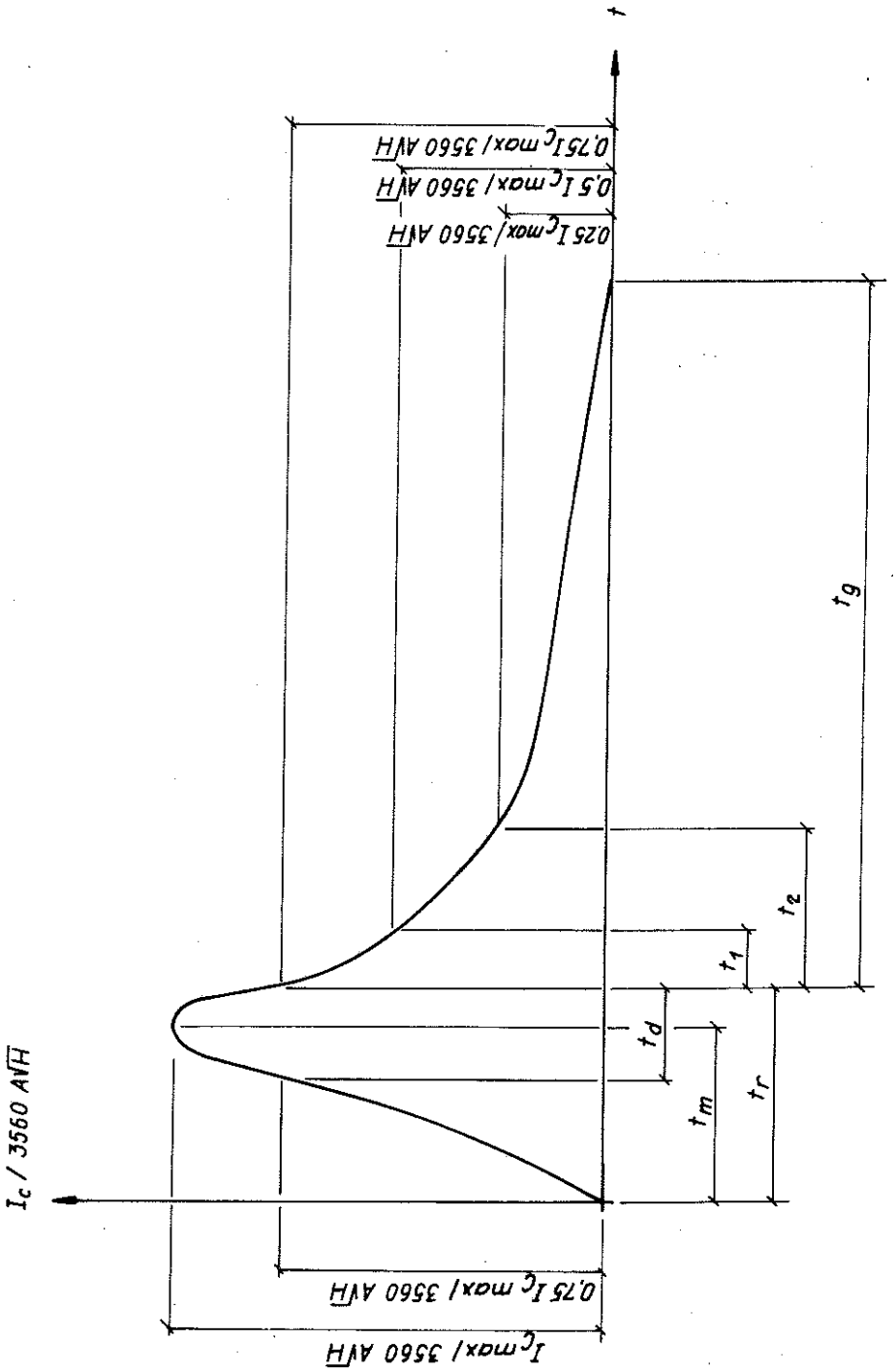

FIG. S 1 Definition of the parameters characterizing the energy-time curve.

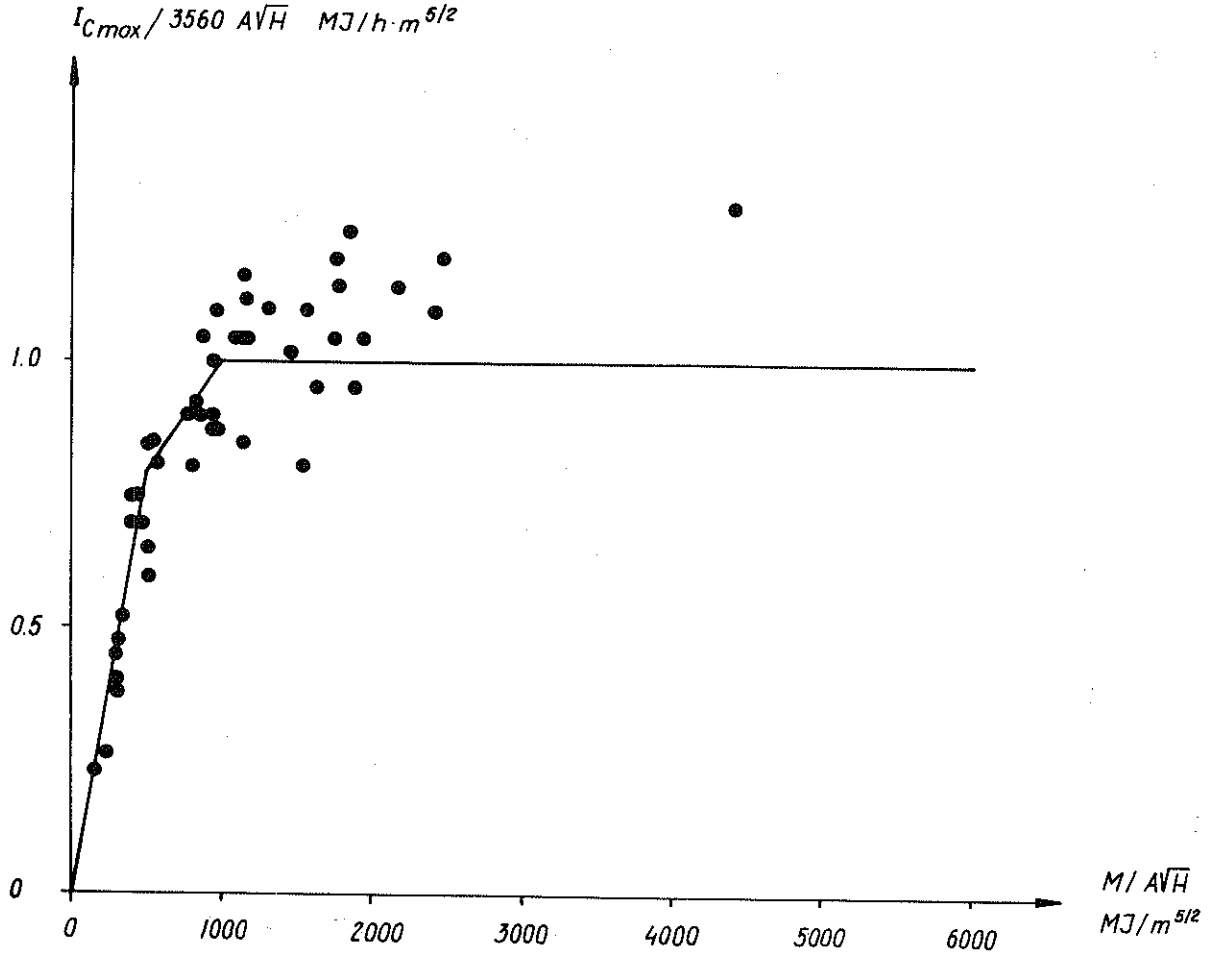

FIG. S 2 The relation, calculated from the results of model tests, between $I_{Cmax}/3560\ A\sqrt{H}$ and $M/A\sqrt{H}$, where M is the total energy content of the fuel. The inserted straight lines are described by Equations (4) - (6). The fire load is in the form of regular wood cribs. In the summary, only the test for which the relations $\phi \gtrsim 0.5$ cm$^{1.1}$ and the stick thickness b = 25 mm are true, have been considered.

$$I_{Cmax} = 5.6\ M \quad MJ/h \tag{4}$$

b) a transitional zone between fuel bed- and ventilation controlled fire processes for $500 \leq M/A\sqrt{H} \leq 1000\ MJ/m^{5/2}$, where

$$I_{Cmax} = 1.52\ M + 2040\ A\sqrt{H} \quad MJ/h \tag{5}$$

and

c) a ventilation controlled range of the fire process for $M/A\sqrt{H} > 1000\ MJ/m^{5/2}$, where

$$I_{Cmax} = 3560\ A\sqrt{H} \quad MJ/h \tag{6}$$

At low values of the porosity factor, $\phi < 0.5\ cm^{1.1}$, and/or large stick dimensions, $b > 30$ mm, the fire process besides depending on the air flow factor, $A\sqrt{H}$, and the total heat content of the fuel, M, will also depend on the other properties of the fire load, whereby the fire process will be combined fuel bed- and crib controlled within the range $M/A\sqrt{H} < 500\ MJ/m^{5/2}$, combined ventilation and crib controlled within the range $M/A\sqrt{H} > 1000\ MJ/m^{5/2}$ and combined ventilation-, fuel bed- and crib controlled within the transitional zone $500 \leq M/A\sqrt{H} \leq 1000\ MJ/m^{5/2}$. Thereby, with a given value for $M/A\sqrt{H}$, the maximum energy development, I_{Cmax}, will assume a value which is lower than that given by Equations (4) - (6).

Guiding principles for the influence of low values of the porosity factor, $\phi < 0.5\ cm^{1.1}$, and large stick dimensions, $b > 30$, on the maximum energy development, I_{Cmax}, and the required modifications at the opening factor $A\sqrt{H}/A_t < 0.04\ m^{1/2}$, are given.

With a known value for I_{Cmax}, the energy-time curve corresponding to the developed energy can be calculated, by the relations described in the report, for all the above-mentioned types of fire processes, with fire load of the type wood cribs, with a precision which is satisfactory for practical applications.

In the report the prerequisites for finding a method to translate the

conditions prevailing in a fire process with fire load of the type real furniture, to a value for the piling density of a wood crib, are discussed through which systematical model scale studies dealing with the influence of the more important influencing factors could be facilitated, using simply shaped fire loads.

REFERENCES

Ahlquist, C. - Thelandersson, S., 1968, Redovisning och bearbetning av fullskaleförsök med bränder utförda av Statens provningsanstalt. Examensarbete vid institutionen för Byggnadsstatik, Lunds Tekniska Högskola, Lund.

Butcher, E.G. - Bedford, G.K. - Fardell, P.J., 1968, Further Experiments on Temperatures Reached by Steel in Building Fires. Behaviour of Structural Steel in Fire, Symposium No. 2, Proceedings of a symposium held at the Fire Research Station, Boreham Wood, Hertz, on 24 Jan. 1967, Her Majesty's Stationary Office, Paper 1.

CTH:s handlingar Nr 274, Träkonstruktioners brandstabilitet-symposium vid Chalmers Tekniska Högskola den 18 juni 1962, Göteborg.

Ehm, H. - Arnault, P., 1969, Versuchsbericht über Untersuchungen mit Natürlichen Bränden im Kleinen Versuchsbrandhaus. Doc. CEACM 3.1-69/29-D, F, Oktober.

Fox, L., 1962, Numerical Solution of Ordinary and Partial Differential Equations. London (Pergamon Press).

Gross, D., 1962, Experiments on the Burning of Cross Piles of Wood. Journal of Research of the National Bureau of Standards. Vol. 66 C, No. 2, April-June.

Harmathy, T.Z., 1972, A New Look at Compartment Fires, Part I. Fire Technology, Vol. 8, No. 3, pp 196-217.

Harmathy, T.Z., 1972, A New Look at Compartment Fires, Part II. Fire Technology, Vol. 8, No. 4, pp 326-350.

Heselden, A.J.M., 1968, Further experiments on Temperatures Reached by Steel in Building Fires. Behaviour of Structural Steel in Fire, Symposium No. 2, Proceedings of a Symposium held at the Fire Research Station, Boreham Wood, Herts, on 24 Jan. 1967, Her Majesty's Stationary Office, Paper 2.

Heselden, A.J.M. - Thomas, P.H. - Law, M., 1970, Burning Rate of Ventilation Controlled Fires in Compartments. Fire Technology, Vol. 6, No. 2, pp 123-125.

ISO/R 834, Fire Resistance Tests of Elements of Building Construction, 1972, ISO/TC 92/WG 11.

Kawagoe, K. 1958, Fire Behaviour in Rooms. Building Research Institute. Report No. 27. Tokyo.

Kawagoe, K. - Sekine, T., 1963, Estimation of Fire Temperature-Time Curve in Rooms. Building Research Institute. Occasional Report. No. 11, Tokyo.

Kawagoe, K., 1967, Estimation of Fire Temperature-Time Curve in Rooms. Building Research Institute, Japan, Research Paper No. 29.

Knublauch, E., 1972, Uber Ausführung und Aussagefähigkeit des Normbrandversuches nach Din 4102, Blatt 2, im Hinblick auf die Nachbildung natürlicher Schadensfeuer. BAM-bericht Nr. 16, Berlin.

Law, M., 1968, Further Experiments on Temperatures Reached by Steel in Building Fires. Behaviour of Structural Steel in Fire, Symposium No. 2, Proceedings of a symposium held at the Fire Research Station, Boreham Wood, Herts, on 24 Jan. 1967, Her Majesty's Stationary Office, Paper 3.

Lundin, S.T. - Fäldt, I., 1968, Fri energi - Temperaturdiagram, Temperatur - Potentialdiagram och Stabilitetsdiagram. Diskussion om principiell uppbyggnad och praktisk tillämpning. Avdelningen för kemisk teknologi, Lunds Tekniska Högskola, Lund.

Magnusson, S.E. - Thelandersson, S., 1970, Temperature-Time Curves of Complete Process of Fire Development. Acta Polytechnica Scandinavica, Civil Engineering and Building Construction, Series No. 65, Stockholm.

Magnusson, S.E. - Thelandersson, S., 1971, Comments on Rate of Gas Flow and Rate of Burning for Fires in Enclosures, Division of Structural Mechanics and Concrete Construction, Lund Institute of Technology, Bulletin 19, Lund.

Nilsson, L., 1970, Brandbelastning i bostadslägenheter (Fire load in flats). Rapport från Byggforskningen R34:1970, Stockholm.

Nilsson, L., 1971, Porositets- och luftflödesfaktorns inverkan på förbränningshastigheten vid brand i slutet rum. Rapport från Byggforskningen R22:1971, Stockholm.

Olsson, B. - Sjöholm, G., 1972, Väggegenskapernas inverkan på förbränningshastigheten vid brand i slutet rum med en fönsteröppning. Examensarbete vid institutionen för Byggnadsstatik, Lunds Tekniska Högskola, Lund.

Pettersson, O., 1965, Structural Fire Engineering Research Today and Tomorrow. Acta Polytechnica Scandinavica, Civil Engineering and Building Construction, Series No 33, Stockholm.

Pettersson, O. - Ödeen, K., 1968, Pågående och planerad byggnadsteknisk brandforskning i Sverige. Rapport från Byggforskningen R34:1968, Stockholm.

Rogowski, B.F.W., 1970, Charring of Timber in Fire Tests. Symposium No. 3, Fire and Structural Use of Timber in Buildings, held at the Fire Research Station, Boreham Wood, Hertz, on 25th October 1967, Her Majesty's Stationary Office, London, 53-59.

Schlyter, S. - Odenmark, N., 1935, Brandsäkerheten hos vissa bjälklagskonstruktioner jämte teoretisk bestämning av brandtemperaturer, uppkommande i byggnadskonstruktioner. Statens provningsanstalt. Meddelande 65. Stockholm.

Sjölin, V., 1970, Experimentella undersökningar av brand i bostadsrum. FOA 4 Rapport C4437-96, Stockholm.

Svensk Byggnorm 67 (SBN 67), 1967, Statens Planverk, publikation nr 1. Stockholm.

Tenning, K., 1961, Brandförsök med limmade träbalkar. Väg- och vattenbyggaren, H. 2, Stockholm.

Thomas, P.H. - Hinkley, P.L. - Theobald, C.R. - Simms, D.L., 1963, Investigations into the Flow of Hot Gases in Roof Venting. Fire Research Technical Paper No. 7. London.

Thomas, P.H. - Heselden, A.J.M. - Law, M., 1967, Fully-Developed Compartment Fires - two kinds of behaviour. Fire Research Technical Paper No. 18, Ministry of Technology and Fire Offices' Committee, Joint Fire Research Organisation, Her Majesty's Office, London.

Thomas, P.H. - Heselden, A.J.M., 1972, Fully-Developed Fires in Single Compartments. A co-operative research programme of the Conseil International du Batiment (C.I.B. Report No. 20). Fire Research Note No. 923.

Ödeen, K., 1963, Teoretisk bestämning av temperaturförloppet i några av brand påverkade konstruktioner. Institutionen för konstruktionslära, Kungl. Tekniska Högskolan. Bulletin No. 9. Stockholm.

Ödeen, K., 1963, Theoretical Study of Fire Characteristics in Enclosed Spaces. Division of Building Construction, Royal Institute of Technology. Bulletin No. 10, Stockholm.

Ödeen, K. - Nordström, Å., 1967, Brand- och rökspridning längs fasader och i ventilationskanaler. Delrapport 1. Instrumentering. Statens råd för byggnadsforskning, Arbetshandling 12. Stockholm.

Ödeen, K., 1968, Experimentellt och teoretiskt studium av brandförlopp i byggnader, Rapport från Byggforskningen 23/68, Stockholm.

Ödeen, K., 1970, Brand- och rökspridning längs fasader och i ventilationskanaler. Delrapport 2. Mätvärden och inledande teoretisk bearbetning av försöksserie I. Statens Provningsanstalt, Brandtekniska laboratoriet, Stockholm.